TU WIEN

**TECHNISCHE
UNIVERSITÄT
WIEN**
Vienna University of Technology

DISSERTATION

The impact of inorganic matter on the performance of dual fluidized bed biomass steam gasification plants

Ausgeführt zum Zwecke der Erlangung des akademischen Grades eines Doktors der technischen Wissenschaften unter der Leitung von

Univ. Prof. Dipl.-Ing. Dr. Hermann Hofbauer

E 166

Institut für Verfahrenstechnik, Umwelttechnik und Technische Biowissenschaften der Technischen Universität Wien

Fakultät für Maschinenwesen und Betriebswissenschaften

von

Dipl.-Ing. Friedrich Kirnbauer

Matr. Nr.: 9825751

Embelgasse 49/11, 1050 Wien

Wien, am 26. Juni 2013   ……………………………………….

Doctoral Committee

Supervisor: Univ. Prof. DI Dr. Hermann Hofbauer, Head of the Institute, Institute of Chemical Engineering, Vienna University of Technology

External reviewer: Prof. Marcus Öhman, Chair Professor and Head of Division, Division of Energy Engineering at Luleå University of Technology

Chairman: Univ. Prof. DI Dr. Anton Friedl, Head of Working Group Sustainable Process Engineering & Chemometrics, Institute of Chemical Engineering, Vienna University of Technology

Date of oral defense: 26.06.2013

Hiermit versichere ich, dass ich die vorliegende Arbeit selbstständig verfasst und keine anderen als die angegebenen Quellen und Hilfsmittel benutzt habe, dass alle Stellen der Arbeit, die wörtlich oder sinngemäß aus anderen Quellen übernommen wurden, als solche kenntlich gemacht sind und, dass die Arbeit in gleicher oder ähnlicher Form noch keiner Prüfungsbehörde vorgelegt wurde.

…………………………………………………..

Friedrich Kirnbauer

Abstract

The utilization of biomass for the substitution of fossil fuels to reduce greenhouse gas emissions in biomass steam gasification plants is a promising technology for the production of electricity, heat, and fuels for transportation. The currently difficult market for the utilization of biomass makes optimization of these plants necessary, in terms of increasing both plant electrical efficiency and availability. Plant availability is often linked to operational problems which are caused by inorganic matters of the fuel. Ash components of biomass fuels can cause fouling, slagging, and bed material agglomeration during thermal utilization in fluidized bed combustion as well as gasification plants. Recently developed biomass gasification plants face similar ash-related problems, but inorganic matter is also linked to their catalytic activity to reduce the tar concentration in the product gas.

This thesis deals with the influence of inorganic matter on the operation and optimization of a dual fluidized bed gasification plant. Analyses of inorganic matter at the biomass steam gasification plant in Güssing, Austria were carried out. Mass balances of inorganic matter are presented, evaluating different loop configuration of solid material flows. Investigations in the bed material from the plant in Güssing, Austria showed a modification of the bed material due to the interaction of the bed material (olivine) with biomass ash components and additives. In this thesis the influence of bed material modification on the gasification properties of used olivine from the plant in Güssing is compared with the case of fresh olivine. The test runs were carried out under similar conditions in a pilot plant at the Vienna University of Technology. Additionally, a variation of the gasification temperature from 870 °C to 750 °C was carried out in a 100 kW pilot plant.

The findings of the pilot plant test runs and investigations in inorganic matter were applied at the plant in Güssing to optimize the plant in terms of efficiency and availability. The main optimization steps included a reduction in gasification temperature, a simplification of ash loops and a focus on the controlling of the combustion reactor. The optimization was evaluated in terms of mass and energy balances, and plant availability.

Analyses of the used bed material show the existence of two calcium-rich layers around the bed material particles. The inner layer is homogeneous, comprised mainly of calcium and silicate, while the outer layer has a similar composition to the fly ash of the plant. Inorganic balances showed an accumulation of potassium in the system during operation of the plant.

Pilot plant test runs comparing fresh and used olivine from the Güssing plant showed an increase in hydrogen and carbon dioxide in the product gas in case of the used bed material while the content of carbon monoxide in the product gas decreased. The exothermal water-gas shift reaction is enhanced by the used bed material, resulting in a lower energy demand for the gasification. Tar content was decreased by around 80% for tars detected by gas chromatography – mass spectrometry (GCMS) and the composition of the tar showed less components during the test run with used bed material.

A reduction of the gasification temperature down to 750 °C reduces the concentration of hydrogen and carbon monoxide in the product gas and increases the concentration of carbon dioxide

and methane. The volumetric concentration of tars in the product gas increases only slightly from 850 °C to 800 °C and nearly doubles when decreasing the gasification temperature to 750 °C.

Applying the findings of the pilot plant test runs and the conclusions of investigations of inorganic matter on the gasification plant in Güssing brought a success in terms of electrical efficiency and plant availability. The electrical efficiency of the plant increased from 21 to 23.8%, with a fuel water content around 30% due to the optimization work. Plant availability was increased from an average of 6600 operating hours per year to 7440 hours in 2012 due to a reduction in fouling tendency.

Kurzfassung

Die energetische Nutzung von Biomasse in Dampfvergasungsanlagen nach dem Prinzip der Zweibettwirbelschicht ist eine zukunftsweisende Technologie zur Produktion von Strom, Wärme und synthetischen Treibstoffen. Das schwierige Marktumfeld macht eine Optimierung dieser Anlagen bezüglich elektrischem Wirkungsgrad und Verfügbarkeit notwendig. Die Verfügbarkeit von Anlagen, die Biomasse thermisch nutzen, ist oft durch aschebasierte Vorgänge begrenzt, beispielsweise Anbackungen an Wärmetauschern, Verschlackungen und Bettmaterialagglomeration. Die relativ neu entwickelten Biomasse-Dampf Vergasungsanlagen nach dem Prinzip der Zweibettwirbelschicht sind mit ähnlichen Problemen konfrontiert, wobei die anorganischen Materialien im System auch eng mit der katalytischen Aktivität des Bettmaterials verbunden sind.

Diese Dissertation befasst sich mit dem Einfluss von anorganischen Bestandteilen auf den Betrieb und die Optimierung einer Biomasse-Dampf Vergasungsanlage nach dem Prinzip der Zweibettwirbelschicht. An dem Blockheizkraftwerk Güssing (Österreich) wurden Analysen der anorganischen Materialien durchgeführt. Begleitet wurden diese durch Massenbilanzen anorganischer Komponenten bei unterschiedlicher Kreislaufführung der Asche. Untersuchungen des Bettmaterials aus der industriellen Anlage in Güssing zeigten eine Modifikation des Bettmaterials während des Betriebs. Der Einfluss dieser Modifikation im Vergleich zu frischem Olivin wurde durch Versuche an einer Pilotanlage untersucht. Zusätzlich wurde an der 100 kW Pilotanlage untersucht, wie sich eine Absenkung der Vergasungstemperatur von 870°C auf 750°C mit gebrauchtem Bettmaterial auswirkt.

Die Erkenntnisse aus den Versuchen an der Pilotanlage und die Schlussfolgerungen aus den Analysen der anorganischen Bestandteile wurden zur Optimierung der Vergasungsanlage in Güssing angewendet. Die wichtigen Optimierungsschritte kann man mit der Reduktion der Vergasungstemperatur, einer Vereinfachung der Aschekreisläufe und einem Fokus auf die Regelung in der Brennkammer zusammenfassen. Die Optimierung wurde durch eine Massen- und Energiebilanz und durch die Evaluierung der Betriebszeit beurteilt.

Die Analysen des Bettmaterials ergaben die Bildung zweier kalziumreicher Schichten an den Bettmaterialpartikeln. Die innere Schicht ist homogen und besteht hauptsächlich aus Kalzium- und Siliziumverbindungen während die äußere Schicht eine ähnliche Zusammensetzung wie die Flugasche aufweist. Die Bilanzen über anorganische Komponenten haben gezeigt, dass es zu einer Anreicherung von Kalium im System kommt.

Der Vergleich von frischem und gebrauchtem Bettmaterial in der Pilotanlage zeigte eine Steigerung des Wasserstoff- und Kohlendioxidgehalts im Produktgas mit gebrauchtem Bettmaterial, während Kohlenmonoxid in geringerer Konzentration messbar ist. Die exotherme Wassergas-shift-Reaktion wird begünstigt, was zu einem geringeren Energiebedarf der Vergasung führt. Der Teergehalt im Produktgas wird durch den Einsatz des gebrauchten Bettmaterials um 80% reduziert (mittels Gaschromatographie bestimmte Teere) und die Vielfalt der Teerkomponenten wird reduziert. Die Absenkung der Vergasungstemperatur bis 750°C reduziert den Wasserstoff- und Kohlenmonoxidgehalt im Produktgas, bei einer Erhöhung des Gehalts an Kohlendioxid und Methan. Die Konzentration von Teeren im Produktgas nimmt zwischen 870°C und 800°C leicht zu und steigt signifikant zwischen 800°C und 750°C.

Die Erkenntnisse der Versuche in der Pilotanlage und die Schlussfolgerungen aus den Untersuchungen der Asche, des Bettmaterials und der Anbackungen wurden zur Optimierung der Vergasungsanlage Güssing erfolgreich angewendet und brachten einen Anstieg des elektrischen Wirkungsgrades von 21 auf 23,8% bei rund 30% Brennstoffwassergehalt. Die Verfügbarkeit der Anlage konnte von einem Durchschnittswert von rund 6600 Betriebsstunden pro Jahr bis 2011 auf 7440 Betriebsstunden im Jahr 2012 gesteigert werden. Maßgeblich dafür war eine Reduktion der Stillstände, die durch aschebedingte Anbackungen hervorgerufen wurde.

List of publications

This thesis is based on the work published in the following articles:

I.   Kirnbauer, F.; Hofbauer, H. Investigations on Bed Material Changes in a Dual Fluidized Bed Steam Gasification Plant in Güssing, Austria. Energy Fuels 2011, 25, 3793–3798.

II.   Kirnbauer, F.; Wilk, V.; Kitzler, H.; Kern, S.; Hofbauer, H. The positive effects of bed material coating on tar reduction in a dual fluidized bed gasifier. FUEL 2012, 95, 553–562.

III. Kirnbauer, F.; Wilk, V.; Hofbauer, H. Performance improvement of dual fluidized bed gasifiers by temperature reduction: The behavior of tar species in the product gas. FUEL 2012, 108, 534–542.

IV.   F. Kirnbauer, H. Hofbauer, The Mechanism of Bed Material Coating in Dual Fluidized Bed Biomass Steam Gasification Plants and its Impact on Plant Optimization, Powder Technology 2013, 245, 94-104. DOI: 10.1016/j.powtec.2013.04.022.

V.   F. Kirnbauer, M. Koch, R. Koch, C. Aichernig, H. Hofbauer, Behavior of Inorganic Matter in a Dual Fluidized Bed Steam Gasification Plant, Energy Fuels 2013. DOI: 10.1021/ef400598h (accepted for publication).

VI.   F. Kirnbauer, M. Koch, R. Koch, C. Aichernig, H. Hofbauer, The role of inorganic matter in the optimization of a dual fluidized biomass steam gasification plant, Fuel Processing Technology 2013 (submitted).

Contribution by the author:

I.   Responsible for data evaluation, writing and responsible for experimental work

II.   Responsible for data evaluation, writing and responsible for experimental work with the support of the operational personnel of the pilot plant at the Vienna University of Technology

III. Responsible for data evaluation, writing and responsible for experimental work with the support of the operational personnel of the pilot plant at the Vienna University of Technology

IV.   Responsible for data evaluation, writing and responsible for experimental work

V.   Responsible for data evaluation, writing and responsible for experimental work with the support of the operational personnel of the CHP plant in Güssing

VI.   Responsible for data evaluation, writing and responsible for experimental work with the support of the operational personnel of the CHP plant in Güssing

Danksagung

Mein erster Dank gebührt meinen Eltern, die es geschafft haben, mein kindliches Interesse an neuen Dingen zu wecken, mir die teils unangenehme Eigenschaft zukommen ließen kritische Fragen zu stellen aber dieses auch bis heute bestehen ließen.

Prof. DI Dr. Hermann Hofbauer verdient meinen besonderen Dank, weil er mir den naturwissenschaftlichen Hintergrund lehrte und es ihm gelang diesem Interesse eine wissenschaftliche Methodik zu hinterlegen, deren Ergebnis nun hiermit vorliegt.

Meine Wertschätzung verdienen auch die Eigentümer, der Geschäftsführer und die Betriebsmannschaft des BHKW Güssing. Die gute Zusammenarbeit mit Dipl.-Ing. Markus Koch als mein erster Ansprechpartner des BHKW Güssing hat maßgeblich zum Erfolg dieser Arbeit beigetragen.

Die Unterstützung der Fa. REPOTEC, insbesondere von Dipl. Ing. Christian Aichernig verdient auch meinen herzlichen Dank.

Danken möchte ich auch den Mitarbeitern und Kollegen des Institut für Verfahrenstechnik für die tatkräftige Unterstützung bei vielfältigen Tätigkeiten, Analysen, Versuchen an der TU Wien. Namentlich möchte ich besonders die „Betriebsmannschaft" der DFB-Versuchsanlage am Institut für Verfahrenstechnik an der TU Wien erwähnen, Veronika Wilk, Hannes Kitzler, Stefan Kern, Johannes Schmid, die maßgeblich an der Zähmung von „Erika", der Versuchsanlage beigetragen haben.

Für die Unterstützung der Analysen an externen Instituten möchte ich Hrn. Zaruba, Hrn. Zbiral und Prof. Kubel danken.

Diese Arbeit wurde im Rahmen des Forschungszentrums „Bioenergy 2020+ GmbH" durchgeführt. Dieses wird durch das Förderprogramm „COMET" gefördert, welches von der österreichischen Forschungsförderungsgesellschaft FFG geleitet wird.

Meinen allergrößten Dank möchte ich meiner Frau Jelka aussprechen! Und meiner Tochter Emma, die mich durch ihr kindliches Interesse und ihren Lerneifer begeistert und inspiriert.

Table of contents

1 Introduction

The utilization of renewable energy sources causes a change of the worldwide energy market. Existing technologies and installed capacities that utilize renewable energy cannot fully replace fossil fuels nowadays but worldwide efforts towards the utilization of renewable energies result in investments in research and development of new technologies. A significant share of fossil fuels is already replaced by renewable fuels. A further increase in the share of renewable energies will cause new challenges in the operation of the plants and controlling of the energy grids.

The role of biomass in the renewable energy system is crucial for the supply of liquid fuels. New technologies can only succeed when they fulfill the demands of the market.

1.1 The demands on new technologies for the utilization of renewable energy

Increasing the share of renewable sources for the supply of energy has become a worldwide aim to reduce greenhouse gas emissions. The greenhouse effect caused by the release of fossil carbon dioxide into the atmosphere is well known by politics, opinion leader, scientists and also a substantial part of the population. Regulations by governments of countries and communities underline worldwide efforts to mitigate climate change.

A program from the European Parliament and the council of the European Union [1] plans a share of 20% renewable energy in gross final energy consumption in average of the EU countries in the year 2020. A share of renewable energies in the transport sector is planned with 10% in 2020. Similar targets are set for other countries [2]. To achieve these targets incentives are given to support investments in research and development, erection, and operation of plants based on renewable energy.

The generation of electricity from renewable energy sources is increasing significantly in the states of the European Union (Figure 1). The main renewable sources for the generation of electricity are hydro power, wind energy, biomass and renewable wastes, and solar energy. Tide, wave and ocean power and geothermal power play a minor role in the generation of energy in the European Union (Figure 2). A significant increase in the utilization of biomass and renewable wastes can be seen since the year 1998. The production of electricity by wind power and solar power is also increasing.
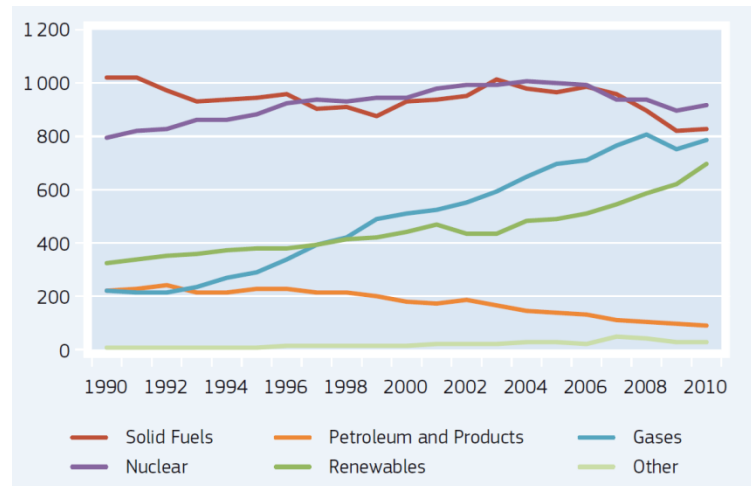
Figure 1: Gross electricity generation in TWh in the EU-27 by fuel [3]

The increase in renewable energy causes the need for a significant increase in investments in the electricity grid [4]. The generation of wind power is spotted on offshore locations or limited rural areas which are barely tapped by the electricity grid. Transport capacities are required to transfer electrical energy from wind rich areas to areas with lower electricity generation.

Another challenge for the utilization of renewable energy sources is that an increase in the number of random variables and operation complexities in the electrical system is caused by the availability of wind and solar power. Reserve capacities have to be built (based on Renewable Energy) which are on standby when wind and solar power are available [5]. Storage capacities for electrical energy are sparse and do not fulfill the challenges of an electrical grid with a high amount of variable renewable energy sources [6,7].
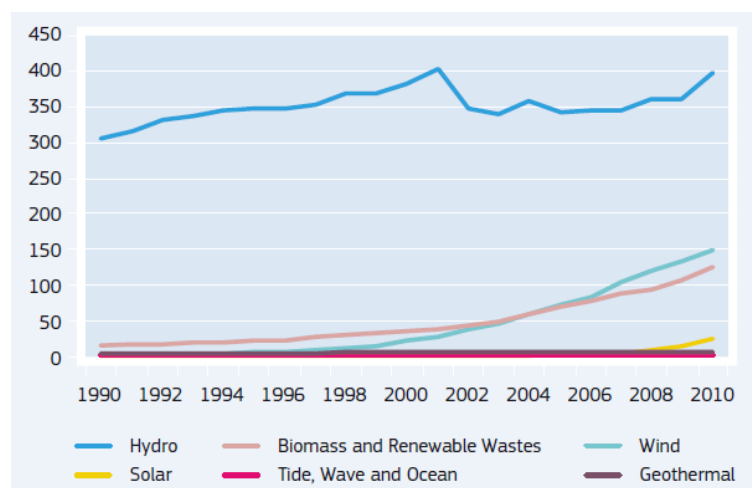
Figure 2: Electricity generation by renewable fuels in TWh in the European Union by energy source [3]

The share of renewable energy sources in fuels for transportation is also increasing within the last years (Figure 3). „First generation" biofuels such as bio-esters, bio-ethanol and biogas appear unsustainable because their production is in direct competition with food commodities. "Second

2

generation" biofuels are based on non-food feedstock such as agricultural and forest residue, grass, aquatic biomass and are considered to be environmentally friendly and not in direct competition with food commodities [8].
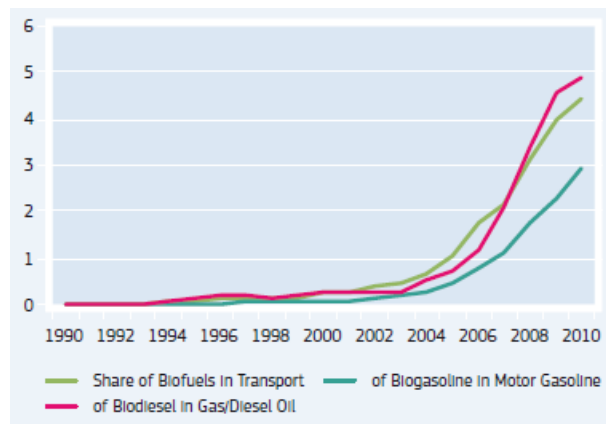
Figure 3: Share of renewable sources in transportation in the EU-27 in % [3]

Various technologies for the supply of second generation biofuels are available: thermo chemical conversion (pyrolysis, gasification, combustion, liquefaction), biological conversion (anaerobic digestion, fermentation, application of enzymes), chemical conversion (hydrolysis, solvent extraction, supercritical conversion of biomass), and physical conversion (mechanical extraction, briquetting, distillation). None of them is installed in industrial scale size with high production capacities which are relevant compared to the share of fossil fuels. A combination of second generation fuel production and electricity generation is not commercially available in industrial scale size.

The demands for new technologies for the generation of electricity and/or fuel for transportation from renewable sources can be summarized as followed:

- Electricity generation should be controllable to complement electricity production from variable renewable energy sources such as wind and solar power

- Additional storage capacities for electricity should be developed to compensate production fluctuations from variable renewable energy sources

- Technologies for the utilization of renewable carbon sources for the production of fuel for transportation are required to be developed which are not in competition with food commodities

These demands are accomplished by the obvious demands of a high economic efficiency and worldwide, high availability of feedstock.

1.2 Biomass as a source for energy production

Biomass can play a significant role by substituting for fossil fuels which cause greenhouse gas emissions in the production of electricity and second generation biofuels [9]. Biomass is a renewable source and releases the same amount of carbon dioxide during energy usage or natural decomposition as it aggregates during the growth period.

Various technologies for the utilization of biomass as an energy source are available. Not all of them include the possibility to generate electricity, heat and fuels for transportation. Different reaction schemes for the utilization of biomass are available: direct conversion in heat (combustion) or the production of intermediate products such as gas which can be used for energy generation or synthesized in different fuels and chemicals. Intermediate products can be generated thermally by carbonization, gasification and pyrolysis but also biologically by anaerobic digestion, fermentation, and the application of enzymes. Physical-chemical conversion schemes are used for the production of oil and oil esters.

The generation of electricity can be carried out by processes that use heat from combustion e.g. a steam process, by combustion e.g. gas turbine, engine or chemically in a fuel cell. The advantage of the generation of intermediate products is that they can be processed to other products such as liquid fuels and chemicals.

The advantages of the utilization of biomass for the generation of energy can be summarized as following:

- Various forms of energy are possible to generate from biomass such as heat, electricity, liquid fuels, chemicals

- Various technologies and conversion paths are possible

- Biomass is stored by nature and can be accessed when required

- The only renewable carbon source that is accessed easily and safely is biomass

The utilization of biomass can be successful when the biomass is used with a high efficiency, when technologies are prepared for high fuel flexibility to compensate seasonal variations and availabilities of feedstock.

1.3 The role of steam gasification in dual fluidized bed reactors for the energetic utilization of biomass

A proven technology for the utilization of woody biomass for electricity generation is biomass steam gasification in a dual fluidized bed (DFB) gasifier. In this process, biomass is gasified thermally and the product gas is used in a gas engine to generate electricity and heat. Various studies are ongoing for the utilization of the product gas to produce fuels for transportation [10-14], making the technology even more suitable for its usage. The polygeneration of electricity, fuels and heat is

considered to be more efficient for the utilization of biomass and higher profits can be generated compared to single-product plants [15,16]. Biomass gasification is described as a key technology for the reduction of greenhouse gas emissions using polygeneration technologies [17].

The advantage of biomass steam gasification in DFB reactors is a nitrogen free product gas with a heating value of around 12-14 MJ/Nm³ and low concentrations of pollutants (tar, higher hydrocarbons, sulfur, nitrogen) that cause problems during further utilization of the product gas. The product gas consists of the main components hydrogen (>40%), carbon monoxide (20-25%), carbon dioxide (20-25%), and methane (8-12%).

The first industrial scale application of a biomass steam gasification plant in a DFB reactor went into operation in 2001 and is located in Güssing (Austria; 8 MWth). Several plants went into operation recently; for example in Oberwart (Austria), Villach (Austria), and Ulm (Germany). The typical plant size is around 8–15 MW but larger plants are planned or are in the realization phase, for example in Goteborg (Sweden; 32 MWth).

Biomass steam gasification in DFB reactors can play an important role for the supply of renewable energy:

- A wide product range can be generated: electricity, heat, fuels for transportation such as Fischer-Tropsch diesel, synthetic natural gas (BioSNG), mixed alcohols or pure hydrogen and synthetic chemicals.

- Electrical efficiencies up to 30% are possible also in plant sizes around 10 MW_{th} [18]

- The production of electricity can be combined with other products to conform the electricity production to the electricity demand, known as polygeneration. During low electricity demand other products can be generated which can be stored easily (e.g. SNG)

- The existing infrastructure for distribution of fuel can be used with the production of e.g. BioSNG and Fischer Tropsch diesel. A synergy between the gas grid and the electricity grid can be achieved by the production of BioSNG during a reduced need for electrical energy

The success of the technology biomass steam gasification is depending on if the demands of the market can be fulfilled. This includes high efficiencies, high availability and a flexibility concerning the fuel type (woody biomass, energy crop, waste etc.) and product flexibility according the demands of the market (electricity, heat, fuel for transportation, chemicals). Furthermore the technology needs to be more efficient and cheaper than conventional technologies for the utilization of renewable energy sources (e.g. steam turbine after combustion).

1.4 Objective, relevance and scope of this work

The utilization of biomass in dual fluidized steam gasification plants is already carried out in industrial scale in Güssing, Austria, Oberwart, Austria and other plants. The operation level of the plants increased significantly within the first years of operation of the plant. An unsolved problem is still a lack of knowledge about the behavior of inorganic matter in the plant and their influence on fouling and slagging in the plant. Fouling and slagging occurs mainly in the combustion reactor and flue gas path in the CHP plant in Güssing and causes unscheduled downtime and a loss of operation time. The operation time which was reached at the CHP plant in Güssing is 7000 hours per year maximum.

This work deals with on the optimization of the CHP plant in Güssing by focusing on a better understanding of inorganic reactions and their influence of the operation on the plant. Samples of inorganic matter were analyzed and discussed, mass balances of inorganic matter were presented and suggestions for the optimization of the CHP plant in Güssing were given. The optimization of the operation at the plant in Güssing is documented and suggestions for the plant design and operation of other plants in future are presented.

This thesis is based on six articles which were published in international journals. The articles are summarized and discussed in this thesis. Full articles are attached in the appendix and can be accessed online at the journals homepages.

Publication I and publication IV focuses on investigations in the bed material which is used in DFB gasification plants. With the new findings of the bed material investigations that bed material is modified during application in the gasifier, test runs were carried out in a 100 kW DFB gasifier pilot plant to evaluate influence of this bed material modification under scientific conditions. The pilot plant findings brought interesting results concerning the catalytic activity of the modified bed material and are presented in publication II and III. Applying the conclusions from the pilot plant test runs to the industrial scale plant in Güssing led to an optimization of the plant. The optimization steps and results of optimization are presented in publication V and publication VI.

2 Fundamentals

This chapter gives an overview over the state of the art of biomass steam gasification in dual fluidized beds. The thermal conversion of biomass in fluidized bed plants often causes various problems in the operation such as slagging, fouling and bed material agglomeration. The background and mechanism of these occurrences which are caused by the inorganic fraction of the fuel and the interaction with the bed material is presented. The thermal gasification of biogenous fuels is linked to the generation of undesired components in the product gas such as tars. Tars are condensable higher carbon hydroxides which condense during cooling down and can cause plugging of heat exchangers and pipes in the product gas path. Therefore, catalytic active bed materials are used for reduction of tar species. The operation of gasification plants is often limited by the generation of tars which is an important edge condition for the design and operation of gasification plants.

2.1 Biomass steam gasification in dual fluidized bed gasifiers

The overall reaction of gasification includes various chemical reactions such as devolatilization of the biomass, gas-gas reactions and gas-solid reactions. Woody biomass consists in 82% of volatile content in mass of the dry substance, typically [19]. The remaining charcoal is gasified by an oxygen-rich gasification agent such as air or pure oxygen, steam or carbon dioxide. The overall reaction of the gasification is endothermic. The main gasification reactions are shown in Table 1. These reactions are considered as equilibrium reactions with variable equilibrium conditions according to Le Chatelier's principle depending on gas concentrations, temperature and pressure. Since various reaction paths are possible, an enhancement of reaction paths is possible through the use of catalysts. Equilibrium conditions cannot be expected under all conditions but are enhanced by the utilization catalytic substances.

Table 1: Typical equilibrium reactions of the main gas components [19,20]

Name of reaction	Chemical equation	ΔH kJ/mol	
Water–gas shift	$CO + H_2O \leftrightarrow CO_2 + H_2$	−40.9	Equation (1)
Methane reforming	$CO + 3\,H_2 \leftrightarrow CH_4 + H_2O$	−225	Equation (2)
Water–gas (i)	$C + H_2O \leftrightarrow CO + H_2$	118.5	Equation (3)
Water–gas (ii)	$C + 2\,H_2O \leftrightarrow CO_2 + 2\,H_2$	103	Equation (4)
Boudouard	$C + CO_2 \leftrightarrow 2\,CO$	159.9	Equation (5)
Methanation	$C + 2\,H_2 \leftrightarrow CH_4$	−87.5	Equation (6)
Oxidation (i)	$C + O_2 \leftrightarrow CO_2$	−393.5	Equation (7)
Oxidation (ii)	$C + 0.5\,O_2 \leftrightarrow CO$	−123.1	Equation (8)

Biomass steam gasification in a DFB gasifier is carried out in two reactors to separate the endothermic reaction from an external heat supply. The main reactor is the gasification reactor operated in a bubbling bed mode where the endothermic steam gasification of the biomass takes

place. In a second reactor, the combustion reactor, thermal heat for gasification is provided by the combustion of char, which is transferred from the gasification reactor to the combustion reactor. The combustion reactor is operated in a fast-fluidized bed regime. The heat is transferred via a circulating bed material between the combustion and the gasification reactor. The product gas consists of the main components, hydrogen, carbon monoxide, carbon dioxide and methane. Trace substances, like higher hydrocarbons, tars, organic sulfur, and nitrogen components are also detectable in the product gas in small amounts. The process is well-described in literature [21-24].

2.2 Thermal utilization of biomass – ash behavior

Inorganic matter plays an important role in the gasification properties but can also lead to fouling, slagging, and bed material agglomeration, which can cause unplanned shutdowns of thermal biomass conversion plants. Various studies of fouling and bed agglomeration are available in the literature, with a focus on the utilization of coal with biomass [25-27], but several studies are also available for woody or other biomass combustion [28-32]. The difference between combustion plants and the DFB biomass gasifier in terms of fouling, slagging, and bed agglomeration is caused by the utilization of two main reactors: a gasification reactor with a reducing atmosphere and a combustion reactor with an oxidizing atmosphere. Intensive exchange of inorganic matters originating from the fuel and bed materials occurs between the two reactors. In contrast to regular fluidized bed combustion plants where quartz sand is used, the bed material in DFB biomass gasification plants is olivine, which is a magnesium iron silicate.

Ash of woody biomass can be described as a system that is dominated by silicates with different contents of basic oxides and a high content of volatile alkaline sulfates and alkaline chlorides. Besides alkali metals, the alkali earth metals also react to form silicates [33,34].

The state of matter of the inorganic material (solid, liquid, gas) plays an important role in the reactivity of the substances. Equation (1) shows general relationships of the state of matter and the reactivity of the substances. Two gaseous components show the highest reactivity, followed by a gaseous and a liquid component. Gaseous and solid components have a higher reactivity than two liquid components, followed by a liquid and a solid component. Two solid components show the lowest reactivity with each other. This is valid for the reactivity and the reaction rate [34].
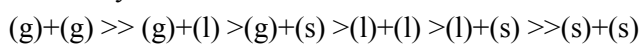
Reactivity of the ash
(g)+(g) >> (g)+(l) >(g)+(s) >(l)+(l) >(l)+(s) >>(s)+(s)   Equation (9) [33]
(g) gaseous elements, (l) liquid elements, (s) solid elements

The substances which are typically detectable in biomass ashes can be split into acid and basic substances (Table 2). The reactivity decreases from the first to the last line [34].

Table 2: Classification of ash compounds [34]

Basic compounds	Acidic compounds
KOH (l, g)	P_2O_5 (g)
NaOH (l, g)	SO_2 (g)/SO_3 (g)
CaO (s)	SiO_2 (s)
MgO (s)	HCl (g)
H_2O (g)	CO_2
	H_2O (g)

Considering the main components of biomass ash, a binary mixture of potassium and silicon oxides is the substance with the lowest melting point, forming a eutectic point at 752 °C with a ratio of 31% K_2O to 69% SiO_2 by weight. Three different crystal phases are formed: K_2O*SiO_2 (melting point 976 °C), $K_2O*2SiO_2$ (melting point 1036 °C), and $K_2O*4SiO_2$ (melting point 765 °C) [35].

The phase diagram for the three-component system of the oxides of potassium, calcium, and silicon which represents the main components of biomass ash forms eutectic points with melting temperatures of around 850 °C [36]. Other elements such as sulfur, chlorine, and potassium have a significant influence on the physical form of the ash mixture at high temperature. The main reactions of ash components were summarized by Boström et al. [34] and are shown in Table 3. These reactions can take place under proper conditions such as temperature, pressure, and availability of reaction partners. Mineral substances can be formed, and amorphous melts can also be detected at fast cooling rates.

The release of alkaline metals in the gas phase is important for the formation of fouling, slagging, and bed material agglomeration because these elements condense after cooling and react with other elements during condensation, which can lead to fouling at heat exchangers. On the other hand the reactivity of elements in the gas phase is higher compared to elements incorporated in a solid crystal structure as described above.
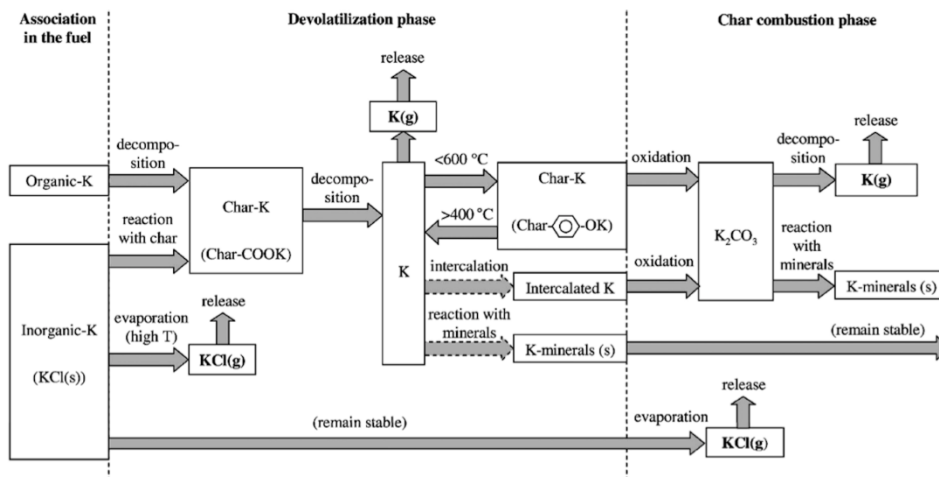
Figure 4: Possible transformations and release mechanisms of organically associated K and KCl during devolatilization and combustion of biomass [37]

Van Lith et al. [37] studied the mechanism and modification of potassium during the devolatilization and combustion of biomass as shown in Figure 4. Due to its metabolic function potassium is highly mobile within all levels of the plant. During drying of the wood, potassium is likely to precipitate in the form of salts such as KCl, K_2SO_4, KOH and K_2CO_3. Some of the potassium is bound in organic structures in carboxyl groups. In spruce and beech about 40 % of the potassium is organically associated. During devolatilization and combustion of biomass organically bound potassium and inorganic bound potassium follow different reaction schemes. Inorganic bound potassium e.g. potassium chlorine is stable and is evaporated at higher temperatures. Carboxyl groups start to decompose at temperatures lower than 300 °C and atomic potassium will be released. This elemental potassium is likely to react with phenol groups which are stable at these temperatures or it remains in the gas phase. At higher temperatures, it is suggested that potassium is bound to phenol groups, which decompose at temperatures higher than 400 °C, while potassium is released to the gas phase, probably in elemental form. During the combustion at temperatures about 850°C organically bound potassium is oxidized to potassium carbonate. Elemental potassium can also react with minerals which remain stable or it reacts with oxygen to form potassium carbonate. The decomposition of potassium carbonate (K_2CO_3) seems to be the dominant mechanism at temperatures higher than 800 °C.

Table 3: Survey of major secondary ash-forming reactions (schematic) [34]

Reaction	Comments	
$P_2O_5(g) + 2KOH\ (g) \leftrightarrow 2KPO_3\ (l,g) + H_2O\ (g)$	Fast reaction,* product molten and partially volatile in residual ash**	Equation (10)
$SO_3(g) + 2KOH\ (g) \leftrightarrow K_2SO_4\ (l,g) + H_2O\ (g)$	Fast reaction, product molten or not	Equation (11)
$HCl(g) + KOH\ (g) \leftrightarrow KCl\ (g,l) + H_2O\ (g)$	Fast reaction, product not stable in residual ash	Equation (12)
$SiO_2(s) + 2KOH\ (g) \leftrightarrow K_2SiO_3\ (l) + H_2O\ (g)$	Medium fast reaction, product stable and molten in residual ash	Equation (13)
$CO_2(g) + 2KOH\ (g) \leftrightarrow K_2CO_3\ (l,g) + H_2O\ (g)$	Fast reaction, product not stable in residual ash	Equation (14)
$P_2O_5(s) + 3CaO\ (s) \leftrightarrow Ca_3P_2O_8\ (s)$	Medium fast reaction, product stable and solid in residual ash	Equation (15)
$SO_3(g) + CaO\ (s) \leftrightarrow CaSO_4\ (s,l)$	Medium fast reaction, product (not) stable and solid in residual ash	Equation (16)
$2HCl(g) + CaO\ (s) \leftrightarrow CaCl_2\ (g,l) + H_2O\ (g)$	Medium fast reaction, product not stable in residual ash	Equation (17)
$SiO_2(s) + CaO\ (s) \leftrightarrow CaSiO_3\ (s)$	Slow reaction,*** product stable and solid in residual ash	Equation (18)
$CO_2(g) + CaO\ (s) \leftrightarrow CaCO_3\ (s)$	Medium fast reaction, product not stable in residual ash**	Equation (19)
$K_2SiO_3(l) + CaO\ (s) \leftrightarrow K-Ca-Silicate\ (l)$	Rather slow reaction,*** product stable and molten in residual ash	Equation (20)

* The reaction rates are classified into four categories on an arbitrary scale

** The stability in residual ash varies according to the thermal condition of the specific appliance.

*** These reaction rates are also highly dependent upon the dispersion of fuel and reactant particles.

Novaković et al. [38] showed in laboratory scale test runs with mixtures of potassium, calcium, and silicon that the release of potassium into the gas phase is mainly dependent on the calcium content in the mixture, the water content in the gas phase, and the temperature. The release rate is independent of the origin of the calcium (e.g. $CaCO_3$ or $Ca(OH)_2$). The absence of steam reduces the release of potassium, while doubling the calcium content brings a higher release of potassium.

The chemical mechanism of the release of potassium from potassium carbonate is shown in Equation (14), Table 3. An excess of water moves the equilibrium according to Le Chatelier's principle towards KOH(g) and CO_2(g) and, with that, towards a higher release rate of potassium into the gas phase.

Comparing the release of potassium into the gas phase in an oxidizing atmosphere (combustion) and a reducing atmosphere (gasification), a higher release rate can be expected in the reducing atmosphere of the gasification reactor at the same temperatures [39,40].

The consequences of ash melting or the release of inorganic matter into the gas phase can be fouling, slagging, and bed material agglomeration. Deposits occurring in the high temperature sections of furnaces are called slagging. Radiative heat transfer is dominant in the areas where slagging occurs. Deposits in the convective heat transfer zones of the boiler are called fouling and takes place in the areas where the gases are cooled [27]. Bed material agglomeration is the consequence of sticking bed material particles which glue together to larger particles (agglomerates). These undesired large particles decrease the mixing in the fluidized bed and may result in a collapse of the fluidized bed.

2.3   Bed material fundamentals

The type of bed material used is important for the gasification performance of the plant. Using olivine, a magnesium-iron silicate, is state of the art for these gasifiers due to its catalytic properties. The positive effects of olivine on tar reduction have been shown in various studies [41-46].

In industrial scale applications which are working at high availabilities of around 8,000 operating hours per year a long-term interaction of bed material with other inorganic substances that are available is possible. In the following possible interactions of olivine with ash components are presented and discussed. An interaction and modification of the bed material by ash components of the biomass is considered to influence the catalytic properties of the bed material.

An overview over the influence of the catalytic activity of the olivine on the gasification performance is given.

2.3.1   The characteristics of olivine and its interaction with other inorganic elements in thermal biomass conversion plants

Due to high temperatures in combustion and also gasification plants interactions between inorganic matter (biomass ash and additives) and bed material is possible. These high temperature reactions can cause bed material agglomeration and fouling. Agglomeration is often initiated by a layer formation on the bed material particles. A layer formation at the surface of bed material particles in biomass combustion plants is described in literature for quartz sand [47-51] but also for olivine [29,52-54].

The formation mechanism of the layers on the bed material particles is described by Öhman et al. [55] and was improved by Brus et al. [48], De Geyter [56], and Grimm et al. [57] for quartz as bed

material. This mechanism is summarized by Grimm et al. [52] as follows: (a) Initiation by coating: ash components are melted and sintered onto the surface of the particle. This is initiated by potassium silicate melting accompanied by the diffusion or dissolution of calcium into the melt. This mechanism is suggested to be typical for woody fuels with ash rich in calcium and potassium with small amounts of silicon and phosphor. (b) Potassium compounds in gaseous or aerosol phase react directly with the particle surface, forming potassium silicates at the surface followed by sintering and agglomeration. This mechanism is suggested to be typical for fuels with high alkali content and relatively low silicon and phosphor contents. (c1) Direct adhesion of melted potassium silicate particles or droplets: this mechanism is typical for fuels with high potassium content and high content of organically bound silicon. (c2) Direct adhesion by partly molten potassium-calcium phosphates or magnesium phosphates: this is typical for biomass rich in phosphor, potassium, and calcium or magnesium.

Scala et al. [58] described the formation of agglomerates around burning particles where the temperatures are locally higher than in the rest of the fluidized bed.

Phosphor is described in literature to have significant influence on the agglomeration behavior which is relevant with alternative fuels [52,57,59]. The influence of phosphor on the adhesion of potassium and its influence on the layer formation with woody biomass are considered to be low because of low phosphor concentrations in the fuel ash and in the particles.

Olivine the bed material in DFB plants is a natural mineral that has its origin in basaltic magma. It is a magnesium iron silicate and the first or an early crystallization phase from basalts [60]. Various authors from different disciplines have published examinations of the crystal structure and properties of olivine. Calcium diffusion in olivine is of interest in mineralogy for determining the cooling rate of samples from meteorites. These studies also show interesting results regarding the utilization of olivine in DFB gasifiers, its modification during long-term utilization, and the interaction with biomass ash.

Olivine consists of two crystal structures: fayalite and forsterite. Fayalite is an iron-containing silicate, Fe_2SiO_4, and forsterite is the phase which is rich in magnesium, Mg_2SiO_4. The crystal structure of olivine is orthorhombic; it has two distinct metal sites (called M1-O and M2-O in literature) of the octahedrally coordinated cations, which can be Fe, Mg, Ni, Mn, or Ca. These two positions are interchangeable with different ions. At temperatures higher than 600 °C the angular distortion of the M1 and M2 octahedra increases and the exchange of ions at these positions is enabled [61]. With increasing temperature the distances at the M-O positions increase while the Si-O distances show zero or slightly negative expansions [61]. The behavior of fayalite is similar to forsterite with increasing temperature [61]. The position M2 is suggested to be preferred by calcium ions when exchanging Fe ions [61]. The Ca-Fe substitution in olivine is more extensive than Ca-Mg substitution because of the difference between the radii of Fe and Mg cations [62]. The diffusion rate of calcium into olivine is lower than the diffusion of iron or magnesium [62,63]. The diffusion rates along the different axes of the crystal structures show that diffusion occurs four to eight times faster along one axis compared to the other two axes [63]. The diffusion rates of calcium into the olivine structure increase with increasing oxygen fugacity because the partial oxidation of the Fe^{2+} ions to Fe^{3+} is charge balanced by the formation of these vacancies [63].

These findings seem to be relevant to the application of olivine in DFB gasification. They can help understanding the influence of the calcium rich woody biomass ash on layer formation, and its influence on the gasification properties. The modification of olivine due to the mobility of the iron ion at high temperatures is reported to have a positive influence on tar cracking in biomass gasification [42,44]. Fredriksson et al. [64] reported that unused olivine in a DFB gasifier is modified by the different atmospheres in the combustion reactor and the gasification reactor. In the combustion atmosphere, iron is mostly available as Fe_2O_3 and Fe_3O_4 or $MgFe_2O_4$, but it is reconverted under a reducing atmosphere to Fe and Fe_3C and the formation of graphitic carbon can be detected [64].

2.3.2 The catalytic properties of olivine for tar reduction

Undesired by-products of biomass gasification are described by the collective term "tars". Tars are defined as follows: "The organics, produced under thermal or partial-oxidation regimes (gasification) of any organic material, are called 'tars' and are generally assumed to be largely aromatic" [65].

Table 4: Possible reactions of hydrocarbons in hot gas cleaning conditions, with toluene as model hydrocarbon [20]

Name of reaction	Chemical equation	ΔH kJ/mol	
Steam reforming	$C_7H_8 + 7\ H_2O \rightarrow 7\ CO + 11\ H_2$	876	Equation (21)
	$C_7H_8 + 14\ H_2O \rightarrow 7\ CO_2 + 18\ H_2$	647	Equation (22)
Steam dealkylation	$C_7H_8 + H_2O \rightarrow C_6H_6 + 2\ H_2 + CO$	123	Equation (23)
	$C_7H_8 + 2\ H_2O \rightarrow C_6H_6 + 3\ H_2 + CO_2$	90	Equation (24)
Hydrocracking	$C_7H_8 + 10\ H_2 \rightarrow 7\ CH_4$	−713	Equation (25)
Hydrodealkylation	$C_7H_8 + H_2 \rightarrow C_6H_6 + CH_4$	−104	Equation (26)
Dry reforming	$C_7H_8 + 7\ CO_2 \rightarrow 14\ CO + 4\ H_2$	1105	Equation (27)
	$C_7H_8 + 11\ CO_2 \rightarrow 18\ CO + 4\ H_2O$	1236	Equation (28)
Thermal cracking	$nC_7H_8 \rightarrow m\ C_xH_y + p\ H_2$	−	Equation (29)
Carbon formation	$C_7H_8 \rightarrow 7\ C + 4\ H_2$	−73	Equation (30)

These tars cause operational problems when cooled down and condensed at heat exchangers, plugging pipes, and so on. Various research activities focus on reduction of these tars before further utilization of the product gas. The chemical reactions concerning tar reduction are described in Table 4 for toluene as a model component. Similar reactions can be described for the other tar components. These chemical equations allow a wide range of reaction schemes and show the complexity of the topic.

To decrease the amount of tar in the product gas, catalytic active material for further tar reduction is used in the fluidized bed. The use of olivine as a bed material has become state of the art in industrial scale DFB steam gasification plants. Additionally calcium-rich additives such as calcite or dolomite are used for further reduction of the tar content in the producer gas.

The positive effect of olivine on tar reduction has been reported by various authors with regard to various fuels [41-44,66-70]. A better catalytic activity of the olivine can be achieved by calcination of olivine [42,71]. Even better conversion is achieved by the use of modified olivine such as Ni-olivine, Fe-olivine [41,69,72-75] or synthetic catalysts [76-78].

Dolomite also showed good results with regard to the catalytic activity for reducing tars [23,41,67,79-82].

A comparison of dolomite and inert bed material was carried out by Ruoppolo et al. [76] They reported a 50% higher tar conversion in a fluidized bed using dolomite as bed material compared to quartzite as well as a reduction of the number of tar components.

Corella et al. [67] reported that the tar removal efficiency with dolomite was ~ 1.4 times better compared to olivine in a fluidized reactor. In a previous publication the authors concluded [83] that the introduction of dolomite into the fluidized bed gives better results compared to a down-stream usage of dolomite in a second reactor. The polymerization of tars is suspected to take place when using a gasification reactor with silica sand and a down-stream reactor with dolomite.

A laboratory scale quartz tube reactor was used by Simell et al. [20] to study the decomposition of toluene, which was used as a model component for tar over dolomite and nickel catalyst. They concluded that the dry reforming reaction (Equation (27) and Equation (28)) and steam reforming reaction (Equation (21), Equation (22)) take place with both catalysts. The presence of steam inhibits the dry reforming reaction but tar decomposition is carried out with steam reforming. The presence of gasification gas on dolomite reduced the tar decomposition on dolomite due to the inhibition of active sites by CO_2, CO and H_2.

Alarcon et al. [84] studied the catalytic activity of a mixture of CaO with MgO for naphthalene steam gasification in a fixed bed. While pure MgO and CaO achieved carbon conversion of 54 and 62%, respectively, a mixture of 10% CaO and 90% MgO showed the highest carbon conversion, 79%. A catalytic synergy between the two oxides was described.

Similar results were published by Delgado et al [85]. The authors studied the catalytic activity of calcined dolomite, calcite, and magnesite in a fixed bed reactor reforming product gas of a fluidized bed gasification reactor. The fixed bed reactor was loaded with the catalyst. They reported better gas yields and tar reduction with dolomite followed by calcite and magnesite.

Kyotani et al. [86] investigated the mechanism of calcium catalysis of carbon gasification with oxygen. They found that calcium enhances the formation of CO_2 in carbon gasification with O_2. The process was explained as follows: O_2 dissociatively chemisorbs on CaO particles to form CaO(O). The active oxygen from CaO(O) quickly migrates to the carbon surface to form C(O). When active sites around CaO are occupied by C(O), oxygen reacts with the C(O) at the active site to CO_2 which is released leaving an active site on the CaO.

Nair et al. [87] studied the tar removal of biomass-derived fuel gas by pulsed corona discharge with respect to the decomposition scheme of naphthalene. They concluded that the most favorable pathway for tar decomposition is the direct attack of oxygen radicals.

This theory is also confirmed by studies by Chen and Yang [88] on alkali and earth alkali metals where the authors catalyzed gasification reactions of graphite by CO_2 and H_2O. They reported the formation of C-O-M groups, where M denotes for the metal. Oxygen radicals have their origin in CO_2 and H_2O. In earlier studies they found that particles are more active than single C-O-K groups [89].

However, the usage of bed materials with better catalytic activity than olivine is desired. Alternative bed materials to olivine often face problems with attrition (e.g. dolomite [41,68]) or their preparation is expensive (e.g. synthetic catalysts). The disposal of wastes of alternative bed materials such as nickel coated bed material is also problematic.

3 Facilities for investigation

Research activities were carried out at the industrial-scale plant in Güssing, Austria and at different test facilities in pilot plant scale and laboratory scale. Various analyses methods were carried out to characterize samples.

Due to the fact that fouling could not be reproduced at small scale plants, various samples had been investigated from the CHP plant Güssing. Assumptions which were made from investigations at the CHP plant Güssing could be confirmed in a 100 kW pilot plant at the Institute for Chemical Engineering at the Vienna University of Technology and a lab scale fluidized bed test rig from Bioenergy 2020+ GmbH.

3.1 CHP plant Güssing

The CHP plant Güssing is part of a concept of the municipality of Güssing to replace fossil fuels by renewable energy sources. The DFB biomass-steam gasification plant has a thermal power of 8 MW and an electrical power of 2 MW. The plant went into operation in late 2001 and had an operation time of ~72,000 h at the gasifier and ~66,000 h at the gas engine up to April 2013. Wood residues harvested in the local area are used as fuel. Various literature is available about the plant [21,22,24].

Figure 5 shows the basic flow sheet of the DFB process operated at the plant in Güssing. Woody biomass is gasified with steam at 850-900°C in a stationary fluidized bed. The required heat is transferred with the bed material from the combustion reactor, which is operated at 950-1000°C, to the gasification reactor.

The product gas leaves the gasifier at 850°C through the product gas cooler, where it is cooled down to 160°C. Mostly inorganic particles with fine char particles that are not gasified leave the gasification reactor with the product gas. This fly char—containing fine char particles, tars, and mainly inorganic matter such as biomass ash, bed material attrition, and catalytic additives—is separated from the product gas flow in the product gas filter and is burnt in the combustion reactor to utilize the remaining energy of the char. The product gas is further washed at a rapeseed methyl ester (RME) scrubber and compressed for further utilization.

A part of the fuel that is not converted in the gasifier is transported together with bed material via a chute to the combustion reactor where it is burnt. After the combustion reactor, bed material is separated from the flue gas in the cyclone and the hot bed material is fed to the gasifier, supplying the required heat for gasification. Fine particles like ash, bed material attrition, and additives leave the cyclone with the flue gas at 970-1000°C. Depending on the performance of the cyclone, the fly ash can contain a considerable content of bed material. The flue gas is cooled down in several heat exchangers to 160°C, and fly ash is separated in the flue gas filter. A part of the fly ash is recirculated to the gasifier due to its catalytic activity for gasification (fly ash circulation) while the other part is disposed (ash container).
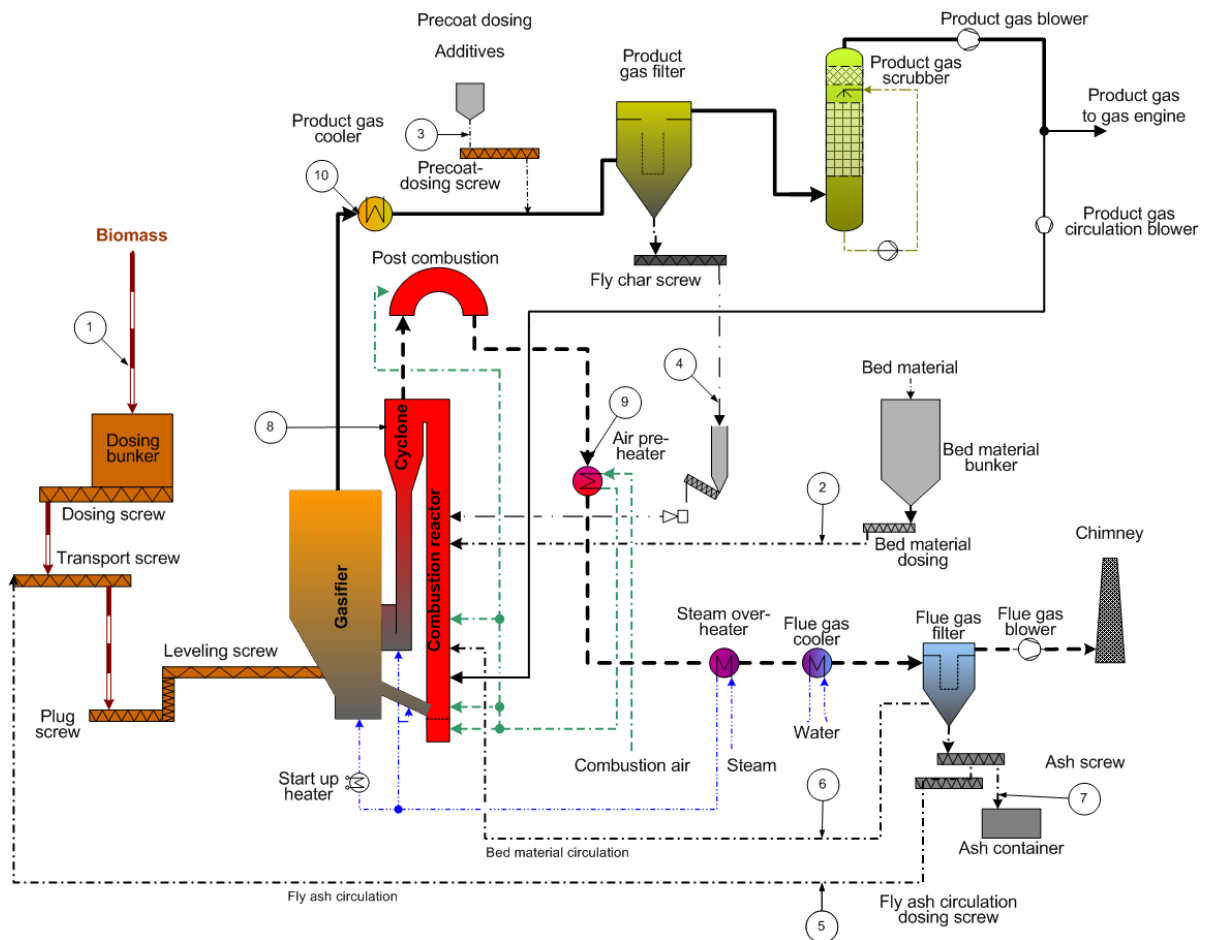
Figure 5: Basic flow sheet of the DFB gasification plant in Güssing (including sampling points)

Inorganic flows enter the plant with the biomass ash into the gasifier, fresh bed material is added to the combustion reactor, and calcium-rich additives such as dolomite or calcium oxide are used as catalytic agents either prior to the gasifier or right before the product gas filter. Inorganic matter is discharged only at the flue gas filter to the ash container.

Due to the demo character of the Güssing plant, the potential for its improvement in terms of design and engineering was determined and applied in later plants which are described in the following.

One of the main differences between the scale of the Güssing prototype plant and those constructed in the following years is the size of the combustion reactor and flue gas pathway. While the Güssing plant was designed for 15% fuel water content, later plants were constructed with higher levels of water in mind due to the low availability of wood chips and wood residues with water content of around 15% on the Austrian and European markets. However, the plant at Güssing now operates using fuel with significantly higher water content (20-45%). Besides the larger size of the combustion reactor, a low temperature biomass dryer positioned prior to the gasifier in more modern plants can be considered state of the art.

The flue gas path in the Güssing plant includes a post combustion chamber followed by a shell and tube heat exchanger, with the flue gas contained inside the tubes. In contrast, the current state

of the art design for flue gas cooling involves convection after the post combustion chamber in order to cool the gas to below the melting temperature of all ash components. A comparison of both flue gas pathways is shown in Figure 6.
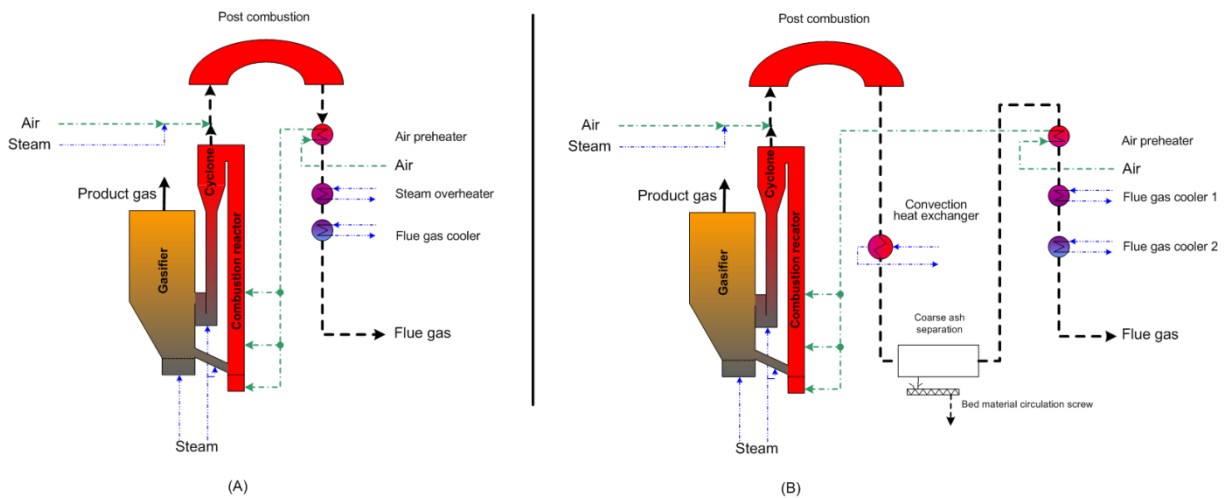
Figure 6: Comparison of flue gas cooling at the Güssing plant (A) and the current state of the art (B)

The Güssing plant currently operates at levels unsuited to its size. This results in the fouling and slagging of the combustion reactor, cyclone and at the first heat exchanger (air preheater), issues which are not seen in newer plants such as that e.g. in Oberwart/Austria. Nevertheless, the operating conditions and scale of the Güssing plant, as well as the resulting problems, can be used to form the basis for developing a better understanding of the DFB gasifier in terms of inorganic matter. Indeed, various research activities have recently been carried out in order to understand the behavior of inorganic matter in the system, and to increase the efficiency and availability of the plant.

3.2 Pilot plant gasifier at Vienna University of Technology

At the pilot plant at the Institute of Chemical Engineering, Vienna University of Technology, the basic design parameters of the gasifier in Güssing, Austria were developed. The basic principal of the gasifier is the same as that of the industrial scale plant in Güssing but due to its size some details are different. The pilot plant shown in Figure 7 is well-described in literature [41,91,92].

However, the gasifier consists of a gasification reactor with a bubbling bed, which is fluidized by steam, and a combustion reactor with a fast fluidized bed, which is fluidized by air. The bed material is circulated between the two reactors to carry the heat from the combustion reactor to the gasification reactor. The separation of the bed material and the flue gas after the combustion reactor is carried out using a gravity separator. Siphons are located between the gasification reactor and the combustion reactor to avoid leakage of gases from the combustion reactor such as air of flue gas into the gasification reactor.
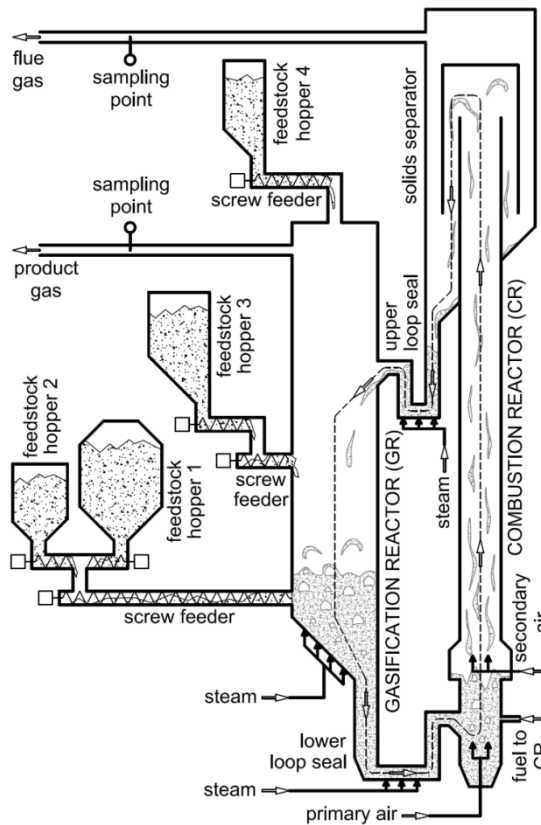
Figure 7: 100 kW gasifier at the VUT [93]

The fuel is dosed into the fluidized bed of the gasifier where water and volatile components of the fuel are released. The remaining char is gasified with steam. A part of the char is transported with the bed material to the combustion reactor, where the char is burnt.

In contrast to the industrial scale plant the pilot plant is designed to add fuel into the combustion reactor to provide a part of the required heat for the gasification not via transport of char through the chute but from outside of the whole system. Light fuel oil is used in the pilot plant. The amount of fuel in the combustion reactor with constant gasification temperatures allows a qualitative evaluation of the gasification properties of the fuel. In the industrial scale gasifier, fly coke from the filters, tar, saturated RME, and a small quantity of product gas are injected into the combustion reactor. The product gas is used to control the temperature of the gasification system.

The pilot plant is equipped with temperature, pressure and volume flow measurements which were logged continuously. Gas measurement in the product gas stream and in the flue gas stream is carried out. Gas analyses of the pilot plant are described in chapter 4.4.1.

3.3 Lab scale fluidized bed test rig

A bench-scale fluidized bed reactor was used to evaluate the influence of the surrounding gas atmosphere on the crystal structure of the bed material particles. The test rig consists of a reactor, a gas-supplying system, a solid-fuel-dosing system, and off gas handling (heat exchanger, cyclone, and filter). The off gas leaving the reactor and cooling section at gasification operation conditions has to be finally burnt before released to the environment. A flow sheet of the test rig is shown in Figure 8.
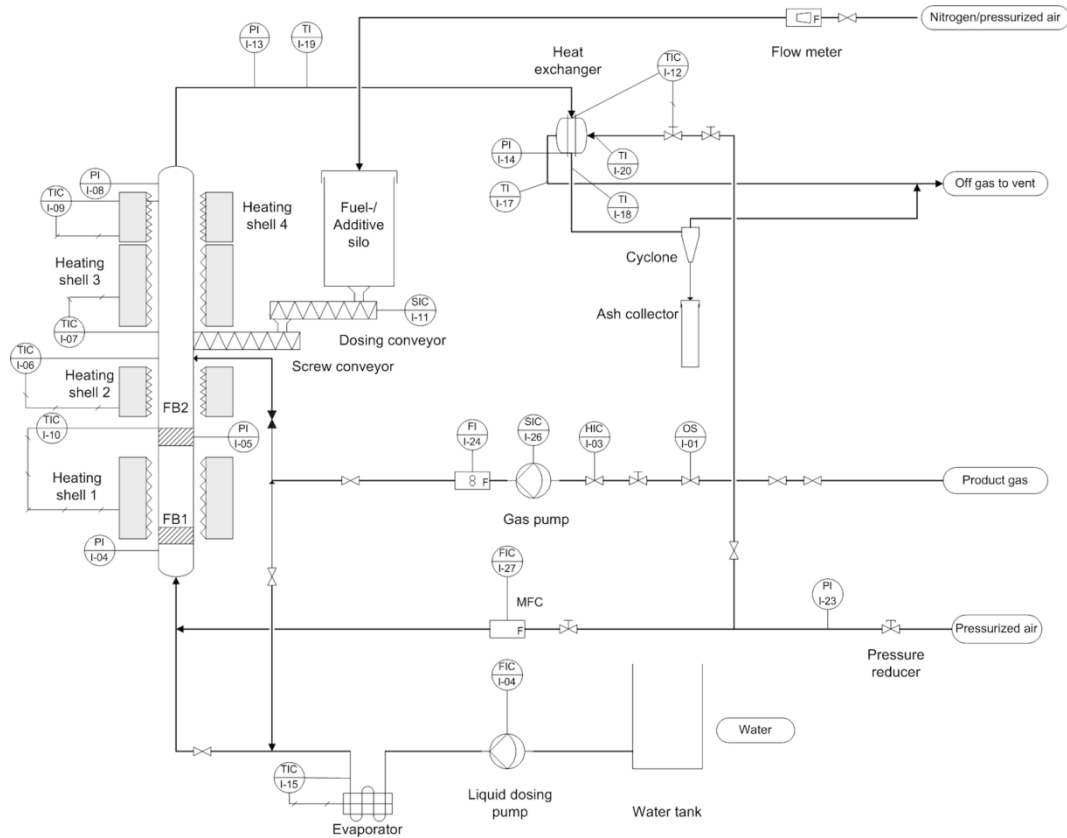
Figure 8: Flow sheet of the 5 kW lab-scale reactor

The bench-scale reactor is made of stainless steel (1.4841) with a total height of 1.85 m, inner diameter of 65 mm, and wall thickness of 3 mm in the bed section. The reactor consists of two fluidized beds located above each other (FB1, FB2). Two perforated stainless steel plates are used as distributors. The lower fluidized bed serves for pre-heating the gas and the upper fluidized bed is used for the reaction and investigations. The lower fluidized bed has a height of 550 mm between the two distributors and the lower bed itself has a height of 100 mm; the upper fluidized bed is 1200 mm in height from the distributor to the gas exit. At the beginning of the experiments bed material is fed in to obtain also a bed height of 100 mm.

The gas composition and flow rate are controlled by mass flow controllers. An electrically heated steam generator is used for supplying steam at atmospheric pressure. A bin with a screw-dosing

system can be used for adding material into the fluidized bed. The conveying screw is speed-controlled by a frequency converter.

Before leaving the flue gas to the atmosphere, the gas is cooled down in a tube heat exchanger and cleaned in a cyclone and filter, and at operation in gasification conditions it has to be burned before it is released into the atmosphere.

To heat the fluidized bed and keep the temperature constant, the reactor is equipped with electrical wall-heating elements which are regulated with proportional controllers. One heating shell is used for heating the lower fluidized bed (heating shell 1). The upper fluidized bed is heated with three heating elements.

The temperature is measured with one thermocouple at the lower fluidized bed and with three thermocouples at the upper fluidized bed and freeboard sections. All thermocouples are of type K with a measuring range of up to 1050 °C.

4 Results

For better understanding of the behavior of inorganic matter and the influence of the operating conditions in the CHP plant Güssing on formation of fouling samples of inorganic matter in the plant were taken. Bed material represents the biggest fraction of inorganic matter in the system.

Investigations of the bed material brought the new finding, that the bed material is modified by long-term interaction with the biomass ash during the operation of the system. Based on this finding, further investigations were carried out to clarify where bed material modification takes place: in the gasification reactor or in the combustion reactor and theories for the mechanism of the modification were discussed.

The influence of this bed material modification on the gasification properties was studied in pilot plant test runs at the gasifier at the Vienna University of Technology. Based on these pilot plant test runs, conclusions were drawn for the optimization of the CHP in Güssing. These optimization steps included an analysis and modification of the inorganic loops in the plant and a focus on operational parameters.

An evaluation of the success of the optimization measures at the CHP plant Güssing was carried out with mass and energy balances.

4.1 Bed material investigations

Bed material samples were investigated to evaluate the influence of inorganic matters such as biomass ash and additives on the bed material which is presented in Publication I. These investigations are related to the composition of biomass ash and fly ash. Fresh bed material particles which were not utilized in the system and bed material particles which were sampled at the plant were compared. A second study presented in Publication IV compares the elemental composition of micrographs which represent the inside of the particle with the elemental composition of particle surface examinations. A study of the thermal behavior in different atmospheres is presented. The mechanism of bed material modification is discussed and a suggestion whether modification takes place in the gasification reactor or in the combustion reactor is given.

4.1.1 Sampling and analysis of bed material

Unused bed material samples were taken at the delivery of fresh olivine. Used bed material was taken from the bottom of the combustion reactor during shutdown after cooling down the plant. Since the retention time of the bed material in the reactor varies due to the continuous supply of small amounts of fresh olivine to replace bed material loss due to abrasion, a number of samples were taken for elemental analyses.

The elemental composition of the samples was determined using X-ray fluorescence (XRF) and calculated as oxides. Samples for XRF were melted in a Merck Spectromelt at 1050°C and dumped on a 400°C stainless steel plate. The analyses were carried out with a PANalytical Axios Advanced

analyzer under vacuum atmosphere with a rhodium anode and an excitation voltage of 50 kV and a tube current of 50 mA. The results indicate the elemental composition of the total sample calculated in oxides. Two bed material samples were analyzed by X-ray diffraction measurements. X-ray diffraction measurements were performed on a PANalytical X'Pert PRO system. Refinements were performed using the TOPAS 4.2 program package.

The samples for the SEM-EDX analysis were mounted in epoxy, sanded and polished. Analyses were carried out on a Scanning Electron Microscope FEI Philips model XL30 combined with energy dispersive X-ray spectroscopy (SEM with EDX). A number of spot analyses were taken for composition of the layers of different particles and average compositions were calculated. The EDX indicates the elemental composition of the surface of the sample.

Thermo-gravimetric analysis (TGA), differential thermal analysis (DTA), and differential scanning calorimetry analysis (DSC) of fresh and used bed material particles were carried out in a NETZSCH STA 449 C Jupiter System. The sample crucible is equipped with a thermocouple for direct measurement of the temperature. The mass is measured by an electromagnetically compensated microbalance with a resolution of 0.1µg and a maximum capacity of 5g. The furnace allows temperatures of up to 1650 °C with heating rates between 0.01 and 50 K/min. Heating rates of 10 K/min were chosen to ensure minor mass or heat transfer limitations. The signal-to-noise ratio of the DSC is 15µW. The gas used to provide the desired atmosphere flows upwards and the desired gas composition is mixed out of gas bottles with the aid of mass flow controllers. Gas flows were set to $40*10^{-6}$ m³/min. The mass for each sample was chosen to be approximately 70 mg. The results of the TGA were related to the mass at 250 °C as a reference mass. Temperatures below 250 °C are not considered due to inaccurate temperature controlling of the oven and because temperatures lower than 250°C are not from interest for this topic. The thermal analyses were carried out once for each sample in three different atmospheres.

A bench-scale fluidized bed reactor (see chapter 3.3) was used to evaluate the influence of the surrounding gas atmosphere on the crystal structure of the particles to obtain a better knowledge of whether the bed material modification takes place in the gasification or the combustion reactor of the DFB system.

Table 5: Test conditions for gasification and combustion in the test rig

	Unit	Gasification	Combustion
Temperature	°C	840 ± 8	960 ±10
Duration of the test run	min	150	150
Fluidization gases and supplements		Product gas (from industrial scale gasification plant, dry, after scrubber) Steam	Air Product gas Char dust Steam

To generate similar gasification and combustion conditions compared to the industrial-scale DFB gasification plant, similar fuels are used. The gasification atmosphere is generated by using product

gas from the Güssing plant for fluidization as the test rig was located in a laboratory just beside the Güssing plant. Since the tapping point of the product gas in the industrial-scale plant is located after the product gas cleaning (filter and scrubber), the gas is mixed with steam to generate a water content similar to that in the gasifier. The test conditions used in the test rig are summarized in Table 5. The combustion conditions were generated by combustion of product gas and char from the industrial-scale plant. To ensure similar steam content in the combustion atmosphere, steam is added. The gas atmospheres of the gasification and combustion conditions are summarized in Table 6. The detailed product gas composition is described elsewhere [14,21].

Table 6: Gas composition of combustion and gasification atmosphere

Component	Unit	Gasification atmosphere	Combustion atmosphere
H_2	%db	~42	–
CO	%db	~20	–
CO_2	%db	~23	~9
CH_4	%db	~9	–
O_2	%db	<0.2	8.5
N_2	%db	<1.5	rest
C_nH_m		<4.3	-
Water	%	40	19

4.1.2 *Results of bed material investigations*

The retention time of bed material in the CHP plant in Güssing during regular operation is between 50 and 100 hours in average. Bed material which is described as "used bed material" was sampled after regular production of around 4 weeks which ensures retention time of the samples of 50 – 100 hours in the system.

The results of the XRF analyses of used and unused olivine are shown in Table 7. The natural mineral olivine consists of magnesium, silicon and iron (($Mg, Fe)_2SiO_4$) as its main components. The results for the elemental analysis were as expected. The elemental composition of the used bed material showed a significant increase in calcium and potassium content. A comparison of the elemental composition of the main components is visualized in Figure 9.

Table 7: Comparison of unused and used olivine

	Unused olivine	Used olivine
	wt.-%	wt.-%
MgO	46.8	40.0
SiO_2	39.8	34.9
CaO	0.9	10.0
Fe_2O_3	10.3	8.1
K_2O	0.32	3.8
Na_2O	0.43	0.73
Al_2O_3	0.40	0.60
Cr_2O_3	0.28	0.55
MnO	0.15	0.29
P_2O_5	0.03	0.25
Cl	0.10	0.21
NiO	0.31	0.20
SO_3	0.06	0.06
Others	0.12	0.31
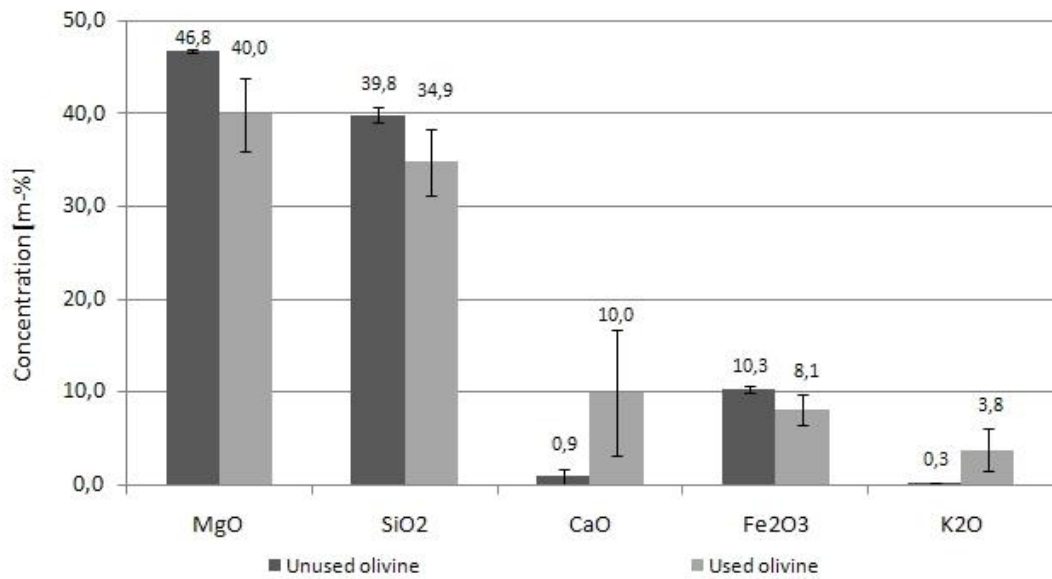
Figure 9: XRF analysis – comparison of unused and used olivine

Table 8: XRD results of unused and used olivine

		Unused Olivine Sample A	Used Olivine Sample B	Comparison unused olivine vs. used olivine
Forsterite	Mg_2SiO_4	S	S	Sample A>> sample B
Bredigite	$Ca_{14}Mg_2(SiO_4)_8$	n/a	S-M	New phase in sample B
Periclase	MgO	n/a	M	New phase in sample B
Larnite	Ca_2SiO_4	n/a	M	New phase in sample B
"Pyrophyllite 1A (dehydroxylated)"	$Al_2Si_4O_{10}(OH)_2$	n/a	TR-M	New phase in sample B
Magnetite	Fe_3O_4	M	TR-M	Sample A > sample B
Fayalite	Fe_2SiO_4	n/a	TR-W	New phase in sample B
Gehlenite	$Ca_2Al(AlSi)O_7$	n/a	TR	New phase in sample B
Lazulite	$(Mg, Fe) Al_2(PO_4)_2(OH)_2$	W	n/a	Phase vanishes in sample B

S, Strong diffraction; M, medium; W, weak; TR, trace; n/a, not applicable

These results are confirmed by the XRD analysis shown in Table 8. While unused olivine has forsterite (Mg_2SiO_4) as a dominant component and calcium silicates such as bredigite ($Ca_{14}Mg_2(SiO_4)_8$), larnite (Ca_2SiO_4) or gehlenite ($Ca_2Al(AlSi)O_7$) are not detectable. The absence of iron silicate is caused by the calcination at 1400°C of the olivine before it is delivered and used in the plant. A calcination of olivine at this temperature leads to a decomposition of the iron silicates [71]. The XRD analyses of the used olivine showed significant amounts of calcium silicates such as bredigite and larnite. Periclase (MgO) and fayalite (Fe_2SiO_4) are detectable in the sample of used bed material.

An SEM image of unused olivine is shown in Figure 10. The image shows a particle with cavities and inclusions with different composition as expected from a natural mineral. However, the particle shows the same composition inside and on the surface. EDX analyses from inside the particle are shown in Table 9. The particle consists mainly of the elements magnesium, silicon, iron and oxygen.

An image of the used olivine (Figure 11) shows the formation of a layer on the surface of the particle. By more detailed analysis (Figure 12), two layers can be determined. The inner layer (1) seems to be more homogeneous than the outer layer (2). This kind of formation of layers could be seen on the majority of particles. Particles with a circular shape like the particle shown in Figure 11 have distinctive layer formation, while particles with a less pronounced circular shape show a less distinctive layer formation. This is caused by the different retention time of the particles in the bed due to a constant feeding of fresh olivine to compensate for bed material losses because of abrasion and loss with the fly ash.
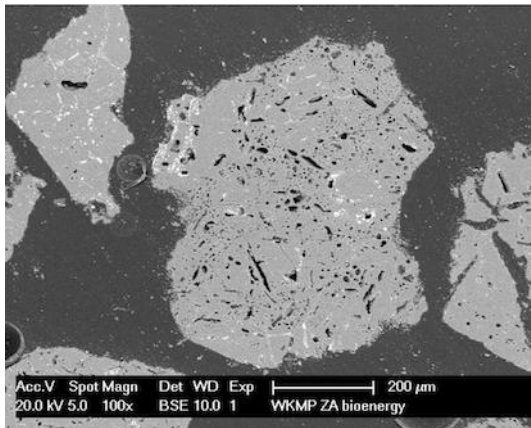
Figure 10. SEM image of unused olivine
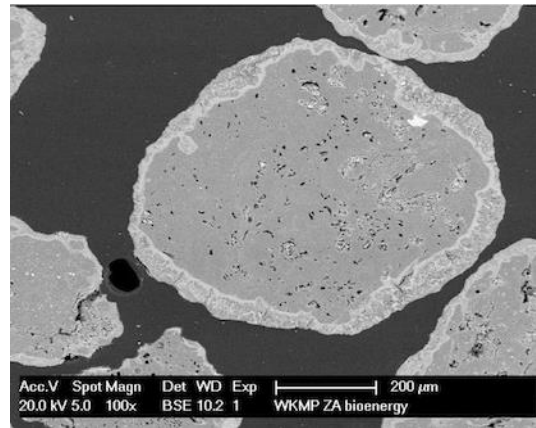
Figure 11. SEM image of used olivine
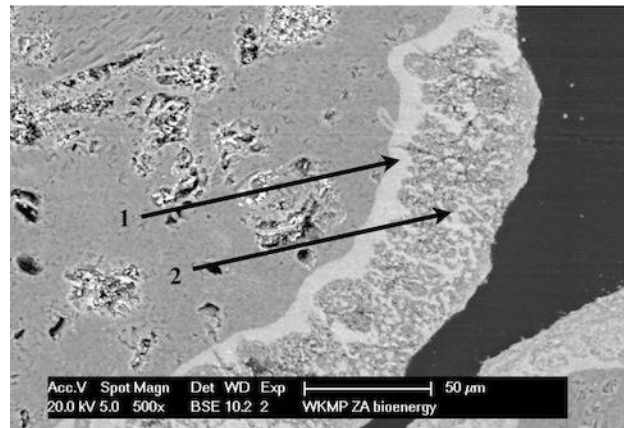
Figure 12. SEM image of inner and outer layer of used olivine.
(1) - inner layer, (2) - outer layer

The EDX analyses of the two layers shown in Table 8 indicate a high concentration of calcium in the inner layer (1) with the two main components of silicon and oxygen. The concentration of magnesium and iron is decreased compared to the unused particle. The composition of the outer layer (2) is dominated by the main components of ash such as calcium, magnesium, silicon and oxygen.

Table 9: Comparison of EDX micrograph examinations of fresh and used olivine

Olivine	Unused olivine particle inside wt.-%	Used olivine particle inside wt.-%	Used olivine inner layer wt.-%	Used olivine outer layer wt.-%
C	n/a	n/a	5.3	9.8
O	15.2	14.2	12.9	13.7
Mg	37.4	30.3	8.6	18.5
Al	0.1	0.7	0.1	0.1
Si	35.5	32.2	17.3	15.4
P	n/a	0.0	n/a	0.3
K	n/a	8.5	2.6	3.2
Ca	n/a	1.8	46.5	33.5
Cr	n/a	n/a	2.7	0.4
Mn	n/a	0.0	0.9	1.2
Fe	11.8	12.5	3.0	3.7

n/a … not applicable

The inside of the used olivine particles (Table 9) shows an increase in potassium and a slight increase in calcium while the concentrations of other elements such as magnesium, silicon and iron remain in the range of unused olivine.

A picture of the surface of one particle is shown in Figure 13. A non-porous surface can be seen, with small dimples as the suggested origin of abrasion in the fluidized bed or elsewhere in the plant. A more detailed picture of the surface is shown in Figure 14, revealing small cracks in the surface, which is mainly smooth.
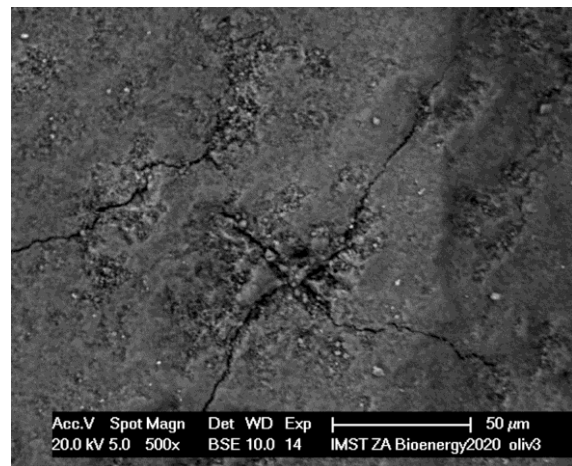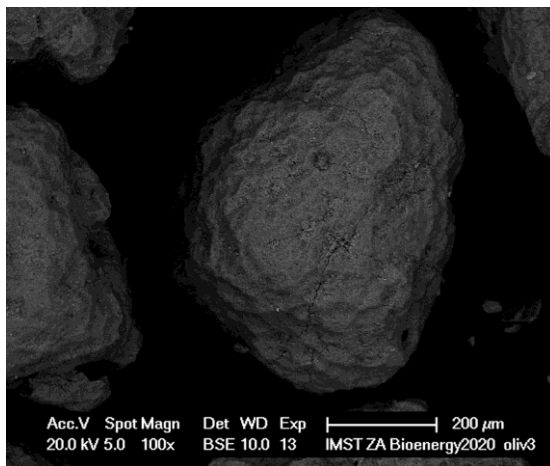
Figure 13: REM picture of a used olivine particle (surface)

Figure 14: REM picture of used olivine – surface detail

A comparison of the elemental composition of the surface of the particle is shown in Figure 15. Both the outer layer and also the analysis of the surface showed that calcium had the highest concentration, followed by magnesium and silicon. The concentration of silicon is lower at the

surface of the particle than in the outer layer, while the concentrations of potassium and phosphor are higher. The other elements are in the same range in both pictures. In general the composition on the surface of the particle is similar to that in the outer layer in the micrograph.
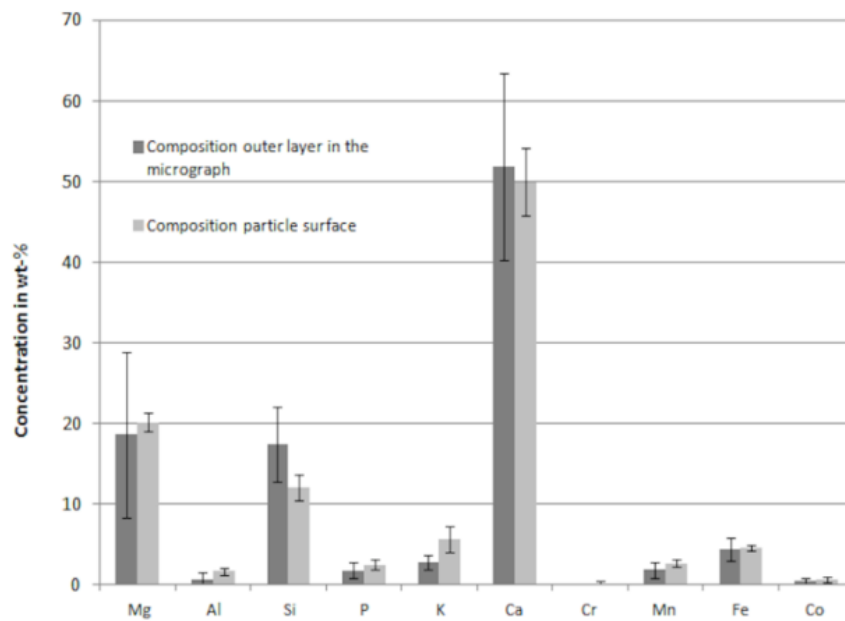
Figure 15: Comparison of the elemental composition shown in the micrograph and the surface (C- and O-free basis)

An analysis of the surface of the particle at different gas atmospheres simulating the atmospheres in the gasifier and the combustion reactor is shown in Figure 16. No significant change in the composition of the surface between the reference case and the treatment under gasification conditions and combustion conditions can be observed. Gasification conditions showed slight increases in iron, chrome, and nickel, which are considered to come from the stainless steel reactor walls of the test rig. The composition of the stainless steel wall is removed in the fourth column of Figure 16 by calculation and shows a similar composition compared to the reference case and the combustion atmosphere.
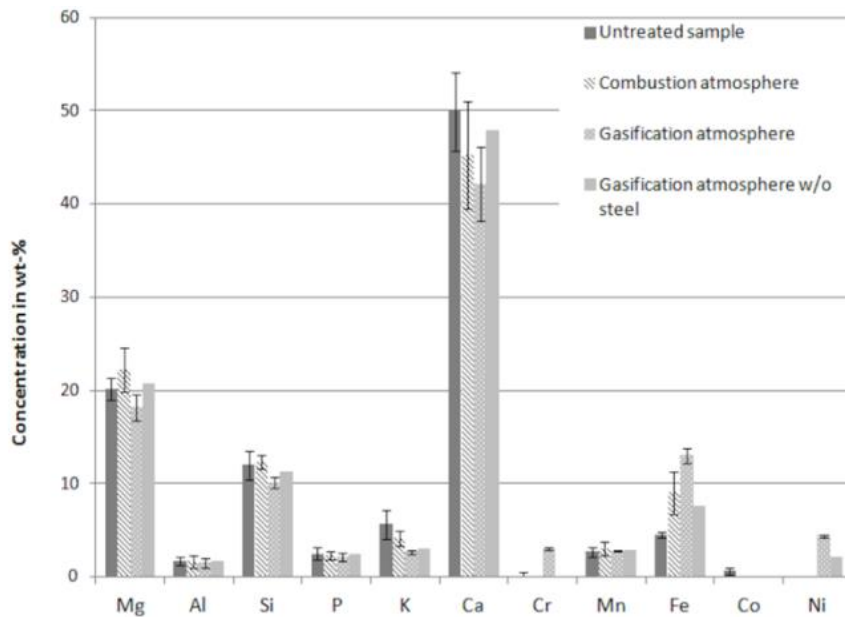
Figure 16: Elemental composition of the particle surface under different atmospheres (C- and O-free basis)

The examination of the crystal structure by XRD analysis under gasification and combustion conditions is shown in Figure 17. The main crystal structure is forsterite, which is the main component of olivine; periclase, calcium silicates such as larnite, and iron oxides such as magnetite and hematite could be detected. Small amounts of potassium silicates were also detectable.

A comparison of the samples under gasification conditions and combustion conditions showed an increase of monticellite, which is a calcium-magnesium silicate, in the combustion atmosphere. Larnite could be detected in a slightly higher amount under combustion conditions compared to gasification conditions. The amount of magnetite decreased under combustion conditions compared to gasification conditions. A slightly weaker signal of forsterite could be detected under combustion conditions.

Figure 17: Crystal structures under different gas atmospheres

Figure 18 and Figure 19 show a comparison of the thermal behavior (TGA) of fresh and used olivine particles, respectively, in different atmospheres.

A TGA shows moderate weight losses for fresh, unused olivine in all atmospheres at different temperatures (Figure 18). The only exemption is air, where an increase in weight can be seen at temperatures higher than 900 °C. The weight loss is around 0.05% up to 0.1 % of the total mass. The DSC signals shows a plateau between 250 and 450 °C with an endothermic weight loss and a change of thermal properties over the whole temperature range but no characteristic peak with a weight loss at temperatures above 450 °C.
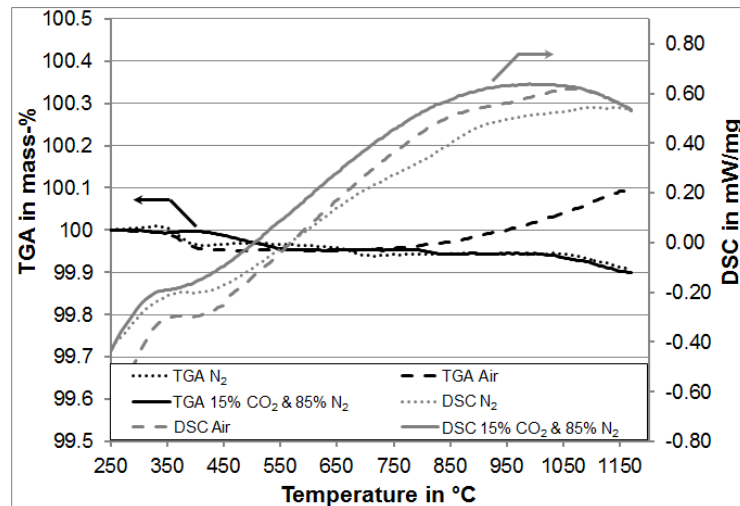
Figure 18: Thermal analysis of fresh, unused olivine in different atmospheres
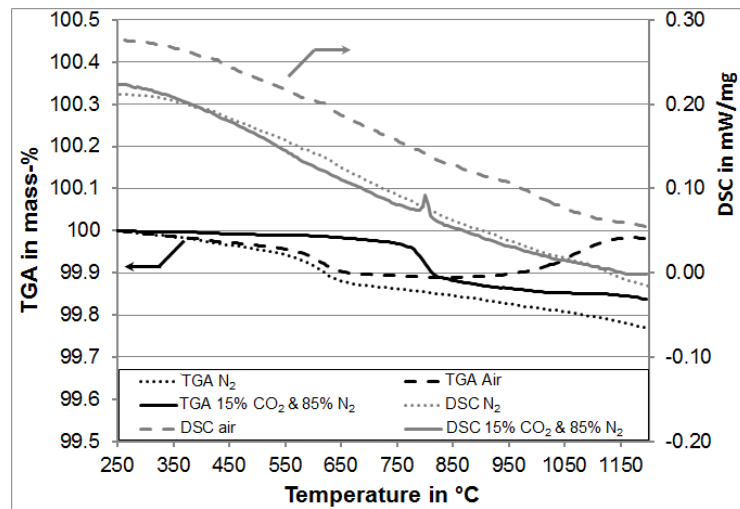
Figure 19: Thermal analysis of used olivine in different atmospheres

Used olivine shows weight losses of around 0.1% (up to 0.2 %) of the mass in the TGA (Figure 19). In nitrogen and air atmosphere, the weight loss occurs at temperatures of around 550 to 600 °C. In a mixture of 15% carbon dioxide and 85% nitrogen by volume a weight loss can be seen at around 800 °C. In a carbon-dioxide-rich atmosphere, the DSC signals only indicate a significant endothermic peak at 800 °C, where the weight loss occurs. At higher temperature (> 850 °C) a slight decrease in mass can be observed which amounts about 0.2 % above 2100 °C.

In an air atmosphere, both the fresh and the used olivine showed significant increases in weight at temperatures higher than 850 °C.

4.2 Investigations in streams of inorganic matter

For better understanding of high temperature reactions of inorganic matter different methods were applied to investigate streams of inorganic matter to understand their behavior at high temperatures. The elemental composition was determined and thermal analyses in different atmospheres were carried out.

4.2.1 Sampling and analyses of streams of inorganic matter

Wood samples were taken during regular production and analyzed for ash content and their elemental composition. To obtain representative values, the samples were taken according to CEN/TS 14780:2005 from the wood chips pile. Samples were taken on two different days and ash was produced according to DIN CEN/TS 14775 to determine the ash content. The remaining ash was analyzed using XRF analysis.

Samples of fouling were taken during stops after cooling down the plant. Fly ash samples (ash exiting the plant into the container, fly ash circulation, bed material circulation) were sieved with a

vibratory sieve with 200 μm mesh size. The fraction smaller than 200 μm is defined as fine ash; the other fraction is defined as coarse ash.

The elemental composition was determined using X-ray fluorescence method and thermal analyses (TGA, DSC) were carried out as described in chapter 4.1.1.

Table 10. Sampling points and flow determination; sampling point numbers are according to Figure 5

Sample type	Sampling point #	Description	Determination of flow
Input flow	1	Biomass ash	Mass flow of biomass, ash content
Input flow	2	Bed material	Level measurement DCS
Input flow	3	Precoat material	Weight measurement DCS
Internal flow	4	Fly char	Weight measurement DCS/calculated after rebuild
Internal flow	5	Fly ash circulation	Manual weight determination
Internal flow	6	Bed material circulation	Manual weight determination
Output flow	7	Ash to container	Manual weight determination

The sampling points are shown in Figure 5 and described in Table 10. Mass flows that were not measured via the distributed control system (DCS) of the plant were measured manually and typically three measurements were carried out over a period of 30 minutes.

4.2.2 Results of investigations in streams of inorganic matter

The composition of the biomass ash has a significant influence on fouling, slagging, and bed material agglomeration tendencies in the plant because it is the only source of components with low melting points. The quality of the biomass is constantly determined by the operational personnel only in terms of water content but not ash content, bark content, or wood type. Table 11 shows the average biomass ash compositions and their standard deviations from samples taken in the years 2010 and 2011 from the present study. The main component of the biomass ash is calcium oxide, which represents about half of the weight, followed by silicon oxide and potassium oxide. Magnesium oxide, phosphorus oxide, aluminum oxide, and sodium oxide are detectable in the low percentage range. The composition of the biomass ash is typical for hardwood ash as shown in literature [94]. The values of the standard deviation indicate a wide variation in biomass quality.

Precoat material is used for precoating the product gas filter and is added to the system. The precoat material described in Table 12 shows a typical composition of the natural mineral dolomite, whose main components are calcium and magnesium oxide, with a high ignition loss at 1050 °C, where the carbonates are released. Other elements are available in the low percentage range, such as sodium oxide, silicon oxide, and aluminum oxide.

Table 11: Results of XRF for the average composition of biomass ash

| Component | Wood chip ash | |
	Average	Standard deviation
	wt.%	*wt.%*
Na_2O	2.77	2.66
MgO	5.13	0.45
Al_2O_3	2.57	1.10
SiO_2	15.36	7.52
P_2O_5	2.36	0.24
SO_3	1.26	0.51
K_2O	12.40	2.75
CaO	52.47	6.16
MnO	1.67	0.43
Fe_2O_3	1.73	0.66
Cl	0.42	0.36
Others	1.86	
Ash content (ds)	1.42	0.10

Table 12: Typical composition of the precoat material dolomite

Component	Precoat material
	wt.%
Na_2O	2.32
MgO	32.01
Al_2O_3	1.36
SiO_2	1.48
P_2O_5	0.38
SO_3	0.44
K_2O	0.87
CaO	59.87
Fe_2O_3	0.63
Cl	0.30
Others	0.35
Loss on ignition 600 °C, 1 h	2.77%
Loss on ignition 1050 °C, 1 h	44.66%

4.2.2.1 Results of fly ash analyses

An overview of the composition of the fine ash (particles < 200 µm) and coarse ash (particles > 200 µm) which leave the process and enter the ash container is shown in Table 13. Coarse ash consists of the main components of olivine, such as magnesium oxide, silicon oxide, and iron oxide, but also significant contents of calcium oxide (nearly 12 wt.%) and potassium oxide (nearly 4 wt.%), which originate from biomass ash. Fine ash mainly consists of calcium oxide, silicon oxide, magnesium oxide, and also potassium oxide. A high content of iron oxide is available and other elements were detected such as sodium oxide, phosphorus oxide, and aluminum oxide. Important for the fouling tendency is the amount of potassium oxide, which is present in the fine ash, where it represents around 7 wt.%, and in the coarse ash, where it represents only 4 wt.%. Standard deviations indicate high variations of the composition of the fly ash for both, the fine ash fraction and the coarse ash fraction.

Table 13: Typical composition of the fly ash entering the container

Component	Fine ash Average values	Standard deviation	Coarse ash Average values	Standard deviation
	wt.%	*wt.%*	*wt.%*	*wt.%*
Na_2O	1.19	1.00	1.20	0.92
MgO	19.67	2.06	37.27	2.61
Al_2O_3	1.52	0.90	0.52	0.21
SiO_2	20.28	8.97	35.70	4.00
P_2O_5	1.22	0.16	0.34	0.05
SO_3	0.39	0.22	0.08	0.03
K_2O	6.97	1.62	3.81	1.16
CaO	42.45	11.08	11.70	3.96
Fe_2O_3	4.08	1.60	8.01	0.58
Cl	0.26	0.17	0.19	0.13
Others	1.97		1.18	
Loss on ignition 600 °C, 1 h	4.94%		0.56%	
Loss on ignition 1050 °C, 1 h	6.81%		1.05%	

The thermal behavior of the fine fraction of fly ash in different atmospheres (air, N_2, CO_2 and N_2) using a TGA is shown in Figure 20. Two main peaks can be seen up to 1200 °C. At temperatures lower than 100 °C, small changes in weight are detectable. A weight loss with an endothermic signal in the DSC at around 400 °C and a significant endothermic weight loss at temperatures of around 720 °C to 820 °C are detectable. The results in air and nitrogen are similar; a different behavior can be seen in the mixture of nitrogen with 15% CO_2. In a CO_2-rich atmosphere, an endothermic weight loss at 400 °C is not present anymore but an increase in weight can be seen at temperatures higher than 400 °C with a strong endothermic peak at 820 °C.
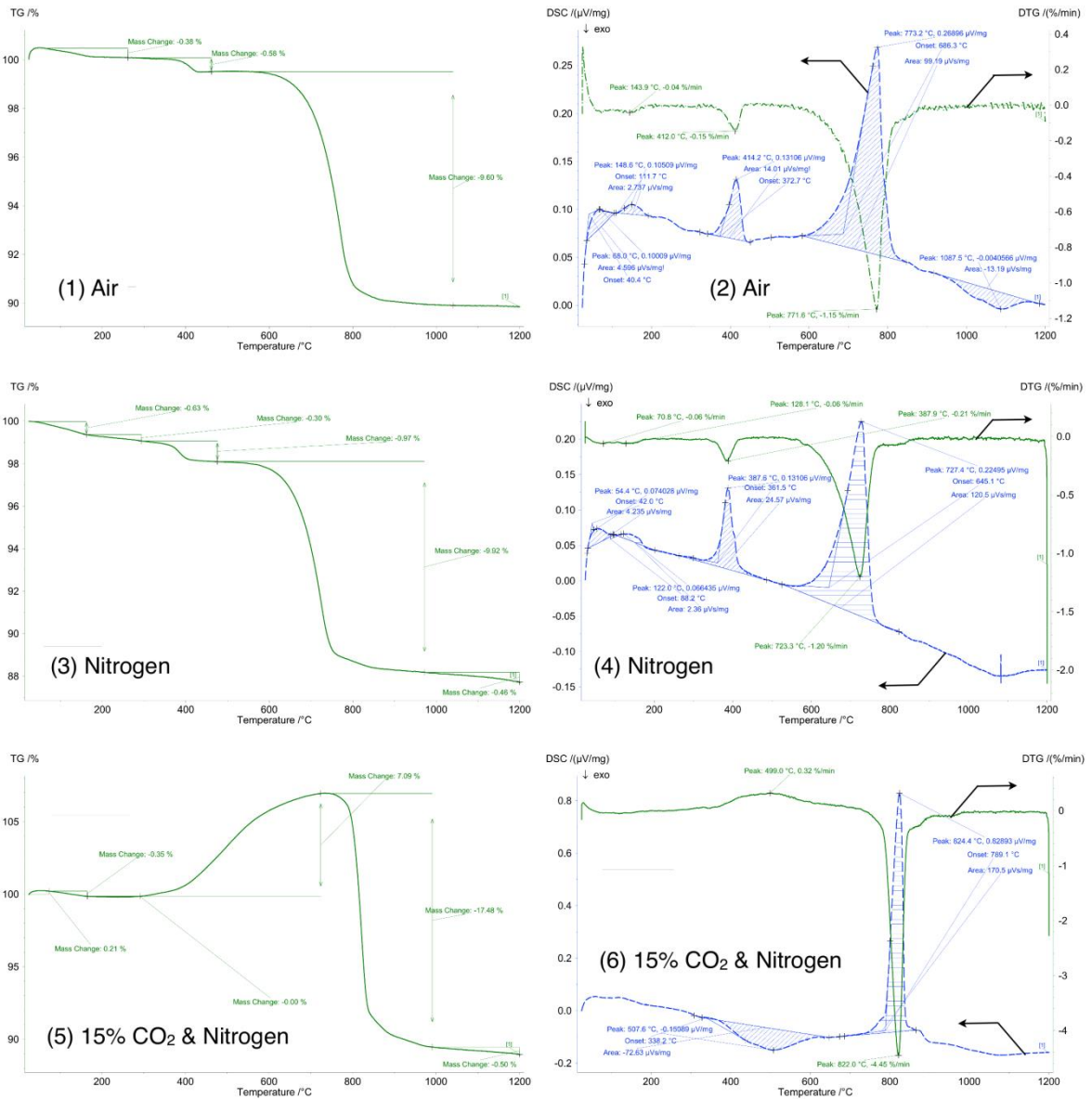
Figure 20: Thermal analysis of fly ash with particle size < 200 μm in different atmospheres

The weight loss at temperatures around 100 °C is considered to be caused by the evaporation of water. An endothermic peak with weight loss at around 400 °C which is not seen in the CO_2-rich atmosphere is considered to be due to the calcination of magnesium carbonate. In the CO_2-rich atmosphere this is interfered by the adsorption of CO_2 on calcium oxide, which can be seen from the increase in weight. Decomposition of calcium hydroxide is not considered at temperatures around 400 °C because it is expected at temperatures around 550 °C. Combustion and decomposition of organic matter (unburned wood) are not assumed to happen because a peak can also be seen in the nitrogen atmosphere.
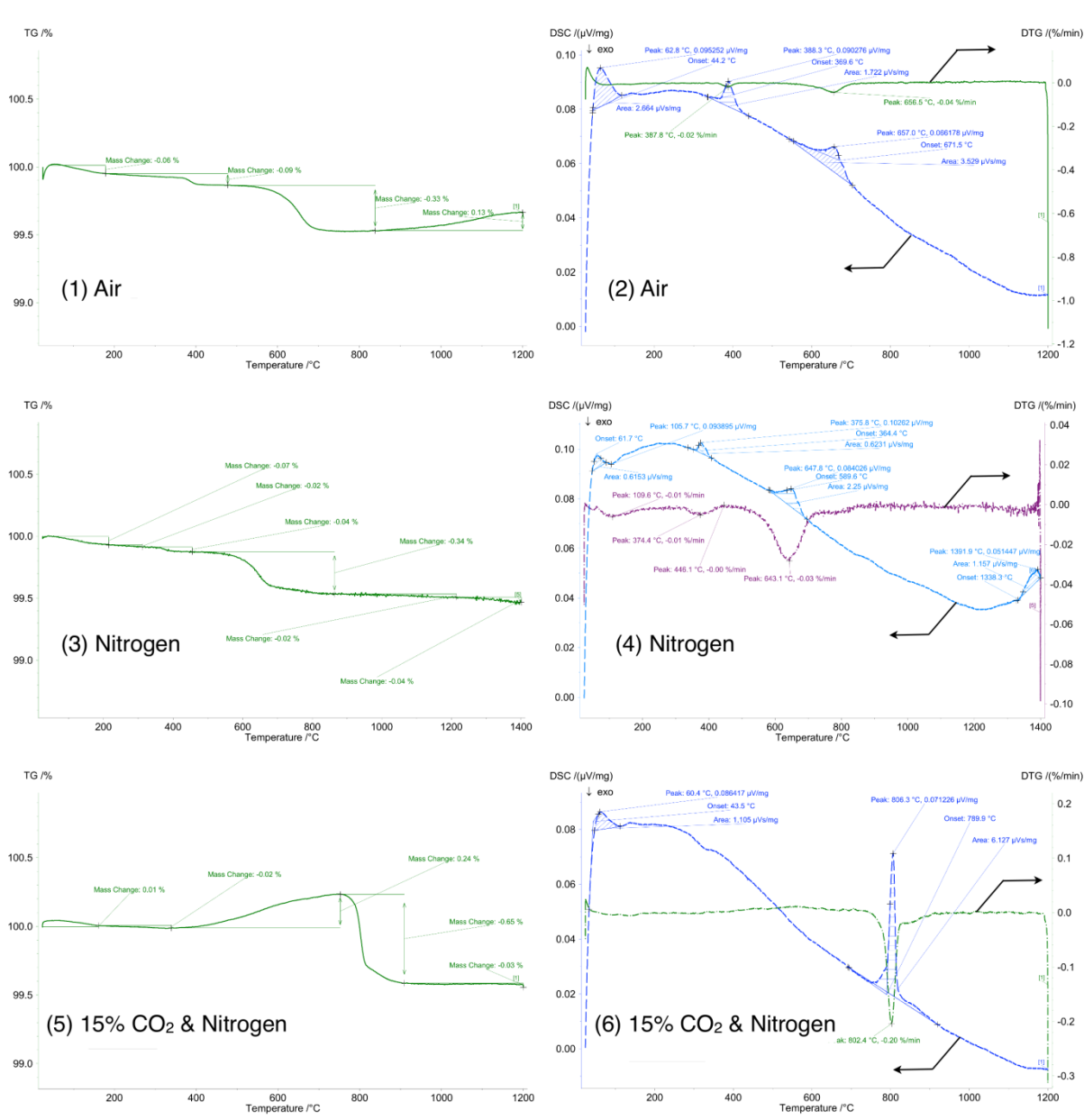
Figure 21: Thermal analysis of fly ash with particle size > 200 μm in different atmospheres

The thermal analysis of the coarse ash fraction of the fly ash shows a behavior similar to those of the fine ash but less pronounced (Figure 21). In contrast to the fine ash, an increase in weight can be seen at temperatures higher than 900 °C. The weight loss of the fine ash fraction is around 10% while that of the coarse ash fraction is only around 0.5%.

Coarse fly ash is considered to consist mainly of bed material, which is confirmed by the iron content which is the same concentration as in olivine. An increase in weight in the thermal analysis at temperatures higher than 900 °C might be caused by the oxidation of magnetite [64] or by the decomposition of fayalite with the oxidation of iron.

4.2.2.2 Results of fly char analyses

The investigations of the properties of the fly char include an analysis similar as for fuels because of the high carbon content of the char. The fuel analysis is shown in Table 14 and reveals that the fly char consists mainly of ash (73%) and carbon (26%). The heating value justifies the utilization of the fly char as a fuel in the combustion reactor. The elemental analysis shown in Table 15 reveals the highest concentrations of substances as calcium oxide, magnesium oxide, silicon oxide potassium oxide, and iron oxide.

Table 14: Analysis of the fly char before modification of the ash loops

		Dry base	Raw
Water content	wt.%	–	0.91
Carbon content	wt.%	26.14	25.9
Hydrogen content	wt.%	0.48	0.48
Nitrogen content	wt.%	0.06	0.06
Ash content (db)	wt.%	73.32	
Upper heating value	kJ/kg	8301	8225
Lower heating value	kJ/kg	8196	8097

Table 15: Elemental analysis of inorganic matter of fly char (sample date 2010)

Component	Mean value	Standard deviation
	wt.%	
Na_2O	1.94	1.36
MgO	25.02	2.83
Al_2O_3	2.38	0.63
SiO_2	22.13	2.17
P_2O_5	1.18	0.22
SO_3	0.38	0.26
K_2O	6.09	0.94
CaO	33.11	5.95
Fe_2O_3	5.24	0.19
Cl	0.52	n/a
Others	2.0	
Loss on ignition 1050 °C, 1 h	36%	

Figure 22: Thermal analysis of fly char in different atmospheres

The thermal analysis of fly char in different gas atmospheres (Figure 22) shows two significant endothermic peaks in air and nitrogen atmosphere at around 417 °C and around 730 °C. A low weight loss can be detected at temperatures up to 100 °C. In a mixture of 15% CO_2 in nitrogen an exothermic peak can be seen at temperatures around 412 °C and a complex endothermic weight loss can be seen at temperatures between 795 °C and 880 °C.

The thermal analysis of the fly char showed combustion in air (exothermic peak) at 400 °C. In nitrogen atmosphere an endothermic weight loss can be seen at around 400 °C which is considered to be due to the decomposition of magnesium carbonate. The low amount of oxygen in the char excludes the pyrolysis of organic matter which could be also expected at this temperature. The endothermic weight loss at around 730 °C in air and nitrogen atmosphere is considered to be caused

by the decomposition of calcium carbonate and dolomite [95]. This reaction interferes in the CO_2-rich atmosphere with the CO_2-gasification of carbon with the peak at 880 °C.

4.3 Investigations in deposits

Various samples of fouling at two different locations were analyzed. Fouling at the air preheater occur regularly, fouling in the cyclone randomly. Fouling can randomly be seen also on other locations such as combustion reactor, product gas cooler and siphon walls but due to a lack of occurrence detailed scientific examinations could not be carried out.

4.3.1 Sampling and analyses of deposits

Deposits can be seen at different locations in the plant (Table 16). Multiple samples of fouling were taken at the first heat exchanger (air preheater) of the flue gas after the combustion reactor. Two different representative samples with different textures are presented as an example in this study.

Various samples of fouling in the cyclone were taken and representative results are presented here. Due to the different appearance of the whole piece of the fouling (see Figure 23), three different parts were analyzed: sample A was located at the surface of the fouling, sample B is material taken 3–4 mm below the surface, sample C was taken from the inner layer of the fouling close to the refractory lining.

Table 16. Sampling points and flow determination; sampling point numbers are according to Figure 5

Sample type	Sampling point #	Description	Description
Deposits	8	Cyclone	Deposits at cyclone walls located close to the cyclone inlet and the gas outlet tube
Deposits	9	Air preheater entry	Deposits at the top plate of a tube in tube heat exchanger
Deposits	10	Product gas cooler	Deposits at the top plate of a tube in tube heat exchanger (no analysis presented)

4.3.2 Results of investigations in deposits

Results of analyses from deposits which occur frequently are presented in this chapter. Fouling at air preheater can be determined in average once a month. Fouling in cyclone happens randomly but affects the operation due to worse separation of bed material.

4.3.2.1 Results from analyses of fouling at air preheater

The nature of fouling at the air preheater is not always the same but varies. A typical picture of the fouling is shown in Figure 23. The texture of the fouling varies from powder debris to hard and rocky material which is difficult to remove. Soft and hard layers can be observed within one position

but also at different locations. Due to the need for high availability of the plant, the inspection intervals for the heat exchanger are around four weeks and an exact determination of the formation of the fouling is not possible. The results of analyses of two different samples with different textures are shown in Table 17. Fouling that disaggregates easily to a powder (right column in Table 17) has calcium oxide as its main component, accounting for nearly half of the mass of the sample. Magnesium and silicon oxide are detectable in about the same amount. The hard and rocky fouling (left column in Table 17) shows a higher magnesium oxide concentration and lower calcium oxide and silicon oxide concentrations. Potassium oxide is significantly more highly concentrated in the hard fouling, where it represents around 9 wt.%, compared to 3.4 wt.% in soft fouling.

Figure 23: Fouling at the air preheater – view from the top at the tube sheet on the flue gas side

Table 17: Elemental analysis of fouling at the air preheater

Sample date	10.03.10	09.07.10
Description	Hard fouling at air preheater – untreated	Fouling at air preheater that disaggregates easily
Component	wt.%	wt.%
Na_2O	1.17	1.22
MgO	25.89	18.37
Al_2O_3	1.28	2.31
SiO_2	16.72	18.91
P_2O_5	1.68	1.92
SO_3	0.18	0.21
K_2O	9.15	3.40
CaO	36.29	47.81
Fe_2O_3	4.81	4.12
Cl	0.18	0.22
Others	2.67	1.48
Loss on ignition 1050 °C, 1 h	13.94%	3.71%

The thermal analysis of the fouling shown in Figure 24 gave different results compared to coarse ash and fine ash. The TGA shows a more or less constant and significant weight loss of 8 to 10 wt.% up to 1200 °C. The weight loss can be seen over the whole temperature range but increases at temperatures higher than 800 °C, and this is independent from the gaseous atmosphere. The DSC signal shows various endothermic peaks. Significant endothermic weight losses can be determined at around 100 °C, at 509 °C in air (526 °C in nitrogen and 532 °C in CO_2-nitrogen respectively), around 755 to 791 °C depending on the atmosphere, 864 to 978 °C, and above 1000 °C.

The first peak of the thermal analysis of the fouling occurs at temperatures around 100 °C, which is considered to be caused by evaporation of water. A significant peak can be observed at 509–530 °C, which is similar to the temperature at which the recrystallization of K_2O*SiO_2 [96] takes place and similar to the temperature at which α-quartz is modified to β-quartz (573 °C) [97].

A peak at 755–791 °C with a high weight loss in air and nitrogen atmosphere and a moderate weight loss in CO_2-rich atmosphere might be caused by the decomposition of dolomite, calcium carbonate, or spurrite [98-100]. In the CO_2-rich atmosphere this peak can be seen at 791 °C but the peak at 879 °C has a significantly higher weight loss. A high partial pressure of CO_2 can shift the decomposition of carbonates ($CaCO_3$ or spurrite) to higher temperatures. An overlapping of different reactions is suggested, where released CO_2 reacts with another component and is only released at higher temperatures. At temperatures between 864 and 878 °C, a recrystallization of quartz in β-tridymite [101] without weight loss is expected. Arvelakis et al. [99] showed that a mixture of K_2CO_3 and SiO_2 reacts to form potassium silicates at this temperature, leading to a weight loss because of the released carbonates.

In CO₂-rich atmosphere, significant decomposition and melting can be seen (endothermic DSC signal with a weight loss), which agrees with the findings of Arvelakis et al. [99] that at temperatures higher than 1000 °C excessive decomposition and release in the gas phase of potassium rich compounds (KCl, K_2CO_3, K_2SO_4) as KOH are occurring.
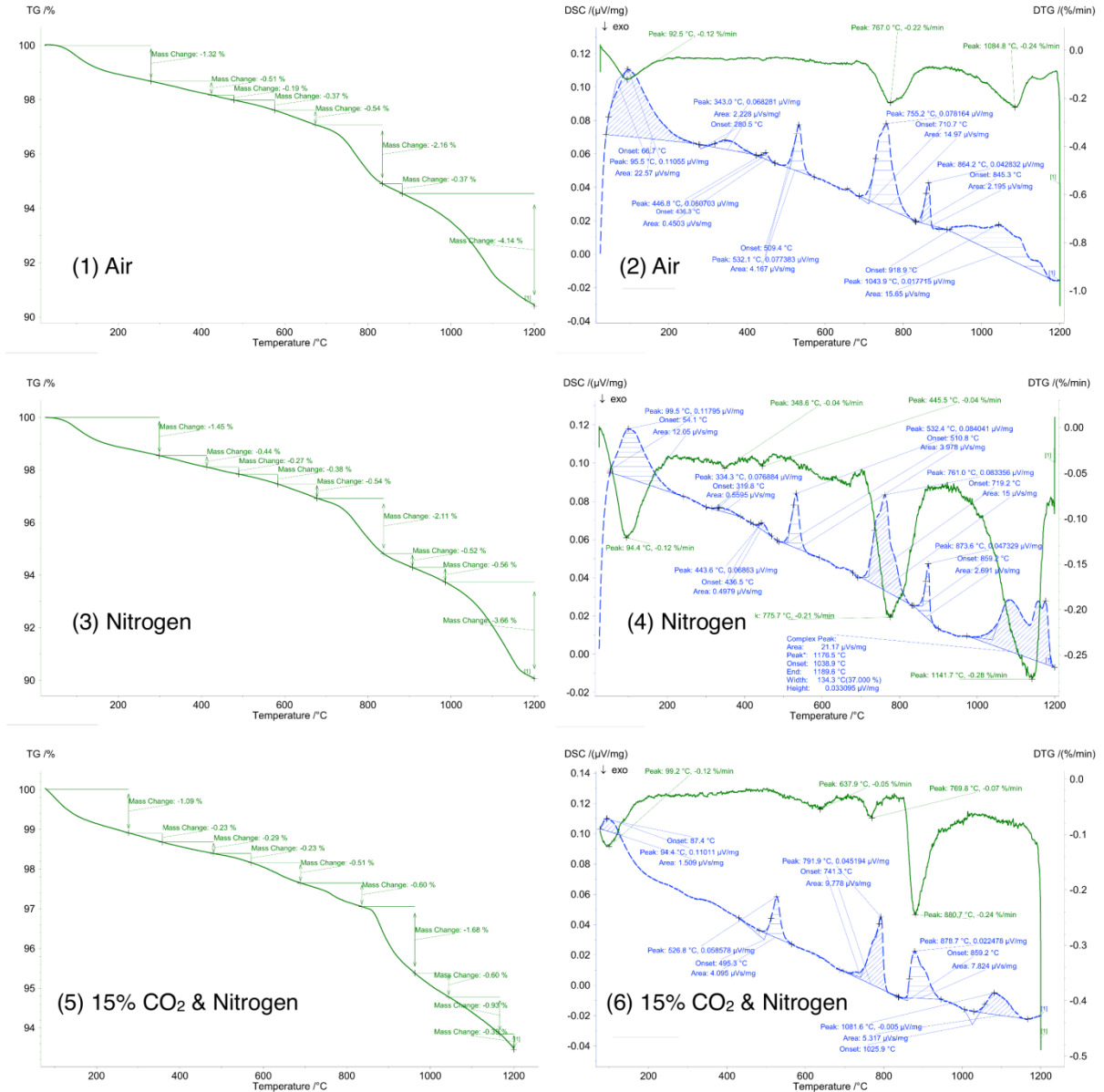
Figure 24: Thermal analyses of fouling at the air preheater in different atmospheres

4.3.2.2 Results from analyses of depositions in the cyclone

A picture of the different samples at the cyclone is shown in Figure 15. The results of the elemental composition of the depositions in the cyclone are shown in Table 18. The elemental analysis confirms the visual impression of the inhomogeneity of the deposits over its thickness. Bed material particles can be visually detected in sample C, which is confirmed by the high iron content of the sample. The amount of potassium in samples A and B, 23.6 and 19.1% respectively, is significantly higher than is expected from the biomass ash. Calcium oxide content is lower in all samples

compared to biomass ash. That means that potassium is enriched in the deposits compared to the fly ash which can be "diluted" by bed material. Due to the fact, that components of fly ash act like a glue between the bed material particles the high concentration in potassium shows that it is causing slagging.
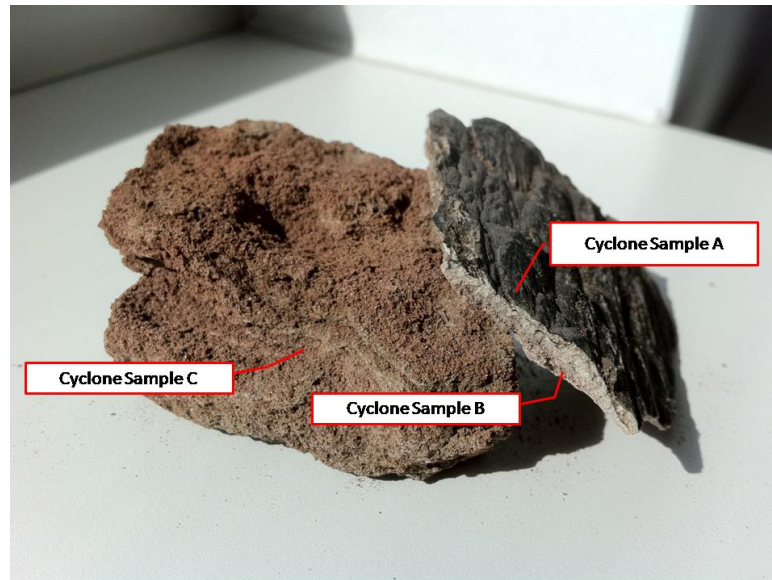
Figure 25. Example of fouling from the cyclone

The cyclone is located directly after the combustion reactor before the post combustion chamber. Due to the fact, that the temperatures in the cyclone are similar to that of the combustion reactor and post combustion chamber these deposits can be defined as slagging.

Table 18: Elemental composition of the fouling in the cyclone (main components)

	Cyclone sample A Total sample *wt.%*	Cyclone sample B Total sample *wt.%*	Cyclone sample C Total sample *wt.%*
Na_2O	0.53	0.35	2.88
MgO	11.09	14.82	28.51
Al_2O_3	1.22	2.51	0.89
SiO_2	25.84	29.34	36.84
P_2O_5	0.75	0.96	0.30
SO_3	0.13	0.03	0.06
K_2O	23.63	19.13	9.98
CaO	33.13	27.88	13.07
Fe_2O_3	2.36	3.42	6.03
Cl	0.08	0.06	0.44
Others	1.26	1.50	1.00

4.4   Pilot plant test runs

The influence of the calcium rich layers at the bed material particles on the gasification performance was known from the experience of the plant in Güssing. Experience also showed that the catalytic properties of the bed material improve with a higher retention time of the bed material in the system. An exact quantification of this occurrence had not been carried out yet.

To quantify the influence of the calcium-rich surface on the catalytic activity of the bed material test runs were carried out under scientific conditions in a 100 kW pilot plant. Unused bed material and used bed material taken from the CHP plant Güssing were investigated by test runs at the pilot plant and the results obtained compared. Another test run was carried out to investigate the influence of the gasification temperature on gasification and tar formation.

4.4.1   Preparation and sampling of the pilot plant test runs

To ensure similar fluidization and gasification conditions with used and with unused bed material, a similar particle size distribution is required for both bed materials. Wood pellets were used as fuel in both test runs in the pilot plant. Wood pellets were chosen because they have better conveying properties in the screw feeder of the pilot plant and because their composition is similar to that of the used fuel in the industrial plant. Only the water content of the pellets (6.74%) is significantly lower than the water content of the wood chips used in the plant in Güssing.

Gas and tar analysis of the product gas of the pilot plant is well-described in the literature [41,91,92,102]. Carbon monoxide, carbon dioxide, methane and hydrogen were measured by a Rosemount NGA2000. The product gas components nitrogen, ethylene, ethane, and propane were measured by a gas chromatograph (Syntech Spectras GC 955). For the calculation of average values a stationary operation period of the plant was taken into consideration. Tars are absorbed in toluene and analyzed similarly to the tar protocol. Detailed descriptions of the tar measurement are given by Wolfesberger et al. [90] and Aigner et al. [103]. Gravimetric tars represent the heavy tars while GCMS tars represent the smaller tar molecules. As the measurement ranges of both tar analyses overlap, they cannot be added. Three samples of tar were taken during each test run and mean values were calculated.

The GCMS tars were classified into substance groups according to Wolfesberger et al. [90], shown in Table 19.

Table 19: Tar substance groups

Substance group	Component
Phenols	phenol, 2-methylphenol, 4-methylphenol, 2,6-dimethylphenol, 2,5 and 2,4-dimethylphenol, 3,5-dimethylphenol, 2,3-dimethylphenol, 3,4-dimethylphenol, 2-methoxy-4-methylphenol, 1,2-dihydroxybenzene
Furans	1-benzofuran, 2-methylbenzofuran, dibenzofuran
Aromatic compounds	phenylacetylene, styrene, mesitylene, 1H-indene, 1-indanone,
Aromatic nitrogen compounds	isoquinoline, indole, carbazole, quinoline
Naphthalenes	naphthalene, 2-methylnaphthalene, 1-methylnaphthalene
PAH	biphenyl, acenaphthylene, acenaphthene, flourene, anthracene, phenanthrene, 4,5-methylphenanthrene, 9-methylanthracene, flouranthene, pyrene, benz[a]anthracene, chrysene, benz[b]flouranthene, benz[k]flouranthene, benz[a]pyrene, benz[g,h,i]perylene, indeno[1,2,3-cd]pyrene, dibenz[a,h]anthracene
Guaiacols	eugenol, isoeugenol
Thiophenes	1-benzothiophen, dibenzothiophen
Phthalates	dimethylphthalate, diethylphthalate, butylbenzylphthalate

The simulation software IPSEpro was used to calculate mass and energy balance to determine gas yields. The software and model library is described by Pröll and Hofbauer [104].

4.4.2 Comparison of the performance of fresh and used olivine in the pilot plant

The operational parameters at the pilot plant were chosen to be similar to those of the industrial scale plant in Güssing. Table 20 shows a summary of important operational parameters. The marked values are the measurements of set points. The other values are given by the operating conditions. The chosen gasification temperature for the comparison of the bed materials is 850 °C because experience at the plant in Güssing has shown that this gasification temperature ensures safe operation. A higher steam-to-carbon ratio was required in the pilot plant compared to the plant in Güssing to reach smooth fluidization properties.

	Unit	Reference test run at the pilot plant with fresh olivine	Pilot plant with used bed material from Güssing	Industrial scale plant in Güssing
Gasifier bed temperature	°C	852 ± 2*	850 ± 1*	850*
Riser temperature	°C	897 ± 2	872 ± 1	~930
Fuel input	kW	97*	97*	8 000*
Fuel into the combustion reactor	kg/h	3.23	2.54	–
	kW	38	29	
Total fuel input	kW	135 **	127 **	–
Steam to carbon ratio	– (kg/kg)	1.8*	1.8*	1.2–1.6

* Set points and target values respectively

** Results from mass and energy balance

Table 21 shows the performance parameters of the pilot plant for the test run with fresh olivine and used olivine. The gasification conditions in the gasifier were similar and performance difference is indicated mainly by the oil consumption. To get a good comparison of the efficiency the total gas yield is referred to the total fuel input which consists of fuel to gasifier and fuel to combustion reactor.

Table 21: Performance parameters of the pilot plant (results from mass and energy balance)

	Unit	Reference test run at the pilot plant with fresh olivine	Pilot plant with used bed material from Güssing
Gas yield	Nm³/kg wood (db)	1.06	1.09
Total gas yield	Nm³/kW total fuel input (db)	0.157	0.172

The gas composition of the two test runs in the pilot plant and the industrial scale plant is shown in Figure 26. While the test run with the used olivine in the pilot plant shows similar results compared to the industrial scale plant, the results for fresh bed material in the pilot plant show a significantly higher CO content and significantly lower CO_2 and H_2 contents. The values from the industrial scale plant show a larger deviation compared to the pilot plant due to varying fuel quality (water content) and instability of inorganic flows (e.g. bed material consumption and ash circulation).
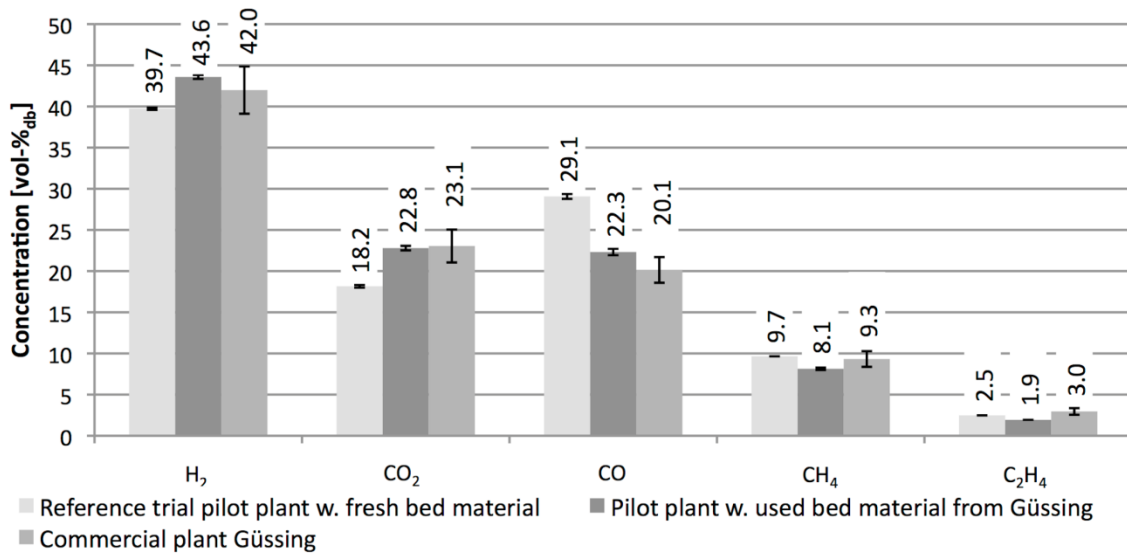
Figure 26: Product gas composition of unused and used bed material at the pilot plant compared with the industrial scale plant

Comparison of the results of the test runs at the pilot plant with fresh, unused and used bed materials reveals an enhancement of the water–gas shift reaction, Equation (1), with used bed material, which leads to higher H_2 and higher CO_2 contents, while the CO content decreases. Additionally, the water–gas shift reaction is slightly exothermal, which explains the lower fuel consumption in the combustion reactor in the test run with the used bed material, as shown in Table 20, considering a similar bed material circulation.

The tar content of the product gas in the pilot plant is shown in Figure 27. It indicates that substantially lower tar content was found with the used olivine from the plant in Güssing independently of the method of analysis. The GCMS measured tars decreased by 82% and the gravimetric tars decreased by 65%.
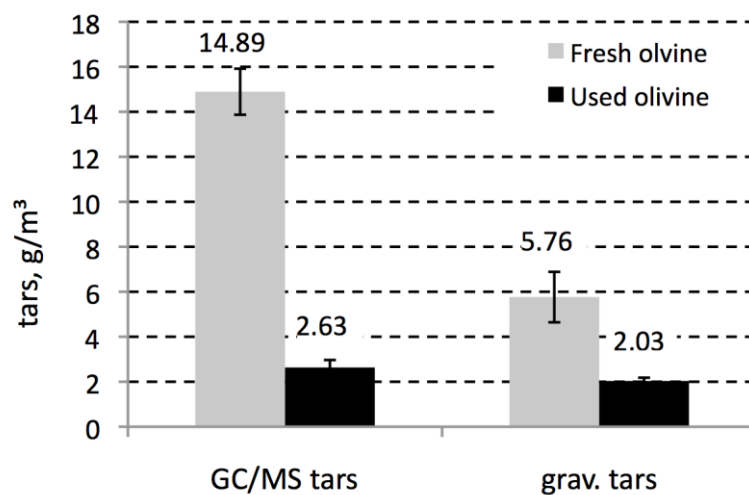
Figure 27: Tar contents with fresh, unused and used olivine in the pilot plant

The comparison of the gas composition from the industrial plant in Güssing and the test run with used bed material from Güssing presented in Figure 26 shows very similar gas compositions of the pilot plant and the industrial scale plant with the same bed material. Also, the results of tar analyses of the test run with the used olivine are in the range of published values of the plant in Güssing. Rauch et al. published values of around 1–2 g/Nm³, assuming that the only reason for the tar reduction was the calcination of the olivine [71]. Results from the plant in Güssing published recently by Aigner indicate GCMS tar values of around 2 g/Nm³ and gravimetric tars values of around 1.8 g/Nm³ for wood as a fuel [105].

As shown with these results, the performance of the pilot plant can be easily transferred to the industrial scale plant. A good scale-up of the 100 kW pilot plant to industrial scale plants in terms of gas quality seems to be possible when the long term interaction of ash and additives with the bed material is considered.

4.4.3 Variation of the gasification temperature in the pilot plant

The operational parameters at the pilot plant, except those of the gasification temperature, were chosen to be similar to those of the industrial scale plant in Güssing. Table 22 shows a summary of the most important operational parameters at different temperatures. The marked values are set points while the other values given were measured. The temperature range was chosen between 750 °C and 870 °C. The upper limit of the gasification temperature was chosen to be slightly higher than the regular operational temperature of the industrial scale plants which is 850 °C. The lower limit was considered to be governed by the setup and fluidization properties of the pilot plant. The fuel input into the gasifier was kept constant for each temperature. The fuel input into the combustion reactor decreased from 3.1 kg/h light fuel oil at 870 °C to 0.1 kg/h at 750 °C gasification temperature. The steam to carbon ratio was kept constant for all test runs.

Table 23 shows gas yields and calorific values for the product gas from the pilot plant for the test runs between 750 °C and 870 °C. The specific gas yield, which is the volume flow of product gas related to the wood pellets input, is reduced from 1.18 Nm³ (db) per kg of pellets at 870 °C to 0.75 Nm³ per kg of pellets at 750 °C. This is due to the decrease of reaction rates which leads to lower gas yields at same residence times. At the same time more char is transported to the combustion reactor that reduces the light oil demand (Table 22). The total gas yield which is the volume flow of product gas related to the energy of the total fuel input (pellets to gasifier plus fuel to combustion reactor), is reduced when the temperature is reduced. An increase of the lower calorific value of the product gas can be seen with decreased gasification temperature.

Table 22: Operational parameters during temperature variation

	Unit					
Target gasification temperature*	°C	**870**	**830**	**800**	**780**	**750**
Measured gasifier bed temperature	°C	869±4	835±6	803±5	784±3	751±3
Temperature of the combustion reactor	°C	905±4	862±4	832±5	811±3	776±2
Fuel input*	kW	97	97	97	97	97
Fuel into the combustion reactor	kg/h kW	3.1 36	1.9 22	1.4 17	0.5 5	0.1 1
Total fuel input**	kW	133	119	114	103	98
Steam to carbon ratio*	– (kg/kg)			1.6		

* Set points and target values respectively

** Results from mass and energy balance

Table 23: Gas yields and calorific values (results from mass and energy balance)

Gasification temperature	°C	870	830	800	780	750
Specific gas yield	Nm³/kg pellets	1.18	1.00	0.94	0.80	0.75
Total gas yield	Nm³/kW total fuel	0.178	0.170	0.166	0.155	0.153
Lower calorific value of the product gas	MJ/Nm³	12.22	12.37	12.40	12.76	12.64

Considering the main components of the product gas, shown in Figure 28, the trend is linear. The trends show reducing contents of hydrogen and carbon monoxide in the product gas with decreasing gasification temperatures. In contrast, the content of carbon dioxide and methane increases. Trace substances, such as ethylene, ethane, nitrogen and higher hydrocarbons, were detected but are not indicated in the graph. In general the higher hydrocarbons are lower at higher temperatures.
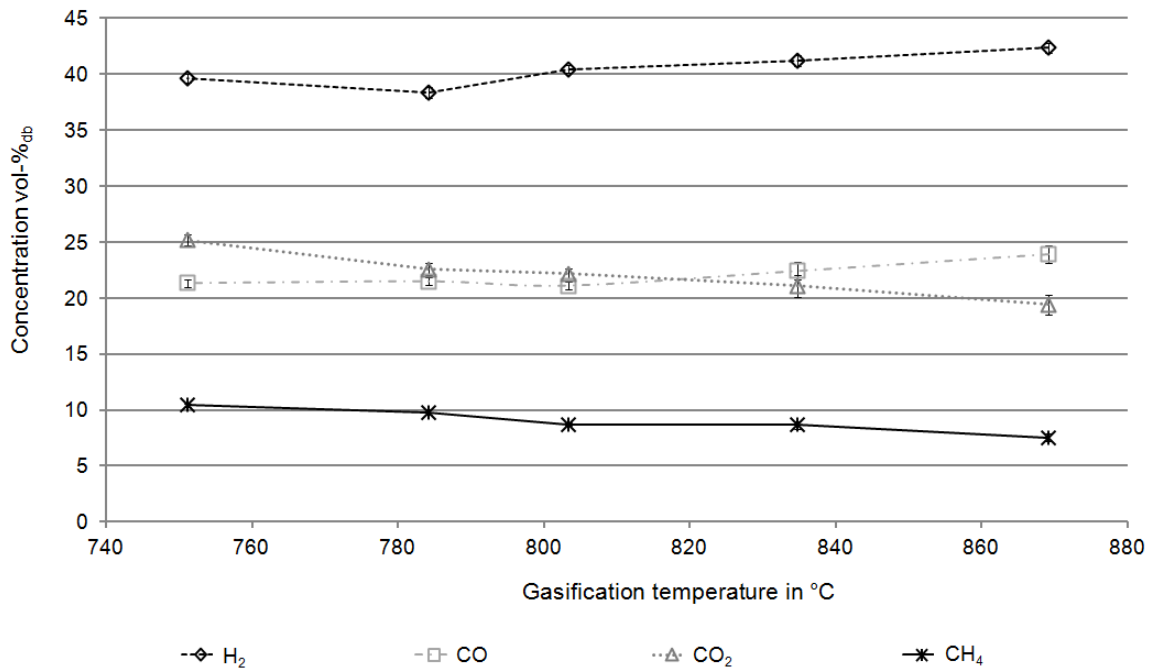
Figure 28: Product gas composition during temperature variation

The amount of tars in the product gas (Figure 29) shows a similar trend for the GCMS detectable tars and the tars measured with the gravimetric method. The amount of GCMS tars are generally higher than that of gravimetric tar. Concerning temperature dependence similar values between 870 °C and 800 °C and increasing values below 800 °C were detected.
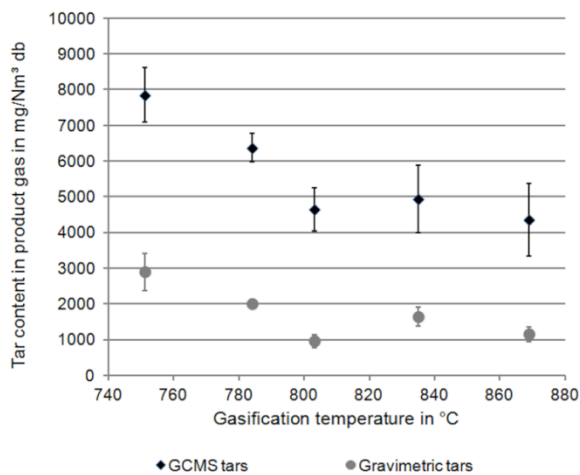
Figure 29: Gravimetric tars and sum of GCMS tars related to the gas volume at different gasification temperatures
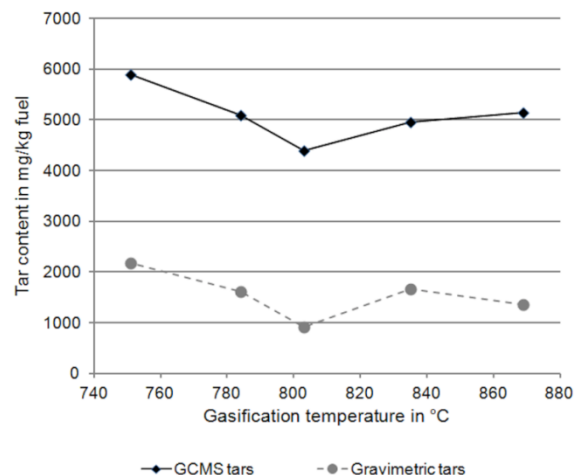
Figure 30: Gravimetric and sum of GCMS tars related to fuel input into gasification reactor

The tars detected with both measurement methods related to the input of fuel into the gasifier are shown in Figure 30. The trends are slightly different compared to those in Figure 29 as the product gas yields are different for different temperatures. Both measurement methods show a minimum of tar concentration related to the fuel input into the gasifier at 800 °C. This trend is more evident when considering the concentration of the tar groups related to the fuel input into the gasification reactor that is shown in Figure 31.
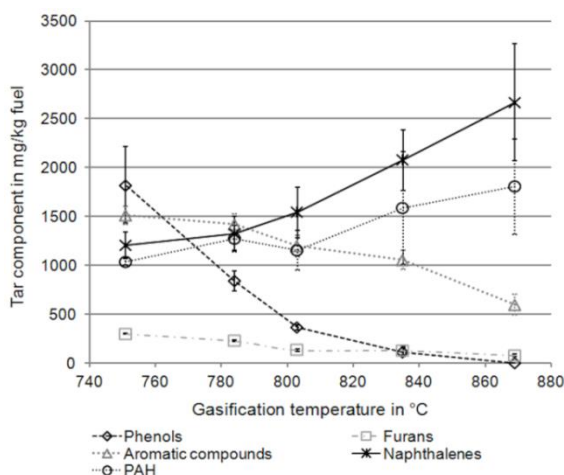
Figure 31: Tar concentration of GCMS tar groups related to fuel input into the gasification reactor
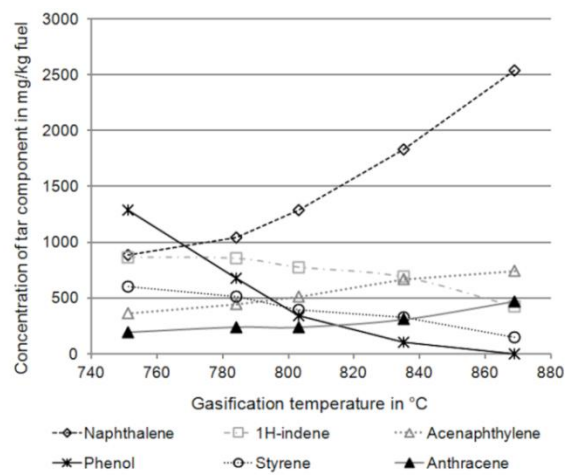
Figure 32: Main GCMS tar components related to fuel input into the gasification reactor

The content of naphthalenes and PAHs related to the fuel input to the gasifier, decreases with decreasing temperatures while the group of phenols and furans increase as shown in Figure 31. The aromatic compounds also increase with lower gasification temperatures with a maximum at 780 °C and slightly decrease at lower gasification temperatures. The increase in phenols is significant and follows an exponential trend with decreasing temperatures.

The main components representing 70–85% of the GCMS tars, depending on the temperature, are naphthalene, 1H-indene, acenaphthylene, phenol, styrene and anthracene. The composition of these main components of GCMS tars is shown in Figure 32. The concentration of anthracene and acenaphthylene decreases slightly when lowering the gasification temperature while styrene and 1H-indene increases. A significant decrease of naphthalene can be seen, while the content of phenol increases significantly at lower gasification temperatures.

Guaiacols, thiophenes and phthalates were not detectable at any temperature. Aromatic nitrogen compounds were measured in concentrations below 30 mg/Nm² db in the product gas and are not shown in the graphs. A clear trend of aromatic nitrogen compounds in connection with the gasification temperature could not be seen.

4.5 Mass balances of inorganic matter

Investigations in the mass flows of inorganic matter through the plant were carried out to determine whether substances are accumulated in the system and in this case where they are accumulated. Therefore mass balances for the main elements were carried out and discussed. As a consequence ash flows were changed to decrease accumulation tendencies and minimize the total flows.

4.5.1 Sampling and calculations for mass balances of inorganic matter

The mass balances for inorganic matter were based on elements calculated in oxides without considering the different chemical conditions were the elements are bond. The balances were based on calculations of total balances of the sum of inorganic matter and elemental balances of the main components.

Ash flows were determined at different locations, shown in Table 10, for the preparation of the mass balances. The ash content was determined and the elemental composition was measured by XRF and calculated in oxides. For the determination of the mass flows of the inorganic matter, the samples were calcined at 1050 °C to release carbonates and organic matter, and the mass flows are related to the calcined samples.

Mass balances of inorganic matter were calculated using the software STAN [106]. The software allows data reconciliation with the method of least squares considering the deviations of the flows and compositions. The balances represent the highest possible probability based on the results of the flow measurements and analyses including their deviations. The inorganic balances are based on (a) the total balance of coarse and fine ash, (b) the elemental balance of CaO, MgO, SiO_2, Fe_2O_3, K_2O, and the sum of other elements for fine and coarse ash mass flows. The composition of bed material and precoat material was considered to be constant and average values were taken. For the composition of biomass ash, an average composition was considered.

Various assumptions were made for the simplification of the system:

- Mass flows of biomass ash, precoat material, fly char, and the mass flow from the combustion reactor to the gasifier were considered to have a particle size smaller than 200 μm.
- Bed material supplement and the flow from the gasification reactor to the combustion reactor are assumed to have a particle size bigger than 200 μm.
- The system is considered to be in a steady state condition, without accumulation of material in the system.
- Bed material circulation between the gasification reactor and the combustion reactor is considered to be balanced in terms of mass flow and composition. All variation of this balance is shown in the results. The balanced bed material circulation is not shown in the diagrams.
- Abrasion is the same in the combustion reactor as in the gasification reactor.
- Abraded material has the same composition as the fresh bed material

- No inorganic matter is detectable in the gas after the product gas filter and the flue gas filter.

The bed material circulation mass flow between the gasifier and the combustion reactor was considered to be balanced and is not indicated in the balances because the mass flow of around 100 tons per hour is much higher than the other inorganic flows and would predominate over all other flows.

The standard deviation for the measured mass flows used is given in Table 24. Higher deviations are adjusted more by the model to reach the best fitting model. Mass flows which are measured by DCS are considered to have a standard deviation of 2%, while manually measured mass flows are assumed to have a standard deviation of 10%. The abrasion is estimated from the coarse and fine ash balance and the standard deviation is chosen with 50% to be adjusted by the calculation method of the balance. Averages of analyses were obtained for the composition of biomass ash, precoat material, and bed material and the standard deviation of the composition of these mass flows was assumed to be 5%. Those analyses with specific analysis for the balance were considered to have 2% standard deviation.

Table 24: Determination of the mass flows and assumed standard deviations for the inorganic balances

Description	Determination of flow	Standard deviation of the mass flow [%]	Standard deviation of the elemental composition [%]
Biomass ash	Mass flow of biomass, ash content	20	5
Bed material	Level measurement DCS	2	5
Precoat material	Weight measurement DCS	2	5
Fly char	Weight measurement DCS (calculated in Figure 34)	20	2
Fly ash circulation	Manual weight determination	10	2
Bed material circulation	Manual weight determination/weight measurement DCS	2	2
Ash to container	Manual weight determination	10	2
Layer formation at the bed material	Calculated	Calculated	Calculated
Abrasion in combustion reactor	Estimated	50/calculated	5
Abrasion in gasification reactor	Estimated	50/calculated	5

Various balances were prepared but two are presented which represent the status before the optimization project and the actual status after optimization. Before optimization, ash circulation is used (called "fly ash circulation" in Figure 5) where fly ash is circulated into the gasifier to minimize bed material consumption and to increase the amount of catalytic substances in the system. Bed material circulation was not implemented at the beginning of the project. During the optimization of the ash loops a gravity separator was implemented in the system to separate bed material particles elutriated with the flue gas path from fly ash ("bed material circulation"). The second balance shows the status after the optimization project after the implementation of the bed material circulation and after turning off the fly ash circulation.

4.5.2 Results of mass balances of inorganic matter

The ash balances were carried out for different operation modes of the ash loops. The status at the beginning of the optimization project is shown in Figure 33. A high amount of ash (coarse and fine) is circulated back into the gasifier before being released into the container to reduce bed material consumption and to increase the amount of catalytic substances in the system. It can be seen that this circulation of fine ash and coarse ash increases the total amount of ash in the system significantly. Considering that potassium is assumed to be responsible for fouling, the total input and output, respectively, from the system is 2.6 kg/h, while the potassium flow in the fly char is 16.8 kg/h. A significant amount of potassium is transferred from the combustion reactor to the gasification reactor via the siphon.
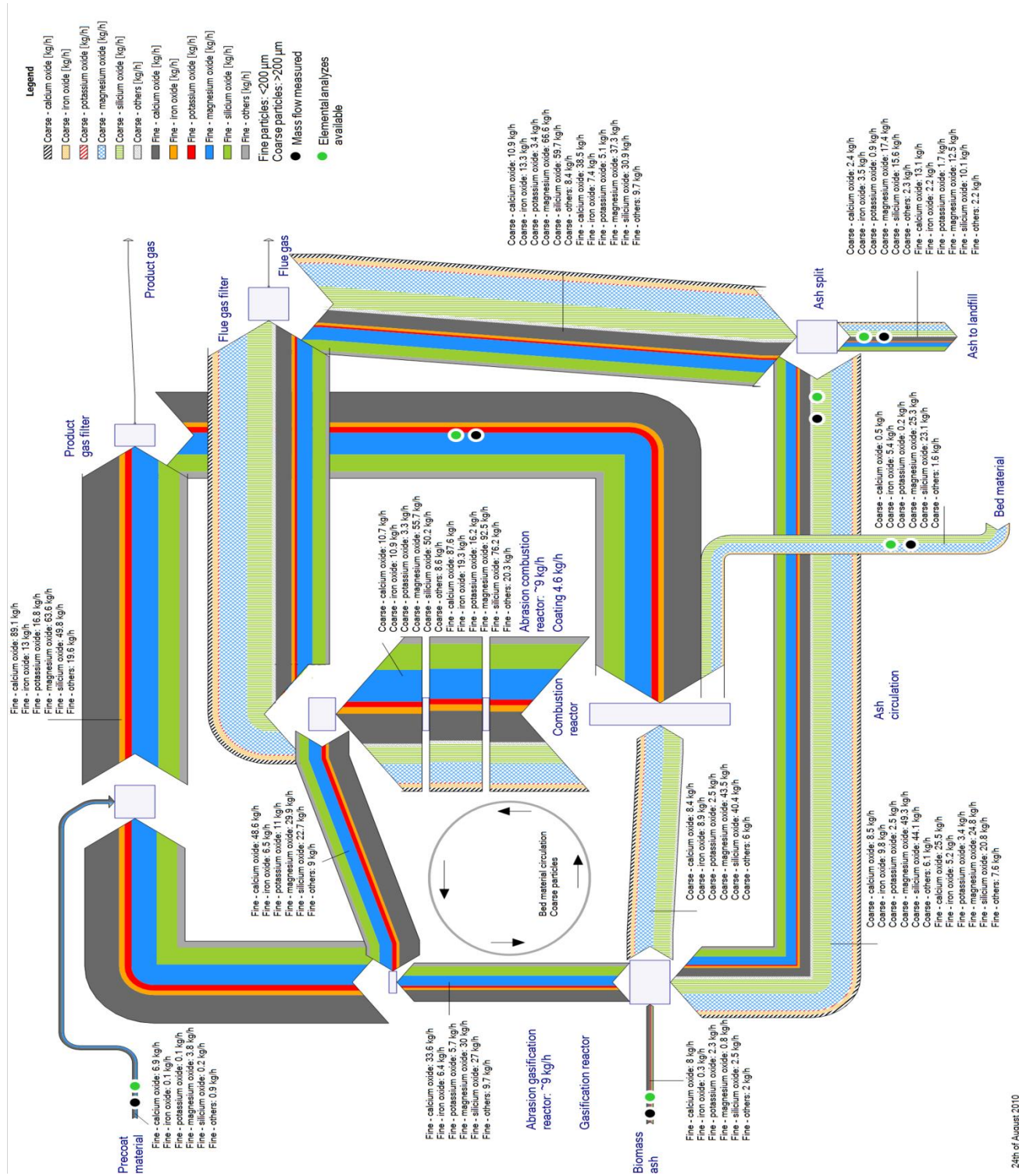
Figure 33: Mass balance of inorganic matters before optimization
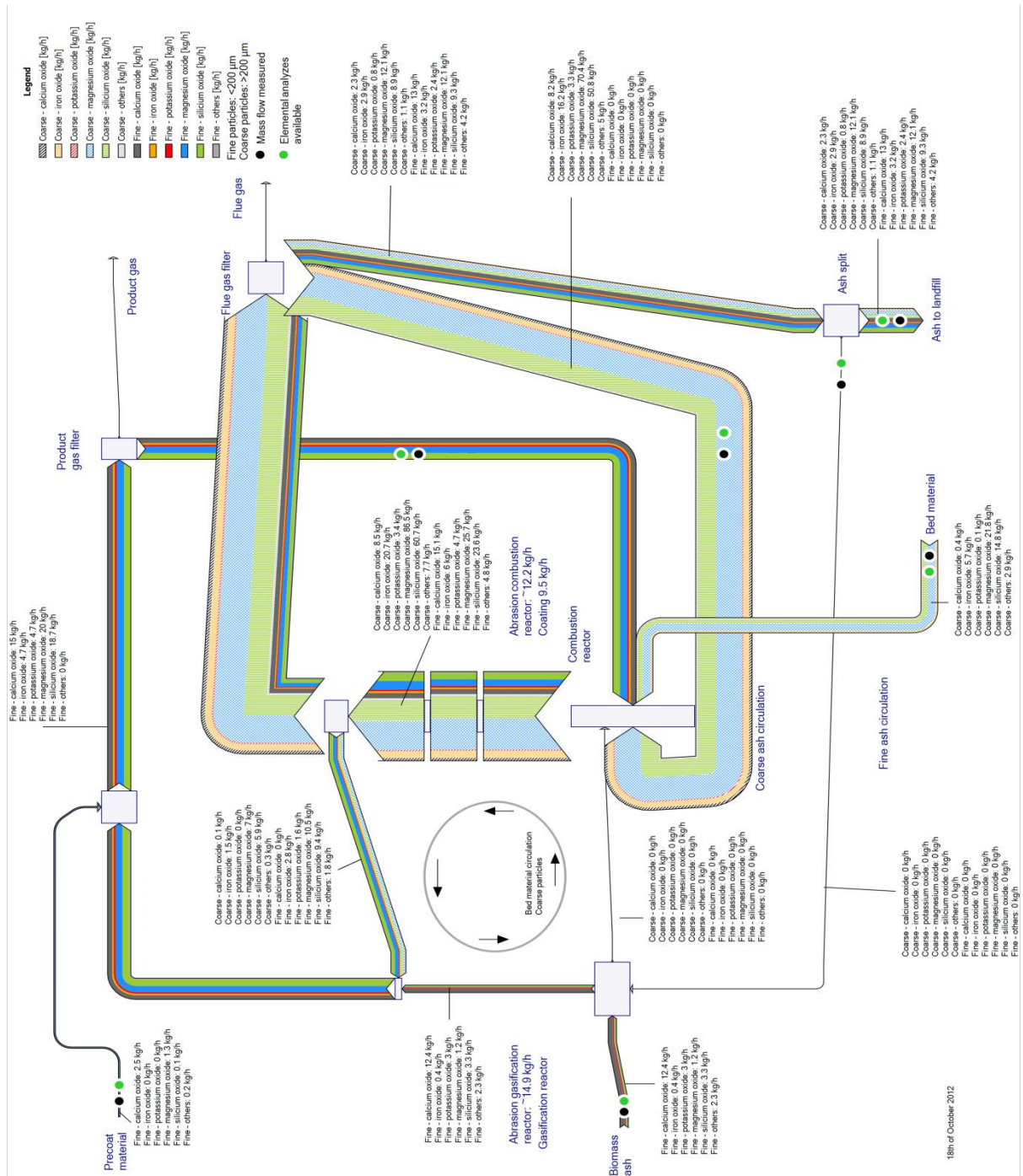
Figure 34: Mass balance of inorganic matter with bed material circulation into the combustion reactor and fine ash turned off

The status after the optimization of the ash loops is shown in Figure 34. The bed material circulation is fed into the combustion reactor while the fly ash circulation is turned off and all fine ash is released into the container. A significant reduction of the fine ash in the system can be seen. The amount of potassium that is transferred between combustion reactor and gasification reactor is reduced to 1.6 kg/h, which is around half of the amount of potassium which enters the plant with the biomass.

4.6 Optimization of the CHP plant Güssing

Based on the knowledge gained from analyses at the CHP plant Güssing and investigations in the 100 kW pilot plant at the Vienna University of Technology, a strategy for the optimization of the CHP in Güssing was developed. The success of the optimization was evaluated in terms of mass and energy balance, and plant availability.

4.6.1 Optimization steps at the CHP plant Güssing

The investigation of inorganic matter, specifically the nature of its modification and its influence on gasification and plant operation, formed the basis for optimization work at the CHP plant Güssing.

Previously-acquired data regarding the modification of the bed material (Publication I and IV) and its influence on gasification properties (Publication II, III), as well as the accumulation of low melting species in the system by ash loops, resulted in the development of the following optimization points:

(a) The catalytic activity of bed material increases with retention time in the system (Publication II, III). A high retention time of the bed material in the system should be aimed.

(b) The source of low melting species such as potassium is fine wood ash (Publication V). Fine ash should therefore be released from the process immediately and not recycled back into the gasifier.

(c) High concentrations of potassium can be found in the fly char burnt in the combustion reactor (Publication V). Accurate dosing of fly char is therefore required to ensure perfect combustion conditions in the combustion reactor.

(d) High catalytic activity of the bed material enables temperature reduction in the gasification and combustion reactors (Publication III).

Based on these four points, the following optimization and modernization procedure was carried out at the Güssing DFB gasification plant during the period from 2009 to 2012:

- Reducing ash loops by turning off the ash circulation and immediately releasing fine ash from the system.
- Focusing on bed material consumption and its retention time in the system via the installation of bed material circulation after the cyclone in order to compensate for the latter's malfunction.
- Improving constant fly char dosing into the combustion reactor.
- Focusing on the control of combustion air inside the combustion reactor.
- Reducing the gasification temperature from 850 - 870°C to a target of 830°C.
- Reducing the volume of product gas in the combustion reactor by lowering temperatures inside the combustion reactor, improving bed material circulation, and air staging.
- Increasing the efficiency of the gas engine to state of the art level by the supplier of the engine.

The above optimization procedure was carried out stepwise by the plant operator. After the temperature was reduced inside the gasification reactor, the plant was operated for 12 months at the new set points before the optimization process was evaluated.

4.6.2 Results of optimization of the CHP plant Güssing

The operational parameters of the Güssing gasification plant varied considerably in both 2009 and 2012, likely as a result of variation in fuel water content, as shown in Figure 35. Despite this, two representative points were chosen as the basis for simulation.
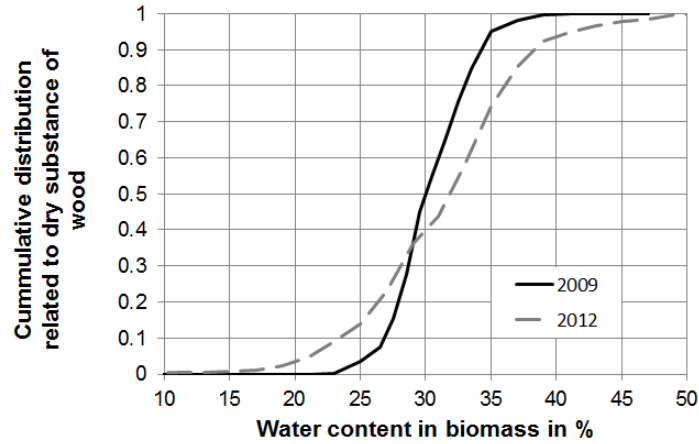
Figure 35: Water content of delivered biomass

The reference product gas composition values are shown in Table 25. As the table reveals, whereas hydrogen content decreased between 2009 and 2012, levels of the main components all increased. In contrast, the concentration of higher gaseous hydrocarbons such as ethane, propane and propene fell significantly.

Table 25: Comparison of product gas composition before and after optimization

Species		Status before optimization (2009) [105]	Status after optimization (2012)
		vol-%db	*vol-%db*
Hydrogen	H_2	39.4	34.9
Carbon monoxide	CO	21.5	24.6
Carbon dioxide	CO_2	23.5	25.3
Methane	CH_4	9	11.3
Ethylene	C_2H_4	2.72	3.6
Nitrogen	N_2	1.3	0.05
Higher gaseous hydrocarbons	C_nH_m	2.58	0.29

The results of the simulation are shown in Table 26. The gasification temperature in the reference year of 2009 was 866°C, a figure which was state of the art at the time. As a result of subsequent temperature reduction in the gasifier, a gasification temperature of 844°C was used in the calculation of plant status after optimization. Electrical efficiency rose from 21% in 2009 to 23.8% after optimization, representing an increase of 13%, cold gas efficiency rose from 65.4 to 69.4, representing an increase of 6%. (Figure 36) These values are confirmed by the amount of wood purchased during the year; with similar generator load, the fuel input decreased accordingly. Cold gas efficiency increased from 65.4% to 69.4%, an improvement of 6%.
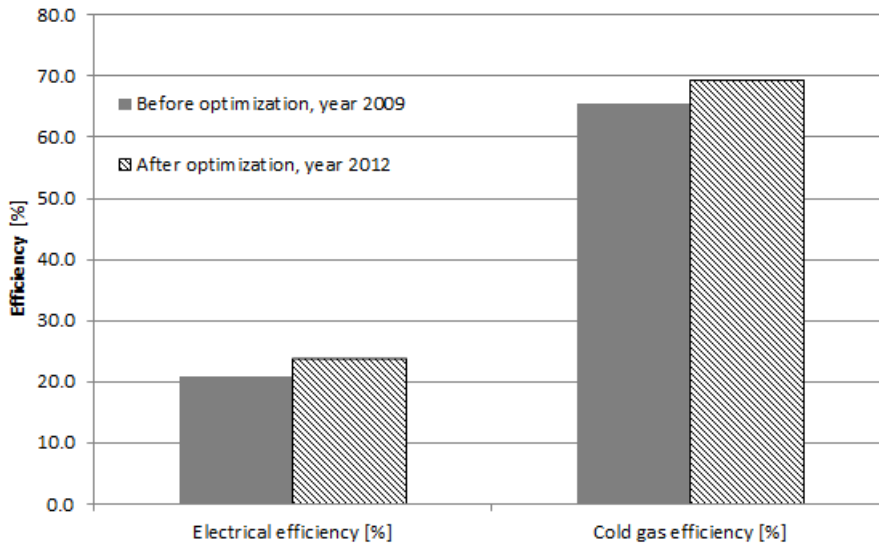
Figure 36: Increase in efficiencies before and after optimization

The installation of a low temperature biomass dryer would increase plant electrical efficiency to 26.2% and cold gas efficiency to 76.6%. Heat output used in a distributed heat net would decrease from 4.1 MW to 3.5 MW as a result of drying of the biomass.

Table 26: Performance parameters of the Güssing CHP plant before and after optimization

		Initial plant design value	Reference 2009	After optimization 2012	Potential with biomass dryer
Origin of values		-	Measured and simulated	Measured and simulated	Simulated
Fuel water content	*%*	15	32.2	28.3	36 - dried to 20
Gasification temperature	*°C*	900	866.2	844.0	844.0
Fuel power	*kW*	8000	9420	8250	7830
Net power of product gas (LHV)	*kW*	5600	6160	5720	5720
Generator output	*kW*	2000	1980	1960	1960
Heat output	*kW*	4500	4150	4100	3550
Product gas in combustion reactor	*Nm³/h*	450	316	77	77
Cold gas efficiency	$\eta_{chem,G}$ *[%]*	70	65.4	69.4	76.6
Electrical efficiency	$\eta_{el,brut}$ *[%]*	25	21.0	23.8	26.2

The optimization measures described above had a significant influence on plant availability, reducing downtime associated with unscheduled shutdowns (Figure 37). The mean availability of the gas engine between 2005 and 2011, excluding the year 2008, was around 6600 h with a maximum of 7950 operating hours per year. Plant optimization could increase the operation hours in the year 2012 to 7442 hours.
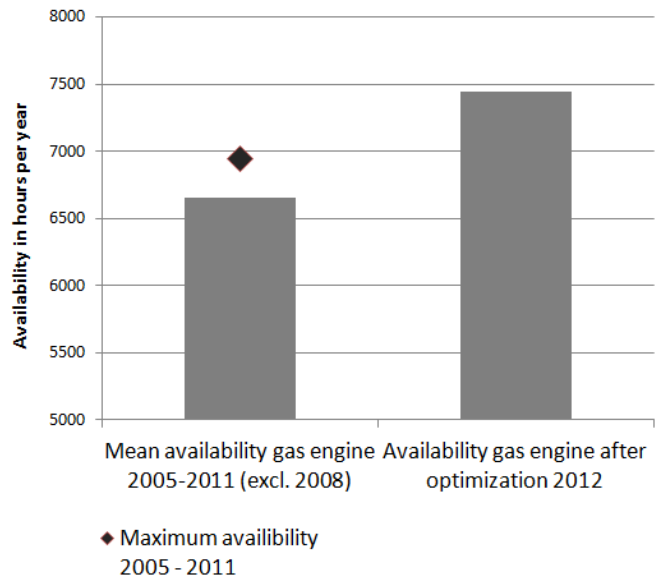
Figure 37: Comparison of plant availability in turns of operation hours per year before and after optimization (yearly average)

The relationship between bed material calcium content and product gas carbon monoxide content is shown in Figure 38. The results of test runs carried out in the 100 kW pilot plant at the Vienna University of Technology are included for comparison and can be taken as a reference for bed material containing no calcium oxide.
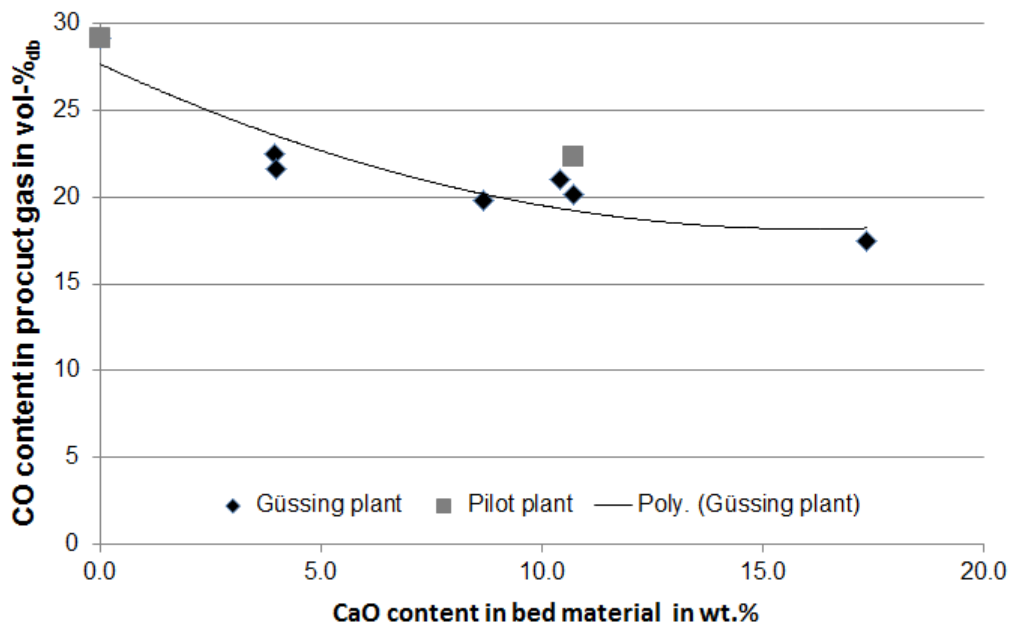
Figure 38: Relationship between bed material calcium oxide content and product gas carbon monoxide content

5 Conclusion and outlook

Biomass steam gasification in dual fluidized bed plants is a promising technology for the generation of electricity, heat, and fuels for transportation. Due to its novelty and complexity various optimization potentials can be determined in terms of operation of the plants, utilization of feedstock and production of fuels for transportation.

This thesis addresses the technical optimization of the gasification system in terms of better understanding of the behavior of inorganic matter and decreasing of the risk of fouling. Higher plant availability and electrical efficiencies are aimed as well.

The following conclusions can be drawn from the work included in this thesis:

Bed material is modified during long term operation of the plant. Two Ca-rich layers are built on the surface of the particles; the inner layer consists mainly of calcium silicates while the outer layer has a similar composition to fine ash. The formation of calcium-rich layers is attributed to the high calcium content of the wood ash and to the addition of Ca-rich additives to improve the catalytic properties of the bed material in terms of tar reduction.

The long term interaction between biomass ash and bed material needs to be considered for the control of inorganic flows and also for the development of new catalytic bed material.

The elemental composition at the surface of the used bed material particles is similar to the composition of the outer layer measured in micrographs and does not change significantly between the gasification and combustion atmospheres.

The investigation of the crystal structure of the used bed material showed an increase of calcium-silicates in the combustion atmosphere, which is in accordance with theoretical considerations. Higher diffusion rates can be expected at higher temperatures and higher oxygen concentrations in the combustion reactor.

An intensive contact of olivine particles and ash promotes the formation of the layers in the combustion reactor. Burning char particles promotes layer formation due to melt formation and random collisions of bed material with burning char particles.

The calcium-rich surface of the used bed material particles allows the reaction with CO_2. At typical temperatures of DFB biomass steam gasification plants, CO_2 transport from the gasification to the combustion reactor is not expected.

The comparison of fresh unused olivine and used olivine from an industrial scale plant showed significant influence on the gas composition and catalytic effects on tar reduction in a 100 kW pilot plant. The difference between the effects of fresh olivine and the used olivine on the gasification properties is caused by the formation of a calcium-rich layer on the used bed material due to the interaction of bed material with biomass ash and additives.

The calcium-rich catalytic bed material promotes the exothermic water–gas shift reaction, which increases the hydrogen and carbon dioxide content in the product gas while the carbon monoxide content is decreased. The lower energy demand for the gasification confirms the assumption of the promotion of the water–gas shift reaction.

The comparison of the results of the test run with used bed material from Güssing in the 100 kW pilot plant with data from the industrial scale plant in Güssing showed good agreement and consequently good scale-up properties.

A reduction of the gasification temperature from 850°C is of interest due to lower fouling tendencies. The test runs at the pilot plant showed that reducing the gasification temperature has an influence on the product gas composition, the tar concentration and GCMS tar composition in the product gas. By reducing the temperature the hydrogen and carbon monoxide contents in the product gas are reduced while the carbon dioxide and methane contents increase. The specific gas yield decreases with lower temperatures.

The concentration of tars related to the volume of product gas increases at temperatures lower than 800 °C. Related to the fuel input, the tar concentration has a minimum of around 800 °C.

A closer examination of the tar components shows that the group of naphthalenes and PAHs decreases when the gasification temperatures are lowered and the group of phenols, furans and aromatic components increases.

The minimization of the tar content related to the fuel input by reducing the gasification temperature is an optimization of the increasing components, which are considered as decomposition products, and the components, which accumulate at higher temperatures. This leads to moderate increase of the sum of GCMS tar concentration related to the volume of product gas to temperatures down to 800°C.

The comparison of the tar concentrations of the temperature variations with a test run with unused olivine showed the importance of the calcium-rich layer on the used olivine. This leads to the conclusion that the retention time of the bed material in the system and the formation of the calcium-rich layer has a higher influence on tar reduction in the product gas than the gasification temperature.

With accurate controlling of the bed material inventory, ash flows and retention time of the bed material in the system, further optimization of the plant is considered to be possible by reducing the gasification temperature to 800 °C without the risk of condensation of tars on the heat exchanger walls or in pipes.

Ash loops can lead to significant higher material streams and to an accumulation of substances with low melting points in the system.

Potassium, which is considered to be mainly responsible for fouling, slagging, and bed material agglomeration in this case, is transferred from the combustion reactor to the gasification reactor. The mechanism of the transfer is still unknown.

An accumulation of potassium can be seen in the fly char.

The concentration of potassium in fine ash is nearly twice that in the coarse ash and bed material.

Based on the knowledge gained from the analyses and the pilot plant test runs, the optimization of the CHP plant Güssing brought the following conclusions:

A focus on control of inorganic matter and bed material composition led to improved plant operation, with reduced fouling tendency observed in terms of inorganic matter.

Gasification temperatures in the DFB biomass gasifier can be reduced to 830°C without any subsequent problems for tar condensation in the product gas path. This procedure is applicable for plants operating using woody biomass.

Electrical efficiencies of 23% can be obtained when employing fuel with 33% water content. The installation of a biomass dryer would increase efficiency to 26%, while still higher values could be achieved with the implementation of an Organic Rankine Cycle (ORC) to utilize heat at temperatures of around 450°C, as shown in the CHP in Oberwart/Austria [18].

Biomass steam gasification in a DFB reactor represents a competitive alternative for the generation of heat and electricity, with the potential for high availabilities and electrical efficiencies (>30%) even in small-scale industrial plants.

Further investigations are required regarding the utilization of biomass fuels other than woody biomass. The interaction between fuel ash and olivine bed material has been observed to vary with different fuels [52].

5.1 Mechanism for modification of inorganic matter and fouling formation

Based on the conclusions of this thesis, a suggestion for the mechanism of the bed material modification and fouling is suggested.

The suggested mechanism of ash transformation in the combustion reactor is shown in Figure 39; the elements indicated in this diagram are not considered to be oxides but rather bound in different minerals. The first step of the decomposition of the biomass is carried out in the gasification reactor. Water and volatile organic matter are released into the gas phase. A part of the char is gasified with the gasification agent steam. Inorganic matter is introduced into the combustion reactor with organic

matter and char, which is transferred with the bed material from the gasification reactor via the chute, as well as fly char from the product gas filter. Organic matter is burnt in the combustion reactor and inorganic matter released from the char particles. These burning particles are the source of heat in fluidized beds and are, therefore, associated with the highest temperatures [36]. Inorganic matter which are set free from the burning material either melts or is released into the gaseous phase or are present as solid particles. The release rate of potassium, which forms compounds with the lowest melting temperatures, is considered crucial for the initiation of fouling and is influenced by temperature, the amount of calcium in the system and water content [38]. Not only is the temperature affected by that of the fluidized bed, but the local temperature of burning particles is also influenced by the excess air ratio and the adiabatic combustion temperature of the particle. A release of inorganic matter into the gas phase is also considered to happen in the gasification reactor but due to the lower temperatures this effect is considered to be lower. On the other hand a reducing atmosphere in the gasification reactor promotes the release of inorganic matter [39,40].
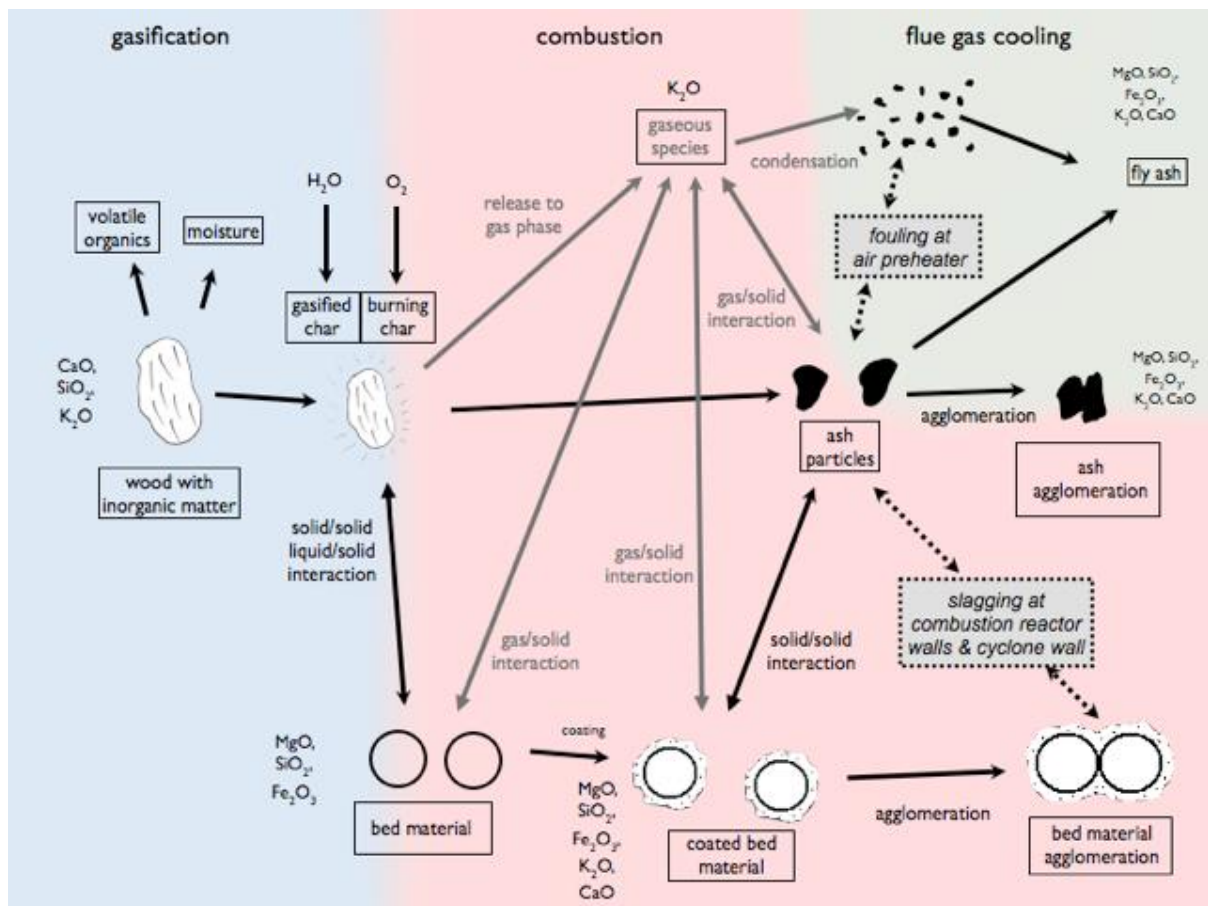
Figure 39: Mechanisms of ash transformation (adapted from Frandsen et al. [107])

Inorganic matter released into the gaseous phase in the combustion reactor but also in the gasification reactor condenses after cooling in the heat exchangers, which can result in fouling, presumably as a result of a reaction which takes place during condensing and cooling with other inorganic matter in the fly ash solid phase. This is assumed to take place in the air preheater.

Due to the high reactivity of the gaseous species, e.g. potassium, a reaction with solid or melted matter can be expected [34]. Such reactions are considered to increase the risk of the formation of deposits in high temperature sections of the combustion reactor and cyclone (Publication V). In the fluidized bed (bubbling bed regime and fast fluidized regime) bed material can be highly affected of these melting processes resulting in layer formation at the bed material, bed material agglomeration and also slagging. Due to high velocities in the combustion reactor and cyclone, bed agglomeration cannot be seen, but at locations with lower velocities e.g. at the top of the cyclone, slagging occurs.

Due to the high temperatures which appear locally around burning char particles, the ash components of the fuel which are released can react with the bed material to form the observed layers around the bed material particles (Publication IV).

All these phenomena can be observed in the Güssing plant. An intervention in the operating parameters but also in the design of the plant can influence these reaction paths.

5.2 Recommendation for design and operation of future biomass steam gasification plants in dual fluidized bed reactors

At present the full potential of the CHP plant Güssing in terms of efficiency and availability of the plant is not being exploited to the full. A simulation including a low temperature biomass dryer showed the potential for an increase of the electrical efficiency of around 2.4 percent-points when the drying is carried out from 36% water content to 20% as shown in Table 26. Trends concerning reduction of fouling tendencies in terms of operation were presented earlier. Further improvements could be achieved by an upgrade of the flue gas path to the design which is state of the art.
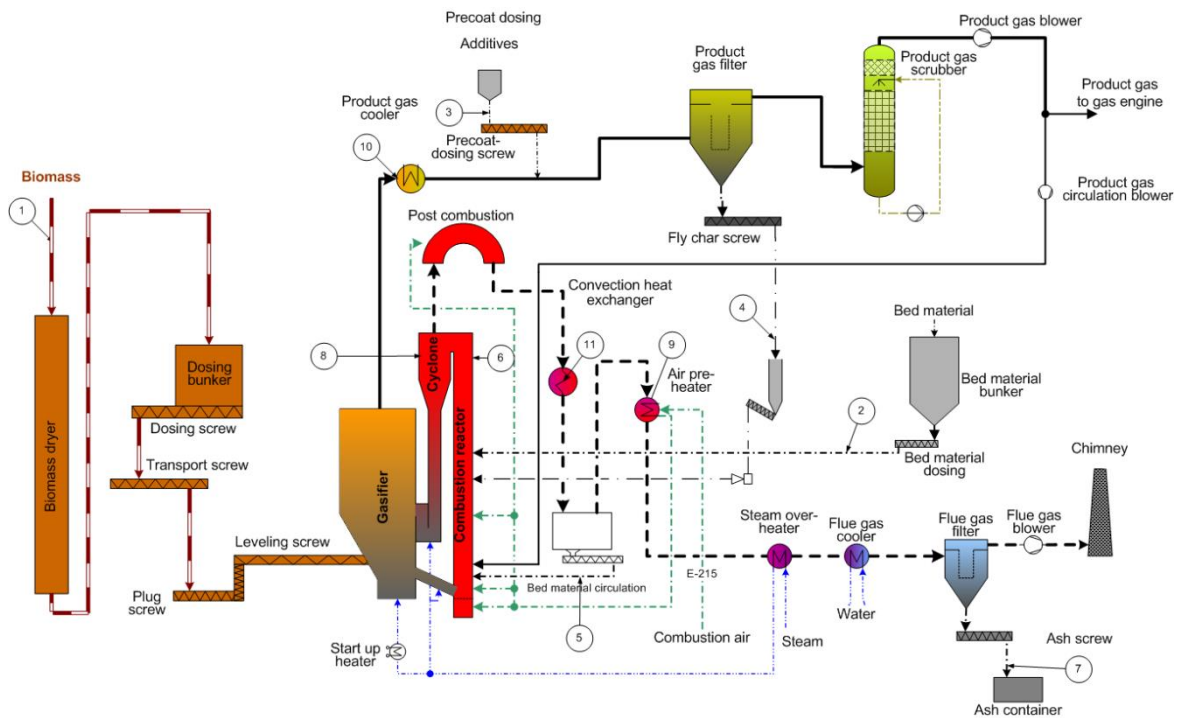
Figure 40: Recommendation for state of the art DFB biomass steam gasification plants

For the design and operation of the DFB plants, recommendations are given in Table 27.

Table 27: Recommendations for design and operation (positions refer to Figure 40)

Measure	Consequence
Consequent and immediate discharge of fine ash (pos. 7)	Potassium is considered to be responsible for the risk of fouling and slagging. The concentration of potassium is around double in the fine ash compared to the coarse ash which is mainly bed material. The potassium concentration in the system can be reduced and fouling, slagging and bed material agglomeration can be avoided. (pos. 6, 8, 9, 10, 11)
Circulation of fine ash should be avoided (pos. 7)	Beside of the high potassium content, also calcium oxide is available in high concentrations in the fine ash fraction. In general, calcium oxide influences the gasification properties positively on the other hand it increases the potassium release rate with negative impact on deposition risk (pos. 6, 8, 9, 10, 11). The catalytic benefit of calcium in the fine ash is not utilized because of a short retention time in the bed and a lack of contact with the gas species.
Measurement and controlling of inorganic loops, supply and discharge of inorganic matter	Catalytic properties of the bed material and melting behavior of inorganic matters is significantly influenced by inorganic streams. A constant monitoring of bed material consumption, ash discharge, and internal flows ensures early detection of malfunctions. (pos. 2, 3, 4, 5, 7)
Controlling of fly char dosing (pos. 4)	Potassium is enriched in fly char which is normally burned in the combustion reactor. Fly char is highly reactive. Due to the close bonding of potassium and burning fly char, the release rate of potassium from the fly char is considered to be high but can be reduced by low adiabatic combustion temperatures. Inconstant dosing of fly char can lead to a lack of combustion air and to high adiabatic combustion temperatures around the char particles which increases the potassium release rate (pos. 6, 8, 9, 11).
Controlling of combustion and fluidization air	The adiabatic combustion temperature of char particles is linked to the release of potassium which is responsible for fouling. Controlling of the combustion air ensures good combustion conditions to avoid too high temperatures.
Installation of a convective path in the flue gas path (pos. 11)	The flue gas path should be designed so that the gas is cooled first via convection to temperatures below the initial melting temperature of potassium silicates (approximately 600°C). This avoids contact of melted particles with heat exchanger walls and plate sheets.
Installation of a convective path in the product gas path (pos. 10)	The release of potassium to the gas phase can happen also in the product gas path where it can condense at heat exchangers. High potassium concentrations in the fuel (e.g. alternative fuels) or an accumulation of potassium in the system can lead to fouling in the product path. A convective path reduces the risk for fouling.
Reduction of gasification temperature to 800-830°C	A consequent monitoring of the catalytic properties of the bed material creates the possibility of a reduction of the gasification temperature. Lower gasification temperature reduces also the temperatures in the combustion reactor. The risk for fouling, slagging and bed material agglomeration is reduced (pos. 6, 8, 9, 10, 11) and higher electrical efficiencies can be reached.
Installation of a biomass dryer	A biomass dryer reduces the amount of water in the system and increases the electrical efficiency. Gas flows are reduced due to less steam. Variations in the operation can be reduced due to controlling of the water content of the biomass in the dryer.

5.3 Outlook

To reduce operation costs, increase efficiencies and increase operational time per year further developments are required. Future research should examine the influence of fuels other than woody ash on fouling and bed material layer formation because the price of woody biomass is higher compared to alternative fuels.

5.3.1 Alternative fuels

Further research activities are required for the utilization of cheaper biogenous fuels such as energy crops, straw, sewage sludge, and so on which are considered to have negative impact on ash melting behavior. The influence of different ash composition of alternative fuels on the layer formation at the bed material and its influence on gasification properties cannot be quantified yet. Grimm et al. showed that the layer formation at olivine particles with other fuels than woody biomass differs from the experience of woody biomass fuels [52]. Methods for the active manipulation of ash melting behavior by the introduction of additives had not been investigated in this thesis. This would be of interest e.g. for the immobilization of gaseous potassium for fuels with high potassium content. The manipulation of the ash composition could be also carried out by fuel blending.

The utilization of alternative fuels will also challenge the fuel feeding system. The systems which are built with plug screw feeders (as built in Güssing) or gate locks (as built in Villach and Senden) cannot be used for all fuels.

5.3.2 Bed material

The findings of this work are important for the development of alternative bed material that is not based on the olivine. Olivine is compared to quartz sand or calcite expensive and worse available, it contains also heavy metals such as chrome and nickel what brings disadvantages during deposition. The development of an alternative, cheap bed material with low contamination of heavy metals which is modified during the utilization in the gasification plant by the formation of a calcium rich layer is considered to be possible. Research concerning the influence on catalytic properties and fouling tendencies are required.

References

[1]   T. Howes, The EU's New Renewable Energy Directive (2009/28/EC), The New Climate Policies of the European Union: Internal Legislation and Climate Diplomacy. (2010) 117.

[2]   M. Downing, L.M. Eaton, R.L. Graham, M.H. Langholtz, R.D. Perlack, A.F. Turhollow Jr, et al., US Billion-Ton Update: Biomass Supply for a Bioenergy and Bioproducts Industry, (2011).

[3]   EU Energy in Figures 2012, European Commission, 2012.

[4]   D.J. Swider, L. Beurskens, S. Davidson, J. Twidell, J. Pyrko, W. Prüggler, et al., Conditions and costs for renewables electricity grid connection: Examples in Europe, Renewable Energy. 33 (2008) 1832–1842.

[5]   M. Matos, J.P. Lopes, M. Rosa, R. Ferreira, A. Leite da Silva, W. Sales, et al., Probabilistic evaluation of reserve requirements of generating systems with renewable power sources: The Portuguese and Spanish cases, International Journal of Electrical Power and Energy Systems. 31 (2009) 562–569.

[6]   M. Beaudin, H. Zareipour, A. Schellenberglabe, W. Rosehart, Energy storage for mitigating the variability of renewable electricity sources: An updated review, Energy for Sustainable Development. 14 (2010) 302–314.

[7]   H. Chen, T.N. Cong, W. Yang, C. Tan, Y. Li, Y. Ding, Progress in electrical energy storage system: A critical review, Progress in Natural Science. 19 (2009) 291–312.

[8]   S.N. Naik, V.V. Goud, P.K. Rout, A.K. Dalai, Production of first and second generation biofuels: A comprehensive review, Renewable and Sustainable Energy Reviews. 14 (2010) 578–597.

[9]   A.V. Bridgwater, The Technical and economic feasibility of biomass gasification for power generation, Fuel. 74 (1995) 631–653.

[10]   R. Rauch, H. Hofbauer, S. Săcăreanu, A. Chiru, FROM GASIFICATION TO SYNTHETIC FUELS VIA FISCHER-TROPSCH SYNTHESIS, Bulletin of the Transsilvania University of Brasov - Series I - Engineering Sciences. 3 (2011).

[11]   B. Rehling, H. Hofbauer, Bio-SNG from biomass - First results of a demonstration plant, in: Self-published, Vienna, Austria, 2009.

[12]   B. Rehling, H. Hofbauer, R. Rauch, C. Aichernig, BioSNG—process simulation and comparison with first results from a 1-MW demonstration plant, Biomass Conv. Bioref. 1 (2011) 111–119.

[13]   A. Sauciuc, Z. Abostreif, G. Weber, A. Potetz, R. Rauch, H. Hofbauer, et al., Influence of pressure on the performance of biomass based Fischer-Tropsch synthesis, in: 2011.

[14]   A. Sauciuc, A. Potetz, G. Weber, R. Rauch, H. Hofbauer, L. Dumitrescu, Synthetic diesel from biomass by Fischer-Tropsch synthesis, (n.d.).

[15]   Y. Chen, T.A. Adams, P.I. Barton, Optimal Design and Operation of Static Energy Polygeneration Systems, Ind. Eng. Chem. Res. 50 (2012) 5099–5113.

[16]   R.H. Williams, E.D. Larson, G. Liu, T.G. Kreutz, Fischer–Tropsch fuels from coal and biomass: Strategic advantages of once-through ("polygeneration") configurations, Energy Procedia. 1 (2009) 4379–4386.

[17]   E. Wetterlund, M. Söderström, Biomass gasification in district heating systems – The effect of economic energy policies, Applied Energy. 87 (2010) 2914–2922.

[18]   J. Kotik, *Über den Einsatz von Kraft-Wärme-Kopplungsanlagen auf Basis der Wirbelschicht-Dampfvergasung fester Biomasse am Beispiel des Biomassekraftwerks Oberwart*, PhD thesis, Vienna University of Technology, 2010.

[19]   M. Kaltschmitt, H. Hartmann, H. Hofbauer, Energie aus Biomasse, Springer, Berlin, Heidelberg, 2009.

[20]   P.A. Simell, J.O. Hepola, A.O.I. Krause, Effects of gasification gas components on tar and ammonia decomposition over hot gas cleanup catalysts, Fuel. 76 (1997) 1117–1127.

[21]   H. Hofbauer, R. Rauch, G. Loeffler, S. Kaiser, E. Fercher, H. Tremmel, Six years experience with the FICFB-GASIFICATION process, in: Self-published, Amsterdam, The Neatherlands, 2002: p. 4.

[22]   M. Bolhar-Nordenkampf, H. Hofbauer, K. Bosch, R. Rauch, C. Aichernig, Biomass CHP Plant Güssing - Using Gasification for Power Generation, in: K. Kirtikara (Ed.), Self-published, Phuket, Thailand, 2003: pp. 567–572.

[23]   S. Koppatz, C. Pfeifer, R. Rauch, H. Hofbauer, T. Marquard-Moellenstedt, M. Specht, H2 rich product gas by steam gasification of biomass with in situ CO2 absorption in a dual fluidized bed system of 8†MW fuel input, Fuel Processing Technology. 90 (2009) 914–921.

[24]   H. Hofbauer, R. Rauch, K. Bosch, R. Koch, C. Aichernig, Biomass CHP Plant Güssing - A Success Story, in: A.V. Bridgwater (Ed.), Pyrolysis and Gasification of Biomass and Waste, CPL Press, 2003: pp. 527–536.

[25]   M. Pronobis, The influence of biomass co-combustion on boiler fouling and efficiency, Fuel. 85 (2006) 474–480.

[26]   P. Plaza, A.J. Griffiths, N. Syred, T. Rees-Gralton, Use of a Predictive Model for the Impact of Cofiring Coal/Biomass Blends on Slagging and Fouling Propensity, Energy Fuels. 23 (2012) 3437–3445.

[27]   P. Teixeira, H. Lopes, I. Gulyurtlu, N. Lapa, P. Abelha, Evaluation of slagging and fouling tendency during biomass co-firing with coal in a fluidized bed, Biomass and Bioenergy. 39 (2012) 192–203.

[28]   T. Valmari, T.M. Lind, E.I. Kauppinen, G. Sfiris, K. Nilsson, W. Maenhaut, Field Study on Ash Behavior during Circulating Fluidized-Bed Combustion of Biomass. 2. Ash Deposition and Alkali Vapor Condensation, Energy Fuels. 13 (1998) 390–395.

[29]   K.O. Davidsson, L.E. Amand, B.M. Steenari, A.L. Elled, D. Eskilsson, B. Leckner, Countermeasures against alkali-related problems during combustion of biomass in a circulating fluidized bed boiler, Chemical Engineering Science. 63 (2008) 5314–5329.

[30]   T.R. Miles, L.L. Baxter, R.W. Bryers, B.M. Jenkins, L.L. Oden, Boiler deposits from firing biomass fuels, Biomass and Bioenergy. 10 (1996) 125–138.

[31]   H.P. Nielsen, L.L. Baxter, G. Sclippab, C. Morey, F.J. Frandsen, K. Dam-Johansen, Deposition of potassium salts on heat transfer surfaces in straw-fired boilers: a pilot-scale study, Fuel. 79 (2000) 131–139.

[32]   T.R. Miles, L. Baxter, R.W. Bryers, B.M. Jenkins, L.L. Oden, Alkali deposits found in biomass power plants: a preliminary investigation of their extent and nature, (1995).

[33]   D. Boström, M. Broström, N. Skoglund, C. Boman, Ash Transformation Chemistry during Energy Conversion of Biomass, in: Saariselkä, Lapland, Finland, 2010.

[34]   D. Boström, N. Skoglund, A. Grimm, C. Boman, M. Öhman, M. Broström, et al., Ash Transformation Chemistry during Combustion of Biomass, Energy Fuels. 26 (2012) 85–93.

[35]   F.C. Kracek, N.L. Bowen, G.W. Morey, The System Potassium Metasilicate-Silica, The Journal of Physical Chemistry. 33 (1929) 1857–1879.

[36]   F. Scala, R. Chirone, An SEM/EDX study of bed agglomerates formed during fluidized bed combustion of three biomass fuels, Biomass and Bioenergy. 32 (2008) 252–266.

[37]   S.C. van Lith, P.A. Jensen, F.J. Frandsen, P. Glarborg, Release to the Gas Phase of Inorganic Elements during Wood Combustion. Part 2: Influence of Fuel Composition, Energy Fuels. 22 (2008) 1598–1609.

[38]   A. Novaković, S.C. van Lith, E. al, Release of Potassium from the Systems K−Ca−Si and K−Ca−P, Energy Fuels. 23 (2012).

[39]   D.A. Sams, T. Talverdian, F. Shadman, Kinetics of catalyst loss during potassium-catalysed CO_2 gasification of carbon, Fuel. 64 (1985) 1208–1214.

[40]   D.C. Dayton, R.J. French, T.A. Milne, Direct observation of alkali vapor release during

biomass combustion and gasification. 1. Application of molecular beam/mass spectrometry to switchgrass combustion, Energy Fuels. 9 (1995) 855–865.

[41] C. Pfeifer, S. Koppatz, H. Hofbauer, Catalysts for dual fluidised bed biomass gasification— an experimental study at the pilot plant scale, Biomass Conv. Bioref. (2011) 1–12.

[42] L. Devi, M. Craje, P. Th ne, K.J. Ptasinski, F.J.J.G. Janssen, Olivine as tar removal catalyst for biomass gasifiers: Catalyst characterization, Applied Catalysis, a: General. 294 (2005) 68–79.

[43] L. Devi, K.J. Ptasinski, F.J.J.G. Janssen, S.V.B. van Paasen, P.C.A. Bergman, J.H.A. Kiel, Catalytic decomposition of biomass tars: use of dolomite and untreated olivine, Renewable Energy. 30 (2005) 565–587.

[44] L. Devi, K.J. Ptasinski, F.J.J.G. Janssen, Pretreated olivine as tar removal catalyst for biomass gasifiers: investigation using naphthalene as model biomass tar, Fuel Processing Technology. 86 (2005) 707–730.

[45] C. Pfeifer, S. Koppatz, H. Hofbauer, Steam gasification of various feedstocks at a dual fluidised bed gasifier: Impacts of operation conditions and bed materials, Biomass Conv. Bioref. 1 (2011) 39–53.

[46] S. Koppatz, E. al, Comparison of the performance behaviour of silica sand and olivine in a dual fluidised bed reactor system for steam gasification of biomass at pilot plant scale, Chemical Engineering Journal. (2011).

[47] M. Öhman, L. Pommer, A. Nordin, Bed Agglomeration Characteristics and Mechanisms during Gasification and Combustion of Biomass Fuels, Energy Fuels. 19 (2005) 1742–1748.

[48] E. Brus, M. Öhman, A. Nordin, Mechanisms of Bed Agglomeration during Fluidized-Bed Combustion of Biomass Fuels, Energy Fuels. 19 (2005) 825–832.

[49] S. De Geyter, M. Öhman, D. Boström, M. Eriksson, A. Nordin, Effects of Non-Quartz Minerals in Natural Bed Sand on Agglomeration Characteristics during Fluidized Bed Combustion of Biomass Fuels, Energy Fuels. 21 (2007) 2663–2668.

[50] L.H. Nuutinen, M.S. Tiainen, M.E. Virtanen, S.H. Enestam, R.S. Laitinen, Coating Layers on Bed Particles during Biomass Fuel Combustion in Fluidized-Bed Boilers, Energy Fuels. 18 (2003) 127–139.

[51] M. Zevenhoven-Onderwater, M. Öhman, B.-J. Skrifvars, R. Backman, A. Nordin, M. Hupa, Bed Agglomeration Characteristics of Wood-Derived Fuels in FBC, Energy Fuels. 20 (2006) 818–824.

[52] A. Grimm, M. Öhman, T. Lindberg, A. Fredriksson, D. Boström, Bed Agglomeration Characteristics in Fluidized-Bed Combustion of Biomass Fuels Using Olivine as Bed Material, Energy Fuels. 26 (2012) 4550–4559.

[53] A. Pettersson, L.-E. Amand, B.-M. Steenari, Chemical fractionation for the characterisation of fly ashes from co-combustion of biofuels using different methods for alkali reduction, Fuel. 88 (2009) 1758–1772.

[54] L.E. Fryda, K.D. Panopoulos, E. Kakaras, Agglomeration in fluidised bed gasification of biomass, Powder Technology. 181 (2008) 307–320.

[55] M. Öhman, A. Nordin, B.-J. Skrifvars, R. Backman, M. Hupa, Bed Agglomeration Characteristics during Fluidized Bed Combustion of Biomass Fuels, Energy Fuels. 14 (2000) 169–178.

[56] S. De Geyter, The role of sulphur in preventing bed agglomeration during combustion of biomass, 2006.

[57] A. Grimm, N. Skoglund, D. Boström, M. Öhman, Bed Agglomeration Characteristics in Fluidized Quartz Bed Combustion of Phosphorus-Rich Biomass Fuels, Energy Fuels. 25 (2011) 937–947.

[58] F. Scala, R. Chirone, Characterization and early detection of bed agglomeration during the fluidized bed combustion of olive husk, Energy Fuels. 20 (2006) 120–132.

[59] A. Grimm, N. Skoglund, D. Boström, C. Boman, M. Öhman, Influence of Phosphorus on

Alkali Distribution during Combustion of Logging Residues and Wheat Straw in a Bench-Scale Fluidized Bed, Energy Fuels. 26 (2012) 3012–3023.

[60] P.L. Roeder, R.F. Emslie, Olivine-liquid equilibrium, Contrib Mineral Petrol. 29 (1970) 275–289.

[61] J. Smyth, High temperature crystal chemistry of fayalite, Am Mineral. (1975).

[62] G. Libourel, Systematics of calcium partitioning between olivine and silicate melt: implications for melt structure and calcium content of magmatic olivines, Contrib Mineral Petrol. 136 (1999) 63–80.

[63] R. Dohmen, H.-W. Becker, S. Chakraborty, Fe–Mg diffusion in olivine I: experimental determination between 700 and 1,200°C as a function of composition, crystal orientation and oxygen fugacity, Phys Chem Minerals. 34 (2007) 389–407.

[64] H.O.A. Fredriksson, R.J. Lancee, P.C. Thüne, H.J. Veringa, J.W.H. Niemantsverdriet, Olivine as tar removal catalyst in biomass gasification: Catalyst dynamics under model conditions, Applied Catalysis, B: Environmental. (2012) 1–23.

[65] T. Milne, N. Abatzoglou, Biomass gasifier "tars": their nature, formation, and conversion, National Renewable Energy Laboratory, 1998.

[66] L. Devi, K.J. Ptasinski, F.J.J.G. Janssen, Decomposition of Naphthalene as a Biomass Tar over Pretreated Olivine: Effect of Gas Composition, Kinetic Approach, and Reaction Scheme, Ind. Eng. Chem. Res. 44 (2005) 9096–9104.

[67] J. Corella, J.M. Toledo, R. Padilla, Olivine or Dolomite as In-Bed Additive in Biomass Gasification with Air in a Fluidized Bed:‚Äâ Which Is Better? Energy Fuels. 18 (2004) 713–720.

[68] S. Rapagná, N. Jand, A. Kiennemann, P.U. Foscolo, Steam-gasification of biomass in a fluidised-bed of olivine particles, Biomass and Bioenergy. 19 (2000) 187–197.

[69] M.L. Mastellone, U. Arena, Olivine as a tar removal catalyst during fluidized bed gasification of plastic waste, AIChE Journal. 54 (2008) 1656–1667.

[70] U. Arena, L. Zaccariello, M.L. Mastellone, Tar removal during the fluidized bed gasification of plastic waste, Waste Management. 29 (2009) 783–791.

[71] R. Rauch, C. Pfeifer, K. Bosch, H. Hofbauer, Comparison of Different Olivines for Biomass Steam Gasification, in: Conference, 2004.

[72] S. Rapagná, M. Virginie, K. Gallucci, C. Courson, M. Di Marcello, A. Kiennemann, et al., Fe/olivine catalyst for biomass steam gasification: Preparation, characterization and testing at real process conditions, Catalysis Today. 176 (2011) 163–168.

[73] L. Di Felice, C. Courson, D. Niznansky, P.U. Foscolo, A. Kiennemann, Biomass Gasification with Catalytic Tar Reforming: A Model Study into Activity Enhancement of Calcium- and Magnesium-Oxide-Based Catalytic Materials by Incorporation of Iron, Energy Fuels. 24 (2010) 4034–4045.

[74] D. Swierczynski, C. Courson, A. Kiennemann, Study of steam reforming of toluene used as model compound of tar produced by biomass gasification, Chemical Engineering and Processing: Process Intensification. 47 (2008) 508–513.

[75] D. Swierczynski, C. Courson, L. Bedel, A. Kiennemann, J. Guille, Characterization of Ni−Fe/MgO/Olivine Catalyst for Fluidized Bed Steam Gasification of Biomass, Chem. Mater. 18 (2006) 4025–4032.

[76] G. Ruoppolo, F. Miccio, R. Chirone, Fluidized Bed Cogasification of Wood and Coal Adopting Primary Catalytic Method for Tar Abatement, Energy Fuels. 24 (2010) 2034–2041.

[77] F. Miccio, B. Piriou, G. Ruoppolo, R. Chirone, Biomass gasification in a catalytic fluidized reactor with beds of different materials, Chemical Engineering Journal. 154 (2009) 369–374.

[78] Y. Xie, J. Xiao, L. Shen, J. Wang, J. Zhu, J. Hao, Effects of Ca-Based Catalysts on Biomass Gasification with Steam in a Circulating Spout-Fluid Bed Reactor, Energy Fuels. 24 (2010)

3256–3261.

[79] A. Olivares, M.P. Aznar, M.A. Caballero, J. Gil, E. Frances, J. Corella, Biomass Gasification: Produced Gas Upgrading by In-Bed Use of Dolomite, Ind. Eng. Chem. Res. 36 (1997) 5220–5226.

[80] N.H. Florin, A.T. Harris, Enhanced hydrogen production from biomass with in situ carbon dioxide capture using calcium oxide sorbents, Chemical Engineering Science. 63 (2008) 287–316.

[81] J. Delgado, M.P. Aznar, J. Corella, Biomass Gasification with Steam in Fluidized Bed: Effectiveness of CaO, MgO, and CaO–MgO for Hot Raw Gas Cleaning, Ind. Eng. Chem. Res. 36 (1997) 1535–1543.

[82] C. Myrén, C. Hörnell, E. Björnbom, K. Sjöström, Catalytic tar decomposition of biomass pyrolysis gas with a combination of dolomite and silica, Biomass and Bioenergy. 23 (2002) 217–227.

[83] J. Corella, M. Aznar, J. Gil, Biomass gasification in fluidized bed: where to locate the dolomite to improve gasification? Energy Fuels. 13 (1999) 1122–1127.

[84] N. Alarcón, X. García, M.A. Centeno, P. Ruiz, A. Gordon, New effects during steam gasification of naphthalene: the synergy between CaO and MgO during the catalytic reaction, Applied Catalysis, a: General. 267 (2004) 251–265.

[85] J. Delgado, M.P. Aznar, J. Corella, Calcined Dolomite, Magnesite, and Calcite for Cleaning Hot Gas from a Fluidized Bed Biomass Gasifier with Steam: Life and Usefulness, Ind. Eng. Chem. Res. 35 (1996) 3637–3643.

[86] T. Kyotani, S. Hayashi, A. Tomita, Study of calcium catalysis on carbon gasification with molecular oxygen-18, Energy Fuels. 5 (1991) 683–688.

[87] S.A. Nair, K. Yan, A.J.M. Pemen, E.J.M. van Heesch, K.J. Ptasinski, A.A.H. Drinkenburg, Tar Removal from Biomass-Derived Fuel Gas by Pulsed Corona Discharges. A Chemical Kinetic Study, Ind. Eng. Chem. Res. 43 (2004) 1649–1658.

[88] S.G. Chen, R.T. Yang, Unified Mechanism of Alkali and Alkaline Earth Catalyzed Gasification Reactions of Carbon by CO2 and H2O, Energy Fuels. 11 (1997) 421–427.

[89] S.G. Chen, R.T. Yang, The Active Surface Species in Alkali-Catalyzed Carbon Gasification: Phenolate (C---O---M) Groups vs Clusters (Particles), Journal of Catalysis. 141 (n.d.) 102–113.

[90] U. Wolfesberger, I. Aigner, H. Hofbauer, Tar content and composition in producer gas of fluidized bed gasification of wood—Influence of temperature and pressure, Environ. Prog. Sustainable Energy. 28 (2009) 372–379.

[91] V. Wilk, H. Kitzler, S. Koppatz, C. Pfeifer, H. Hofbauer, Gasification of waste wood and bark in a dual fluidized bed steam gasifier, Biomass Conv. Bioref. 1 (2011) 91–97.

[92] I. Aigner, C. Pfeifer, H. Hofbauer, Co-gasification of coal and wood in a dual fluidized bed gasifier, Fuel. 90 (2011) 2404–2412.

[93] J.C. Schmid, U. Wolfesberger, S. Koppatz, C. Pfeifer, H. Hofbauer, Variation of feedstock in a dual fluidized bed steam gasifier—influence on product gas, tar content, and composition, Environ. Prog. Sustainable Energy. 31 (2012) 205–215.

[94] S.V. Vassilev, D. Baxter, L.K. Andersen, C.G. Vassileva, An overview of the chemical composition of biomass, Fuel. 89 (2010) 913–933.

[95] B.V. L'Vov, Mechanism of thermal decomposition of alkaline-earth carbonates, Thermochimica Acta. 303 (1997) 161–170.

[96] E. Roedder, Silicate melt systems, Physics and Chemistry of the Earth. 3 (1959) 224–297.

[97] W. Bragg, R.E. Gibbs, The Structure of Formula and Formula Quartz, Proceedings of the Royal Society a: Mathematical, Physical and Engineering Sciences. 109 (1925) 405–427.

[98] P. Engler, M.W. Santana, M.L. Mittleman, D. Balazs, Non-isothermal, in situ XRD analysis of dolomite decomposition, Thermochimica Acta. 140 (1989) 67–76.

[99] S. Arvelakis, P.A. Jensen, K. Dam-Johansen, Simultaneous Thermal Analysis (STA) on Ash

from High-Alkali Biomass, Energy Fuels. 18 (2004) 1066–1076.

[100]   G. Goswami, B.P. Padhy, J.D. Panda, Thermal analysis of spurrite from a rotary cement kiln, J Therm Anal Calorim. 35 (1989) 1129–1136–1136.

[101]   F.C. Kracek, N.L. Brown, G.W. Morey, Equilibrium Relations and Factors Influencing Their Determination in the System K2SiO3,AlSiO2, The Journal of Physical Chemistry. 41 (1937) 1183–1193.

[102]   C. Pfeifer, B. Puchner, H. Hofbauer, Comparison of dual fluidized bed steam gasification of biomass with and without selective transport of CO2, Chemical Engineering Science. 64 (2009) 5073–5083.

[103]   I. Aigner, U. Wolfesberger, H. Hofbauer, Tar Content and Composition in Producer Gas of Fluidized Bed Gasification and Low Temperature Pyrolysis of Straw and Wood - Influence of Temperature, in: Vienna, Austria, 2009: pp. 1–9.

[104]   T. Pröll, H. Hofbauer, Development and Application of a Simulation Tool for Biomass Gasification Based Processes, International Journal of Chemical Reactor Engineering. 6 (2008).

[105]   I. Aigner, Co-gasification of coal and wood with steam in a dual fluidized bed gasifier, PhD thesis, Vienna University of Technology, 2010.

[106]   O. Cencic, H. Rechberger, Material flow analysis with software STAN, Journal of Environmental Engineering and Management. 18 (2008) 3–7.

[107]   F.J. Frandsen, Ash Research from Palm Coast, Florida to Banff, Canada: Entry of Biomass in Modern Power Boilers, Energy Fuels. 23 (2013) 3347–3378.

Publication I

Kirnbauer, F.; Hofbauer, H. Investigations on Bed Material Changes in a Dual Fluidized Bed Steam Gasification Plant in Güssing, Austria. Energy Fuels 2011, 25, 3793–3798.

Investigations on Bed Material Changes in a Dual Fluidized Bed Steam Gasification Plant in Güssing, Austria

Friedrich Kirnbauer*,[†] and Hermann Hofbauer[‡]

[†]Bioenergy 2020+ GmbH, Wiener Strasse 49, A-4570 Güssing, Austria

[‡]Institute of Chemical Engineering, Vienna University of Technology, Getreidemarkt 9/166, 1060 Vienna, Austria

ABSTRACT: Bed material coating in fluidized biomass combustion plants is a precursor for bed agglomeration. While bed agglomeration is a well-described problem in connection with biomass combustion plants, the literature on bed agglomeration or bed material coating in gasification plants is sparse. Recently developed biomass gasification plants face similar ash-related problems, but inorganic matter is also linked to their catalytic activity to reduce the tar concentration in the product gas. This paper summarizes recent ash-related research activities at a dual fluidized bed steam gasification plant located in Güssing, Austria. The used fuel is forestry residues; the bed material is olivine. The setup of inorganic flows and loops is described. Bed material analyses were carried out and presented, such as X-ray fluorescence, X-ray diffraction, and scanning electron microscopy with energy-dispersive X-ray spectroscopy. The analyses show the building of two calcium-rich layers around the bed particles. The inner layer is homogeneous, composed mainly of calcium and silicate, while the outer layer has a similar composition to the fly ash of the plant. Analyses of the crystal structure of the used bed material show the formation of calcium silicates that were not detected in the fresh bed material. This has consequences on the performance of the plant concerning the catalytic activity of the bed material and the tendency for fouling in the plant.

■ INTRODUCTION

Biomass steam gasification is a promising technology as a carbon-neutral energy source to produce electricity and heat. Dual fluidized bed (DFB) steam gasification is one of various technologies for biomass steam gasification.[1] This technology was developed at the Vienna University of Technology and is successfully demonstrated at the biomass power plants at Güssing, Austria (8 MW$_{th}$ fuel power),[2] and Oberwart, Austria (8.5 MW$_{th}$ fuel power).[3] The plant in Güssing produces electricity in a gas engine (2 MW$_{el}$) commercially and has had an operation time (until the end of February 2011) of approximately 56 000 h at the gasifier and approximately 51 000 h at the gas engine since startup in late 2001. Research projects are ongoing for usage of the product gas for production of second-generation fuels such as methane, Fischer—Tropsch diesel, and synthetic mixed alcohols.[4,5] Other plants using dual fluidized steam gasification technology are at startup or under construction, for example in Villach, Austria, or Ulm, Germany.[3]

This paper focuses on bed material examinations from the DFB steam gasification of the plant in Güssing, Austria. The plant operates with forestry residues harvested in the local area of the plant.

The basic principle of this biomass gasification technology is the separation of endothermic steam gasification from the exothermic combustion zone. Heat is transferred via a circulating bed material from the combustion zone to the gasification zone to provide heat for gasification. The fluidized bed in the gasification zone is fluidized with steam that also acts as a gasification agent. The combustion zone is fluidized by combustion air in a fast-fluidized bed where a part of the fuel is combusted to provide heat for gasification. Due to its catalytic activity in terms of tar reduction in the product gas, olivine is used as the bed material.

For further reduction of the tar concentration in the product gas, calcium-rich catalytic additives such as dolomite or calcium oxide are used.[6−8] DFB gasification is well-described in the literature.[2,9] Most studies have focused on the gasification properties of different fuels and the catalytic properties of bed materials, focusing on the development of catalytic bed materials.[3,7,8,10−16]

Due to commercial pressure to increase availability, reduce operational supplements, and compete with conventional biomass combustion plants, research had been initiated concerning solid flows, bed material coatings, and agglomeration and fouling to reduce unplanned stops.

High alkali metal content of biomass fuels causes various ash-related problems during combustion in fluidized bed boilers such as bed agglomeration and fouling.[17,18] Use of catalytic bed material such as olivine and addition of catalytic additives to decrease the tar content in the producer gas results in different compositions of the ash and different thermal behavior compared to conventional biomass fluidized bed combustion boilers.

Laboratory-scale examinations on combustion and gasification of woody biomass show the formation of coatings around the bed material used for gasification and combustion.[19−23] The formation of multiple layers was shown with different compositions depending on the fuel and the bed material composition.[20,24] For woody biomass with the bed material quartz sand, laboratory-scale trials showed that the inner layer consists mainly of potassium—calcium silicates, while the outer layer consists of ash components.[19,25] Comparisons of quartz sand and olivine show similar results.[21] Investigations concerning agglomeration
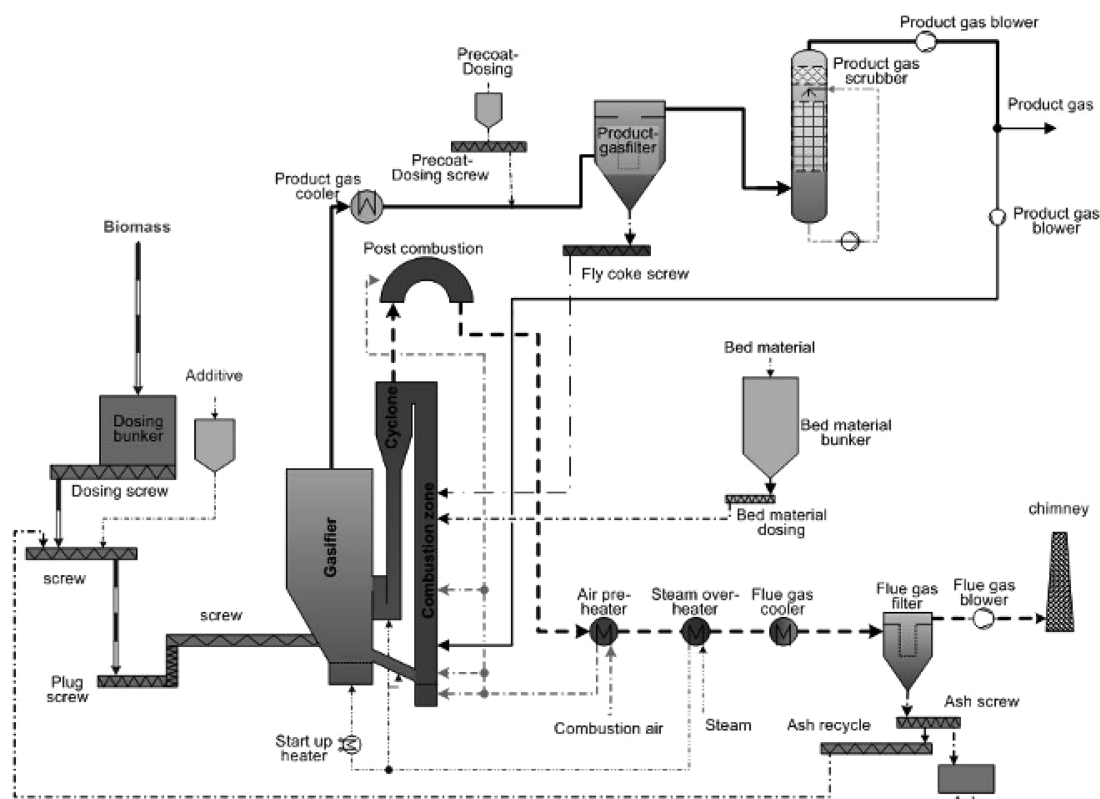
Figure 1. Basic flow sheet of the DFB gasification plant in Güssing.

behavior under gasification conditions showed no significant changes compared to combustion conditions.[19] Studies were carried out for the addition of dolomite or other additives in the bed to reduce the agglomeration tendency of the fuel ash.[26−28] However, literature of lab-scale plants for specific questions under limited conditions is available but not for industrial-scale DFB gasification plants. In DFB gasification, most of the conditions described above are occurring. A gasification atmosphere at 850 °C and a combustion atmosphere at 970 °C is available, and the addition of calcium-rich additives is the difference from the examinations in literature. The ash circles lead to an intensive ash contact in the gasification and the combustion zones between the bed material and the fuel ash.

However, there is no literature available on bed material coatings in DFB gasifiers. The objective of this work is the investigation of bed material coatings in DFB gasification. A better understanding of ash-related issues connected with the catalytic activity of inorganic matter gives prospects for the usage of alternative biomass fuels such as residues from agriculture.

■ EXPERIMENTAL SECTION

DFB Biomass Gasification. Figure 1 shows the basic flow sheet of the DFB process performed at the plant in Güssing. Woody biomass qis gasified in the gasifier with steam at 850−900 °C in a stationary fluidized bed. The required heat is transferred with the bed material from the combustion zone, which is operated at 950−1000 °C, to the gasification zone.

The product gas leaves the gasifier at 850 °C through the product gas cooler, where it is cooled down to 160 °C. Mostly inorganic particles with fine char particles that are not gasified leave the gasification zone with the product gas. This fly char—containing fine char particles, tars, and mainly inorganic matter such as biomass ash, attrition, and catalytic additives—is separated from the product gas flow in the product gas filter and is burnt in the combustion chamber to utilize the remaining energy of the char. The product gas is further washed at a rapeseed methyl ester (RME) scrubber and compressed for further utilization.

A part of the fuel that is not converted in the gasifier is transported together with bed material via a chute to the combustion zone where it is burnt. After the combustion zone, bed material is separated from the flue gas in the cyclone and the hot bed material is fed to the gasifier, supplying the required heat for gasification. Fine particles like ash, bed material attrition, and additives leave the cyclone with the flue gas at 970−1000 °C. Depending on the performance of the cyclone, the fly ash can contain a considerable content of bed material. The flue gas is cooled down in several heat exchangers to 160 °C, and fly ash is separated in the flue gas filter. A part of the fly ash is recirculated to the gasifier due to its catalytic activity for gasification while the other part is disposed.

Inorganic flows enter the plant with the biomass ash into the gasifier, fresh bed material is added to the combustion zone, and calcium-rich additives such as dolomite or calcium oxide are used as catalytic agents either prior to the gasifier or right before the product gas filter. Inorganic matter is discharged only at the flue gas filter.

Sampling. Wood ash samples were taken during regular production and analyzed for elemental composition. To obtain representative values, the samples were taken according to CEN/TS 14780:2005 from the wood chips pile. Samples were taken on two different days and ash

Table 1. Fuel Ash and Fly Ash Composition by XRF Analysis

component	wood chip ash (wt %)	fly ash, <200 μm (wt %)
Na_2O	3.9	2.5
MgO	4.9	29.1
Al_2O_3	2.3	1.5
SiO_2	13.0	24.1
P_2O_5	2.4	1.2
SO_3	1.5	0.4
K_2O	11.0	4.0
CaO	55.3	29.5
TiO_2	0.2	0.1
Cr_2O_3	0.1	0.3
MnO	1.6	0.8
Fe_2O_3	1.5	5.6
Co_3O_4	0.7	0.0
NiO	0.1	0.2
CuO	0.1	0.0
ZnO	0.1	0.0
SrO	0.2	0.1
Sb_2O_3	0.1	0.1
BaO	0.6	n/a[a]
Cl	0.6	0.4

[a] Not applicable.

Table 2. Comparison of Unused and Used Olivine

component	unused olivine (wt %)	used olivine (wt %)
MgO	46.8	40.0
SiO_2	39.8	34.9
CaO	0.9	10.0
Fe_2O_3	10.3	8.1
K_2O	0.32	3.8
Na_2O	0.43	0.73
Al_2O_3	0.40	0.60
Cr_2O_3	0.28	0.55
MnO	0.15	0.29
P_2O_5	0.03	0.25
Cl	0.10	0.21
NiO	0.31	0.20
Co_3O_4	0.03	0.11
ZrO_2	n/a[a]	0.10
SO_3	0.06	0.06
TiO_2	0.02	0.04
ZnO	0.01	0.02
CuO	0.03	0.02
SrO	0.00	0.02
MoO_3	0.01	0.01
CdO	n/a	0.01
Nb_2O_5	0.01	0.01
V_2O_5	0.01	0.00

[a] Not applicable.

was produced according to DIN CEN/TS 14775 to determine the ash content. The remaining ash was analyzed by X-ray fluorescence (XRF) analysis.

Fly ash was taken from the ash container after the flue gas filter. To remove coarse particles of mainly bed material, the samples were sieved with a 200 μm sieve. The elemental composition was determined by XRF.

Unused bed material samples were taken at the delivery of the olivine. Used bed material was taken from the bottom of the combustion zone during shutdown after cooling down the plant. Since the retention time of the bed material in the reactor varies, a number of samples were taken for elemental analyses.

The elemental composition of the samples was determined by XRF and calculated as oxides. Samples for XRF were melted in a Merck Spectromelt at 1050 °C and dumped on a 400 °C stainless steel plate. The analyses were carried out with a PANalytical Axios Advanced analyzer under vacuum atmosphere with a rhodium anode, an excitation voltage of 50 kV, and a tube current of 50 mA. The results indicate the elemental composition of the total sample calculated in oxides.

Two bed material samples were analyzed by X-ray diffraction measurements. X-ray diffraction measurements were performed on a PANalytical X'Pert PRO system. Refinements were performed with the TOPAS 4.2 program package.

The samples for the SEM-EDX analysis were mounted in epoxy, sanded, and polished. Analyses were carried out on a scanning electron microscope (SEM), FEI Philips model XL30, combined with energy-dispersive X-ray spectroscopy (EDX). A number of spot analyses were taken for composition of the layers of different particles, and average compositions were calculated. The EDX indicates the elemental composition of the surface of the sample.

■ RESULTS AND DISCUSSION

The ash composition of the fuel is shown in Table 1. The result shows that calcium is the dominating element in biomass ash. Silicate and magnesium are in the range that is expected for woody biomass. A significant high content of potassium and sodium is

caused by high bark content in the fuel. For comparison of the influence of attrition of the bed material and the catalytic additives, the composition of fly ash is also shown in Table 1. Due to the varying performance of the cyclone, the fly ash was sieved with a 200 μm sieve to remove remaining bed material particles.

The results of XRF analyses of used and unused olivine are shown in Table 2. The natural mineral olivine consists of magnesium, silicon, and iron [$(Mg, Fe)_2SiO_4$] as its main components. The results for the elemental analysis brought expected results. The elemental composition of the used bed material showed a significant increase in calcium and potassium content. A comparison of the elemental composition of the main components is visualized in Figure 2.

These results are confirmed by the X-ray diffraction (XRD) analysis shown in Table 3. While unused olivine has forsterite (Mg_2SiO_4) as a dominant component and calcium silicates such as bredigite [$Ca_{14}Mg_2(SiO_4)_8$], larnite (Ca_2SiO_4), or gehlenite [$Ca_2Al(AlSi)O_7$] are not detectable. The absence of iron silicate is caused by the calcination at 1400 °C of the olivine before it is delivered and used in the plant. A calcination of olivine at this temperature leads to decomposition of iron silicates.[29] The XRD analyses of the used olivine showed significant amounts of calcium silicates such as bredigite and larnite. Periclase (MgO) and fayalite (Fe_2SiO_4) are detectable in the sample of used bed material.

An SEM image of unused bed material is shown in Figure 3. The image shows a particle with cavities and inclusions with different composition, as expected from a natural mineral. However, the particle shows the same composition inside and on the surface. EDX analyses from inside the particle are shown in
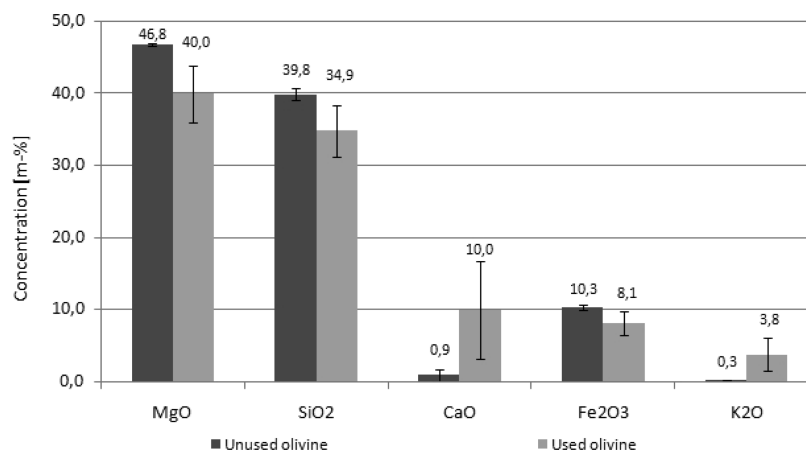
Figure 2. XRF analysis: comparison of unused and used olivine.

Table 3. XRD Results of Unused and Used Bed Material[a]

		unused olivine, sample A	used olivine, sample B	comparison, unused vs used olivine
forsterite	Mg_2SiO_4	S	S	sample A≫ sample B
bredigite	$Ca_{14}Mg_2(SiO_4)_8$	n/a	S-M	new phase in sample B
periclase	MgO	n/a	M	new phase in sample B
larnite	Ca_2SiO_4	n/a	M	new phase in sample B
"pyrophyllite 1A (dehydroxylated)"	$Al_2Si_4O_{10}(OH)_2$	n/a	TR-M	new phase in sample B
magnetite	Fe_3O_4	M	TR-M	sample A > sample B
fayalite	Fe_2SiO_4	n/a	TR-W	new phase in sample B
gehlenite	$Ca_2Al(AlSi)O_7$	n/a	TR	new phase in sample B
lazulite	$(Mg, Fe) Al_2(PO_4)_2(OH)_2$	W	n/a	phase vanishes in sample B

[a] S, strong diffraction; M, medium; W, weak; TR, trace; n/a, not applicable.

Table 4. The particle consists of the elements magnesium, silicon, iron, and oxygen.

An image of used olivine (Figure 4) shows the formation of a layer on the surface of the particle. By more detailed analysis (Figure 5), two layers can be determined. The inner layer seems to be more homogeneous than the outer layer. This kind of formation of layers could be seen on the majority of particles. Particles with a circular shape like the particle shown in Figure 4 have distinctive layer formation, while particles with a less pronounced circular shape show less distinctive layer formation. This is caused by the different retention time of the particles in the bed due to a constant feeding of fresh olivine to compensate for bed material losses because of abrasion and loss with the fly ash.

EDX analyses of the two layers shown in Table 4 indicate a high concentration of calcium in the inner layer with the two main components silicon and oxygen. The concentration of magnesium and iron is decreased compared to the unused particle. The composition of the outer layer is dominated by the main components of ash such as calcium, magnesium, silicon, and oxygen.

The inside of the used olivine particles shows an increase in potassium and a slight increase in calcium while the concentrations of other elements such as magnesium, silicon, and iron remain in the range of unused olivine.
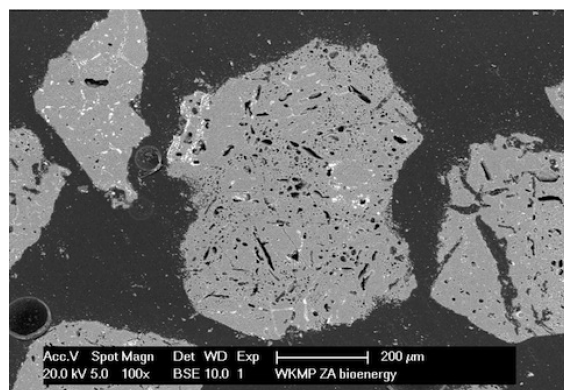
Figure 3. SEM image of unused olivine.

These results of the bed material analyses confirm the observations from the literature. The high concentration of calcium in the particle layers is caused by the addition of calcium-rich additives. The circulation of fly ash (bed material and fine ash) leads to the formation of layers in the bed material.

Table 4. EDX Comparison of Olivines

	unused olivine	used olivine		
element	particle inside (wt %)	particle inside (wt %)	inner layer (wt %)	outer layer (wt %)
C	n/a[a]	n/a	5.3	9.8
O	15.2	14.2	12.9	13.7
Mg	37.4	30.3	8.6	18.5
Al	0.1	0.7	0.1	0.1
Si	35.5	32.2	17.3	15.4
P	n/a	0.0	n/a	0.3
K	n/a	8.5	2.6	3.2
Ca	n/a	1.8	46.5	33.5
Cr	n/a	n/a	2.7	0.4
Mn	n/a	0.0	0.9	1.2
Fe	11.8	12.5	3.0	3.7

[a] Not applicable.
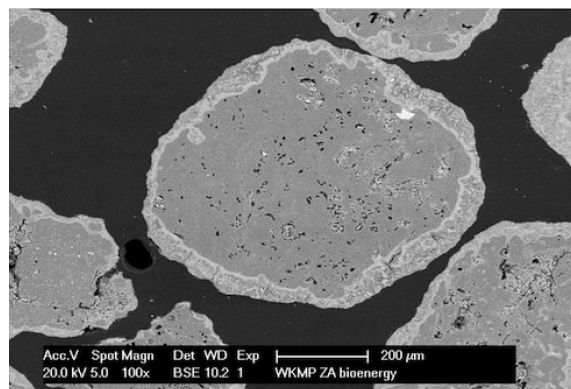
Figure 4. SEM image of used olivine.

Risnes et al.[30] describes the preferred formation of liquid salt melts in wheat ashes when calcium is added to the raw fuel. Calcium silicates are formed, while potassium silicates decrease.

The layer formation of the examined olivine particles confirms this theory. When high amounts of calcium are detectable in the inner layer, the potassium concentration in this layer is lower. Crystalline phases of potassium were not detectable. The higher potassium concentration in the particle inside the used olivine is caused by the high volatile content of potassium at the temperatures of gasification (850 °C) and combustion (970 °C).[19]

According to the literature,[25] three mathods of layer formation are possible: (a) the layer grows outward from the particle, (b) the layer grows into the particle, or (c) a combination of cases a and b. In case a, the composition of the layer consists mainly of fuel ash components. In case b, reactive components are inserted into the particle structure. The examinations in this study showed both cases: the inner layer with a constant thickness within each particle and the homogeneous structure and composition indicates that the layer grows into the particle, forming a stable crystal structure. The crystal structure of olivine is modified with the implementation of calcium. On the contrary, the outer layer is inhomogeneous with a different thickness that indicates that the layer grows outward from the particle.
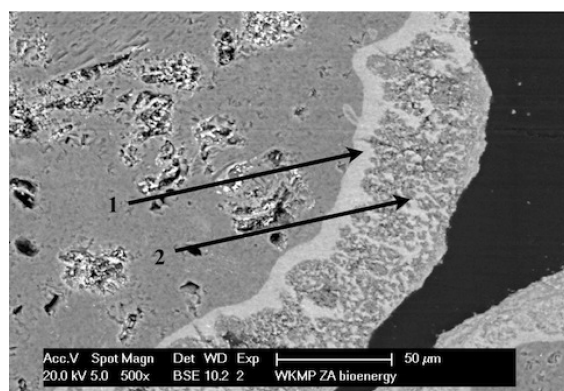
Figure 5. SEM image of (1) inner and (2) outer layers of used olivine.

Layer formation is described in the literature as an interaction between potassium, calcium, and silicon.[24,25] Silicon has its main origin in the bed material, but the fuel ash also contains a considerable amount of silicon. The origin of potassium is only the fuel ash, while calcium is detectable at considerable levels in fuel ash and additives.

The low amount of potassium in the layer can be explained because high calcium concentrations inhibit the redeposition of potassium into the silicates, since these positions are preferentially filled by calcium.[30−32]

Layer formation on the bed material is often linked to bed agglomeration problems in the literature and operational problems in the plant. Bed material agglomeration has not been encountered in the DFB plant in Güssing. An influence on catalytic activity is assumed, and operational problems due to fouling are considered to be linked to the bed material coating.

■ CONCLUSIONS

Bed material of biomass steam gasification in a dual fluidized bed gasifier located in Güssing/Austria was studied. These studies should give a better understanding of the long-term changes to the bed material during regular production in a commercial DFB gasifier and the influence of these changes on the operation of the plant. The bed material was analyzed by XRF, XRD, and SEM/EDX techniques. These analyses show layer formation on the bed material. Two calcium-rich layers are built; the inner layer consists mainly of calcium silicates while the outer layer has a similar composition to fine ash. The formation of calcium-rich layers is attributed to the high calcium content of wood ash and to the addition of calcium-rich additives to improve the catalytic properties of the bed material in terms of tar reduction.

The long-term interaction between biomass ash and bed material needs to be considered for the control of inorganic flows and also for the development of new catalytic bed material.

■ AUTHOR INFORMATION

Corresponding Author
*Phone + 43 (0) 3322 42606-156; fax + 43 (0) 3322 42606-199; e-mail friedrich.kirnbauer@bioenergy2020.eu.

■ ACKNOWLEDGMENT

■ REFERENCES

(1) E4Tec. *Review of Technologies for Gasification of Biomass and Wastes*; NNFCC Publications Final Report, 9th ed.; NNFCC, The UK's National Centre for Biorenewable Energy, Fuels and Materials, 2009; p 130.

(2) Hofbauer, H.; Rauch, R.; Loeffler, G.; Kaiser, S.; Fercher, E.; Tremmel, H. In *Proceedings of the 12th European Conference on Biomass and Bioenergy*, Amsterdam, 2002; p 4.

(3) Pfeifer, C.; Koppatz, S.; Hofbauer, H. *Biomass Convers. Biorefinery* **2011**, 1–12.

(4) Rehling, B.; Hofbauer, H. In *ICPS 09 - International Conference on Polygeneration Strategies*, Vienna, Austria, 2009.

(5) Rauch, R.; Hofbauer, H.; Săcăreanu, S.; Chiru, A. *Bull. Transilvania Univ. Brasov, Ser. I: Eng. Sci.* **2011**, *3*, 33–40.

(6) Rapagná, S.; Jand, N.; Kiennemann, A.; Foscolo, P. U. *Biomass Bioenergy* **2000**, *19*, 187–197.

(7) Devi, L.; Ptasinski, K. J.; Janssen, F. J. J. G.; van Paasen, S. V. B.; Bergman, P. C. A.; Kiel, J. H. A. *Renewable Energy* **2005**, *30*, 565–587.

(8) Koppatz, S.; Pfeifer, C.; Rauch, R.; Hofbauer, H.; Marquard-Moellenstedt, T.; Specht, M. *Fuel Process. Technol.* **2009**, *90*, 914–921.

(9) Bolhar-Nordenkampf, M.; Hofbauer, H.; Bosch, K.; Rauch, R.; Aichernig, C. In *Proceedings of the International Conference on Biomass Utilisation*; Kirtikara, K., Ed.; Phuket, Thailand, 2003; Vol. *1*, pp 567−572.

(10) Pfeifer, C.; Puchner, B.; Hofbauer, H. *Chem. Eng. Sci.* **2009**, *64*, 5073–5083.

(11) Pfeifer, C.; Rauch, R.; Hofbauer, H. *Ind. Eng. Chem. Res.* **2004**, *43*, 1634–1640.

(12) García, L.; Salvador, M. L.; Arauzo, J.; Bilbao, R. *Energy Fuels* **1999**, *13*, 851–859.

(13) Mitsuoka, K.; Hayashi, S.; Amano, H.; Kayahara, K.; Sasaoka, E.; Uddin, M. A. *Fuel Process. Technol.* **2011**, *92*, 26–31.

(14) Rapagná, S.; Virginie, M.; Gallucci, K.; Courson, C.; Di Marcello, M.; Kiennemann, A.; Foscolo, P. U. *Catal. Today* **2011**(in press).

(15) Miccio, F.; Piriou, B.; Ruoppolo, G.; Chirone, R. *Chem. Eng. J.* **2009**, *154*, 369–374.

(16) Ruoppolo, G.; Miccio, F.; Chirone, R. *Energy Fuels* **2010**, *24*, 2034–2041.

(17) Valmari, T.; Lind, T. M.; Kauppinen, E. I.; Sfiris, G.; Nilsson, K.; Maenhaut, W. *Energy Fuels* **1998**, *13*, 379–389.

(18) Davidsson, K. O.; Amand, L. E.; Steenari, B. M.; Elled, A. L.; Eskilsson, D.; Leckner, B. *Chem. Eng. Sci.* **2008**, *63*, 5314–5329.

(19) Öhman, M.; Pommer, L.; Nordin, A. *Energy Fuels* **2005**, *19*, 1742–1748.

(20) Brus, E.; Öhman, M.; Nordin, A. *Energy Fuels* **2005**, *19*, 825–832.

(21) De Geyter, S.; Öhman, M.; Boström, D.; Eriksson, M.; Nordin, A. *Energy Fuels* **2007**, *21*, 2663–2668.

(22) Nuutinen, L. H.; Tiainen, M. S.; Virtanen, M. E.; Enestam, S. H.; Laitinen, R. S. *Energy Fuels* **2003**, *18*, 127–139.

(23) Fryda, L. E.; Panopoulos, K. D.; Kakaras, E. *Powder Technol.* **2008**, *181*, 307–320.

(24) Brus, E.; Öhman, M.; Nordin, A.; Boström, D.; Hedman, H.; Eklund, A. *Energy Fuels* **2004**, *18*, 1187–1193.

(25) Zevenhoven-Onderwater, M.; Öhman, M.; Skrifvars, B.-J.; Backman, R.; Nordin, A.; Hupa, M. *Energy Fuels* **2006**, *20*, 818–824.

(26) Steenari, B. M.; Lindqvist, O. *Biomass Bioenergy* **1998**, *14*, 67–76.

(27) Steenari, B. M.; Karlfeldt Fedje, K. *Fuel* **2010**, *89*, 2026–2032.

(28) Öhman, M.; Boström, D.; Nordin, A.; Hedman, H. *Energy Fuels* **2004**, *18*, 1370–1376.

(29) Rauch, R.; Pfeifer, C.; Bosch, K.; Hofbauer, H. In *Proceedings of the Conference for Science in Thermal and Chemical Biomass Conversion*, Victoria, Canada, 2004.

(30) Risnes, H.; Fjellerup, J.; Henriksen, U.; Moilanen, A.; Norby, P.; Papadakis, K.; Posselt, D.; Sorensen, L. H. *Fuel* **2003**, *82*, 641–651.

(31) Thy, P.; Lesher, C. E.; Jenkins, B. M. *Fuel* **2000**, *79*, 693–700.

(32) Thy, P.; Jenkins, B. M.; Grundvig, S.; Shiraki, R.; Lesher, C. E. *Fuel* **2006**, *85*, 783–795.

Publication II

Kirnbauer, F.; Wilk, V.; Kitzler, H.; Kern, S.; Hofbauer, H. The positive effects of bed material coating on tar reduction in a dual fluidized bed gasifier. FUEL 2012, 95, 553–562.

The positive effects of bed material coating on tar reduction in a dual fluidized bed gasifier

Friedrich Kirnbauer [a],*, Veronika Wilk [a], Hannes Kitzler [b], Stefan Kern [b], Hermann Hofbauer [b]

[a] Bioenergy 2020+ GmbH, Wiener Straße 49, A-7540 Güssing, Austria
[b] Vienna University of Technology, Institute of Chemical Engineering, Getreidemarkt 9/166, 1060 Vienna, Austria

ABSTRACT

The utilization of biomass for the substitution of fossil fuels to reduce greenhouse gas emissions in biomass steam gasification plants is a promising technology for the production of electricity, heat, and fuels for transportation. Experience from industrial scale dual fluidized bed steam gasification plants showed a modification of the bed material due to the interaction of the bed material (olivine) with biomass ash components and additives. In this paper the influence of bed material modification on the gasification properties of used olivine from an industrial scale plant in Güssing is compared with the case of fresh olivine. The trials were carried out under similar conditions in a pilot plant at the Vienna University of Technology. The pilot plant trials showed an increase in hydrogen and carbon dioxide in the product gas with the used bed material while the content of carbon monoxide in the product gas decreased. The exothermal water–gas shift reaction is enhanced by the used bed material, resulting in a lower energy demand for the gasification. Tar content was decreased by around 80% for tars detected by gas chromatography–mass spectrometry (GCMS) and the composition of the tar showed less components during the trial with used bed material.

The results obtained with the used bed material at the 100 kW pilot plant are in good agreement with those for the 8 MW industrial plant in Güssing, confirming good scale-up properties from the 100 kW plant to industrial scale plants.

© 2011 Elsevier Ltd. All rights reserved.

1. Introduction

Biomass can play a significant role by substituting for fossil fuels which cause greenhouse gas emissions in the production of electricity and second generation biofuels [1]. Biomass is a renewable source and releases the same amount of carbon dioxide during energy usage or natural decomposition as it aggregates during the growth period. Using woody biomass for steam gasification is a promising technology that has been successfully demonstrated since late 2001.

The basic principle of biomass gasification is the thermal decomposition of biomass using a gasification agent such as steam, air, or carbon dioxide to produce a combustible gas consisting mainly of hydrogen, carbon monoxide, carbon dioxide, and methane. If air is used as a gasification agent a high amount of nitrogen is present in the producer gas, which reduces its heating value. The gas can be utilized for electricity production, fuel synthesis or synthetic natural gas.

Dual fluidized bed (DFB) steam gasification for biomass was developed by the Institute of Chemical Engineering, Vienna University of Technology [2]. A pilot plant (100 kW) is in operation at the Institute of Chemical Engineering, Vienna University of Technology, with various research activities concerning bed material [3–5] or different fuels [6,7]. This process was brought to the market by the first plant in Güssing (Austria; 8 MW[th]) in 2001, followed by plants in Oberwart (Austria; 8.5 MW[th]), Villach (Austria; 15 MW[th]), Ulm (Germany; 11.5 MW[th]), Götheborg (Sweden; 32 MW[th]), which commenced operation recently or are currently in the realization phase [4]. Various research activities concerning further utilization of the product gas in addition to production of heat and electricity are ongoing at the plants in Güssing and Oberwart [8,9].

The advantage of DFB steam gasification is the usage of steam as a gasification agent to avoid the introduction of nitrogen into the producer gas. It results in a producer gas with a high caloric value of 12–14 MJ/Nm³ (referred to as dry gas) and a high hydrogen content. To supply the thermal energy that is required for the endothermic gasification reactions in the bubbling bed a separate combustion zone with a fast fluidized bed is used. The bed material, which is heated up in the combustion zone, is transferred to the gasification zone.

* Corresponding author. Tel.: + 43 (0) 3322 42606 156; fax: + 43 (0) 3322 42606 199.
E-mail address: friedrich.kirnbauer@bioenergy2020.eu (F. Kirnbauer).

The main gasification reactions are shown in Table 1. These reactions are considered as equilibrium reactions with variable equilibrium conditions according to Le Chatelier's principle depending on gas concentrations, temperature and pressure. Since various reaction paths are possible, an enhancement of reaction paths is possible through the use of catalysts.

Undesired by-products of biomass gasification are described by the collective term "tars". Tars are defined as follows: "The organics, produced under thermal or partial-oxidation regimes (gasification) of any organic material, are called 'tars' and are generally assumed to be largely aromatic" [10].

These tars cause operational problems when cooled down and condensed at heat exchangers, plugging pipes, and so on. Various research activities focus on reduction of these tars before further utilization of the product gas. The chemical reactions concerning tar reduction are described in Table 2 for toluene as a model component. Similar reactions can be described for the other tar components. These chemical equations allow a wide range of reaction schemes and show the complexity of the topic.

To decrease the amount of tar in the product gas, catalytic material is used in the fluidized bed.

The use of olivine as a bed material has become state of the art in industrial scale DFB steam gasification plants. Additionally calcium-rich additives such as calcite or dolomite are used for further reduction of the tar content in the producer gas. Experience from the industrial scale plant in Güssing, Austria, showed that biomass ash and additives interact with bed material, building calcium-rich layers around the particles. The inner layer is homogeneous, composed mainly of calcium and silicate, while the outer layer has a similar composition to the fly ash of the plant [13]. Fig. 1 shows a micrograph of a used bed material particle and the results of energy-dispersive X-ray (EDX) spectroscopy are shown in Table 3. The positive effects of this calcium-rich layer on the tar reduction and the influence on the gas composition are known from the experience of the plant in Güssing. Experience also showed that the catalytic properties of the bed material improve with a higher retention time of the bed material in the system. This effect has not yet been described in detail or quantified.

The significant increase in calcium in the surface layer of the bed material leads to the assumption that the catalytic properties of the used bed material are dominated by the calcium-rich surface. Small amounts of potassium are also detected.

The positive effect of olivine on tar reduction has been reported by various authors with regard to various fuels [4,14–21]. A better catalytic activity of the olivine can be achieved by calcination of olivine [14,22]. Even better conversion is achieved by the use of modified olivine such as Ni-olivine, Fe-olivine [4,20,23–26] or synthetic catalysts [27–29].

Dolomite also showed good results with regard to the catalytic activity for reducing tars [3,4,18,30–33].

A comparison of dolomite and inert bed material was carried out by Ruoppolo et al. [27]. They reported a 50% higher tar conversion in a fluidized bed using dolomite as bed material compared to quartzite as well as a simplification of tar components.

Corella et al. [18] reported that the tar removal efficiency with dolomite was ~1.4 times better compared to olivine in a fluidized reactor. In a previous publication the authors concluded [34] that the introduction of dolomite into the fluidized bed gives better results compared to a down-stream usage of dolomite in a second reactor. The polymerization of tars is suspected to take place when using a gasification reactor with silica sand and a down-stream reactor with dolomite.

A laboratory scale quartz tube reactor was used by Simell et al. [11] to study the decomposition of toluene, which was used as a model component for tar over dolomite and nickel catalyst. They concluded that the dry reforming reaction (Formulas (15) and (16)) and steam reforming reaction (Formulas (9) and (10)) take place with both catalysts. The presence of steam inhibits the dry reforming reaction but tar decomposition is carried out with steam reforming. The presence of CO on dolomite strongly inhibited the tar decomposition on dolomite.

Alarcón et al. [35] studied the catalytic activity of a mixture of CaO with MgO for naphthalene steam gasification in a fixed bed. While pure MgO and CaO achieved carbon conversion of 54% and 62%, respectively, a mixture of 10% CaO and 90% MgO showed the highest carbon conversion, 79%. A catalytic synergy between the two oxides was described.

Similar results were published by Delgado et al. [36]. The authors studied the catalytic activity of calcined dolomite, calcite, and magnesite in a fixed bed reactor reforming product gas of a fluidized bed gasification reactor. The fixed bed reactor was loaded with the examined catalyst. They reported better gas yields and tar reduction with dolomite followed by calcite and magnesite.

Kyotani et al. [37] investigated the mechanism of calcium catalysis of carbon gasification with oxygen. They found that calcium enhances the formation of CO_2 in carbon gasification with O_2. The process was explained as follows: O_2 dissociatively chemisorbs on CaO particles to form CaO(O). The active oxygen from CaO(O) quickly migrates to the carbon surface to form C(O). When active sites around CaO are occupied by C(O), oxygen reacts with the C(O) at the active site to CO_2 which is released leaving an active site on the CaO.

Nair et al. [38] studied the tar removal of biomass-derived fuel gas by pulsed corona discharge with respect to the decomposition scheme of naphthalene. They concluded that the most favorable pathway for tar decomposition is the direct attack of oxygen radicals.

This theory is also confirmed by studies by Chen and Yang [39] on alkali and earth alkali metals where the authors catalyzed gasification reactions of graphite by CO_2 and H_2O. They reported the formation of C–O–M groups, where M denotes for the metal. Oxygen radicals have their origin in CO_2 and H_2O. In earlier studies they found that particles are more active than single C–O–K groups [40].

However, the usage of bed materials with better catalytic activity than olivine is desired. Alternative bed materials to olivine often face problems with attrition (e.g. dolomite [4,19]) or their preparation is expensive (e.g. synthetic catalysts). The disposal of wastes of alternative bed materials such as nickel coated bed material is also problematic.

An exact statement about the influence of the formation of a calcium-rich layer on the catalytic properties of the bed material is not available. To study this effect, used bed material from the industrial scale gasification plant in Güssing, Austria, was used in the 100 kW DFB steam gasification pilot plant at the Institute of Chemical Engineering, Vienna University of Technology, and compared with the results of the utilization of unused olivine under the same conditions.

This paper summarizes the latest investigations of the catalytic properties of used olivine with a calcium-rich layer with regard to

Table 1
Typical equilibrium reactions of the main gas components [11,12].

Name of reaction	Chemical equation	ΔH (kJ/mol)	
Water–gas shift	$CO + H_2O \leftrightarrow CO_2 + H_2$	−40.9	Formula (1)
Methane reforming	$CO + 3 H_2 \leftrightarrow CH_4 + H_2O$	−225	Formula (2)
Water–gas (i)	$C + H_2O \leftrightarrow CO + H_2$	118.5	Formula (3)
Water–gas (ii)	$C + 2 H_2O \leftrightarrow CO_2 + 2 H_2$	103	Formula (4)
Boudouard	$C + CO_2 \leftrightarrow 2 CO$	159.9	Formula (5)
Methanation	$C + 2 H_2 \leftrightarrow CH_4$	−87.5	Formula (6)
Oxidation (i)	$C + O_2 \leftrightarrow CO_2$	−393.5	Formula (7)
Oxidation (ii)	$C + 0.5 O_2 \leftrightarrow CO$	−123.1	Formula (8)

Table 2
Possible reactions of hydrocarbons in hot gas cleaning conditions, with toluene as model hydrocarbon[11].

Name of reaction	Chemical equation	ΔH kJ/mol	
Steam reforming	$C_7H_8 + 7\ H_2O \rightarrow 7\ CO + 11\ H_2$	876	Formula (9)
	$C_7H_8 + 14\ H_2O \rightarrow 7\ CO_2 + 18\ H_2$	647	Formula (10)
Steam dealkylation	$C_7H_8 + H_2O \rightarrow C_6H_6 + 2\ H_2 + CO$	123	Formula (11)
	$C_7H_8 + 2\ H_2O \rightarrow C_6H_6 + 3\ H_2 + CO_2$	90	Formula (12)
Hydrocracking	$C_7H_8 + 10\ H_2 \rightarrow 7\ CH_4$	−713	Formula (13)
Hydrodealkylation	$C_7H_8 + H_2 \rightarrow C_6H_6 + CH_4$	−104	Formula (14)
Dry reforming	$C_7H_8 + 7\ CO_2 \rightarrow 14\ CO + 4\ H_2$	1105	Formula (15)
	$C_7H_8 + 11\ CO_2 \rightarrow 18\ CO + 4\ H_2O$	1236	Formula (16)
Thermal cracking	$nC_7H_8 \rightarrow m\ C_xH_y + p\ H_2$	–	Formula (17)
Carbon formation	$C_7H_8 \rightarrow 7\ C + 4\ H_2$	−73	Formula (18)
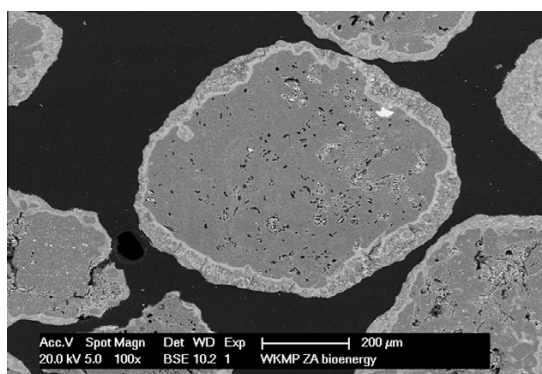
Fig. 1. Layer formation on used olivine [13].

Table 3
EDX: Comparison of unused and used olivine [13].

Olivine	Unused olivine	Used olivine		
	Particle inside (wt.%)	Particle inside (wt.%)	Inner layer (wt.%)	Outer layer (wt.%)
C	n/a	n/a	5.3	9.8
O	15.2	14.2	12.9	13.7
Mg	37.4	30.3	8.6	18.5
Al	0.1	0.7	0.1	0.1
Si	35.5	32.2	17.3	15.4
P	n/a	0.0	n/a	0.3
K	n/a	8.5	2.6	3.2
Ca	n/a	1.8	46.5	33.5
Cr	n/a	n/a	2.7	0.4
Mn	n/a	0.0	0.9	1.2
Fe	11.8	12.5	3.0	3.7

n/a = not applicable.

gas composition and tar reduction, and the results from an industrial scale plant are compared with results from the pilot plant.

2. Experimental section

Two trials were carried out at a 100 kW pilot plant, one using fresh olivine as a reference and one using used olivine from the industrial plant in Güssing. The results of these trials were compared with the results of the industrial scale plant in Güssing.

2.1. DFB biomass gasification

The DFB biomass-steam gasification plant in Güssing, Austria, has a thermal power of 8 MW and an electrical power of 2 MW. The plant went into operation in late 2001 and had an operation

time of 60,000 h at the gasifier and 54,500 h at the gas engine up to September 2011. Wood residues harvested in the local area are used as fuel. Various literature is available about the plant [2,41,42].

A basic flow sheet of the plant is shown in Fig. 2. Biomass is fed into the gasifier via a screw system and is gasified in a bubbling bed in the gasifier at 850 °C using steam as a gasification agent. Bed material also containing char is transferred to the combustion zone, where char is combusted in a fast fluidized bed at 930 °C. Air is used for fluidization in the combustion zone. The bed material is separated from the flue gas in the cyclone and transported back into the gasifier, providing the heat for the gasification. The flue gas is further cooled down and the fly ash is separated in the flue gas filter. A part of the fly ash is circulated into the gasifier due to its positive effects on tar reduction and to save bed material consumption.

The product gas is cooled down after leaving the gasifier and particles are separated from the gas stream in the product gas filter. The fly coke from the product gas filter contains inorganic matter such as biomass ash, additives, and products of bed material abrasion as well as unconverted char and tar. To utilize the remaining combustible substances, the fly coke is burnt in the combustion zone. After the separation of the particles from the product gas in the product filter, the gas is washed in a rapeseed methyl ester (RME) scrubber to remove water and tars. The cleaned gas is then utilized in a gas engine to produce electricity and heat. A small amount of the product gas is used to control the temperature of the combustion zone.

2.2. Description of the pilot plant

At the pilot plant at the Institute of Chemical Engineering, Vienna University of Technology, the basic design parameters of the gasifier in Güssing, Austria were developed. The basic principal of the gasifier is the same as that of the industrial scale plant in Güssing but due to its size some details are different. The pilot plant shown in Fig. 3 is well-described in literature [4,6,7].

However, the gasifier consists of a gasification zone with a bubbling bed, which is fluidized by steam, and a combustion zone with a fast fluidized bed, which is fluidized by air. The bed material is circulated between the two zones to carry the heat from the combustion zone to the gasification zone. The separation of the bed material and the flue gas after the combustion zone is carried out using a gravity separator. Siphons are located between the gasification zone and the combustion zone to avoid leakage of gases from the combustion zone such as air of flue gas into the gasification zone.

The fuel is dosed into the fluidized bed of the gasifier where water and volatile components of the fuel are released. The remaining char is gasified with steam. A part of the char is trans-
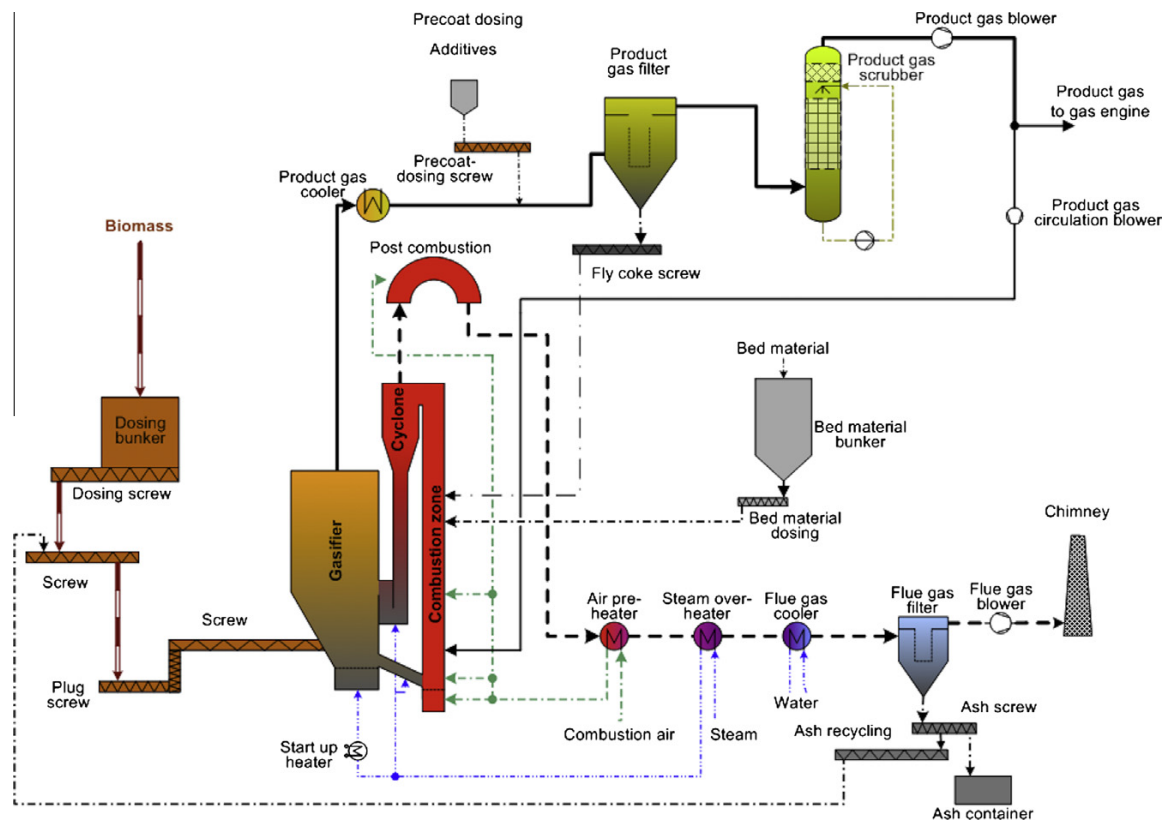
Fig. 2. Basic flow sheet of the DFB gasification in Güssing, Austria [13].

ported with the bed material to the combustion zone, where the char is burnt.

In contrast to the industrial scale plant the pilot plant is designed to add fuel into the combustion zone to provide a part of the required heat to the gasification not via transport through the chute but from outside the system. Light fuel oil is used in the pilot plant. The amount of fuel in the combustion zone with constant gasification temperatures allows a qualitative evaluation of the gasification properties of the fuel or a comparison of the bed material using the same fuel. In the industrial scale gasifier, fly coke from the filters, tar, saturated RME, and a small quantity of product gas are injected into the combustion reactor. The product gas is used to control the temperature.

The pilot plant is equipped with gas measurement in the product gas stream and in the flue gas stream.

2.3. Sampling at the industrial scale plant

The required amount of used bed material (150 kg) for the trial in the pilot plant was taken from the plant in Güssing in December 2010. The bed material was taken during regular operation from the bottom of the combustion zone. To avoid impact on the production of the plant, several batches were taken over a period of 2 days.

To have a similar particle size distribution compared to fresh olivine, the used bed material was sieved and the fractions smaller than 400 μm and bigger than 1 mm were removed to avoid the presence of fine ash or nails and broken refractory lining in the pilot rig.

Gas analyses at the industrial scale plant were carried out with a Clarus 500 gas chromatograph (GC) made by Perkin Elmer. The GC is equipped with three different columns: one molecular and two non-polar (Porapak) sieves, connected with two automated valves and an injection loop of 500 μl. Helium is used as the carrier gas. Two types of detectors are used: a thermal conductivity detector (TCD) for the permanent gases (O_2, N_2, CO, CO_2) and a flame ionization detector (FID) for hydrocarbons up to a carbon number of three. The hydrogen concentration is calculated as 100 minus the sum of the gas concentration given by the two detectors.

The average values of various measurements taken over the period from the beginning of October until the middle of January were calculated and used for comparison.

2.4. Sampling at the pilot plant

Wood pellets were used as a fuel in the trials in the pilot plant. A wood pellet sample was taken before both trials in the pilot plant and analyzed. The same batch of wood pellets was used for both trials. To obtain representative values the samples were taken on the basis of DIN 51701. Ash content was determined according to DIN 51719 but at 550 °C. The content of volatile matter was determined using DIN 51720 and the higher and lower heating values according to DIN 51900 T2.

The elemental composition of the unused and used bed material was determined by X-ray fluorescence (XRF) and calculated as oxides. Samples for XRF were melted in a Merck Spectromelt at 1050 °C and dumped on a 400 °C stainless steel plate. The analyses were carried out with a PANalytical Axios Advanced analyzer under a vacuum atmosphere with a rhodium anode, an excitation
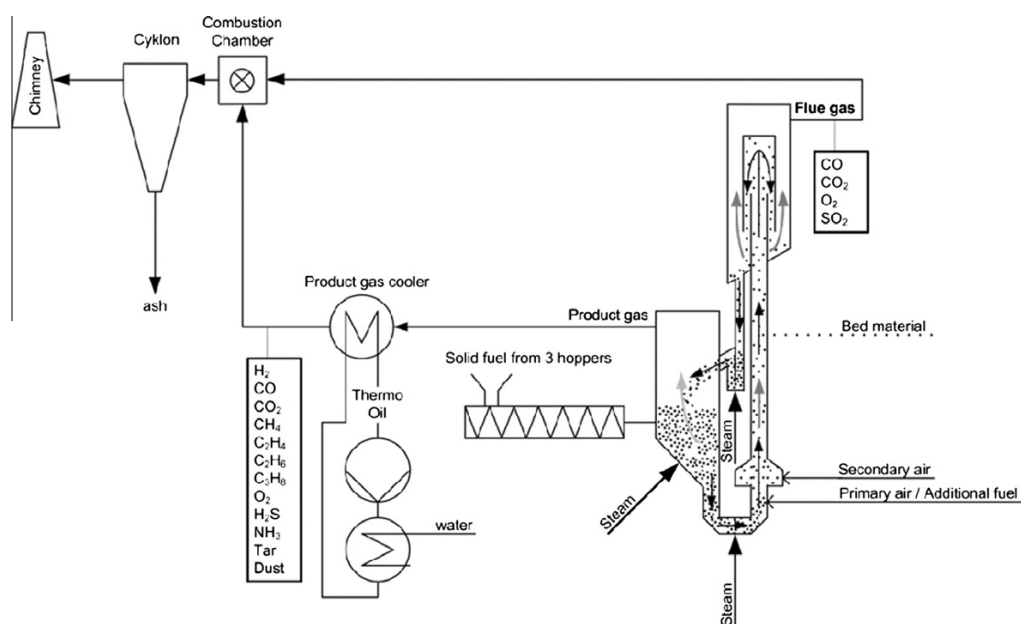
Fig. 3. 100 kW pilot plant [7].

voltage of 50 kV, and a tube current of 50 mA. The results indicate the elemental composition of the total sample calculated in oxides.

Gas and tar analysis of the product gas of the pilot plant is well-described in the literature [4–7]. Carbon monoxide, carbon dioxide, methane and hydrogen were measured by a Rosemount NGA2000. The components nitrogen, ethylene, ethane, and propane were measured by a gas chromatograph (Syntech Spectras GC 955). For the calculation of average values a stationary phase of the plant was taken into consideration. The stationary phase for the trial with unused bed material lasted for 2:25 h, while the one for the trial with used bed material lasted for 1:05 h. Tars are absorbed in toluene and measured similarly to the tar protocol. Detailed descriptions of the tar measurement are given by Wolfesberger et al. [43] and Aigner et al. [44]. Gravimetric tars represent the heavy tars while GCMS tars represent the smaller tar molecules. As the measurement ranges of both tar analyses overlap, they cannot be added. Three samples of tar were taken during each trial and averages were calculated.

The simulation software IPSEpro was used to calculate mass and energy balance to determine gas yields. The software and model library is described by Proell and Hofbauer [45].

2.5. Used materials at the pilot plant trials

To ensure similar fluidization and gasification conditions with used and with unused bed material, a similar particle size distribution is required for both bed materials. Fig. 4 shows the particle size distribution of both bed materials and Table 4 shows the characteristic values for the particle size of the bed material.

Due to variations in the operating conditions at the industrial plant in Güssing, the used bed material that was used for the trial in the pilot plant was analyzed to determine the elemental composition. The results are shown in Table 5. The main difference between the elemental compositions of the unused and the used bed material is the content of calcium and potassium. From earlier investigations it is known that calcium occurs mainly in the layers on the surface of the particle [13].

Wood pellets were used as fuel in both trials in the pilot plant. The composition of the fuel used in both trials is shown in Table 6. Wood pellets were chosen because they have better conveying properties in the screw feeder of the pilot plant and because their composition is similar to that of the used fuel in the industrial plant. The water content of the pellets (6.74%) is significantly lower than the water content of the wood chips used in the plant in Güssing, which is 20–30% [22].

3. Results and discussion

The operational parameters at the pilot plant were chosen to be similar to those of the industrial scale plant in Güssing. Table 7 shows a summary of important operational parameters. The marked values are the measurements of set points. The other values are given by the operating conditions. The chosen operating temperature of the gasifier is 850 °C because experience at the plant in Güssing has shown that this gasification temperature ensures safe production. A higher steam-to-carbon ratio was required in the pilot plant compared to the plant in Güssing to reach fluidization properties.
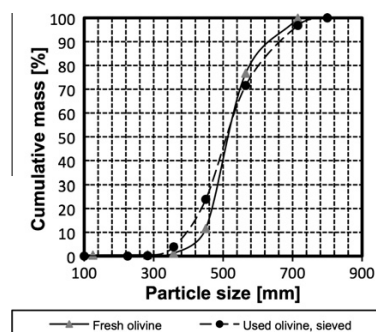
Fig. 4. Particle size distribution of the bed material.

Table 4
Particle size of the bed material.

	Unit	Fresh olivine	Used olivine, sieved
d_{p10}	μm	445	395
d_{p50}	μm	514	510
d_{p90}	μm	630	662

Table 5
Elemental composition of the bed material.

Metal oxide	Fresh olivine (wt.%)	Used olivine (wt.%)
Na_2O	0.43	1.67
MgO	46.76	40.52
Al_2O_3	0.40	0.44
SiO_2	39.84	33.60
P_2O_5	0.03	0.19
SO_3	0.06	0.08
K_2O	0.32	3.89
CaO	0.90	10.71
Cr_2O_3	0.28	0.38
MnO	0.15	0.24
Fe_2O_3	10.32	7.45
NiO	0.31	0.33
Cl	0.10	0.27
Others	0.11	0.23

Table 6
Fuel analysis of the fuel for the pilot plant.

Parameter	Value	Unit
C	51.07	mass% db
H	5.79	mass% db
N	0.13	mass% db
S	0.005	mass% db
Volatile matter content	86.12	mass% db
LHV (dry base)	19.0	MJ/kg db
HHV (dry base)	20.3	MJ/kg db
Ash	0.32	mass% db
Water content	6.74	mass%

db – dry base with ash.

Table 8 shows the performance parameters of the pilot plant for the trial with fresh olivine and used olivine. The gasification conditions in the gasifier were similar and performance difference is indicated mainly by the oil consumption. To get a good comparison of the efficiency the total gas yield is referred to the total fuel input which consists of fuel to gasifier and fuel to combustion zone.

The gas composition of the two trials in the pilot plant and the industrial scale plant is shown in Fig. 5. While the trial with the used olivine in the pilot plant shows similar results compared to the industrial scale plant, the results for fresh bed material in the pilot plant show a significantly higher CO content and significant lower CO_2 and H_2 contents. The values from the industrial scale plant show a higher deviation compared to the pilot plant due to

Table 8
Performance parameters of the pilot plant (results from mass and energy balance).

|	Unit	Reference trial at the pilot plant with fresh olivine	Pilot plant with used bed material from Güssing
Gas yield	Nm^3/kg wood (db)	1.06	1.09
Total gas yield	Nm^3/kW total fuel input (db)	0.157	0.172

varying fuel quality (moisture content) and instability of inorganic flows (e.g. bed material consumption and ash circulation).

Comparison of the trials from the pilot plant with fresh and used bed materials reveals an enhancement of the water–gas shift reaction, Formula (1), with used bed material, which leads to higher H_2 and higher CO_2 contents, while the CO content decreases. Additionally, the water–gas shift reaction is slightly exothermal, which explains the lower fuel consumption in the combustion chamber in the trial with the used bed material, as shown in Table 7, considering a similar bed material circulation. The pressure profile of the pilot plant is shown in Fig. 6 indicates similar operating conditions in the trials. The pressure difference at the combustion zone can be explained by the slightly higher means particle size for the used bed material shown in Table 4. This pressure difference may indicate a lower circulation rate, which should cause a higher temperature in the combustion chamber when the same energy demand is assumed in the gasifier. However, the temperature in the combustion zone is significantly lower with used olivine at the same gasification temperature, indicating again a lower energy demand for gasification.

The tar content of the product gas in the pilot plant is shown in Fig. 7. It indicates that substantially lower tar content was found with the used olivine from Güssing independently of the method of analysis. The GCMS measured tars decreased by 82% and the gravimetric tars decreased by 65%.

Fig. 8 shows the detailed GCMS analyses of tar components for both trials including the chemical structure of the components. The concentrations are presented on a logarithmic scale. The trial with used bed material showed fewer components in the tar composition. Various components mostly large multi-ring hydrocarbons, were not detectable. This reduction in tar species due to gasification with calcium-rich bed material was also described by Ruoppolo et al. [27].

The tar component with the highest content in both cases was naphthalene. Anthracene was the component with the second highest concentration in the trial with the unused olivine but due to a better reduction rate with used bed material it had the third highest content in the trial with used bed material, while acenaphthylene had the second highest content. Acenaphthylene showed a lower relative reduction rate than the average of the

Table 7
Operational parameters at the industrial scale plant and the pilot plant.

	Unit	Reference trial at the pilot plant with fresh olivine	Pilot plant with used bed material from Güssing	Industrial scale plant in Güssing
Gasifier bed temperature	°C	852 ± 2[a]	850 ± 1[a]	850[a]
Riser temperature	°C	897 ± 2	872 ± 1	∼930
Fuel input	kW	97[a]	97[a]	8 000[a]
Fuel into the combustion zone	kg/h	3.23	2.54	–
Total fuel input	kW	135[b]	127[b]	–
Steam to carbon ratio	– (kg/kg)	1.8[a]	1.8[a]	1.2–1.6

[a] Set points and target values respectively.
[b] Results from mass and energy balance.

Fig. 5. Product gas composition of unused and used bed material at the pilot plant compared with the industrial scale plant.

Fig. 6. Pressure profile over the DFB pilot plant.

Fig. 7. Tar contents with fresh and used olivine in the pilot plant.

GCMS tars. Anthracene showed the highest absolute reduction from the components which were detected in both trials, followed by naphthalene and acenaphthylene. Styrene had the lowest relative reduction rate (45%) and had the fourth highest absolute concentration in the trial with the used bed material. Multi-ring hydrocarbons with four or more rings such as benz(a)anthracene, chrysene, benzo(b)fluoranthene, benzo(k)fluoranthene, benzo(a)-pyrene, benzo(g,h,i)perylene, and indeno(1,2,3-c,d)pyrene were detected in the trial with the fresh bed material but not in the trial with used bed material. One exception was pyrene, which could be detected in the trial with used bed material but showed a higher relative reduction rate (91%) compared to the total tars. Phenol and phenylacetylene were detected in the trial with fresh bed material but not detected in the trial with used bed material. Methylnaphthalene showed low relative reductions, with 2-methylnaphtalene achieving better reduction. Benzofuran and dibenzofuran showed above average relative reduction rates of 88% and 92% respectively. Fluorene also had a high relative reduction rate of 95%. Phenanthrenes showed similar contents; 73 mg/Nm^3 for phenantrene and 71 mg/Nm^3 for 4,5-methylphenantrene. The relative reduction rate of phenanthrene was significantly high-er (97%) compared to that of 4,5-methylphenantrene (66%). The reduction rate of 1H-Indene was above average at 87%, while that of biphenyl was slightly below average at 80%. Fluoranthene showed a reduction rate of 85% which was slightly above the average.

The decrease in multi-ring polycyclic aromatic hydrocarbons with the usage of calcium-rich bed material is in accordance with experience from the literature. Longwell, summarized by Milne et al. [10], states that thermal treatment with CaO in coal gasification removes newly formed pyrolysis tars and pure aromatic compounds such as multi-ring polycyclic aromatic hydrocarbons and benzene respectively. Devi et al. [16] suggest the reaction scheme of naphthalene decomposition. In agreement with this reaction scheme these trials confirmed the theory that the recombination of cyclic hydrocarbons into multi-ring hydrocarbons is inhibited. The tar composition of the trial with used bed material showed no multi-cyclic hydrocarbon with more than three rings. The decomposition products of naphthalene seem to react with small molecules to form small single-ring hydrocarbons such as styrene, methylnaphthalene, and acenaphthylene.

Milne et al. [10] summarize examinations by Alden et al., stating that almost all components of tar are non-polar after catalytic cracking with dolomite. This is confirmed by this study. Phenol was not detectable in the trial with the used bed material.

While phenanthrene was reduced in the trial with used bed material to close to the detection limit, anthracene is available in significant amounts and has the second highest concentration after naphthalene.

Summarizing the tar analyses, it can be concluded that the layer formation on the bed particles shows very positive effects on tar reduction.
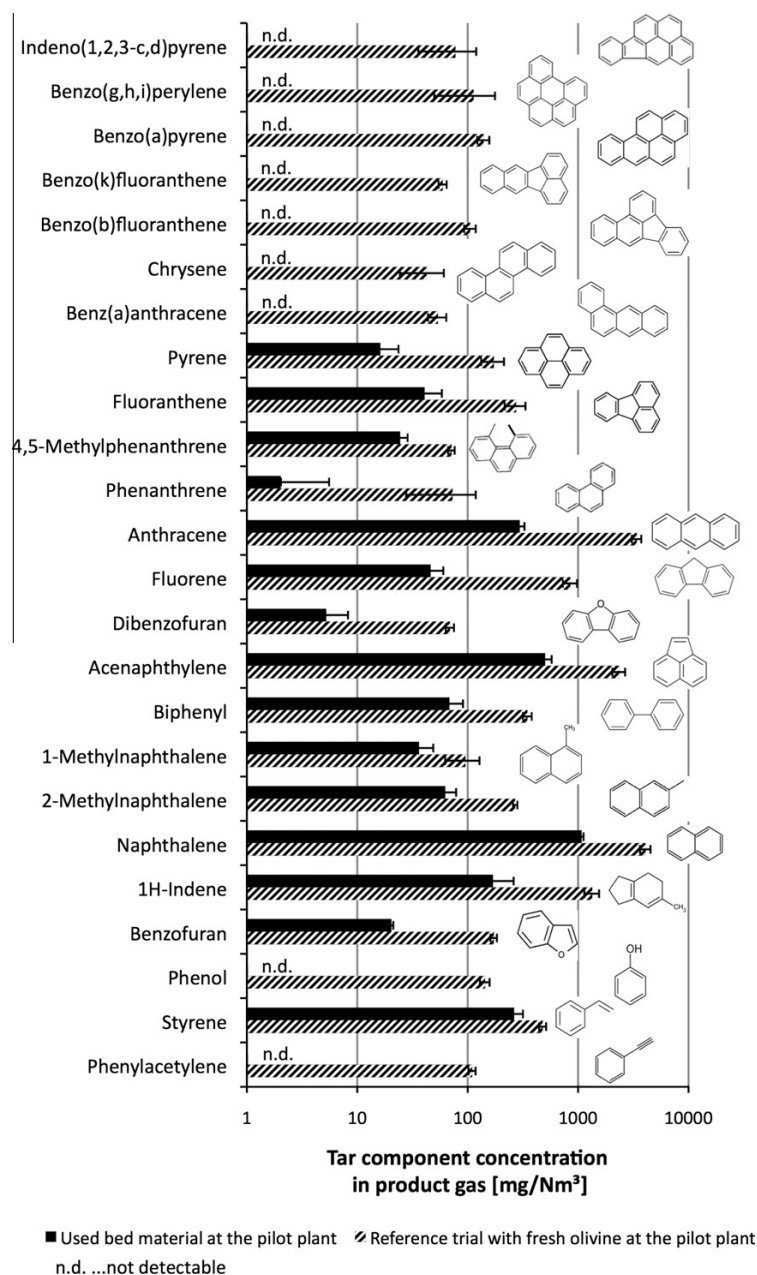
Fig. 8. Comparison of tar components in the pilot plant.

Considering the main components of the layer on the bed material the following elements have to be considered catalytically active: calcium oxide, magnesium oxide, and potassium oxide.

Potassium is available in concentrations of about 4% in bed material and fly ash but not detectable in crystal structures [13]. The catalytic activity of potassium is lower compared to dolomite [46]. According to Thy et al. [47], potassium is forced out of the crystal structure with high CaO concentration and is mainly present in gasified form. Considering this along with the finding of Chen and Yang [40] that the catalytic activity of clusters (particles) is significantly higher than that of C–O–M groups, the catalytic activity of potassium can be considered to be insignificant in this case.

The catalytic properties of olivine are well-proven. Since the results of the trial with used bed material showed these significant improvements in the catalytic activity, calcium and probably the mix of calcium and magnesium are considered to be the component that causes the catalytic improvements.

The comparison of the gas composition from the industrial plant in Güssing and the trial with the used bed material from Güssing presented in Fig. 5 shows very similar gas compositions of the pilot plant and the industrial scale plant with the same bed mate-

rial. Also, the results of tar analyses of the trial with the used olivine are in the range of published values of the plant in Güssing. Rauch et al. published values of around 1–2 g/Nm^3, assuming that the only reason for the tar reduction was the calcination of the olivine [22]. Results from the plant in Güssing published recently by Aigner indicate GCMS tar values of around 2 g/Nm^3 and gravimetric tars values of around 1.8 g/Nm^3 for wood as a fuel [48].

As shown with these results, the performance of the pilot plant can be easily transferred to the industrial scale plant. A good scale-up of the 100 kW pilot plant to industrial scale plants seems to be possible when the long term interaction of ash and additives with the bed material is considered.

4. Conclusions

The comparison of fresh olivine and used olivine from an industrial scale plant showed significant influence on the gas composition and catalytic effects on tar reduction. The difference between the effects of fresh olivine and the used olivine on the gasification properties is caused by the formation of a calcium-rich layer on the used bed material due to the interaction of bed material with biomass ash and additives.

The calcium-rich catalytic bed material promotes the exothermic water–gas shift reaction, which increases the hydrogen and carbon dioxide content of the product gas while the carbon monoxide content is decreased. The lower energy demand for the gasification confirmed the assumption of the promotion of the water–gas shift reaction.

The comparison of the results of the trial with used bed material from Güssing in the 100 kW pilot plant with data from the industrial scale plant in Güssing showed good scale-up properties.

Acknowledgments

References

[1] Bridgwater AV. The technical and economic feasibility of biomass gasification for power generation. Fuel 1995;74(5):631–53.
[2] Hofbauer H, Rauch R, Loeffler G, et al. Six years experience with the FICFB-gasification process. In: 12th European conf biomass and bioenergy. Amsterdam, The Netherlands: self-published; 2002.p. 4.
[3] Koppatz S, Pfeifer C, Rauch R, et al. H$_2$ rich product gas by steam gasification of biomass with in situ CO$_2$ absorption in a dual fluidized bed system of 8 MW fuel input. Fuel Process Technol 2009;90(7–8):914–21.
[4] Pfeifer C, Koppatz S, Hofbauer H. Catalysts for dual fluidised bed biomass gasification – an experimental study at the pilot plant scale. Biomass Convers Bioref 2011:1–12.
[5] Pfeifer C, Puchner B, Hofbauer H. Comparison of dual fluidized bed steam gasification of biomass with and without selective transport of CO$_2$. Chem Eng Sci 2009;64(23):5073–83.
[6] Wilk V, Kitzler H, Koppatz S, Pfeifer C, Hofbauer H. Gasification of waste wood and bark in a dual fluidized bed steam gasifier. Biomass Convers Bioref 2011;1(2):91–7.
[7] Aigner I, Pfeifer C, Hofbauer H. Co-gasification of coal and wood in a dual fluidized bed gasifier. Fuel 2011;90(7):2404–12.
[8] Rauch R, Hofbauer H, Săcăreanu S, Chiru A. From gasification to synthetic fuels via Fischer-Tropsch synthesis. Bull Transsilv Univ Brasov – Series I – Eng Sci 2011:3.
[9] Rehling B, Hofbauer H. Bio-SNG from biomass – first results of a demonstration plant. In: ICPS 09 – Int conf polygeneration strategies. Vienna, Austria: self-published; 2009.
[10] Milne T, Evans R, Abatzoglou N. Biomass gasifier "tars": their nature, formation, and conversion. National Renewable Energy Laboratory; 1998.
[11] Simell PA, Hepola JO, Krause AOI. Effects of gasification gas components on tar and ammonia decomposition over hot gas cleanup catalysts. Fuel 1997;76(12):1117–27.
[12] Kaltschmitt M, Hartmann H, Hofbauer H. Energie aus Biomasse. Berlin, Heidelberg: Springer; 2009. p. 1032.
[13] Kirnbauer F, Hofbauer H. Investigations on bed material changes in a dual fluidized bed steam gasification plant in Güssing, Austria. Energy Fuels 2011:110722151257027.
[14] Devi L, Craje M, Thüne P, Ptasinski KJ, Janssen FJJG. Olivine as tar removal catalyst for biomass gasifiers: catalyst characterization. Appl Catal A: Gen 2005;294(1):68–79.
[15] Devi L, Ptasinski KJ, Janssen FJJG, et al. Catalytic decomposition of biomass tars: use of dolomite and untreated olivine. Renew Energy 2005;30(4):565–87.
[16] Devi L, Ptasinski KJ, Janssen FJJG. Decomposition of naphthalene as a biomass tar over pretreated olivine: effect of gas composition, kinetic approach, and reaction scheme. Ind Eng Chem Res 2005;44(24):9096–104.
[17] Devi L, Ptasinski KJ, Janssen FJJG. Pretreated olivine as tar removal catalyst for biomass gasifiers: investigation using naphthalene as model biomass tar. Fuel Process Technol 2005;86(6):707–30.
[18] Corella J, Toledo JM, Padilla R. Olivine or dolomite as in-bed additive in biomass gasification with air in a fluidized bed: which is better? Energy Fuels 2004;18(3):713–20.
[19] Rapagná S, Jand N, Kiennemann A, Foscolo PU. Steam-gasification of biomass in a fluidised-bed of olivine particles. Biomass Bioenergy 2000;19(3):187–97.
[20] Mastellone ML, Arena U. Olivine as a tar removal catalyst during fluidized bed gasification of plastic waste. AIChE J 2008;54(6):1656–67.
[21] Arena U, Zaccariello L, Mastellone ML. Tar removal during the fluidized bed gasification of plastic waste. Waste Manage 2009;29(2):783–91.
[22] Rauch R, Pfeifer C, Bosch K, Hofbauer H. Comparison of different olivines for biomass steam gasification. In: Proc conf science in thermal and chemical biomass conversion, Victoria, Canada Conference; 2004.
[23] Rapagná S, Virginie M, Gallucci K, et al. Fe/olivine catalyst for biomass steam gasification: preparation, characterization and testing at real process conditions. Catal Today 2011;176:163–8.
[24] Di Felice L, Courson C, Niznansky D, Foscolo PU, Kiennemann A. Biomass gasification with catalytic tar reforming: a model study into activity enhancement of calcium- and magnesium-oxide-based catalytic materials by incorporation of iron. Energy Fuels 2010;24(7):4034–45.
[25] Swierczynski D, Courson C, Kiennemann A. Study of steam reforming of toluene used as model compound of tar produced by biomass gasification. Chem Eng and Process: Process Intensif 2008;47(3):508–13.
[26] Swierczynski D, Courson C, Bedel L, Kiennemann A, Guille J. Characterization of Ni–Fe/MgO/olivine catalyst for fluidized bed steam gasification of biomass. Chem Mater 2006;18(17):4025–32.
[27] Ruoppolo G, Miccio F, Chirone R. Fluidized bed cogasification of wood and coal adopting primary catalytic method for tar abatement. Energy Fuels 2010;24(3):2034–41.
[28] Miccio F, Piriou B, Ruoppolo G, Chirone R. Biomass gasification in a catalytic fluidized reactor with beds of different materials. Chem Eng J 2009;154(1–3):369–74.
[29] Xie Y, Xiao J, Shen L, et al. Effects of Ca-based catalysts on biomass gasification with steam in a circulating spout-fluid bed reactor. Energy Fuels 2010;24(5):3256–61.
[30] Olivares A, Aznar MP, Caballero MA, et al. Biomass gasification: produced gas upgrading by in-bed use of dolomite. Ind Eng Chem Res 1997;36(12):5220–6.
[31] Florin NH, Harris AT. Enhanced hydrogen production from biomass with in situ carbon dioxide capture using calcium oxide sorbents. Chem Eng Sci 2008;63(2):287–316.
[32] Delgado J, Aznar MP, Corella J. Biomass gasification with steam in fluidized bed: effectiveness of CaO, MgO, and CaO–MgO for hot raw gas cleaning. Ind Eng Chem Res 1997;36(5):1535–43.
[33] Myrén C, Hörnell C, Björnbom E, Sjöström K. Catalytic tar decomposition of biomass pyrolysis gas with a combination of dolomite and silica. Biomass Bioenergy 2002;23(3):217–27.
[34] Corella J, Aznar M, Gil J. Biomass gasification in fluidized bed: where to locate the dolomite to improve gasification? Energy Fuels 1999;13(6):1122–7.
[35] Alarcón N, García X, Centeno MA, Ruiz P, Gordon A. New effects during steam gasification of naphthalene: the synergy between CaO and MgO during the catalytic reaction. Appl Catal A: Gen 2004;267(1–2):251–65.
[36] Delgado J, Aznar MP, Corella J. Calcined dolomite, magnesite, and calcite for cleaning hot gas from a fluidized bed biomass gasifier with steam: life and usefulness. Ind Eng Chem Res 1996;35(10):3637–43.
[37] Kyotani T, Hayashi S, Tomita A. Study of calcium catalysis on carbon gasification with molecular oxygen-18. Energy Fuels 1991;5(5):683–8.
[38] Nair SA, Yan K, Pemen AJM, et al. Tar removal from biomass-derived fuel gas by pulsed corona discharges. A chemical kinetic study. Ind Eng Chem Res 2004;43(7):1649–58.
[39] Chen SG, Yang RT. Unified mechanism of alkali and alkaline earth catalyzed gasification reactions of carbon by CO$_2$ and H$_2$O. Energy Fuels 1997;11(2):421–7.

[40] Chen SG, Yang RT. The active surface species in alkali-catalyzed carbon gasification: phenolate (C–O–M) groups vs clusters (Particles). J Catal 1993;141(1):102–13.

[41] Bolhar-Nordenkampf M, Hofbauer H, Bosch K, Rauch R, Aichernig C. Biomass CHP plant Güssing – using gasification for power generation. In: Kirtikara K, editor. Int conf biomass utilisation. vol 1. Phuket, Thailand: self-published; 2003. p. 567–72.

[42] Hofbauer H, Rauch R, Bosch K, Koch R, Aichernig C. Biomass CHP plant Güssing – a success story. In: Pyrolysis and gasification of biomass and waste. CPL Press; 2003. p. 527–36.

[43] Wolfesberger U, Aigner I, Hofbauer H. Tar content and composition in producer gas of fluidized bed gasification of wood – influence of temperature and pressure. Environ Prog Sustain Energy 2009;28(3):372–9.

[44] Aigner I, Ute W, Hofbauer H. Tar content and composition in producer gas of fluidized bed gasification and low temperature pyrolysis of straw and wood – influence of temperature. In: ICPS 09 – Int conf polygeneration strategies. Vienna, Austria; 2009. p. 1–9.

[45] Proell T, Hofbauer H. Development and application of a simulation tool for biomass gasification based processes. Int J Chem Reactor Eng 2008:6.

[46] Abu El-Rub Z, Bramer EA, Brem G. Review of catalysts for tar elimination in biomass gasification processes. Ind Eng Chem Res 2004;43(22):6911–9.

[47] Thy P, Lesher CE, Jenkins BM. Experimental determination of high-temperature elemental losses from biomass slag. Fuel 2000;79(6):693–700.

[48] Aigner I. In: Hofbauer H, Pfeifer C, editors. Co-gasification of coal and wood with steam in a dual fluidized bed gasifier. Vienna University of Technology; 2010. p. 1–179.

Publication III

Kirnbauer, F.; Wilk, V.; Hofbauer, H. Performance improvement of dual fluidized bed gasifiers by temperature reduction: The behavior of tar species in the product gas. FUEL 2012, 108, 534–542.

Performance improvement of dual fluidized bed gasifiers by temperature reduction: The behavior of tar species in the product gas

Friedrich Kirnbauer [a,*], Veronika Wilk [a], Hermann Hofbauer [b]

[a] Bioenergy 2020+ GmbH, Wiener Straße 49, A-7540 Güssing, Austria
[b] Vienna University of Technology, Institute of Chemical Engineering, Getreidemarkt 9/166, 1060 Vienna, Austria

HIGHLIGHTS

▶ Olivine is modified by the ash during biomass steam gasification which enhances the gasification properties.
▶ Reducing the gasification temperature is desired to increase the efficiency of the plant and to reduce fouling issues.
▶ The reduction of the gasification temperature leads to slightly higher tar concentrations in the product gas.
▶ The condition of the bed material is more important for tar decomposition than the gasification temperature.

ABSTRACT

To meet the aims of the worldwide effort to reduce greenhouse gas emissions, product gas from biomass steam gasification in DFB (dual fluidized bed) gasification plants can play an important role for the production of electricity, fuel for transportation and chemicals. Using a catalytically active bed material, such as olivine, brings advantages concerning tar reduction in the product gas. Experience from industrial scale gasification plants showed that a modification of the olivine occurs during operation due to the interaction of the bed material with ash components from the biomass and additives. This interaction leads to a calcium-rich layer on the bed material particles which influences the gasification properties and reduces tar concentration in the product gas. In this paper, the influence on the gasification performance, product gas composition and tar formation of a reduction of the gasification temperature are studied. A variation of the gasification temperature from 870 °C to 750 °C was carried out in a 100 kW pilot plant. A reduction of the gasification temperature down to 750 °C reduces the concentration of hydrogen and carbon monoxide in the product gas and increases the concentration of carbon dioxide and methane. The product gas volume produced per kg of fuel is reduced at lower gasification temperatures but the calorific value of the product gas increases. The volumetric concentration of tars in the product gas increases slightly until 800 °C and nearly doubles when decreasing the gasification temperature to 750 °C. The tars detected by gas chromatography–mass spectrometry (GCMS) were classified into substance groups and related to the fuel input to the gasifier and showed a decrease in naphthalenes and polycyclic aromatic hydrocarbons (PAHs) and an increase in phenols, aromatic compounds and furans when reducing the gasification temperature. The comparison with results from an earlier study, where the gasification properties of unused fresh olivine were compared with used olivine, underlines the importance of a long retention time of the bed material in the gasifier, ensuring the formation of a calcium-rich layer in the bed material.

© 2012 Elsevier Ltd. All rights reserved.

1. Introduction

Various countries are aiming to utilize renewable sources for the supply of energy, such as heat, electrical energy or fuels for transportation. The European Commission is aiming to substitute nearly all fossil fuels by renewable sources for the production of electricity by the year 2050 [1]. Similar strategies are also promoted by decision-makers, opinion leaders, societal groups and scientists in the United States [2] and other countries.

Electrical energy produced from biomass may make redundant partly the randomly produced electricity from wind and photovoltaic materials because biomass is stored by nature and can be utilized by proper technology with varying energy loads at any time.

A proven technology for the utilization of woody biomass for electricity generation is biomass steam gasification in a dual fluidized bed (DFB) gasifier. In this process, biomass is gasified

---

thermally and the product gas is used in a gas engine to generate electricity and heat. Various studies are ongoing for the utilization of the product gas to produce fuels for transportation [3–7], making the technology even more suitable for usage and electricity production with different loads depending on the demand of the consumers. The polygeneration of electricity, fuels and heat is considered to be more efficient for the utilization of biomass and higher profits can be generated compared to single-product plants [8,9]. Biomass gasification is described as a key technology for the reduction of greenhouse gas emissions using polygeneration technologies [10].

The first industrial scale application of a biomass steam gasification plant in a DFB reactor went into operation in 2001 and is located in Güssing (Austria; 8 MWth). Several plants went into operation recently; for example in Oberwart (Austria), Villach (Austria), and Ulm (Germany). The typical plant size is around 8–15 MW but larger plants are planned or are in the realization phase, for example in Goteborg (Sweden; 32 MWth).

Biomass steam gasification in a DFB gasifier is carried out in two reactors. The main reactor is the gasification reactor operated in a bubbling bed mode where the endothermic steam gasification of the biomass takes place. In a second reactor, the combustion reactor, thermal heat for gasification is provided by the combustion of char, which is transferred with the bed material from the gasification reactor to the combustion reactor. The combustion reactor is operated in a fast-fluidized bed regime. The heat is transferred via a circulating bed material between the combustion and the gasification reactor. The product gas consists of the main components, hydrogen, carbon monoxide, carbon dioxide and methane. Trace substances, like higher hydrocarbons, tars, and organic sulfur, and nitrogen components are also detectable in the product gas in small amounts. In industrial scale applications, the product gas is cooled down, dust is separated and tar components are removed in a rapeseed methyl ester (RME) scrubber before further utilization of the product gas in a gas engine to produce heat and electricity. The RME loaded with tars from tar washing is burnt in the combustion reactor. The process is well-described in literature [11–16].

The type of bed material used is important for the gasification performance of the plant. Using olivine, a magnesia-iron silicate, is state of the art for these gasifiers. The positive effects of olivine on tar reduction have been shown in various studies [17–22].

Earlier investigations carried out in the industrial scale plant in Güssing by the authors showed that the biomass ash of the fuel interacts with the olivine during the long-term operation of the plant [14]. Calcium-rich layers accumulate on the surface of the particles. The influence of olivine particles with this calcium-rich layer on gasification compared to unused fresh olivine as bed material was investigated in a pilot plant at the Vienna University of Technology (VUT), showing that the "coated" bed material reduced the tar content by around 80% for tars detected by gas chromatography–mass spectrometry (GCMS) and 65% for tars detected by gravimetric analyses [15]. These studies were carried out at 850 °C because industrial scale plants regularly run at this temperature where safe operation is ensured.

Decreasing the gasification temperature has various advantages, for example higher efficiencies of the plant are expected and the risk of ash related problems, such as slagging, fouling and bed material agglomeration is reduced. Different low grade biogeneous fuels other than woody biomass are available for lower prices but ash related problems such as fouling, slagging and bed material agglomeration are even more expected for these fuels [23,24]. A reduction of the gasification temperature can, therefore, bring advantages also in terms of greater fuel flexibility.

Operational experience at the industrial scale plant in Güssing showed also that good gasification performance at 850 °C can lead, in some cases, to high hydrogen contents in the product gas, which can limit the maximum power of the gas engine because of a lower specific energy density of the product gas with a high hydrogen content. By reducing the gasification temperature it is expected to decrease the amount of hydrogen in the product gas and to increase the specific heat of the gas and further to improve the operation of the engine.

Tars, which are the collective term for higher, mainly aromatic, hydrocarbons, are undesired byproducts of gasification. A high amount of tars in the product gas can lead to deposits and even plug heat exchangers, pipes and vessels and cause unplanned shutdowns of the plant.

The formation mechanism of tars, depending on the temperature and state of pyrolysis or gasification, was described by Milne et al. [25]. The authors classified the tars in primary, secondary, alkyl tertiary and condensed tertiary products. Cellulose-derived products characterize primary products; secondary products are characterized by phenolics and olefins; alkyl tertiary products include methyl-derivative aromatics such as methyl acenaphthylene, methylnaphthalene, toluene, and indene; condensed tertiary products are characterized by polycyclic aromatic hydrocarbon (PAH) series without substituents: benzene, naphthalene, acenaphthylene, anthracene/phenanthrene, and pyrene. The formation of each group of tars depends on the pyrolysis/gasification temperature as shown in Fig. 1.

A reduction of the gasification temperature is generally assumed to lead to higher tar content in the product gas. Various studies confirm this assumption.

Wolfesberger et al. [26] summarized results from various test runs at the pilot plant at VUT and concerning GCMS tar contents and their compositions. These test runs were carried out with unused fresh olivine. The trend by decreasing the temperature from 850 °C to 800 °C showed a slight increase in GCMS tar content in the product gas. Since various test runs under different conditions are compared, a clear trend cannot be seen. The relative composition of the tars during the gasification of wood chips showed a decrease in naphthalene and PAHs and an increase in aromatic compounds when lowering the gasification temperature from 850 °C to 800 °C. The relative amount of phenols in the GCMS tars increased significantly; furans and aromatic nitrogen compounds did not show a trend when reducing the temperature. During the gasification of wood pellets, the relative amount of naphthalene also decreased when decreasing the temperature from around 870 °C to around 830 °C. In contrast to wood chips, the relative amount of PAHs (without naphthalenes) increases with lower temperatures as do the relative amounts of phenols and furans.

Shen et al. simulated the gas composition of steam gasification in a similar gasifier to the DFB gasifier [27]. The gas composition changed by decreasing the gasification temperature from 900 °C to 650 °C. As expected an increase of carbon dioxide and methane was seen and a decrease of hydrogen and carbon monoxide.

Pfeifer et al. studied the gasification of wood pellets in the DFB gasifier at the VUT using nickel-enriched olivine as bed material [28]. The tar content in the product gas increased 3 or 4-fold when the gasification temperature was lowered from 900 °C to about 780 °C. The gas yield decreased from about 1.1 Nm³/kg biomass to about 0.9 Nm³/kg biomass at the same time.

A model for steam gasification of biomass in a DFB gasifier, applying thermodynamic equilibrium calculations, was used by Schuster et al. to simulate the effect of the gasification temperature on the gas composition of the product gas [29]. A decrease in the concentration of carbon monoxide and an increase in the carbon dioxide and methane content in the product gas were calculated at temperatures between 1000 °C and 700 °C. Hydrogen stays constant and drops at temperatures lower than 850 °C. The tar content of the product gas was not considered in this simulation work.
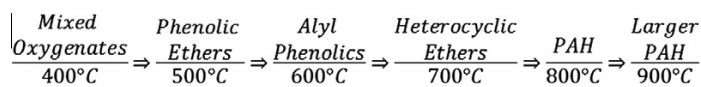
$$\left|\frac{Mixed}{Oxygenates}_{400°C} \Rightarrow \frac{Phenolic}{Ethers}_{500°C} \Rightarrow \frac{Alyl}{Phenolics}_{600°C} \Rightarrow \frac{Heterocyclic}{Ethers}_{700°C} \Rightarrow \frac{PAH}{800°C} \Rightarrow \frac{Larger}{PAH}_{900°C}\right.$$

Fig. 1. Tar formation at different temperatures [25].

A parametric study of the gasification of biomass using olivine in a lab-scale bubbling-bed gasifier was published by Rapagna et al. [30]. The authors reported a decrease in the carbon monoxide and hydrogen content in the product gas and an increase in the carbon dioxide and methane content when reducing the temperature from 820 °C to 700 °C. The tar content increased significantly from 0.5 to 1 g/Nm^3 db to more than 6 g/Nm^3 db.

Hofbauer and Rauch [31] presented an extensive parametric study in a DFB gasifier with "a natural mineral", which is considered to be olivine, as the bed material. The gas composition changed by lowering the temperature from 900 °C to 780 °C with reducing hydrogen from 40 to 35 vol.%, carbon monoxide decreased slightly, while the carbon dioxide and methane content increased. The tar content increased significantly from 1 to 2 g per normal cubic meter of gas at 880 °C to approximately 4–7 g/Nm^3 - db at 800 °C. The measurement method for the tar is not indicated but is assumed to be the gravimetric method.

Koppatz et al. [22] compared the behavior of the bed material olivine with silica sand in the 100 kW pilot plant of the VUT, including a temperature variation for olivine. The authors conclude that the variation in the gasification temperature influences the hydrogen content in the product with a decrease in the hydrogen content when decreasing the temperature from 850 °C to 770 °C. A moderate increase in carbon monoxide content is reported. The content of tars in the product gas increases by decreasing the temperature. Tar values were twice as high at 770 °C compared to 850 °C. The composition of the tars shows a decrease of naphthalene, acenaphthylene and anthracene while phenol and styrene increase when reducing the gasification temperature from 850 °C to 770 °C.

Similar studies are also available for air blown gasification [32], showing a decrease of hydrogen and CO$_2$ when decreasing the temperature from 850 °C to 800 °C with dolomite as a bed material. An increase in the tar content of the product gas is reported.

However, in these studies described above unused fresh olivine or dolomite as a bed material were applied. The influence of the calcium-rich layer at the surface of used olivine bed material particles in DFB steam gasification plants is unknown. A study of temperature variations with this bed material has not yet been published. The exact influence of the gasification temperature with used olivine particles on gas composition and tar content of the producer gas is not quantified. Since the bed material is built up under regular operational conditions in an industrial scale DFB gasifier, these results can have a significant impact on the operation of these plants.

This paper summarizes the influence of the gasification temperature on the tar concentration and the composition of tars with different temperatures. Used olivine from the industrial scale plant in Güssing is used and the results are compared with results using fresh olivine from a previous study [15]. The knowledge about the behavior of tars at reduced gasification temperatures is the basis to reduce the gasification temperature in an industrial scale plant in Güssing/Austria as a part of an optimization program.

2. Experimental section

Test runs with different gasification temperatures were carried out at a 100 kWth pilot plant at the VUT. Used olivine taken out from the industrial plant in Güssing, which is described in earlier publications [14,15], was used as a bed material.

2.1. DFB biomass gasification

The DFB biomass steam gasification plant in Güssing, Austria, from where the bed material was taken, has a thermal power of 8 MW and an electrical output of 2 MW. The plant went into operation in late 2001 and, up to July 2012, has had an operation time of 66,000 h for the gasifier and 60,500 h for the gas engine. Wood residues harvested in the local area are utilized as fuel. Olivine is applied as a bed material. Various literature is available about the Güssing plant [11,12], therefore no further description is given here.

2.2. Sampling of the bed material at the industrial scale plant

The required amount of used bed material for the tests in the pilot plant was 150 kg. The bed material was taken during regular operation from the bottom of the combustion reactor of the industrial plant. To avoid impact on the production of the plant, several batches were taken over a period of two days.

To get a similar particle size distribution compared to fresh olivine, the used olivine from the Güssing plant was sieved and fractions smaller than 400 μm and bigger than 1 mm were removed to avoid the presence on the one hand of fine ash and on the other hand of nails and a broken refractory lining in the pilot rig.

The sieved used olivine which was applied as bed material in the pilot plant has a mean particle size d_{p50} of 510 μm, a d_{p10} of 395 μm and a d_{p90} of 662 μm analyzed by a sieve analysis. The elemental composition calculated as oxides of the bed material is shown in Table 1. The calcium content of the bed material occurs mainly in the layers on the surface of the particle, which was described in earlier studies [14]. A polished micrograph of a particle with a layer is shown in Fig. 2.

2.3. Description of the pilot plant

The pilot plant at the Institute of Chemical Engineering, VUT has got a fuel power of 100 kW. The good scale-up properties of the results obtained from this pilot plant to industrial scale plants have been proven by performing specific test runs [15]. For this purpose used olivine from the Güssing plant were used in the pilot plant and the test runs were carried out at the same operation conditions as normally applied at the Güssing plant. A comparison showed

Table 1
Bed material composition.

Metal oxide	Used olivine wt.%
Na$_2$O	1.67
MgO	40.52
Al$_2$O$_3$	0.44
SiO$_2$	33.60
P$_2$O$_5$	0.19
SO$_3$	0.08
K$_2$O	3.89
CaO	10.71
Cr$_2$O$_3$	0.38
MnO	0.24
Fe$_2$O$_3$	7.45
NiO	0.33
Cl	0.27
Others	0.23
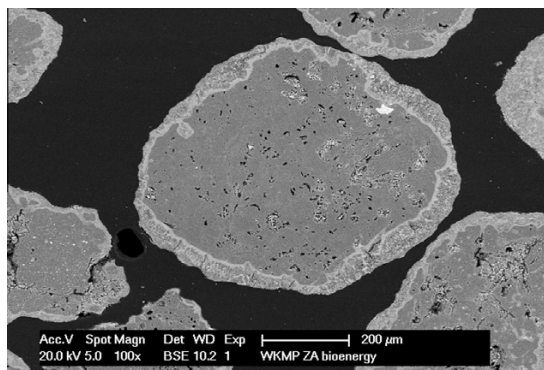
Fig. 2. Polished micrograph of used olivine particles [14].

good agreement of the data from the pilot plant with those from the industrial scale plant in Güssing/Austria [15].

The pilot plant shown in Fig. 3 is well-described in literature [17,21,22,33–36].

The gasifier consists of a gasification reactor operated with a bubbling bed, which is fluidized by steam, and a combustion reactor with a fast-fluidized bed, which is fluidized by air. The bed material is circulated between the two reactors to carry the heat from the combustion reactor to the gasification reactor. The

separation of the bed material and the flue gas after the combustion reactor is carried out using a gravity separator. Siphons are located in the tubes between the gasification reactor and the combustion reactor to avoid gas leakages from the combustion reactor, such as air or flue gas, into the gasification reactor and vice versa.

The fuel can be fed from various hoppers at different locations. During these test runs, feedstock hopper 1 (see Fig. 3) is used and the fuel is fed directly into the fluidized bed of the gasifier where water and volatile components of the fuel are released. The remaining char is gasified with steam. A part of the char is transported with the bed material to the combustion reactor, where the char is burnt.

The pilot plant is designed to add also fuel into the combustion reactor to provide a part of the required heat for gasification, not via transport through the chute, but from outside the system. Light fuel oil is used in the pilot plant as fuel for the combustion chamber. Industrial scale plants are designed to recycle product gas and to avoid external fuel addition to the combustion reactor, but for research proposes, separate fuel addition to the combustion reactor is useful. The pilot plant is equipped with gas composition measurements in the product gas stream as well as in the flue gas stream. Relevant temperatures and pressures are registered by a data acquisition tool.

2.4. Sampling at the pilot plant

Wood pellets were used as a fuel during the test runs in the pilot plant. A wood pellet sample was taken before the test runs in the pilot plant and analyzed. To obtain representative values, the samples were taken on the basis of the standard DIN 51701. Ash content was determined according to DIN 51719 but at 550 °C. The content of volatile matter was determined using DIN 51720 and the higher and lower heating values according to DIN 51900 T2. The same batch of wood pellets was used for all test runs.

Gas and tar analysis of the product gas of the pilot plant is well-described in the literature [17,33–35,37]. Carbon monoxide, carbon dioxide, methane were measured by a non-dispersive infrared analyzer; hydrogen by thermal conductivity and oxygen was measured by a paramagnetic sensor (Rosemount NGA2000). The components, nitrogen, ethylene, ethane, and propane, were measured by a gas chromatograph (Perkin Elmer Arnel 1015 Refinery Gas Analyzer). Tars are absorbed in toluene and measured similarly to the tar protocol. Detailed descriptions of the tar measurement are given by Wolfesberger et al. [26] and Aigner et al. [38]. Gravimetric tars represent the heavy tars while GCMS tars represent the smaller tar molecules. As the measurement ranges of both tar analyses overlap, they cannot be added. Three samples of tar were taken during each test run and averages were calculated. The test runs were carried out on two days to ensure enough time for stationary conditions for each operation point. At day one the operation points at gasification temperatures of 870, 800 and 750 °C were studied, at day two the temperatures 830 °C, 780 °C and remaining tar measurements at 750 °C were carried out. For the calculation of average values of continuous measurements, a stationary phase of the plant was taken into consideration. The duration of the stationary phases is summarized for each temperature in Table 2.

The GCMS tars were classified into substance groups according to Wolfesberger et al. [26], shown in Table 3. For the calculation of the average values, the results of each sample were split into the substance groups and the average of these values was ascertained for each gasification temperature. The relative content of the substance groups was calculated by relating to the average of the total GCMS tars. The tar analyses were also related to the biomass fuel input (including water and ash).
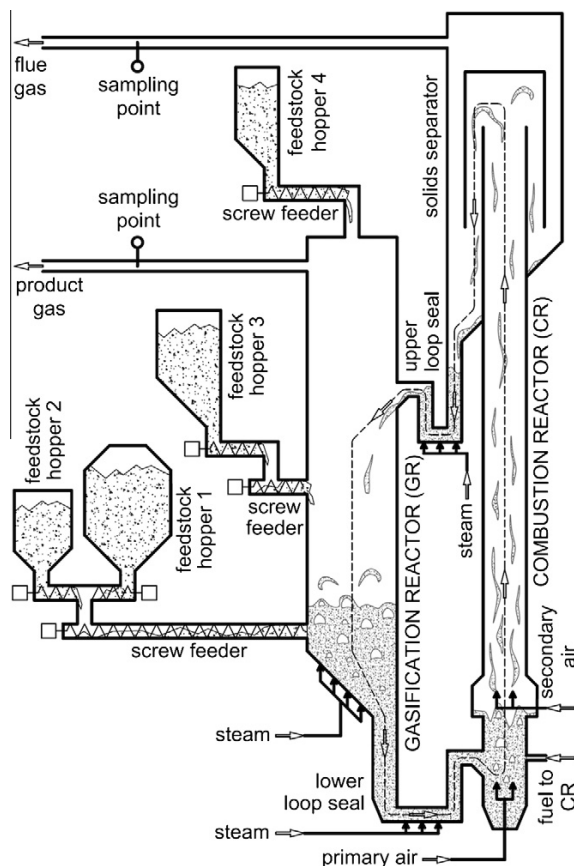
Fig. 3. 100 kW gasifier at the VUT [35].

Table 2
Duration of the stationary phases.

Target temperature (°C)	Duration stationary phase (h)
750	1:49
780	1:45
800	1:55
830	1:31
870	0:48

Table 4
Typical fuel composition.

Parameter	Value	Unit
C	51.07	mass% db
H	5.79	mass% db
N	0.13	mass% db
S	0.005	mass% db
Volatile matter content	86.12	mass% db
Lower heating value (db)	19.0	MJ/kg db
Higher heating value (db)	20.3	MJ/kg db
Ash	0.32	mass% db
Water content	6.74	mass%

db – Dry base with ash.

The simulation software IPSEpro was used to calculate mass and energy balances to determine gas yields. The software and model library is described by Pröll and Hofbauer [39].

2.5. Materials used in the pilot plant trials

Wood pellets were used as fuel in the test runs in the pilot plant. The typical composition of the fuel used is shown in Table 4. Wood pellets were chosen because they have better conveying properties in the screw feeder of the pilot plant and because woody biomass is used in the actual operating industrial scale gasification plants.

Used olivine from the industrial scale plant in Güssing was used as described above.

3. Results

The operational parameters at the pilot plant, except those of the gasification temperature, were chosen to be similar to those of the industrial scale plant in Güssing. Table 5 shows a summary of the important operational parameters at different temperatures. The marked values are set points while the other values given were measured. The temperature range was chosen between 750 °C and 870 °C. The upper limit of the gasification temperature was chosen to be slightly higher than the regular operational temperature of the industrial scale plants which is 850 °C. The lower limit was considered to be governed by the setup and fluidization properties of the pilot plant. The fuel input into the gasifier was kept constant for each temperature. The fuel input into the combustion reactor decreased from 3.1 kg/h light fuel oil at 870 °C to 0.1 kg/h at 750 °C gasification temperature. The steam to carbon ratio was kept constant for all test runs.

The demand for fuel into the combustion reactor, shown in Fig. 4 decreases with reducing gasification temperature. Considering the heat loss of the pilot plant which was estimated in previous test runs with 20 kW and considered to be constant for simplification, the temperature where additional fuel into the combustion reactor is not required can be estimated for similar, larger plants. The gasification temperature where the char which is transferred

with the bed material into the combustion reactor is sufficient can be defined for the pilot plant with around 750 °C. The estimated value for an industrial scale plant with less heat losses is at around 820 °C which is in agreement with the experience of the 8 MW plant in Güssing, where product gas is used in the combustion zone.

Table 6 shows gas yields and calorific values of the pilot plant for the test runs between 750 °C and 870 °C. The specific gas yield, which is the volume flow of product gas related to the wood pellets input, is reduced from 1.18 Nm³ per kg of pellets at 870 °C to 0.75 Nm³ per kg of pellets at 750 °C. The total gas yield, which is the volume flow of product gas related to the energy of the total fuel input (pellets to gasifier plus fuel to combustion zone), is reduced when the temperature is reduced. An increase of the lower calorific value of the product gas can be seen with decreased gasification temperature.

Considering the main components of the product gas, shown in Fig. 5, the trend is linear. The trends show reducing contents of hydrogen and carbon monoxide in the product gas with decreasing gasification temperatures. In contrast, the content of carbon dioxide and methane increases. Trace substances, such as ethylene, ethane, nitrogen and higher hydrocarbons, were detected but are not indicated in the graph. In general the higher hydrocarbons are lower at higher temperatures.

The amount of tars in the product gas (Fig. 6) shows a similar trend for the GCMS detectable tars and the tars measured with the gravimetric method. The amount of GCMS tars are generally higher than that of gravimetric tar. Concerning temperature dependence similar values between 870 °C and 800 °C and increasing values below 800 °C were detected.

The tars detected with both measurement methods related to the input of fuel into the gasifier are shown in Fig. 7. The trends are slightly different compared to those in Fig. 6 as the product gas yields are different for different temperatures. Both measurement methods show a minimum of tar concentration related to

Table 3
Tar substance groups.

Substance group	Component
Phenols	Phenol, 2-methylphenol, 4-methylphenol, 2,6-dimethylphenol, 2,5 and 2,4-dimethylphenol, 3,5-dimethylphenol, 2,3-dimethylphenol, 3,4-dimethylphenol, 2-methoxy-4-methylphenol, 1,2-dihydroxybenzene
Furans	1-Benzofuran, 2-methylbenzofuran, dibenzofuran
Aromatic compounds	Phenylacetylene, styrene, mesitylene, 1H-indene, 1-indanone,
Aromatic nitrogen compounds	Isoquinoline, indole, carbazole, quinoline
Naphthalenes	Naphthalene, 2-methylnaphthalene, 1-methylnaphthalene
PAH	Biphenyl, acenaphthylene, acenaphthene, flourene, anthracene, phenanthrene, 4,5-methylphenanthrene, 9-methylanthracene, flouranthene, pyrene, benz[a]anthracene, chrysene, benz[b]flouranthene, benz[k]flouranthene, benz[a]pyrene, benz[g,h,i]perylene, indeno[1,2,3-cd]pyrene, dibenz[a,h]anthracene
Guaiacols	Eugenol, isoeugenol
Thiophenes	1-Benzothiophen, dibenzothiophen
Phthalates	Dimethylphthalate, diethylphthalate, butylbenzylphthalate

Table 5
Operational parameters.

	Unit					
Target gasification temperature[a]	°C	870	830	800	780	750
Measured gasifier bed temperature	°C	869 ± 4	835 ± 6	803 ± 5	784 ± 3	751 ± 3
Temperature of the combustion reactor	°C	905 ± 4	862 ± 4	832 ± 5	811 ± 3	776 ± 2
Fuel input	kW	97[a]	97[a]	97[a]	97[a]	97[a]
Fuel into the combustion reactor	kg/h	3.1	1.9	1.4	0.5	0.1
	kW	36[b]	22[b]	17[b]	5[b]	1[b]
Total fuel input	kW	133[b]	119[b]	114[b]	103[b]	98[b]
Steam to carbon ratio	– (kg/kg)	1.6[a]				

[a] Set points and target values respectively.
[b] Results from mass and energy balance.
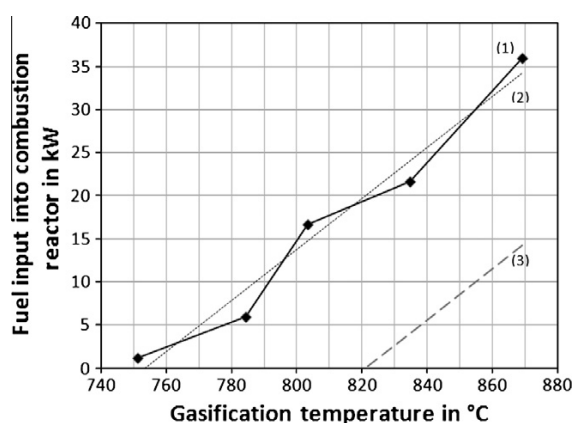
Fig. 4. Fuel input into the combustion chamber depending on the gasification temperature. (1) – Measured values, (2) – linear trend of the measured values, and (3) – estimated trend without 20 kW heat losses.

Fig. 5. Product gas composition, main components.

the fuel input into the gasifier at 800 °C. This trend is more evident when considering the relative concentrations of GCSM tar groups, shown in Fig. 8 or the concentration of the tar groups related to the fuel input into the gasification reactor that is shown in Fig. 9.

The relative content of naphthalenes and PAHs decreases with decreasing temperatures while the group of phenols and furans increase as shown in Fig. 8. The aromatic compounds also increase with lower gasification temperatures with a maximum at 780 °C and slightly decrease at lower gasification temperatures.

Relating the concentration to the fuel input to the gasifier, which considers the different specific gas yields, shows similar results (Fig. 9). The groups of naphthalenes and PAHs decrease while the amount of phenols, furans and aromatic compounds increases. The increase in phenols is significant and follows an exponential trend with decreasing temperatures.

The main components representing 70–85% of the GCMS tars, depending on the temperature, are naphthalene, 1H-indene, acenaphthylene, phenol, styrene and anthracene. The composition of these main components of GCMS tars is shown in Fig. 10. The concentration of anthracene and acenaphthylene decreases slightly when lowering the gasification temperature while styrene and 1H-indene increases. A significant decrease of naphthalene can

Fig. 6. Gravimetric tars and sum of GCMS tars related to the gas volume at different gasification temperatures.

be seen, while the content of phenol increases significantly at lower gasification temperatures.

Guaiacols, thiophenes and phthalates were not detectable at any temperature. Aromatic nitrogen compounds were measured

Table 6
Gas yields and calorific values (results from mass and energy balance).

Gasification temperature	°C	870	830	800	780	750
Specific gas yield	Nm³/kg pellets	1.18	1.00	0.94	0.80	0.75
Total gas yield	Nm³/kW total fuel	0.178	0.170	0.166	0.155	0.153
Lower calorific value of the product gas	MJ/Nm³	12.22	12.37	12.40	12.76	12.64

Fig. 7. Gravimetric and sum of GCMS tars related to fuel input into gasification reactor.
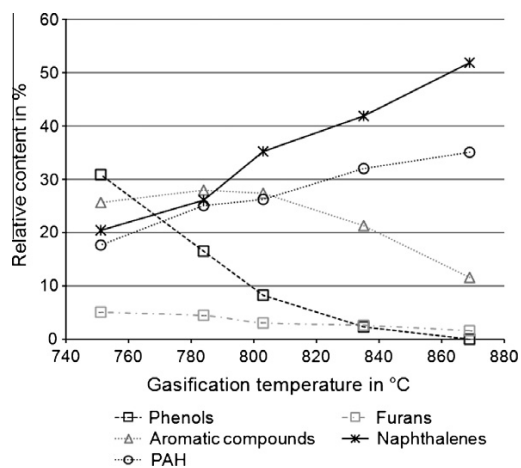
Fig. 8. Relative content of GCMS tar groups at different temperatures.
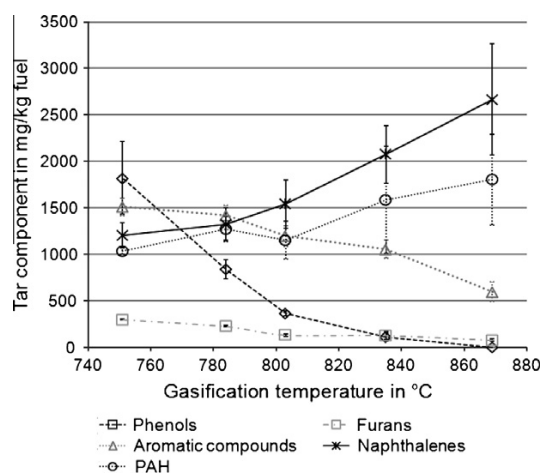
Fig. 9. Tar concentration of GCMS tar groups related to fuel input into the gasification reactor.

in concentrations below 30 mg/Nm² db in the product gas and are not indicated in the graphs. A clear trend of aromatic nitrogen compounds in connection with the gasification temperature could not be seen.

4. Discussion

The results show a clear trend for the decomposition and formation of different tar species dependent on temperature. The concentration of large aromatic compounds, which are described in the literature as tertiary tars, decreases by lowering the gasification temperature, while the concentration of smaller molecules, such as phenols, increases. These findings agree with other studies carried out with unused fresh olivine [22,26].

For the design and operation of DFB gasification plants, the following points are important in terms of tar handling. (1) The concentration of tar per volume of product gas: this concentration influences the temperature to which the product gas can be cooled before condensation of the tars occurs. (2) The amount of tar that is accumulated per unit of fuel: This value influences the size of the tar cleaning unit (in general a RME-scrubber) and the demand for the scrubber liquid. (3) The composition of the tars: Different tar compounds have different boiling points and condense at different temperatures.

Earlier studies showed that biomass gasification with used olivine as a bed material reduces the concentration of tars in the product gas significantly compared to unused fresh olivine [15]. The sum of GCMS tars in the product gas was measured in the earlier study with unused fresh olivine at around 15 g/Nm³ while the sum of GCMS tar concentration with used olivine in this study is between 4.5 g/Nm³ at 870 °C up to 7.8 g/Nm³ at 750 °C. This trend is even clearer when splitting the GCMS tars into groups and relating them to the fuel input, as shown in Fig. 11. The PAH group using fresh olivine in the gasification is the main group. In case of used olivine PAH is significantly lower and a reduction in the gasification temperature even reduces this amount as shown in this study. The group of naphthalenes with unused fresh olivine is also present in a higher concentration compared to the results with used olivine from the temperature variations in this study. Furthermore, the concentration of the group of naphthalenes in the tars can be reduced by decreasing the gasification temperature. The amount of aromatic compounds detected in the product gas using fresh olivine is nearly doubled compared to the results of this
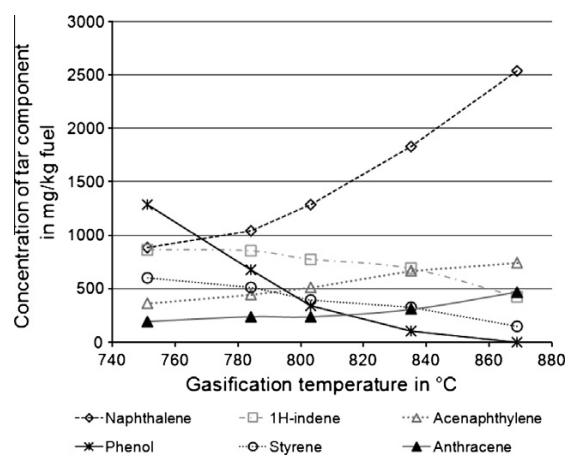
Fig. 10. Main GCMS tar components related to fuel input into the gasification reactor.
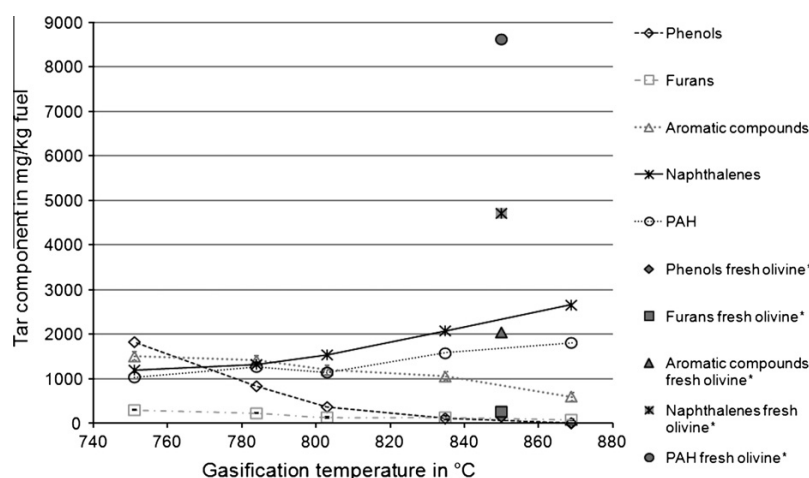
Fig. 11. Comparison of results of the temperature variations with the result of unused olivine from an earlier study (Values marked with ∗ are from an earlier study [15]).

study. But the concentration of aromatic compounds slightly increases when the gasification temperature is reduced. The amounts of phenols and furans with unused fresh olivine are low and also similar to the results in this study.

This study shows that naphthalenes and PAHs are components which accumulate at higher temperatures. The comparison of the results presented in this article with an earlier study [15] shows that utilization of used bed material inhibits the recombination of cyclic hydrocarbons into multi-ring hydrocarbons [40] which are even more inhibited at lower gasification temperatures. This can be explained by the catalytically active Ca-rich surface of the used olivine where O_2 dissociatively chemisorbs onto the calcium-oxide-rich surface to form CaO(O). The active oxygen (O) from CaO(O) reacts with carbon to form C(O) what reacts with additional oxygen and is released as CO_2 from the active sites from the CaO-rich bed material particles. This mechanism was suggested by Kyotani et al. [41] for calcium catalyzed carbon gasification with oxygen. A similar mechanism is suggested for the gasification of biomass. The water gas shift reaction is promoted with calcium rich used bed material [15] which can be explained by a high availability of active oxygen which moves the equation to carbon dioxide and hydrogen. This high availability of active oxygen with low activation energy is considered to influence also the decomposition and recombination of tars.

The increase in phenols at lower temperatures shown in this study confirms this theory. Phenols contain a hydroxyl group (–OH), which can be assumed to be an intermediate product of the decomposition of woody biomass with the participation of oxygen. The decomposition mechanism is inhibited at lower temperatures and the thermodynamically stable hydroxyl groups are not further decomposed.

Tar content of the product gas can cause operational problems of the plant when the product gas is cooled down and tar species are condensing at heat exchangers. The dew point where tars start condensing is depending on the tar concentration and on the tar composition and the boiling point of the components. Inhibiting the formation of PAHs by using used olivine with a calcium-rich layer can be considered to reduce the dew point of the total tar mixture with similar tar concentrations. While the boiling points of naphthalenes and phenols are in the range of 180 °C to 220 °C the boiling points of components which belong in the group of PAHs are at temperatures around 380–500 °C (e.g. chrysene: 448 °C; benzo(a)pyrene; 495 °C). A greater impact on the

condensing properties of tars in the gasification plant can be expected by higher concentrations of PAHs compared to higher concentrations of phenols. This leads to the conclusion that the impact of tar decomposition and formation on the operation of a DFB gasification plant is influenced mainly by inhomogeneous bed material quality rather than the gasification temperature (Fig. 11). High calcium content in the bed material and high catalytic activity of the bed material reduces the tar content and the concentrations of tar components, such as PAHs, which are more relevant for condensation and better than temperature variations in the gasifier.

The utilization of used olivine, that has a calcium-rich layer with a constant quality, leads to an "optimization problem" between the naphthalene and PAHs, which accumulate at higher gasification temperatures, and the phenols, aromatic compounds and furans, which suffer from less decomposition at lower gasification temperatures. This study showed an optimum (minimum) concerning the tar formation related to the fuel input at a gasification temperature of about 800 °C.

This optimization of inhibiting the formation of large multi-ring hydrocarbons at higher temperatures and the decomposition of hydrocarbons could be achieved by accurate controlling of the bed material inventory, ash loops and also the temperature. The controlling of the retention time of the bed material in the system should be prioritized compared to temperature control.

5. Conclusions

Test runs with used olivine of an industrial scale DFB gasification plant in a 100 kW DFB gasifier were carried out to study the influence of the modification which olivine undergoes during long-term usage in industrial plants. The test runs showed that reducing the gasification temperature has an influence on the product gas composition, the tar concentration and GCMS tar composition in the product gas. The hydrogen and carbon monoxide content in the product gas are reduced while the carbon dioxide and methane contents increase. The specific gas yield decreases with lower temperatures.

The concentration of tars related to the volume of product gas increases at temperatures lower than 800 °C. Related to the fuel input, the tar concentration has a minimum of around 800 °C.

A closer examination of the tar components shows that the group of naphthalenes and PAHs decreases when the gasification

temperatures are lowered and the group of phenols, furans and aromatic components increases.

The minimization of the tar content related to the fuel input by reducing the gasification temperature is an optimization of the increasing components, which are considered as decomposition products, and the components, which accumulate at higher temperatures. This leads to moderate increase of the sum of GCMS tar concentration related to the volume of product gas to temperatures down to 800 °C.

The comparison of the tar concentrations of the temperature variations with a test run with unused olivine in an earlier study [15] showed the importance of the calcium-rich layer in the used olivine.

This leads to the conclusion that the retention time of the bed material in the system and the formation of the calcium-rich layer has a higher influence on tar reduction in the product gas than the gasification temperature.

With accurate controlling of the bed material inventory, ash flows and retention time of the bed material in the system, further optimization of the plant is considered to be possible by reducing the gasification temperature to 800 °C without risking condensation of tars on the heat exchanger walls or in pipes.

Acknowledgments

References

[1] EC. A roadmap for moving to a competitive low carbon economy in 2050. vol. 112. European Commission. Brussels; 2011. <http://ec.europa.eu/clima/policies/roadmap/index_en.htm>. COM(2011).
[2] US Department of Energy. US billion-ton update: biomass supply for a bioenergy and bioproducts industry. In: Perlack RD, Stokes BJ (Leads). ORNL/TM-2011/224. Oak Ridge (TN): Oak Ridge National Laboratory; 2011. 227p.
[3] Rauch R, Hofbauer H, Săcăreanu S, Chiru A. From gasification to synthetic fuels via Fischer-Tropsch synthesis. Bull Transsilv Univ Brasov – Ser I – Eng Sci 2011:3.
[4] Rehling B, Hofbauer H. Bio-SNG from biomass – first results of a demonstration plant. In: ICPS 09 – International conference on polygeneration strategies. Vienna (Austria): self-published; 2009.
[5] Rehling B, Hofbauer H, Rauch R, Aichernig C. BioSNG—process simulation and comparison with first results from a 1-MW demonstration plant. Biomass Conv Bioref 2011;1:111–9.
[6] Sauciuc A, Abostreif Z, Weber G, Potetz A, Rauch R, Hofbauer H. Influence of pressure on the performance of biomass based Fischer–Tropsch synthesis. In: Proceedings of the international conference on polygeneration strategies (ICPS11). Vienna, Austria; 30 August–1 September 2011.
[7] Sauciuc A, Potetz A, Weber G, Rauch R, Hofbauer H, Dumitrescu L. Synthetic diesel from biomass by Fischer-Tropsch synthesis. In: International conference of renewable energies and power quality (ICREPQ '11). Spain: Las Palmas de Gran Canaria; 2011. ISBN: 978-84-614-7527-8.
[8] Chen Y, Adams TA, Barton PI. Optimal design and operation of static energy polygeneration systems. Ind Eng Chem Res 2012;50:5099–113.
[9] Williams RH, Larson ED, Liu G, Kreutz TG. Fischer–Tropsch fuels from coal and biomass: strategic advantages of once-through ("polygeneration") configurations. Energy Procedia 2009;1:4379–86.
[10] Wetterlund E, Söderström M. Biomass gasification in district heating systems – the effect of economic energy policies. Appl Energy 2010;87:2914–22.
[11] Hofbauer H, Rauch R, Loeffler G, Kaiser S, Fercher E, Tremmel H. Six years experience with the FICFB gasification process. In: 12th European conference biomass and bioenergy. Amsterdam (The Netherlands): self-published; 2002. p. 4.
[12] Bolhar-Nordenkampf M, Hofbauer H, Bosch K, Rauch R, Aichernig C. Biomass CHP plant Güssing – using gasification for power generation. In: Kirtikara K, editor. International Conference on Biomass Utilisation. vol 1. Phuket (Thailand): self-published; 2003. p. 567–72.
[13] Koppatz S, Pfeifer C, Rauch R, Hofbauer H, Marquard-Moellenstedt T, Specht M. H_2 rich product gas by steam gasification of biomass with in situ CO_2 absorption in a dual fluidized bed system of 8 MW fuel input. Fuel Process Technol 2009;90(7–8):914–21.
[14] Kirnbauer F, Hofbauer H. Investigations on bed material changes in a dual fluidized bed steam gasification plant in Güssing, Austria. Energy Fuels 2011;25:3793–8.
[15] Kirnbauer F, Wilk V, Kitzler H, Kern S, Hofbauer H. The positive effects of bed material coating on tar reduction in a dual fluidized bed gasifier. Fuel 2012;95:553–62.
[16] Hofbauer H, Rauch R, Bosch K, Koch R, Aichernig C. Biomass CHP plant Güssing – a success story. In: Pyrolysis and gasification of biomass and waste. CPL Press; 2003. p. 527–36.
[17] Pfeifer C, Koppatz S, Hofbauer H. Catalysts for dual fluidised bed biomass gasification – an experimental study at the pilot plant scale. Biomass Conv Bioref 2011:1–12.
[18] Devi L, Craje M, Thüne P, Ptasinski KJ, Janssen FJJG. Olivine as tar removal catalyst for biomass gasifiers: catalyst characterization. Appl Catal A: Gen 2005;294:68–79.
[19] Devi L, Ptasinski KJ, Janssen FJJG, van Paasen SVB, Bergman PCA, Kiel JHA. Catalytic decomposition of biomass tars: use of dolomite and untreated olivine. Renew Energy 2005;30:565–87.
[20] Devi L, Ptasinski KJ, Janssen FJJG. Pretreated olivine as tar removal catalyst for biomass gasifiers: investigation using naphthalene as model biomass tar. Fuel Process Technol 2005;86:707–30.
[21] Pfeifer C, Koppatz S, Hofbauer H. Steam gasification of various feedstock at a dual fluidised bed gasifier: impacts of operation conditions and bed materials. Biomass Conv Bioref 2011;1:39–53.
[22] Koppatz S, Pfeifer C, Hofbauer H. Comparison of the performance behaviour of silica sand and olivine in a dual fluidised bed reactor system for steam gasification of biomass at pilot plant scale. Chem Eng J 2011.
[23] Hupa M. Ash-Related issues in fluidized-bed combustion of biomasses: recent research highlights. Energy Fuels 2012;26.
[24] Boström D, Skoglund N, Grimm A, Boman C, Öhman M, Broström M, et al. Ash transformation chemistry during combustion of biomass. Energy Fuels 2012;26:85–93.
[25] Milne T, Abatzoglou N. Biomass gasifier "tars": their nature, formation, and conversion. National Renewable Energy Laboratory; 1998.
[26] Wolfesberger U, Aigner I, Hofbauer H. Tar content and composition in producer gas of fluidized bed gasification of wood – influence of temperature and pressure. Environ Prog Sustain Energy 2009;28:372–9.
[27] Shen L, Gao Y, Xiao J. Simulation of hydrogen production from biomass gasification in interconnected fluidized beds. Biomass Bioenergy 2008;32:120–7.
[28] Pfeifer C, Rauch R, Hofbauer H. In-bed catalytic tar reduction in a dual fluidized bed biomass steam gasifier. Ind Eng Chem Res 2004;43:1634–40.
[29] Schuster G, Löffler G, Weigl K, Hofbauer H. Biomass steam gasification – an extensive parametric modeling study. Bioresour Technol 2001;77:71–9.
[30] Rapagná S, Jand N, Kiennemann A, Foscolo PU. Steam-gasification of biomass in a fluidised-bed of olivine particles. Biomass Bioenergy 2000;19:187–97.
[31] Hofbauer H, Rauch R. Stoichiometric water consumption of steam gasification by the FICFB-gasification process. In: Bridgwater AV, editor. Oxford (UK)/Innsbruck (Austria). Blackwell Science Ltd.; 2000. p. 199–208.
[32] Gil J, Caballero MA, Martin JA, Aznar M-P, Corella J. Biomass gasification with air in a fluidized bed: effect of the in-bed use of dolomite under different operation conditions. Ind Eng Chem Res 1999;38:4226–35.
[33] Wilk V, Kitzler H, Koppatz S, Pfeifer C, Hofbauer H. Gasification of waste wood and bark in a dual fluidized bed steam gasifier. Biomass Conv Bioref 2011;1:91–7.
[34] Aigner I, Pfeifer C, Hofbauer H. Co-gasification of coal and wood in a dual fluidized bed gasifier. Fuel 2011;90:2404–12.
[35] Schmid JC, Wolfesberger U, Koppatz S, Pfeifer C, Hofbauer H. Variation of feedstock in a dual fluidized bed steam gasifier – influence on product gas, tar content, and composition. Environ Prog Sustain Energy 2012;31:205–15.
[36] Koppatz S, Schmid JC, Pfeifer C, Hofbauer H. The effect of bed particle inventories with different particle size in a dual fluidized bed pilot plant for biomass steam gasification. Ind Eng Chem Res 2012.
[37] Pfeifer C, Puchner B, Hofbauer H. Comparison of dual fluidized bed steam gasification of biomass with and without selective transport of CO_2. Chem Eng Sci 2009;64:5073–83.
[38] Aigner I, Wolfesberger U, Hofbauer H. Tar content and composition in producer gas of fluidized bed gasification and low temperature pyrolysis of straw and wood – influence of temperature. In: ICPS 09 – International conference on polygeneration strategies. Vienna, Austria; 2009. p. 1–9.
[39] Pröll T, Hofbauer H. Development and application of a simulation tool for biomass gasification based processes. Int J Chem Reactor Eng 2011;6:1–58.
[40] Devi L, Ptasinski KJ, Janssen FJJG. Decomposition of naphthalene as a biomass tar over pretreated olivine: effect of gas composition, kinetic approach, and reaction scheme. Ind Eng Chem Res 2005;44:9096–104.
[41] Kyotani T, Hayashi S, Tomita A. Study of calcium catalysis on carbon gasification with molecular oxygen-18. Energy Fuels 1991;5:683–8.

Publication IV

The mechanism of bed material coating in dual fluidized bed biomass steam gasification plants and its impact on plant optimization

Friedrich Kirnbauer [a,*], Hermann Hofbauer [b]

[a] Bioenergy 2020 + GmbH, Wiener Straße 49, A-7540 Güssing, Austria
[b] Vienna University of Technology, Institute of Chemical Engineering, Getreidemarkt 9/166, 1060 Vienna, Austria

ABSTRACT

The bed material and especially its catalytic activity plays an important role in biomass steam gasification in dual fluidized bed gasifiers. The bed material is modified by interaction with biomass ash during operation of the gasification plant forming layers at the particles which are induced by the biomass ash. Optimization of dual fluidized biomass steam gasification will have significant influence on the process variables such as temperatures, inorganic composition and product gas composition. The influence of these changes on layer formation is still unknown. This paper summarizes results of investigations about bed material characteristics taken from the industrial-scale biomass steam gasification plant in Güssing where woody biomass is used as fuel. Analyses of the surface and the crystal structures of the bed material particles treated in gasification and combustion atmospheres were carried out. The thermal behavior of used olivine and fresh olivine in different atmospheres was analyzed. A suggestion for the mechanism of formation of the layers is presented and the influence of possible optimization measures is discussed. A change in the elemental composition of the surface was not detectable but a slight change in the crystal structure. Thermal investigations show a weak endothermic weight loss with used olivine in a CO_2-rich atmosphere which could not be determined with fresh olivine. The formation of layers at the olivine particles is considered to be caused by the intensive contact with burning char particles in the combustion reactor.

© 2013 Elsevier B.V. All rights reserved.

1. Introduction

The utilization of biomass for energy generation seems to be indispensable for the supply of energy from renewable energy sources. A well proven technology for the generation of electrical energy and heat is biomass steam gasification in a dual fluidized bed (DFB) gasifier in connection with gas engines [1–6].

Biomass steam gasification in DFB plants is carried out in two fluidized beds. In a gasification reactor that is operated in bubbling bed mode, mainly endothermic gasification reactions take place. The bed is fluidized with steam. A part of the fuel is transported via the bed material in a chute to the combustion reactor where it is combusted and the bed material is heated up. The combustion reactor is operated in a fast fluidized bed regime. Due to circulation of the bed material between the combustion reactor and the gasification reactor, heat is transferred from the combustion reactor to the gasification reactor. The product gas is cooled down and filtered to remove inorganic particles and char. Tars are removed in a scrubber that is operated with rapeseed oil methyl ester (RME). The cleaned product gas is utilized in a gas engine to generate electricity and heat. The flue gas from the combustion reactor is cooled down, and fly ash is separated in a fabric filter and the clean flue gas is released into the atmosphere via a chimney. Detailed descriptions of the process can be found in the literature [1–6]. A flow sheet of the gasification process is shown in Fig. 1.

This technology is developed to industrial-scale size in various plants in operation inEurope [7–9]. The development of different technologies for alternative utilization of the product gas from the dual fluidized steam gasification such as Fischer–Tropsch synthesis, synthesis of synthetic natural gas (BioSNG), and mixed alcohols is ongoing and each type of synthesis has different requirements regarding the composition of the product gas [10–14]. The most efficient way to influence the composition of the product gas is to change the parameters directly in the gasification process rather than the downstream application of upgrading steps, for example, a steam reformer.

On the other hand, the economic pressure which is caused on the one hand by increasing wood prices and on the other hand a constant feed-in tariff for electricity creates demand for a further optimization of the gasification process in terms of economic and technological efficiency. This can be achieved by increasing the product flexibility by generating not only electricity and heat but also synthetic fuels or chemicals. Higher fuel flexibility can have similar positive effects on the economic efficiency due to lower prices of alternative fuels. Woody biomass, which is used in industrial scale biomass steam

---
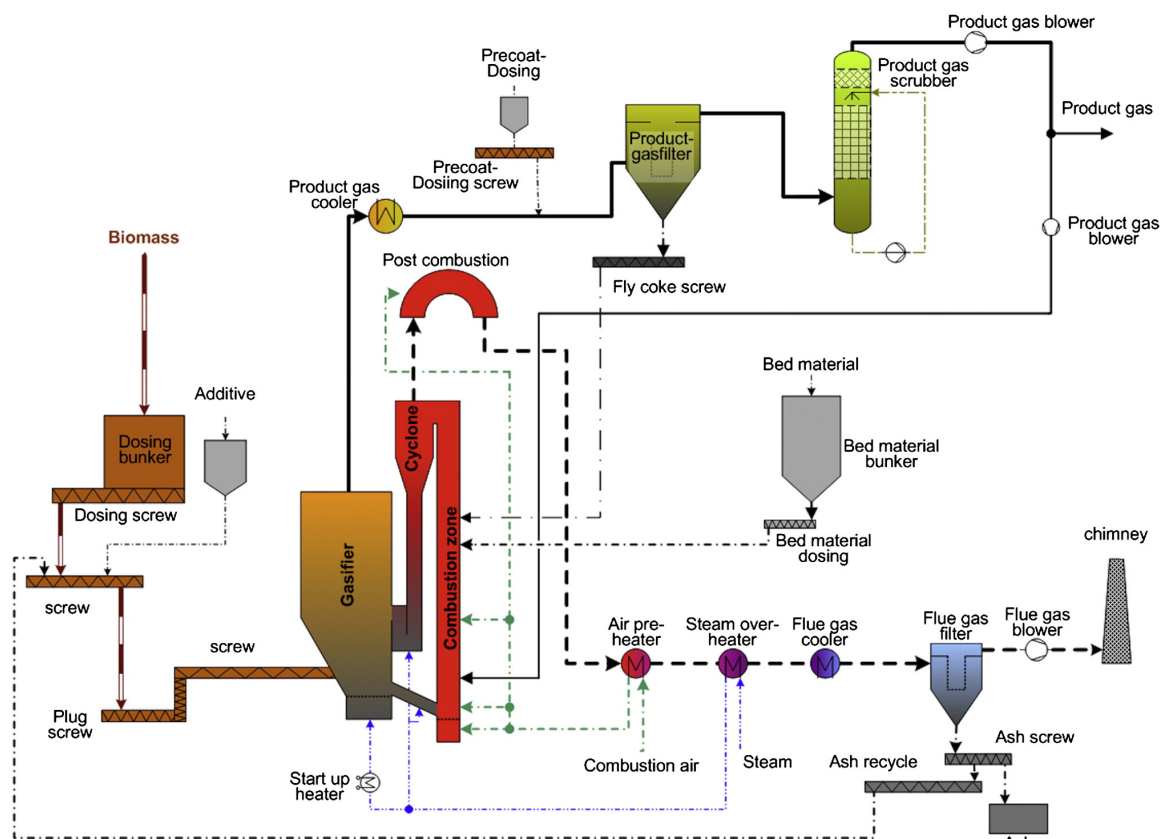
Fig. 1. Basic flow sheet of the DFB gasification in Güssing.

gasification plants nowadays, has a high softening as well as melting temperature of the ash compared to other biomass, which has an impact on the agglomeration behavior [15–17]. Other biogenous fuels such as energy crops or biogenous waste from agriculture such as straw, corn cobs, and others have even a worse melting behavior of the ash and often causes problems in biomass combustion plants [18–22].

A promising way to increase the technological and economic efficiency is to decrease the gasification temperature. A reduced gasification temperature brings advantages in the technical efficiency of the plant [23,24] and reduces the risk of ash related problems such as bed material agglomeration, fouling, and slagging [25,26].

The utilization of catalytic bed material is state of the art for the biomass steam gasification in DFB plants. The natural mineral olivine, which is a magnesium iron silicate, (Mg, Fe) SiO_2, is used in these plants, because it showed good results in laboratory-scale experiments concerning tar reduction in the product gas [27–34].

Olivine which is most frequently used as bed material in the DFB gasification plants interacts with the biomass ash during its utilization [4,35]. The long-term interaction with woody biomass in an industrial scale plant in Güssing was documented in an earlier study [4]. Two different calcium-rich layers are built at the surface of the bed material particles. The inner layer is homogenous and consists mainly of calcium and silicate. The outer layer has a similar composition to the fly ash of the plant.

This calcium-rich layer at the surface of the bed material influences the gasification properties significantly [5,36]. The water–gas shift reaction is enhanced, leading to higher hydrogen and CO_2 content in the product gas and to lower carbon monoxide content and lower content of higher hydrocarbons. The decomposition of primary tars is enhanced and formation of secondary tars is reduced, leading to lower total tar concentrations in the product gas. The enhancement of the water–gas shift reaction was confirmed by Kern et al. [37] in laboratory scale examinations of the bed material.

The high amount of calcium at the surface of the bed material particles can make CO_2 adsorption and transport with the bed material possible. The CO_2 transport with the bed material is desired in the sorption-enhanced reforming (SER) process, where calcium-rich bed material such as calcite is used. The adsorption of CO_2 in the gasification reactor at lower temperatures and the desorption of CO_2 in the combustion reactor at higher temperatures transports CO_2 from the gasification reactor to the combustion reactor, bringing higher hydrogen contents in the product gas from around 55–70 vol.% depending on the bed material and process conditions. Details about the SER process (also called adsorption enhanced reforming, AER) can be found in the literature [3,38–44].

A new, optimized reactor design for a DFB gasifier presented by Schmied et al. [45] proposes significant changes in the reactor design, ash loops, and operating conditions of the process.

A wide range of desired process variations are possible, such as plant optimization by temperature reduction and the utilization of different fuels in industrial plants or overall optimization for the production of second generation biofuel plants via gasification and Fischer–Tropsch synthesis, BioSNG, or production of hydrogen rich gas by selective CO_2 transport. The bed material in a DFB gasifier can play an important role for directing the gas composition of the

syngas to the desired composition according to its application. However, detailed knowledge about the fundamentals of the formation of the calcium rich layer and the influence of the operating conditions of DFB plants would be necessary. Details about the mechanism of the layer formation have not been published and the location in the gasification plant where the layer formation takes place is still matter of speculations.

This paper summarizes recent research activities and analyses of bed material modification in DFB plants and describes the mechanism of formation of the layers. Qualitative statements are made about the thermal behavior of the bed material. The formation mechanism is discussed in the context of different possibilities for optimizing the operation of DFB biomass steam gasification plants. This study aimed on clarifying conditions for lab scale tests and for further investigations of bed material catalysts.

2. Fundamentals

Olivine the bed material in DFB plants is a natural mineral that has its origin in basaltic magma. It is a magnesium iron silicate and the first or an early crystallization phase from basalts [46]. Various authors from different disciplines have published examinations of the crystal structure and properties of olivine. Calcium diffusion in olivine is of interest in mineralogy for determining the cooling rate of samples from meteorites. These studies also show interesting results regarding the utilization of olivine in DFB gasifiers, its modification during long-term utilization, and the interaction with biomass ash.

Olivine consists of two crystal structures: fayalite and forsterite. Fayalite is an iron-containing silicate, Fe_2SiO_4, and forsterite is the phase which is rich in magnesia, Mg_2SiO_4. The crystal structure of olivine is orthorhombic; it has two distinct metal sites (called M1-O and M2-O in literature) of the octahedrally coordinated cations, which can be Fe, Mg, Ni, Mn, or Ca. These two positions are interchangeable with different ions. At temperatures higher than 600 °C the angular distortion of the M1 and M2 octahedra increases and the exchange of ions at these positions is enabled [47]. With increasing temperature the distances at the M−O positions increase while the Si−O distances show zero or slightly negative expansions [47]. The behavior of fayalite is similar to forsterite with increasing temperature [47]. The position M2 is suggested to be preferred by calcium ions when exchanging Fe ions [47]. The Ca−Fe substitution in olivine is more extensive than Ca−Mg substitution because of the difference between the radii of Fe and Mg cations [48]. The diffusion rate of calcium into olivine is lower than the diffusion of iron or magnesium [48,49]. The diffusion rates along the different axes of the crystal structures show that diffusion occurs four to eight times faster along one axis compared to the other two axes [49]. The diffusion rates of calcium into the olivine structure increase with increasing oxygen fugacity because the partial oxidation of the Fe^{2+} ions to Fe^{3+} is charge balanced by the formation of these vacancies [49].

These findings seem to be relevant to the application of olivine in DFB gasification. They can help understanding the influence of the calcium rich woody biomass ash on layer formation, and its influence on the gasification properties. The modification of olivine due to the mobility of the iron ion at high temperatures is reported to have a positive influence on tar cracking in biomass gasification [28,30]. Fredriksson et al. [50] reported that unused olivine in a DFB gasifier is modified by the different atmospheres in the combustion reactor and the gasification reactor. In the combustion atmosphere, iron is mostly available as Fe_2O_3 and Fe_3O_4 or $MgFe_2O_4$, but it is reconverted under a reducing atmosphere to Fe_0 and Fe_3C and the formation of graphitic carbon can be detected [50]. The incorporation of calcium into the olivine structure takes place during long-term interaction with the calcium-rich biomass ash, resulting in a homogeneous inner layer of the particle [4].

Beside the diffusion of calcium into the olivine structure at the surface of bed material particles, a second, outer layer is built. This layer is composed mainly of biomass ash components [4].

The formation mechanism of the layers on the bed material particles is described by Öhman et al. [51] and was improved by Brus et al. [52], De Geyter [53], and Grimm et al. [54] for quartz as bed material. This mechanism is summarized by Grimm et al. [35] as follows: (a) Initiation by coating: ash components are melted and sintered onto the surface of the particle. This is initiated by potassium silicate melting accompanied by the diffusion or dissolution of calcium into the melt. This mechanism is suggested to be typical for woody fuels with ash rich in calcium and potassium with small amounts of silicon and phosphor. (b) Potassium compounds in gaseous or aerosol phase react directly with the particle surface, forming potassium silicates at the surface followed by sintering and agglomeration. This mechanism is suggested to be typical for fuels with high alkali content and relatively low silicon and phosphor contents. (c1) Direct adhesion of melted potassium silicate particles or droplets: this mechanism is typical for fuels with high potassium content and high content of organically bound silicon. (c2) Direct adhesion by partly molten potassium-calcium phosphates or magnesium phosphates: this is typical for biomass rich in phosphor, potassium, and calcium or magnesium.

Scala et al. [55] described the formation of agglomerates around burning particles where the temperatures are locally even higher than in the rest of the fluidized bed.

Phosphor is described in literature to have significant influence on the agglomeration behavior which from interest with alternative fuels [35,54,56]. The influence of phosphor on the adhesion of potassium and its influence on the layer formation are considered to be low because of low phosphor concentrations in the fuel ash and in the particles.

3. Experimental Section

The investigations were carried out with bed material from the 8 MW (thermal) gasification plant in Güssing/Austria. Bed material samples were taken during regular operation. These samples were analyzed and investigations were carried out in small-scale test rigs.

3.1. Sampling and Analyses

The bed material which is described as "fresh olivine" was taken after delivery to the plant before usage in the system. The bed material was already calcined by the supplier at a maximal temperature of 1600 °C before delivery. Bed material which is described as "used olivine" was taken from the bottom of the combustion zone during regular operation. Samples were taken after cooling under ambient conditions.

The used bed material was taken after a period of regular production with wood residues as a fuel. A typical composition of the biomass ash is presented that represents the average composition of the ash.

Sieve analyses of fresh olivine and used olivine were carried out to determine the typical size distribution of the bed material.

The used bed material taken from the bottom of the combustion reactor of the Güssing plant was treated in a lab-scale fluidized reactor under a simulated gasification and combustion atmosphere. One sample was analyzed before treatment in the lab scale reactor as a reference, one sample was analyzed after treatment in gasification conditions, and one sample was analyzed after treatment under combustion conditions.

Used bed material samples after the exposing in combustion and gasification atmosphere were analyzed by X-ray diffraction measurements (XRD). X-ray diffraction measurements were performed with a PANalytical X'Pert PRO system. Refinements were carried out using the program package TOPAS 4.2. The preparation of the samples

Table 1
Typical operation conditions for the bed material.

Parameter	Unit	Range
Temperature in combustion reactor	°C	940–1050 °C
Temperature in gasification reactor	°C	830–870 °C
Average retention time	h	35–70

was carried out in two ways: one analysis of the particles without further treatment and an analysis of grinded particles. Both samples showed similar trends, the sample without grinding will be presented because the trend is more pronounced.

The samples of particles which were exposed in gasification and combustion atmosphere were analyzed using a scanning electron microscope (SEM)–energy dispersive X-ray spectroscopy (EDX) analysis. The samples for analysis of the surface of the particles were fixed on a sample holder without further treatment. For the micrographs the samples were mounted in epoxy, sanded, and polished. Analyses were carried on an FEI Philips model XL30 SEM combined with EDX. At least three spot analyses were carried out to determine the composition of the layers or surfaces on different particles and average compositions were calculated. The EDX-analysis indicates the elemental composition of the surface of the sample. The results were calculated without carbon or oxygen.

Thermo-gravimetric analysis (TGA), differential thermal analysis (DTA), and differential scanning calorimetry analysis (DSC) of fresh

and used bed material particles were carried out in a NETZSCH STA 449 C Jupiter System. The sample crucible is equipped with a thermocouple for direct measurement of the temperature. The mass is measured by an electromagnetically compensated microbalance with a resolution of 0.1 μg and a maximum capacity of 5 g. The furnace allows temperatures of up to 1650 °C with heating rates between 0.01 and 50 K/min. Heating rates of 10 K/min were chosen to ensure minor mass or heat transfer limitations. The signal-to-noise ratio of the DSC is 15 μW. The gas used to provide the desired atmosphere flows upwards and the desired gas composition is mixed out of gas bottles with the aid of mass flow controllers. Gas flows were set to $40 * 10^{-6}$ m^3/min. The mass for each sample was chosen to be approximately 70 mg. The results of the TGA were related to the mass at 250 °C as a reference mass. Temperatures below 250 °C are not considered due to inaccurate temperature controlling of the oven and because temperatures lower than 250 °C are not from interest for this topic.

The thermal analyses were carried out once for each sample in three different atmospheres. These analyses were part of an optimization program in the DFB plant in Güssing where thermal analyses of various inorganic matter were carried out. Due to the good agreement with other results the quality of the analyses are considered as good to conclude on qualitative trends.

Typical conditions for the bed material in the DFB plant in Güssing are summarized in Table 1. The temperature in the combustion reactor is depending on the fuel water content and is varying. The set
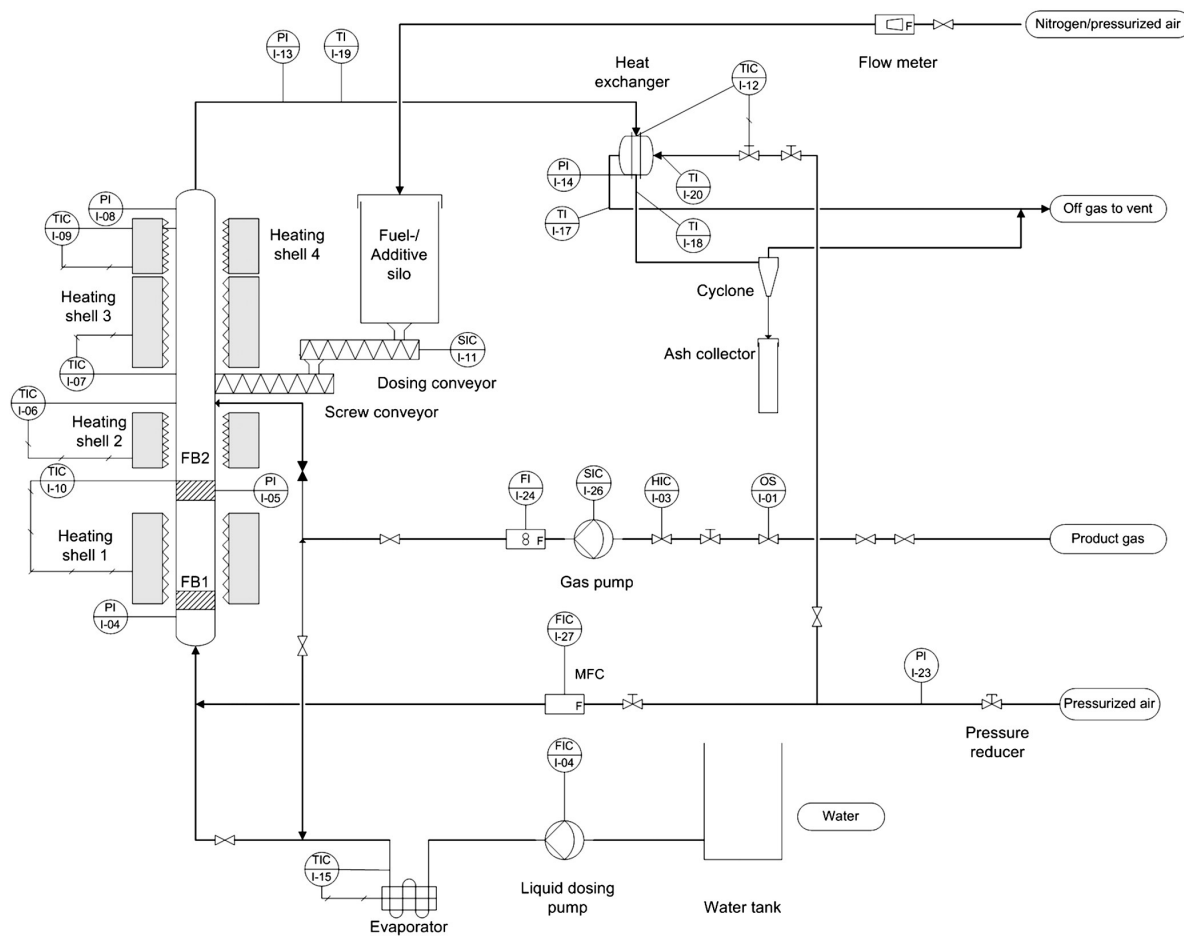
Fig. 2. Flow sheet of the 5 kW lab-scale reactor.

Table 2
Test conditions for gasification and combustion in the test rig.

	Unit	Gasification	Combustion
Temperature	°C	840 ± 8	960 ± 10
Duration of the test run	min	150	150
Fluidization gases and supplements		Product gas (from industrial scale gasification plant, dry, after scrubber)	Air
			Product gas
			Char dust
		Steam	Steam

point for the temperature of the gasification reactor is 850 °C, due to variations in the fuel water content, this temperature can vary between the limits shown in Table 1. The retention time of the bed material in the system is depending on the performance of the cyclone between combustion reactor and gasification reactor. The typical range of the retention time is given in Table 1.

3.2. Lab-scale Fluidized Bed Experiments

A bench-scale fluidized bed reactor was used to evaluate the influence of the surrounding gas atmosphere on the crystal structure of the particles to obtain a better knowledge of whether the incorporation of calcium takes place in the gasification or the combustion reactor of the DFB system. The test rig consists of a reactor, a gas-supplying system, a solid-fuel-dosing system, and off gas handling (heat exchanger, cyclone, and filter). The off gas leaving the reactor and cooling section at gasification operation conditions has to be finally burnt before releasing to the environment. A flow sheet of the test rig is shown in Fig. 2.

The bench-scale reactor is made of stainless steel (1.4841) with a total height of 1.85 m, inner diameter of 65 mm, and wall thickness of 3 mm in the bed section. The reactor consists of two fluidized beds (FB1, FB2). Two perforated stainless steel plates are used as distributors. The lower fluidized bed serves for pre-heating the gas and the upper fluidized bed is used for the reaction and investigations. The lower fluidized bed has a height of 550 mm between the two distributors and the lower bed itself has a height of 100 mm; the upper fluidized bed is 1200 mm in height from the distributor to the gas exit. At the beginning of the experiments bed material is fed in to obtain a bed height of 100 mm.

The gas composition and flow rate are controlled by mass flow controllers. An electrically heated steam generator is used for supplying steam at atmospheric pressure. A bin with a screw-dosing system can be used for adding material into the fluidized bed. The conveying screw is speed-controlled by a frequency converter.

Before leaving the flue gas to the atmosphere, the gas is cooled down in a tube heat exchanger and cleaned in a cyclone and filter, and at operation in gasification conditions it has to be burned before it is released into the atmosphere.

To heat the fluidized bed and keep the temperature constant, the reactor is equipped with electrical wall-heating elements which are regulated with proportional controllers. One heating shell is used for heating the lower fluidized bed (heating shell 1). The upper fluidized bed is heated with three heating elements.

Table 3
Gas composition of combustion and gasification atmosphere.

Component	Unit	Gasification atmosphere	Combustion atmosphere
Hydrogen	%db	~42	–
CO	%db	~20	–
CO_2	%db	~23	~9
CH_4	%db	~9	–
O_2	%db	<0.2	8.5
Nitrogen	%db	<1.5	Rest
Higher hydro-carbons		<4.3	–
Water	%	40	19

The temperature is measured with one thermocouple at the lower fluidized bed and with three thermocouples at the upper fluidized bed and freeboard sections. All thermocouples are of type K with a measuring range of up to 1050 °C.

To generate similar gasification and combustion conditions compared to the industrial-scale DFB gasification plant, similar fuels are used. The gasification atmosphere is generated by using product gas from the Güssing plant for fluidization as the test rig was located in a laboratory just beside the Güssing plant. Since the tapping point of the product gas in the industrial-scale plant is located after the product gas cleaning (filter and scrubber), the gas is mixed with steam to generate a water content similar to that in the gasifier. The test conditions used in the test rig are summarized in Table 2. The product gas composition of the main components is shown in Table 3. The detailed gas composition is described elsewhere [1,13]. The combustion conditions were generated by combustion of product gas and char from the industrial-scale plant. To ensure a similar steam content in the combustion atmosphere, steam is added. The gas atmospheres of the gasification and combustion conditions are summarized in Table 3.

4. Results

The typical composition of the ash of the woody biomass which is utilized as a fuel in the gasification plant in Güssing is shown in Table 4. The composition is typical for woody biomass with a high amount of calcium oxide, silicon oxide, potassium oxide and other elements.

The particle size distribution of the fresh and used olivine which is utilized in the plant in Güssing is shown in Fig. 3. Used olivine has a slightly higher content of fine particles due to abrasion.

Earlier studies only showed micrographs of the particles [4] without recognizing their impact on the gasification performance. But later the influence of the bed material and especially the modification of the particles on the gasification properties became known [5,36]. A detailed examination of the surface of the olivine particle is of interest. A picture of the surface of one particle is shown in Fig. 4. A non-porous surface can be seen, with small dimples as the suggested origin of abrasion in the fluidized bed or elsewhere in the plant. A detailed picture of the surface is shown in Fig. 5, revealing small cracks in the surface, which is mainly smooth. The formation of the two layers outside on the particles is shown in Figs. 6 and 7 in detail. The inner layer could be explained by the diffusion of calcium into the crystal structure of the olivine while the outer layer is similar to the fly ash composition and is considered to grow outward from the particle (see Kirnbauer et al. [4]).

Table 4
Typical composition of the biomass ash results of XRF.

	Wood chip ash	
	Average	Standard deviation
	wt.%	wt.%
Na_2O	2.77	2.66
MgO	5.13	0.45
Al_2O_3	2.57	1.10
SiO_2	15.36	7.52
P_2O_5	2.36	0.24
SO_3	1.26	0.51
K_2O	12.40	2.75
CaO	52.47	6.16
MnO	1.67	0.43
Fe_2O_3	1.73	0.66
Cl	0.42	0.36
Others	1.85	
Water content	26.25	9.00
Ash content (ds)	1.42	0.10
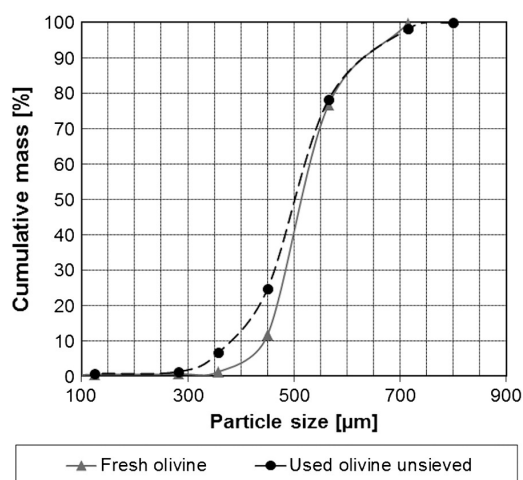
Fig. 3. Typical size distribution of the bed material particle.

Fig. 5. REM picture of used olivine − surface detail.

A comparison of the elemental composition of the surface of the particle is shown in Fig. 8. Both the outer layer and also the analysis of the surface showed that calcium had the highest concentration, followed by magnesium and silicon. The concentration of silicon is lower at the surface of the particle than in the outer layer, while the concentrations of potassium and phosphor are higher. The other elements are in the same range in both pictures. In general the composition in the surface of the particle is similar to that in the outer layer in the micrograph.

An analysis of the surface of the particle at different gas atmospheres simulating the atmospheres in the gasifier and the combustion reactor is shown in Fig. 9. No significant change in the composition of the surface between the reference case and the treatment under gasification conditions and combustion conditions can be observed. Gasification conditions showed slight increases in iron, chrome, and nickel, which are considered to come from the stainless steel reactor walls of the test rig. The composition of the stainless steel wall is removed in the fourth column of Fig. 9 by calculation and shows a similar composition compared to the reference case and the combustion atmosphere.

The examination of the crystal structure by XRD analysis under gasification and combustion conditions is shown in Fig. 10. The main crystal structure is forsterite, which is the main component of olivine; periclase, calcium silicates such as larnite, and iron oxides

such as magnetite and hematite could be detected. Small amounts of potassium silicates were also detectable.

A comparison of the samples under gasification conditions and combustion conditions showed an increase of monticellite, which is a calcium-magnesium silicate, in the combustion atmosphere. Larnite could be detected in a slightly higher amount under combustion conditions compared to gasification conditions. The amount of magnetite decreased under combustion conditions compared to gasification conditions. A slightly weaker signal of forsterite could be detected under combustion conditions.

Figs. 11 and 12 show a comparison of the thermal behavior of fresh and used olivine particles, respectively, in different atmospheres.

A TGA of the bed materials shows moderate weight losses for fresh olivine in air, inert gas (nitrogen) and carbon dioxide gas (mixed with nitrogen) at different temperatures. The only exemption is air, where an increase in weight can be seen at temperatures higher than 900 °C. The weight loss is around 0.05% up to 0.1% of the total mass. The DSC signals shows a plateau between 250 and 450 °C with an endothermic weight loss and a change of thermal properties over the whole temperature range but no characteristic peak with a weight loss at temperatures above 450 °C.

Used olivine shows weight losses of around 0.1% (up to 0.2%) of the mass in the TGA. In nitrogen and air atmosphere, the weight loss occurs at temperatures of around 550 to 600 °C. In a mixture of 15% carbon dioxide and 85% nitrogen by volume a weight loss can be seen at around 800 °C. In a carbon-dioxide-rich atmosphere, the
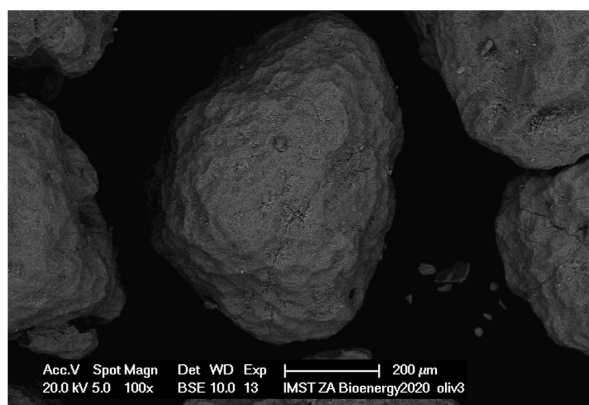
Fig. 4. REM picture of a used olivine particle.
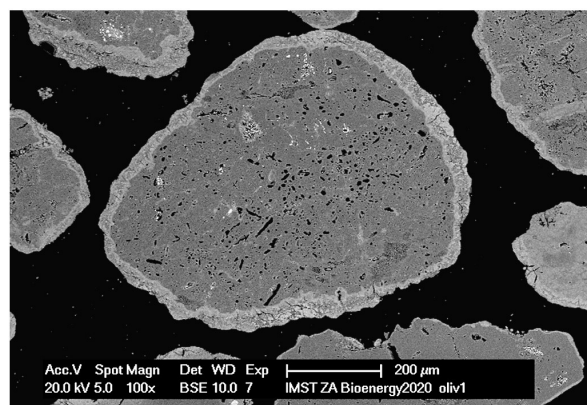
Fig. 6. REM micrograph of used olivine.
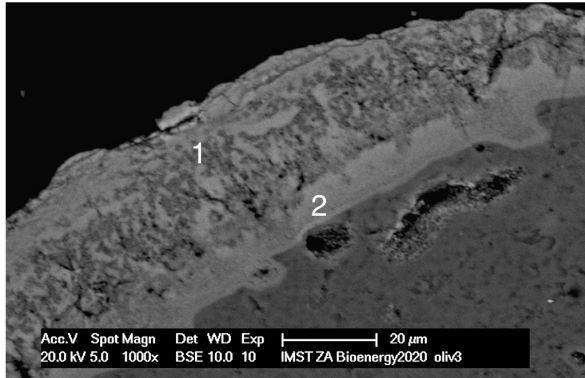
Fig. 7. Micrograph of particle layer of used olivine (1) — outer layer, (2) — inner layer.

DSC signals only indicate a significant endothermic peak at 800 °C, where the weight loss occurs. At higher temperature (>850 °C) a slight decrease in mass can be observed which amounts about 0.2% above 2100 °C.

In an air atmosphere, both the fresh and the used olivine showed significant increases in weight at temperatures higher than 850 °C.

5. Discussion

Investigations of the particle surface of used bed material particles and comparison with the outer layer using micrographs showed no significant differences in the elemental composition. Only small differences in the amount of potassium and phosphor can be seen, which might be explained by condensation reactions during the cooling process when the samples were taken. The difference could be also caused by the accuracy of the measurement the results are average values from multiple samples which reduces the mistake. The relative error of for concentrations between 1 and 5 wt.% is given with 20% by the supplier of the EDX.

The elemental composition of the carbon- and oxygen-free particle surface of used olivine particles also seemed to be stable in different atmospheres during test runs under laboratory conditions. Only the concentration of potassium in the surface decreases compared to the reference in a combustion atmosphere and even more in a gasification atmosphere. This can be explained by the assumption that potassium is mainly available as KOH [35] in the gasification atmosphere and also in the combustion atmosphere and is released from the reactor with the gas phase (product gas and flue gas respectively). Also the high calcium content can be considered to enhance the potassium release in the gas phase [57–59]. In the industrial-scale plant, the conditions can be considered balanced, where a constant balance between incoming potassium that is fed into the gasifier with the biomass and a loss of potassium with the product gas flow leads to a constant potassium concentration in the gas atmosphere and within the bed material. A similar balance can be considered in the combustion reactor, where potassium is fed via ash loops to the combustion reactor and released with the flue gas.

Consideration of the crystal structures of used bed material particles in combustion and gasification atmosphere shows that an increase of monticellite is detected under combustion atmosphere, while forsterite is detected in lower amounts. This can be explained by the incorporation of calcium into the crystal structure of the olivine. The substitution of Fe with Ca is promoted compared to the substitution of Mg with Ca [48]. Nevertheless, a significant amount of MgO can be detected. The diffusion of Ca into the crystal structure of olivine is promoted at higher oxygen fugacities because the partial oxidation of Fe^{2+} to Fe^{3+} is charge-balanced to the formation of these vacancies [49]. In contrast to an earlier study [4], iron silicates are not detected in samples in this study. This might be due to changes in the solid loops (ash circulation and bed material circulation) of the gasification plant which were carried out between this study and the earlier study [4] with the aim of reducing bed material consumption, which leads to a longer retention time of the bed material in the system. Iron silicate structures are considered to be removed from the crystal structures of the olivine during plant operation [30,50].

The detection of crystal structures of potassium silicates in used bed material particles also contrasts with the findings of the earlier study and can be explained again by the change in the ash loops. $K_6Si_6O_{15}$ is a crystal of K_2O and SiO_2 at the ratio of 1:2 on a molar basis. Considering the binary phase diagram of potassium and silicon oxide [60], this structure crystallizes when cooling down a melt to
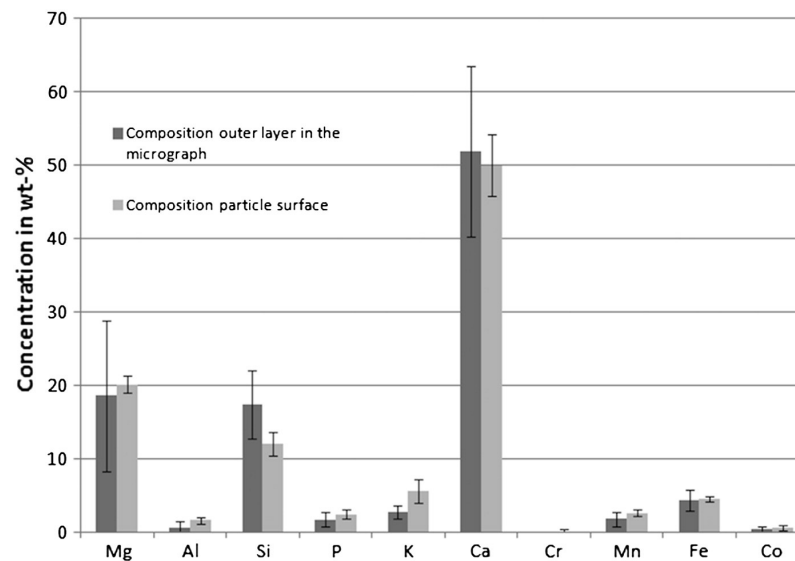
Fig. 8. Comparison of the elemental composition of used olivine shown in the micrograph and the surface (C- and O-free basis).
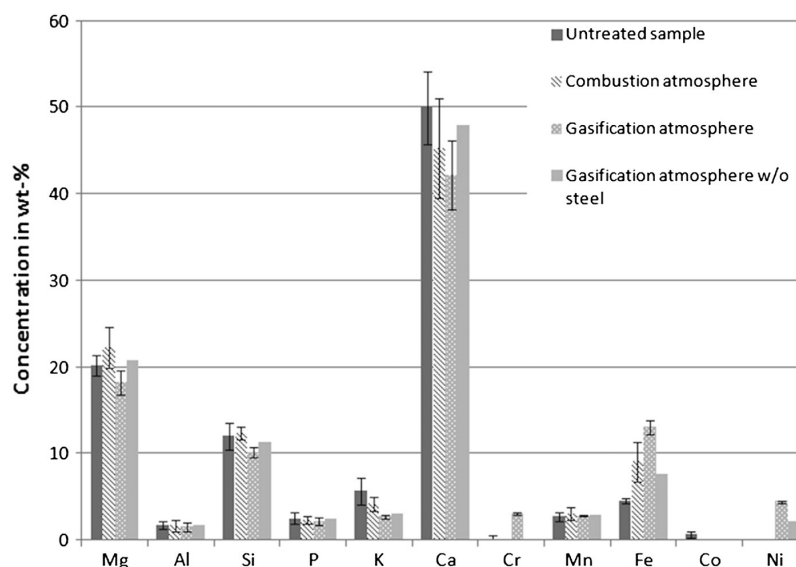
Fig. 9. Elemental composition of the particle surface of used olivine under different atmospheres (C- and O-free basis).

1036 °C, which is the maximum melting temperature of the binary phase in the concentration range between two eutectics points with a potassium oxide concentration of more than 30% on a molar basis. This crystal structure is a mixture of 57% potassium oxide and 43% silicon oxide by weight. Temperatures higher than 1036 °C are considered to be possible locally around burning char particles in the combustion reactor. Considering the mechanism of the layer formation summarized by Grimm et al. [35], described above, the potassium silicate can be considered to be incorporated in the outer layer according to mechanism (a), where melted ash components stick on the surface of the particle and calcium is diffused into the particle. The investigation of the particle surface (see Figs. 4 and 5) shows a smooth surface, which confirms the assumption that layer formation mechanism (a) occurs with a molten surface.

The thermal analysis showed a weight increase of both samples (used and unused bed material) in air at higher temperatures: This might be caused by the oxidation of magnetite [50] or by the decomposition of fayalite with the oxidation of iron. Since fayalite was not detected by analyses of the crystal structure it is evident that the iron of the bed material sample that was taken as a reference was neither oxidized to Fe_2O_3, nor were the samples treated in the combustion atmosphere or gasification atmosphere fully oxidized to Fe_2O_3.

The weight loss at 400 °C with fresh olivine might be caused by the decomposition of magnesium carbonates, which decompose at 400–600 °C [61]. The weight loss of used olivine at around 600 °C is suspected to be caused by the decomposition of calcium hydroxide, which can be built at the surface due to the humidity of the ambient air after sampling.

TGA in an atmosphere of 15% CO_2 in nitrogen shows a similar picture compared to the air and nitrogen atmosphere. The DSC signal of used olivine shows a small but clear endothermic peak at 800 °C during a weight loss of around 0.1 mass%. This peak is considered to be caused by the decomposition of calcium carbonates. The investigations of the
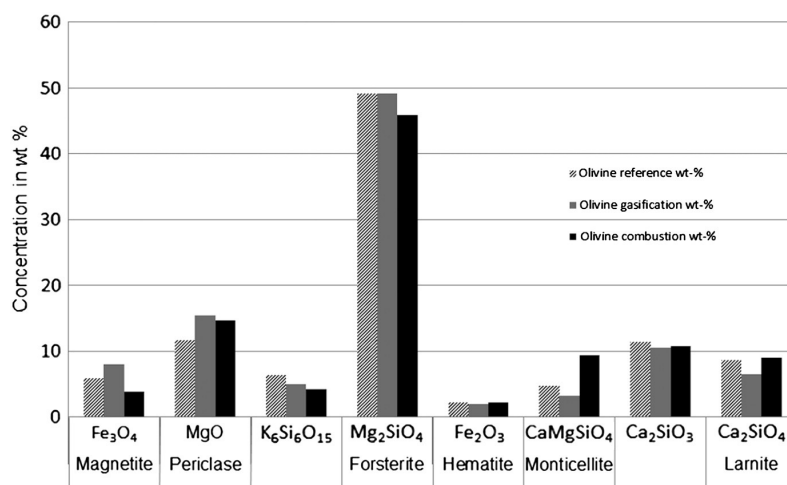
Fig. 10. Crystal structures of used olivine under different gas atmospheres.
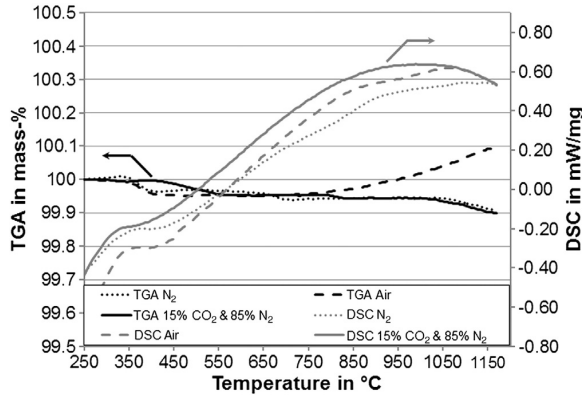
Fig. 11. Thermal analysis of fresh olivine in different atmospheres.

surface of the particles showed a calcium content of 45 to 50%. As the crystal structures showed, at least a part of the calcium is incorporated into the calcium silicate structures but also a part seems to be reactive and can react with CO_2, forming $CaCO_3$ which is released at elevated temperatures. Pure calcium carbonate decomposes in an atmosphere of 15% CO_2 at temperatures of around 800 °C [40,62]. The thermal analysis showed that CO_2 transport of the used olivine is possible in conditions similar to the SER (Sorption Enhanced Reforming) process [3,38–44]. In regular conditions in DFB gasifiers with gasification temperatures of 850 °C and temperatures in the combustion reactor higher than 900 °C, CO_2 transfer between the gasification and combustion reactors is negligible. The surface investigations of the bed material showed a flat surface with a low specific surface of the particle, indicating a low capacity for the transport of CO_2. The weight loss in the CO_2-rich atmosphere is around 0.1%, which represents a far lower specific transport capacity of the bed material compared to bed materials that are typically used in the SER process [63].

Considering optimization potentials of the DFB biomass steam gasification, important results were obtained by this study.

(i) One option for optimization is the reduction of the gasification temperature which increases the electrical efficiency of the plant. By this measure the temperature in the combustion reactor is reduced accordingly. Since the layer formation is suggested to be dependent not only on the temperature of the fluidized bed but also on the combustion temperature of char particles, a lower temperature in the combustion reactor does not necessarily affect the layer formation. The combustion
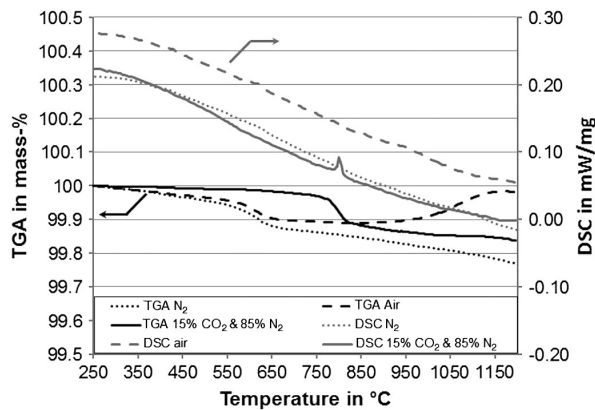
temperature of the char particles can be influenced by the oxygen excess in the combustion reactor.

(ii) The utilization of alternative fuels (other than woody biomass) will have an impact on the composition of inorganic matter in the plant and this will have an impact on the layer formation. According to Grimm et al. [35] the layer formation mechanism and the composition of the layer will change with different fuels, such as fuels rich in potassium or phosphorus. Since the elemental composition of the surface of the particle is similar to the ash composition (see Kirnbauer et al. [4]), a significant impact on the operation of the plant is expected by using different fuels with different ash compositions. Detailed investigations with different fuels and fuel blends are required to evaluate the influence of the different ash compositions on the gasification properties.

(iii) The synthesis of fuels and chemicals such as Fischer–Tropsch synthesis and synthesis of synthetic natural gas (BioSNG), mixed alcohols, or chemicals have different requirements regarding the product gas composition, for example the optimal H_2:CO ratio. A reduction of the gasification temperature will influence the product gas composition [36], and by choosing the correct temperatures of the gasification reactor and the combustion reactor, the transport of CO_2 from the gasification reactor to the combustion reactor is possible. The low CO_2 load capacity of the used bed material limits the influence on the product gas composition.

6. Conclusions

The following conclusions can be drawn from this work:

• The elemental composition at the surface of the used bed material particles is similar to the composition of the outer layer measured in micrographs and does not change significantly between the gasification and combustion atmospheres.
• The investigation of the crystal structure showed an increase of calcium-silicates in the combustion atmosphere, which is in accordance with theoretical considerations. Higher diffusion rates can be expected at higher temperatures and higher oxygen concentrations in the combustion reactor.
• An intensive contact of olivine particles and ash promotes the formation of the layers in the combustion reactor. Burning char particles promotes layer formation due to melt formation and random collisions of bed material with burning char particles.
• The calcium-rich surface of the used bed material particles allows the reaction with CO_2. At typical temperatures of DFB biomass steam gasification plants, CO_2 transport from the gasification to the combustion reactor is not expected.

References

[1] H. Hofbauer, R. Rauch, G. Loeffler, S. Kaiser, E. Fercher, H. Tremmel, Six years experience with the FICFB-GASIFICATION process, Proceedings of the 12th European Conf. on Biomass and Bioenergy, Amsterdam, The Neatherlands, 2002.
[2] M. Bolhar-Nordenkampf, H. Hofbauer, K. Bosch, R. Rauch, C. Aichernig, Biomass CHP Plant Güssing — using gasification for power generation, in: K. Kirtikara (Ed.), Proceedings of the International Conference on Biomass Utilisation, vol. 1, Phuket, Thailand, 2003, pp. 567–572.

Fig. 12. Thermal analysis of used olivine in different atmospheres.

[3] S. Koppatz, C. Pfeifer, R. Rauch, H. Hofbauer, T. Marquard-Moellenstedt, M. Specht, H₂ rich product gas by steam gasification of biomass with in situ CO₂ absorption in a dual fluidized bed system of 8 MW fuel input, Fuel Processing Technology 90 (2009) 914–921.

[4] F. Kirnbauer, H. Hofbauer, Investigations on bed material changes in a dual fluidized bed steam gasification plant in Güssing, Austria, Energy & Fuels 25 (2011) 3793–3798.

[5] F. Kirnbauer, V. Wilk, H. Kitzler, S. Kern, H. Hofbauer, The positive effects of bed material coating on tar reduction in a dual fluidized bed gasifier, Fuel 95 (2012) 553–562.

[6] H. Hofbauer, R. Rauch, K. Bosch, R. Koch, C. Aichernig, Biomass CHP Plant Güssing — a success story, in: A.V. Bridgwater (Ed.), Pyrolysis and Gasification of Biomass and Waste, CPL Press, 2003, pp. 527–536.

[7] J. Kotik, Über den Einsatz von Kraft-Wärme-Kopplungsanlagen auf Basis der Wirbelschicht-Dampfvergasung fester Biomasse am Beispiel des Biomassekraftwerks Oberwart, PhD Thesis Vienna University of Technology, 2010. (in German language).

[8] T. Klotz, A regional energy-supply-showcase–the 15 MW fuel-power biomass gasification plant villach, International Seminar on Gasification, Gothenbourg, Sweden, October 28-29 2010.

[9] I. Gunnarsson, The GoBiGas project — efficient transfer of biomass to biofuels, SGC International Seminar on Gasification, Gothenburg, Sweden, October 28–29 2010.

[10] R. Rauch, H. Hofbauer, S. Săcăreanu, A. Chiru, From gasification to synthetic fuels via Fischer–Topsch synthesis, Bulletin of the Transsilvania University of Brasov Series I - Engineering Sciences 3 (2011) 33–40.

[11] B. Rehling, H. Hofbauer, Bio-SNG from biomass — first results of a demonstration plant, ICPS 09 — Int Conf Polygeneration Strategies., Vienna, Austria, 2009.

[12] B. Rehling, H. Hofbauer, R. Rauch, C. Aichernig, BioSNG—process simulation and comparison with first results from a 1-MW demonstration plant, Biomass Conversion and Biorefinery 1 (2011) 111–119.

[13] A. Sauciuc, A. Potetz, G. Weber, R. Rauch, H. Hofbauer, L. Dumitrescu, Synthetic diesel from biomass by Fischer–Tropsch synthesis, Int. Conf of Renewable Energies and Power Quality (ICREPQ `11), Las Palmas de Gran Canaria, Spain, ISBN: 978-84-614-7527-8, 2011.

[14] A. Sauciuc, Z. Abostreif, G. Weber, A. Potetz, R. Rauch, H. Hofbauer, et al., Influence of pressure on the performance of biomass based Fischer–Tropsch synthesis, Proc of the int conf on polygeneration strategies (ICPS11), August 30–September 1, Vienna, Austria, 2011.

[15] M. Öhman, L. Pommer, A. Nordin, Bed agglomeration characteristics and mechanisms during gasification and combustion of biomass fuels, Energy & Fuels 19 (2005) 1742–1748.

[16] M. Zevenhoven-Onderwater, R. Backman, B.J. Skrifvars, M. Hupa, T. Liliendahl, E. Rosén, et al., The ash chemistry in fluidised bed gasification of biomass fuels. Part II: Ash behaviour prediction versus bench scale agglomeration tests, Fuel 80 (2001) 1503–1512.

[17] S. Arvelakis, P.A. Jensen, K. Dam-Johansen, Simultaneous thermal analysis (STA) on ash from high-alkali biomass, Energy & Fuels 18 (2004) 1066–1076.

[18] T. Valmari, T.M. Lind, E.I. Kauppinen, G. Sfiris, K. Nilsson, W. Maenhaut, Field study on ash behavior during circulating fluidized-bed combustion of biomass. 1. Ash formation, Energy & Fuels 13 (1998) 379–389.

[19] T. Valmari, T.M. Lind, E.I. Kauppinen, G. Sfiris, K. Nilsson, W. Maenhaut, Field study on ash behavior during circulating fluidized-bed combustion of biomass. 2. Ash deposition and alkali vapor condensation, Energy & Fuels 13 (1998) 390–395.

[20] K.O. Davidsson, L.E. Amand, B.M. Steenari, A.L. Elled, D. Eskilsson, B. Leckner, Countermeasures against alkali-related problems during combustion of biomass in a circulating fluidized bed boiler, Chemical Engineering Science 63 (2008) 5314–5329.

[21] T.R. Miles, L.L. Baxter, R.W. Bryers, B.M. Jenkins, L.L. Oden, Boiler deposits from firing biomass fuels, Biomass and Bioenergy 10 (1996) 125–138.

[22] H.P. Nielsen, L.L. Baxter, G. Sclippab, C. Morey, F.J. Frandsen, K. Dam-Johansen, Deposition of potassium salts on heat transfer surfaces in straw-fired boilers: a pilot-scale study, Fuel 79 (2000) 131–139.

[23] T. Pröll, R. Rauch, C. Aichernig, H. Hofbauer, Fluidized bed steam gasification of solid biomass: analysis and optimization of plant operation using process simulation, ASME Conf. Proc. 2005, 2005, pp. 763–770.

[24] T. Pröll, R. Rauch, C. Aichernig, H. Hofbauer, Fluidized bed steam gasification of solid biomass—performance characteristics of an 8 MWth combined heat and power plant, International Journal of Chemical Reactor Engineering 5 (2007) 1–19.

[25] M. Hupa, Ash-Related Issues in Fluidized-Bed Combustion of Biomasses: Recent Research Highlights, Energy & Fuels 26 (2012).

[26] D. Boström, N. Skoglund, A. Grimm, C. Boman, M. Öhman, M. Broström, et al., Ash transformation chemistry during combustion of biomass, Energy & Fuels 26 (2012) 85–93.

[27] C. Pfeifer, S. Koppatz, H. Hofbauer, Catalysts for dual fluidised bed biomass gasification—an experimental study at the pilot plant scale, Biomass Conversion and Biorefinery (2011) 1–12.

[28] L. Devi, M. Craje, P. Th ne, K.J. Ptasinski, F.J.J.G. Janssen, Olivine as tar removal catalyst for biomass gasifiers: catalyst characterization, Applied Catalysis A: General 294 (2005) 68–79.

[29] L. Devi, K.J. Ptasinski, F.J.J.G. Janssen, Decomposition of naphthalene as a biomass tar over pretreated olivine: effect of gas composition, kinetic approach, and reaction scheme, Industrial and Engineering Chemistry Research 44 (2005) 9096–9104.

[30] L. Devi, K.J. Ptasinski, F.J.J.G. Janssen, Pretreated olivine as tar removal catalyst for biomass gasifiers: investigation using naphthalene as model biomass tar, Fuel Processing Technology 86 (2005) 707–730.

[31] J. Corella, J.M. Toledo, R. Padilla, Olivine or dolomite as in-bed additive in biomass gasification with air in a fluidized bed: which is better? Energy & Fuels 18 (2004) 713–720.

[32] S. Rapagná, N. Jand, A. Kiennemann, P.U. Foscolo, Steam-gasification of biomass in a fluidised-bed of olivine particles, Biomass and Bioenergy 19 (2000) 187–197.

[33] M.L. Mastellone, U. Arena, Olivine as a tar removal catalyst during fluidized bed gasification of plastic waste, AICHE Journal 54 (2008) 1656–1667.

[34] U. Arena, L. Zaccariello, M.L. Mastellone, Tar removal during the fluidized bed gasification of plastic waste, Waste Management 29 (2009) 783–791.

[35] A. Grimm, M. Öhman, T. Lindberg, A. Fredriksson, D. Boström, Bed agglomeration characteristics in fluidized-bed combustion of biomass fuels using olivine as bed material, Energy & Fuels 26 (2012) 4550–4559.

[36] F. Kirnbauer, V. Wilk, H. Hofbauer, Performance improvement of dual fluidized bed gasifiers by temperature reduction: the behavior of tar species in the product gas, Fuel 108 (2012) 534–542.

[37] S. Kern, C. Pfeifer, H. Hofbauer, Reactivity tests of the water gas shift reaction on fresh and used fluidized bed materials from industrial DFB biomass gasifiers, Biomass and Bioenergy (2013), http://dx.doi.org/10.1016/j.biombioe.2013.02.001, (in press).

[38] N.H. Florin, A.T. Harris, Enhanced hydrogen production from biomass with in situ carbon dioxide capture using calcium oxide sorbents, Chemical Engineering Science 63 (2008) 287–316.

[39] C. Pfeifer, B. Puchner, H. Hofbauer, Comparison of dual fluidized bed steam gasification of biomass with and without selective transport of CO₂, Chemical Engineering Science 64 (2009) 5073–5083.

[40] G. Soukup, C. Pfeifer, A. Kreuzeder, H. Hofbauer, In situ CO₂ capture in a dual fluidized bed biomass steam gasifier — bed material and fuel variation, Chemical Engineering and Technology 32 (2009) 348–354.

[41] K. Göransson, U. Söderlind, J. He, W. Zhang, Review of syngas production via biomass DFBGs, Renewable and Sustainable Energy Reviews 15 (2011) 482–492.

[42] C. Pfeifer, S. Koppatz, H. Hofbauer, Steam gasification of various feedstocks at a dual fluidised bed gasifier: Impacts of operation conditions and bed materials, Biomass Conversion and Biorefinery 1 (2011) 39–53.

[43] C. Hawthorne, N. Poboss, H. Dieter, A. Gredinger, M. Zieba, G. Scheffknecht, Operation and results of a 200-kWth dual fluidized bed pilot plant gasifier with adsorption-enhanced reforming, Biomass Conversion and Biorefinery 2 (2012) 217–227.

[44] T. Pröll, H. Hofbauer, H₂ rich syngas by selective CO₂ removal from biomass gasification in a dual fluidized bed system — process modelling approach, Fuel Processing Technology 89 (2008) 1207–1217.

[45] J. Schmid, T. Pröll, C. Pfeifer, H. Hofbauer, Improvement of gas-solid interaction in dual circulating fluidized bed systems, Proc. of 9th European Conf on Industrial Furnaces and Boilers (INFUB), Estoril, Portugal, 2011.

[46] P.L. Roeder, R.F. Emslie, Olivine-liquid equilibrium, Contributions to Mineralogy and Petrology 29 (1970) 275–289.

[47] J. Smyth, High temperature crystal chemistry of fayalite, American Mineralogist (1975).

[48] G. Libourel, Systematics of calcium partitioning between olivine and silicate melt: implications for melt structure and calcium content of magmatic olivines, Contributions to Mineralogy and Petrology 136 (1999) 63–80.

[49] R. Dohmen, H.-W. Becker, S. Chakraborty, Fe–Mg diffusion in olivine I: experimental determination between 700 and 1,200°C as a function of composition, crystal orientation and oxygen fugacity, Physics and Chemistry of Minerals 34 (2007) 389–407.

[50] H.O.A. Fredriksson, R.J. Lancee, P.C. Thüne, H.J. Veringa, J.W.H. Niemantsverdriet, Olivine as tar removal catalyst in biomass gasification: catalyst dynamics under model conditions, Applied Catalysis B: Environmental (2012) 1–23.

[51] M. Öhman, A. Nordin, B.-J. Skrifvars, R. Backman, M. Hupa, Bed agglomeration characteristics during fluidized bed combustion of biomass fuels, Energy & Fuels 14 (2000) 169–178.

[52] E. Brus, M. Öhman, A. Nordin, Mechanisms of bed agglomeration during fluidized-bed combustion of biomass fuels, Energy & Fuels 19 (2005) 825–832.

[53] S. De Geyter, The Role of Sulphur in Preventing Bed Agglomeration During Combustion of Biomass, 2006.

[54] A. Grimm, N. Skoglund, D. Boström, M. Öhman, Bed agglomeration characteristics in fluidized quartz bed combustion of phosphorus-rich biomass fuels, Energy & Fuels 25 (2011) 937–947.

[55] F. Scala, R. Chirone, Characterization and early detection of bed agglomeration during the fluidized bed combustion of olive husk, Energy & Fuels 20 (2006) 120–132.

[56] A. Grimm, N. Skoglund, D. Boström, C. Boman, M. Öhman, Influence of phosphorus on alkali distribution during combustion of logging residues and wheat straw in a bench-scale fluidized bed, Energy & Fuels 26 (2012) 3012–3023.

[57] P. Thy, C.E. Lesher, B.M. Jenkins, Experimental determination of high-temperature elemental losses from biomass slag, Fuel 79 (2000) 693–700.

[58] P. Thy, B.M. Jenkins, S. Grundvig, R. Shiraki, C.E. Lesher, High temperature elemental losses and mineralogical changes in common biomass ashes, Fuel 85 (2006) 783–795.

[59] A. Novaković, S.C. van Lith, et al., Release of potassium from the systems K – Ca – Si and K – Ca – P, Energy & Fuels 23 (2012).

[60] F.C. Kracek, N.L. Bowen, G.W. Morey, The system potassium metasilicate-silica, The Journal of Physical Chemistry 33 (1929) 1857–1879.

[61] N. Khan, D. Dollimore, K. Alexander, F.W. Wilburn, The origin of the exothermic peak in the thermal decomposition of basic magnesium carbonate, Thermochimica Acta 367–368 (2001) 321–333.

[62] N.H. Florin, A.T. Harris, Reactivity of CaO derived from nano-sized CaCO3 particles through multiple CO2 capture-and-release cycles, Chemical Engineering Science 64 (2009) 187–191.

[63] G.S. Grasa, J.C. Abanades, CO2 capture capacity of CaO in long series of carbonation/calcination cycles, Industrial and Engineering Chemistry Research 45 (2006) 8846–8851.

Dipl.-Ing. Friedrich Kirnbauer: Mr. Kirnbauer received a Dipl.-Ing. in Process Engineering at Vienna University of Technology. He completed his diploma thesis with a work on the high temperature syngas cleaning of biomass steam gasification. Since 2009 he works for the competence centre BIOENERGY 2020 + as a scientist in the area steam gasification. His research area is biomass steam gasification with the focus on ash related issues and bed material modifications. He is author of scientific articles in international journals in the field bed material modification and its influence on gasification in fluidized bed gasification plants.

Univ.-Prof. Dipl.-Ing. Dr. Hermann Hofbauer: Prof. Hofbauer received a Dipl. Ing. in Mechanical Engineering and Dr. techn. in Chemical Engineering at Vienna University of Technology. He was appointed as full Professor for Chemical Engineering in 1997. He is head of the Chemical Engineering Institute and is leading the research division of Chemical Process Engineering und Energy Technology. He is key researcher at the competence centre BIOENERGY 2020 + and chairman of the scientific board. He is author or co-author of more than 300 scientific publications in the field of thermal biomass conversion and fluidized bed technology. He has got numerous grants for his scientific work.

Publication V

Behavior of Inorganic Matter in a Dual Fluidized Steam Gasification Plant

Friedrich Kirnbauer,*,[†] Markus Koch,[‡] Reinhard Koch,[‡] Christian Aichernig,[§] and Hermann Hofbauer[||]

[†]Bioenergy 2020+ GmbH, Wiener Straße 49, A-7540 Güssing, Austria
[‡]Biomasse-Kraftwerk Güssing GmbH, Europastraße 1, A-7540 Güssing, Austria
[§]Repotec Umwelttechnik GmbH, Europastraße 1, A-7540 Güssing, Austria
[||]Vienna University of Technology, Institute of Chemical Engineering, Getreidemarkt 9/166, 1060 Vienna, Austria

ABSTRACT: Ash components of biomass fuels can cause fouling, slagging, and bed material agglomeration during thermal utilization in fluidized bed combustion and gasification plants. The influence of ash components on these problems in dual fluidized bed biomass gasification plants is investigated in an industrial scale plant in Güssing, Austria. Samples of fouling are analyzed, and the results are evaluated. The samples were analyzed by X-ray fluorescence analysis and thermal analyses such as thermogravimetric analysis, differential thermal analysis, and differential scanning calorimetry. Mass balances of inorganic matter are presented, evaluating different loop configurations. The analyses showed high potassium contents compared to the fuel ash composition in fouling of up to 23% by weight. The potassium content of fly ash with a particle size smaller than 200 μm is half that of coarse fly ash with a particle size larger than 200 μm. The thermal analyses showed a large difference between samples of inorganic streams such as fly ash or fly char and fouling. Different fractions of fly ash samples (particle fraction smaller than 200 μm and particle fraction larger than 200 μm) showed similar thermal behavior: endothermic weight losses at around 400 °C and around 720−820 °C caused by decomposition of carbonates. The composition of inorganic matters of fly ash and fly char is similar. The elemental composition of deposits at the cyclone wall and the first heat exchanger in the flue gas path showed high potassium contents up to 23.6%. While samples of fly ash and fly char did not show significant melting in their thermal behavior, melting could be detected with fouling at temperatures higher than 1000 °C. Mass balances of inorganic matter showed a flow of potassium oxide from the combustion reactor to the gasification reactor, which leads to unexpected high potassium concentrations in the fly char. A reduction of ash loops reduces the amount of potassium that is transferred from the combustion reactor to the gasification reactor. Recommendations are made for the operation of dual fluidized bed gasification plants in terms of ash handling to reduce tendencies for fouling, slagging, and bed material agglomeration.

■ INTRODUCTION

Biomass fuels are well-known to cause operational problems and unscheduled downtime in fluidized bed combustion plants. These problems are often caused by slagging, fouling, and bed material agglomeration.[1,2] Gasification plants face similar problems. Studies published about fouling, slagging, and bed material agglomeration in gasification plants are often carried out in lab-scale test rigs, but studies of these phenomena in industrial-scale gasification plants are sparse. This might be due to a lack of operating fluidized bed biomass gasification plants.[3]

A technology for the gasification of biomass, which is demonstrated successfully at industrial scale, is biomass steam gasification in a dual fluidized bed (DFB) gasifier. Various plants working with the DFB gasification technology are in operation, for example, in Güssing (Austria; 8 MWth),[4] Oberwart (Austria; 8.5 MWth),[5] Villach (Austria; 15 MWth),[6] and Ulm (Germany; 15.1 MWth).[7]

The DFB biomass steam gasification plant in Güssing was the first industrial scale DFB biomass steam gasification plant to go into operation. It began operating in 2002 and demonstrated the DFB process successfully.

Because this plant in Güssing was the first installation of an industrial-scale DFB steam gasification plant, potential for improvements in terms of plant design and engineering was determined. These disadvantages in the design of the Güssing

plant lead to a higher risk of fouling and slagging. Knowledge about design improvements was considered in plants that were constructed recently, and fouling and slagging cannot be determined in the gasification plant in Oberwart, for example. The present operation of the plant in Güssing also differs from what was defined during the planning phase in some aspects.

The fuel−water content has a big influence on the operation, and is 33% on average today; in comparison, the design value was 15%. The consequence is that the combustion chamber is operated with a higher load than designed, which leads to higher velocities and lower excess air.

However, a better understanding of the fouling and slagging mechanism for woody biomass at the plant in Güssing may be a precondition for design improvements in future plants and for the utilization of cheaper alternative fuels in DFB gasifiers such as energy crops, straw, sewage sludge, and so on. By now, the gasification plants are running with woody biomass as a fuel.

This study is part of a process of overall optimization of the plant to increase its efficiency in terms of technological efficiency, economic efficiency, and availability. This paper presents the results of analyses of inorganic matter in solid flow streams and
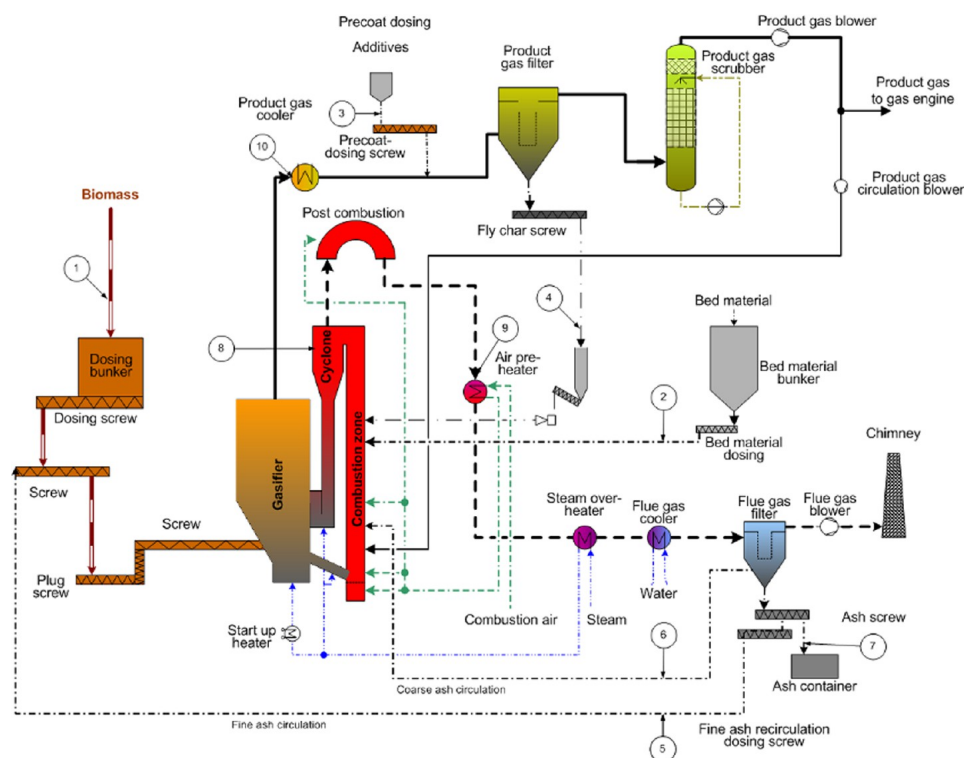
Figure 1. Flow sheet of the CHP plant in Güssing with sampling points.

fouling and documents different ash loop setups with balances of inorganic matter at the plant in Güssing. The formation mechanism of fouling is investigated, and suggestions for a mechanism are given. Proposals for improvements of the inorganic loops and the operation of the plant are given.

■ FUNDAMENTALS

The principle of DFB steam gasification is based on the separation of the endothermic gasification process and the external heat supply from a separate combustion chamber. Heat is transferred via circulating bed material between the gasification zone (gasifier) operated in bubbling bed mode and the combustion reactor operated in fast-fluidized bed mode. Details of the DFB steam gasification process are summarized elsewhere.[4,8−13] A basic flow sheet of the Güssing plant with a focus on inorganic material streams is shown in Figure 1.

Input streams for inorganic matter are biomass streams into the gasifier (wood chips), precoat material (dolomite) prior to the product gas filter, and bed material supplement to the combustion zone. The output stream is only fly ash that leaves the process after the flue gas filter and is collected in a container.

The main internal stream of inorganic matter is the circulation stream of bed material between the gasifier and the combustion zone. A fine fraction of inorganic matter such as biomass ash and abraded bed material leaves the gasifier with the product gas and is separated in the product gas filter (fly char). This dust from the product gas filter contains organic matter that is not gasified, such as char and tar. To utilize this remaining energy, char and tars are burned in the combustion zone.

Inorganic matter plays an important role in the gasification properties but can also lead to fouling, slagging, and bed material agglomeration, which can cause unplanned shutdowns of thermal biomass conversion plants. Various studies of fouling and bed agglomeration are available in the literature, with a focus on the utilization of coal with biomass,[14−16] but several studies are also available for woody or other biomass combustion.[2,17−20] The difference between combustion plants and the DFB biomass gasifier in terms of fouling, slagging, and bed agglomeration is caused by the utilization of two main reactors: a gasification reactor with a reducing atmosphere and a combustion reactor with an oxidizing atmosphere. Intensive exchange of inorganic matters originating from the fuel and bed materials occurs between the two reactors. In contrast to regular fluidized bed combustion plants where quartz sand is used, the bed material in DFB biomass gasification plants is olivine, which is a magnesium iron silicate.

Ash of woody biomass can be described as a system that is dominated by silicates with different contents of basic oxides and a high content of volatile alkaline sulfates and alkaline chlorides.[21,22] Besides alkali metals, the alkali earth metals also react to form silicates.[21,22]

The state of matter of the inorganic material (solid, liquid, gas) plays an important role in the reactivity of the substances. Table 1 shows general relationships of the state of matter and the reactivity of the substances. Two gaseous components show the highest reactivity, followed by a gaseous and a liquid component. Gaseous and solid components have a higher reactivity than two liquid components, followed by a liquid and a solid component. Two solid components show the lowest

Table 1. Influence of the Physical Form of the Substances on the Reactivity[21]

reactivity of the ash[a]	
(g) + (g) ≫ (g) + (l) > (g) + (s) > (l) + (l) > (l) + (s) ≫ (s) + (s)	equation 1

[a](g) gaseous elements, (l) liquid elements, (s) solid elements.

reactivity with each other. This is valid for the reactivity and the reaction rate.[22]

The substances that are typically detectable in biomass ashes can be split into acid and basic substances (Table 2). The reactivity decreases from the first to the last row.[22]

Table 2. Classification of Ash Compounds[22]

basic cmpds	acidic cmpds
KOH (l, g) (K_2O)	P_2O_5 (g)
NaOH (l, g) (Na_2O)	SO_2 (g)/SO_3 (g)
CaO (s)	SiO_2 (s)
MgO (s)	HCl (g) (Cl_2)
H_2O (g)	CO_2
	H_2O (g)

Considering the main components of biomass ash, a binary mixture of potassium and silicon oxides is the substance with the lowest melting point, forming a eutectic point at 752 °C with a ratio of 31% K_2O to 69% SiO_2 by weight. Three different crystal phases are formed: $K_2O{\cdot}SiO_2$ (melting point 976 °C), $K_2O{\cdot}2SiO_2$ (melting point 1036 °C), and $K_2O{\cdot}4SiO_2$ (melting point 765 °C).[23]

The phase diagram for the three-component system of the oxides of potassium, calcium, and silicon, which represents the main components of biomass ash, forms eutectic points with melting temperatures of around 850 °C.[24] Other elements such as sulfur, chlorine, and potassium have a significant influence on the physical form of the ash mixture at high temperature. The main reactions of ash components were summarized by Boström et al.[22] and are shown in Table 3. These reactions can take place under proper conditions such as temperature, pressure, and availability of reaction partners. Mineral substances can be formed, and amorphous melts can also be detected at fast cooling rates.

The release of alkaline metals in the gas phase is important for the formation of fouling, slagging, and bed material agglomeration because these elements condense after cooling and react with other elements during condensation, which can lead to fouling at heat exchangers. On the other hand, the reactivity of elements in the gas phase is higher compared to elements incorporated in a solid crystal structure, as described above.

Van Lith et al.[25] studied the mechanism and modification of potassium during the devolatilization and combustion of biomass, as shown in Figure 2. Due to its metabolic function, potassium is highly mobile within all levels of the plant. During drying of the wood, potassium is likely to precipitate in the form of salts such as KCl, K_2SO_4, KOH, and K_2CO_3. Some of the potassium is bound in organic structures in carboxyl groups. In spruce and beech, about 40% of the potassium is organically associated. During devolatilization and combustion of biomass, organically bound potassium and inorganic bound potassium follow different reaction schemes. Inorganic bound potassium (e.g., potassium chlorine) is stable and is evaporated at higher temperatures. Carboxyl groups start to decompose at temperatures lower than 300 °C, and atomic potassium will be released. This elemental potassium is likely to react with phenol groups, which are stable at these temperatures, or it remains in the gas phase. At higher temperatures, it is suggested that potassium is bound to phenol groups, which decompose at temperatures higher than 400 °C, while potassium is released to the gas phase, probably in elemental form. During the combustion at temperatures about 850 °C, organically bound potassium is oxidized to potassium carbonate. Elemental potassium can also react with minerals that remain stable, or it reacts with oxygen to form potassium carbonate. The decomposition of potassium carbonate (K_2CO_3) seems to be the dominant mechanism at temperatures higher than 800 °C.

Novaković et al.[26] showed in laboratory scale trials with mixtures of potassium, calcium, and silicon that the release of potassium into the gas phase is mainly dependent on the calcium content in the mixture, the water content in the gas phase, and the temperature. The release rate is independent of the origin of the calcium (e.g., $CaCO_3$ or $Ca(OH)_2$). The absence of steam reduces the release of potassium, while doubling the calcium content brings a higher release of potassium.

Table 3. Survey of Major Secondary Ash-Forming Reactions (Schematic)[22]

reaction	comments	
P_2O_5(g) + 2KOH(g) ↔ 2KPO_3(l, g) + H_2O(g)	fast reaction,[a] product molten and partially volatile in residual ash[b]	equation 2
SO_3(g) + 2KOH(g) ↔ K_2SO_4(l, g) + H_2O(g)	fast reaction, product molten or not	equation 3
HCl(g) + KOH(g) ↔ KCl(g, l) + H_2O(g)	fast reaction, product not stable in residual ash	equation 4
SiO_2(s) + 2KOH(g) ↔ K_2SiO_3(l) + H_2O(g)	medium fast reaction, product stable and molten in residual ash	equation 5
CO_2(g) + 2KOH(g) ↔ K_2CO_3(l, g) + H_2O(g)	fast reaction, product not stable in residual ash	equation 6
P_2O_5(s) + 3CaO(s) ↔ $Ca_3P_2O_8$(s)	medium fast reaction, product stable and solid in residual ash	equation 7
SO_3(g) + CaO(s) ↔ $CaSO_4$(s, l)	medium fast reaction, product (not) stable and solid in residual ash	equation 8
2HCl(g) + CaO(s) ↔ $CaCl_2$(g, l) + H_2O(g)	medium fast reaction, product not stable in residual ash	equation 9
SiO_2(s) + CaO(s) ↔ $CaSiO_3$(s)	slow reaction,[c] product stable and solid in residual ash	equation 10
CO_2(g) + CaO(s) ↔ $CaCO_3$(s)	medium fast reaction, product not stable in residual ash[b]	equation 11
K_2SiO_3(l) + CaO(s) ↔ K − Ca − Silicate(l)	rather slow reaction,[c] product stable and molten in residual ash	equation 12

[a]The reaction rates are classified into four categories on an arbitrary scale. [b]The stability in residual ash varies according to the thermal condition of the specific appliance. [c]These reaction rates are also highly dependent upon the dispersion of fuel and reactant particles.

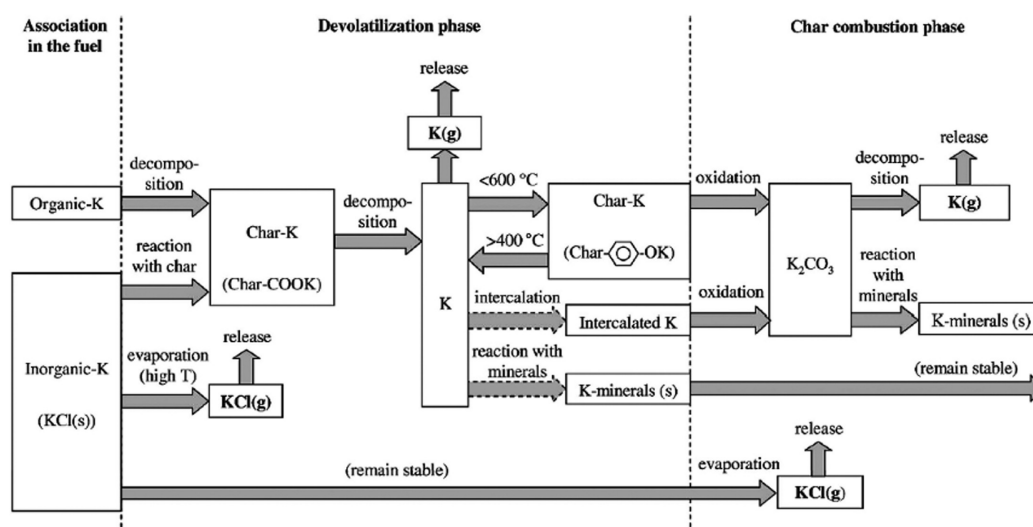**Figure 2.** Possible transformations and release mechanisms of organically associated K and KCl during devolatilization and combustion of biomass.[25]

The chemical mechanism of the release of potassium from potassium carbonate is shown in eq 6. An excess of water moves the equilibrium according to Le Chatelier's principle toward $KOH(g)$ and $CO_2(g)$ and, with that, toward a higher release rate of potassium into the gas phase.

Comparing the release of potassium into the gas phase in an oxidizing atmosphere (combustion) and a reducing atmosphere (gasification), a higher release rate can be expected in the reducing atmosphere of the gasification reactor at the same temperatures.[27,28]

The consequences of ash melting or the release of inorganic matter into the gas phase can be fouling, slagging, and bed material agglomeration. Deposits occurring in the high temperature sections of furnaces are called slagging. Radiative heat transfer is dominant in the areas where slagging occurs. Deposits in the convective heat transfer zones of the boiler are called fouling and take place in the areas where the gases are cooled.[16]

The interaction of biomass ash with the bed material of the fluidized bed can lead to bed material agglomeration. Bed material agglomeration cannot be seen in DFB biomass steam gasification plants because olivine is used as a bed material, which has a lower agglomeration tendency compared to silicon sand.[29]

Earlier studies showed that the bed material olivine is modified during utilization in the plant.[10] Two different calcium-rich layers are formed at the surface of the bed material particles. The inner layer is homogeneous and consists mainly of calcium and silicate. The outer layer has a similar composition to the fly ash.

The importance of this calcium-rich layer concerning the gasification properties was shown in two earlier studies at a 100 kW pilot plant at the Vienna University of Technology.[11,12] The water–gas shift reaction is enhanced, leading to higher hydrogen and CO_2 contents in the product gas and to a lower carbon monoxide content and a lower content of higher hydrocarbons. The decomposition of primary tars is enhanced, and the formation of secondary tars is reduced, leading to lower total tar concentrations in the product gas.

Detailed investigations on the mechanism of the layer formation at the bed material were presented by Kirnbauer et al.[30] Investigations of the composition of the surface of used bed material in gasification and combustion atmosphere did not show a change in the elemental composition but showed a slight change in the crystal structure. Thermal investigations show a weak endothermic weight loss with used bed material in CO_2-rich atmosphere, which could not be determined with fresh olivine. The layer formation is considered by the authors to be caused by the intensive contact of bed material with burning char particles in the combustion reactor.

An unsolved problem of the plant in Güssing is the formation of fouling in the flue gas path after the combustion chamber. The main fouling that reduces the operation time significantly is located at the entrance of the first heat exchanger after the combustion chamber, which is an air preheater. It is a shell in a tube heat exchanger with the flue gas inside the tubes. The flue gas temperature at the entrance of the heat exchanger is around 830 °C, with wall temperatures of around 500 °C.

The influence of changing the ash loops on the behavior of the inorganic matter in the gasification system in terms of layer formation of the bed material and fouling and slagging is still unknown.

■ METHODS

The investigations of inorganic matters and their behavior in the system included analyses of the composition and amount of all flows for a qualitative evaluation of the possible behavior of the components. Balances of the main components of inorganic matter were determined to understand the influence of ash loops on the possible accumulation of substances in the system.

Sampling. Ash samples were taken during operation, and samples of fouling were taken during stops after cooling the plant. Fly ash samples (ash exiting the plant in the container, fine ash circulation, coarse ash circulation) were sieved with a vibratory sieve with 200 μm mesh size. The fraction smaller than 200 μm is defined as fine ash; the other fraction is defined as coarse ash.

The sampling points are shown in Figure 1 and described in Table 4. Mass flows that were not measured via the distributed control system (DCS) of the plant were measured manually, and three measurements were carried out over a period of 30 min.

Multiple samples of fouling were taken at the first heat exchanger (air preheater) of the flue gas after the combustion reactor.

Table 4. Sampling Points and Flow Determination[a]

sample type	sampling point no.	description	determination of flow
input flow	1	biomass ash	mass flow of biomass, ash content
input flow	2	bed material	level measurement DCS
input flow	3	precoat material	weight measurement DCS
internal flow	4	fly char	weight measurement DCS/ calculated after rebuild
internal flow	5	fine ash circulation	manual weight determination
internal flow	6	coarse ash circulation	manual weight determination
output flow	7	ash to container	manual weight determination
fouling	8	cyclone	
fouling	9	air preheater entry	
fouling	10	product gas cooler	(no analysis presented)

[a]Sampling point numbers are according to Figure 1.

Two different representative samples with different textures were presented as an example in this study.

Various samples of fouling in the cyclone were taken, and representative results are presented here. Due to the different appearance of the samples (see Figure 3), three different probes were analyzed: sample A was located at the surface of the fouling, sample B is material taken 3−4 mm below the surface, sample C was taken from the inner layer of the fouling close to the refractory lining.

Analyses. The elemental composition of the samples was determined using X-ray fluorescence (XRF) and calculated as oxides. Samples for XRF were melted in a Merck Spectromelt at 1050 °C and placed on a 400 °C stainless steel plate. The analyses were carried out with a PANalytical Axios Advanced analyzer under vacuum atmosphere with a rhodium anode, an excitation voltage of 50 kV, and a tube current of 50 mA. The results indicate the elemental composition of the total sample calculated in oxides.

Thermogravimetric analysis (TGA), differential thermal analysis (DTA), and differential scanning calorimetry (DSC) analysis were carried out in a NETZSCH STA 449 C Jupiter System. The sample crucible is equipped with a thermocouple for direct measurement of the temperature. The furnace allows temperatures of up to 1650 °C with heating rates of 0.01 to 50 K/min. A heating rate of 10 K/min was chosen. Gas used to provide the desired atmosphere flows upward and the desired gas composition is mixed from gas bottles of pure gases with the aid of mass flow controllers. The mass of each sample was chosen to be approximately 70 mg. Results of the DSC are indicated in microvolts, and calibration with $BaCO_3$ gave a calibration factor of 2.77, allowing the results to be obtained in milliwatts.

The TGA, DTA, and DSC analyses were carried out once for each sample but in three different atmospheres. Air, pure nitrogen as an inert gas, and a mixture of nitrogen with 15% CO_2 by volume were used as atmospheres to simulate reactions with the atmosphere such as combustion and calcination. The purge gas flow was set to 40×10^{-6} m^3/min. Due to the high inhomogeneity of the samples, a low repeatability of the analysis is expected but the authors expect to obtain only qualitative results, which will lead to qualitative conclusions about the operation of the system.

Mass Balances of Inorganic Matter. Ash flows were determined at different locations, shown in Table 4, for the preparation of the mass balances. The ash content was determined, and the elemental composition was measured by XRF and calculated in oxides. For the determination of the mass flows of the inorganic matter, the samples were calcined at 1050 °C to release carbonates and organic matter, and the mass flows are related to the calcined samples.

Mass balances of inorganic matter were calculated using the software STAN.[31] The software allows data reconciliation with the method of least-squares. The balances of inorganic matter are based on (a) the total balance of coarse and fine ash, (b) the elemental balance of CaO, MgO, SiO_2, Fe_2O_3, K_2O, and the sum of other elements for fine and coarse ash mass flows. The composition of bed material and precoat material was considered to be constant, and average values were taken. For the composition of biomass ash, an average composition was considered due to the high inhomogeneity of the fuel due to the utilization of different wood species, log sizes, and bark contents.

Various assumptions were made for the simplification of the system and are shown in Table 5. The bed material circulation mass flow between the gasifier and the combustion reactor was considered to be balanced and is not indicated in the balances because the mass flow of around 100 tons per hour is much higher than the other inorganic flows and would predominate over all other flows.

The standard deviation for the measured mass flows used is given in Table 6. Mass flows that are measured by DCS are considered to have a standard deviation of 2%, while manually measured mass flows are assumed to have a standard deviation of 10%. The abrasion is estimated from the coarse and fine ash balance and the standard deviation is chosen with 50% to be adjusted by the calculation method of the balance. Averages of analyses were obtained for the composition of biomass ash, precoat material, and bed material and the standard
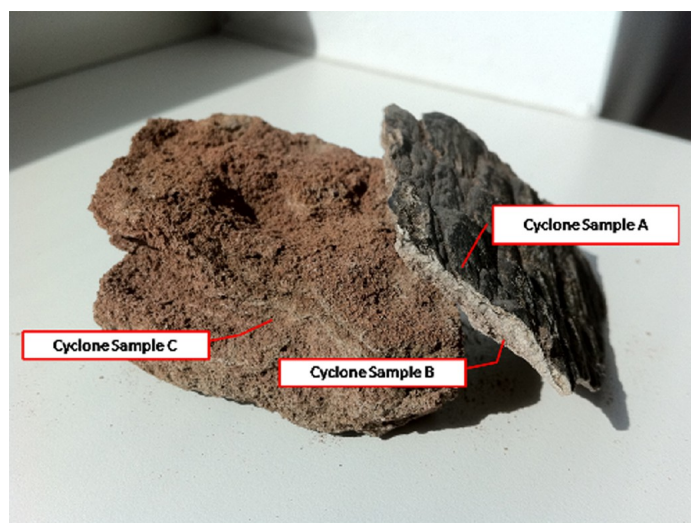

Figure 3. Sampling of fouling in the cyclone.

Table 5. Assumptions for the Mass Balance of the Inorganic Matter

- Mass flows of biomass ash, precoat material, fly char, and the mass flow from the combustion reactor to the gasifier were considered to have a particle size smaller than 200 μm.
- Bed material supplement and the flow from the gasification reactor to the combustion reactor are assumed to have a particle size bigger than 200 μm.
- The system is considered to be in a steady state condition, without accumulation of material in the system.
- Bed material circulation between the gasification reactor and the combustion reactor is considered to be balanced in terms of mass flow and composition. All variation of this balance is shown in the results. The balanced bed material circulation is not shown in the diagrams.
- Abrasion is the same in the combustion reactor as in the gasification reactor.
- Abraded material has the same composition as the fresh bed material.
- No inorganic matter is detectable in the gas after the product gas filter and the flue gas filter.

Table 6. Determination of the Mass Flows and Assumed Standard Deviations for the Mass Balances of Inorganic Matter

description	determination of flow	SD mass flow (%)	SD elemental composition (%)
biomass ash	mass flow of biomass, ash content	20	5
bed material	level meas. DCS	2	5
precoat material	wt meas. DCS	2	5
fly char	wt meas. DCS (calcd in Figure 9)	20	2
fine ash circulation	manual wt determination	10	2
coarse ash circulation	manual wt determination/wt meas. DCS	2	2
ash to container	manual wt determination	10	2
layer formation at the bed material	calcd	calcd	calcd
abrasion in combustion reactor	est.	50/calcd	5
abrasion in gasification reactor	est.	50/calcd	5

Table 7. Results of XRF for the Average Composition of Biomass Ash

	wood chip ash	
	avg (wt %)	SD (wt %)
Na_2O	2.77	2.66
MgO	5.13	0.45
Al_2O_3	2.57	1.10
SiO_2	15.36	7.52
P_2O_5	2.36	0.24
SO_3	1.26	0.51
K_2O	12.40	2.75
CaO	52.47	6.16
MnO	1.67	0.43
Fe_2O_3	1.73	0.66
Cl	0.42	0.36
others	1.85	
ash content (ds)	1.42	0.10

deviation of the composition of these mass flows was assumed to be 5%. Those analyses with specific analysis for the balance were considered to have 2% standard deviation.

Table 8. Typical Composition of the Precoat Material Dolomite

	precoat material (wt %)	
Na_2O	2.32	
MgO	32.01	
Al_2O_3	1.36	
SiO_2	1.48	
P_2O_5	0.38	
SO_3	0.44	
K_2O	0.87	
CaO	59.87	
Fe_2O_3	0.63	
Cl	0.30	
others	0.35	
loss on ignition 600 °C, 1 h		2.77%
loss on ignition 1050 °C, 1 h		44.66%

Table 9. Elemental Analysis of Olivine[10]

	olivine (wt %)
MgO	46.8
SiO_2	39.8
CaO	0.9
Fe_2O_3	10.3
K_2O	0.32
Na_2O	0.43
Al_2O_3	0.40
MnO	0.15
P_2O_5	0.03
Cl	0.10
SO_3	0.06
others	0.71

Table 10. Typical Composition of the Ash Entering the Container

	fine ash		coarse ash	
	avg. values (wt %)	SD (wt %)	avg. values (wt %)	SD (wt %)
Na_2O	1.19	1.00	1.20	0.92
MgO	19.67	2.06	37.27	2.61
Al_2O_3	1.52	0.90	0.52	0.21
SiO_2	20.28	8.97	35.70	4.00
P_2O_5	1.22	0.16	0.34	0.05
SO_3	0.39	0.22	0.08	0.03
K_2O	6.97	1.62	3.81	1.16
CaO	42.45	11.08	11.70	3.96
Fe_2O_3	4.08	1.60	8.01	0.58
Cl	0.26	0.17	0.19	0.13
others	1.96		1.19	
loss on ignition 600 °C, 1 h	4.94%		0.56%	
loss on ignition 1050 °C, 1 h	6.81%		1.05%	

Various balances were prepared, but two are presented that represent the status before the optimization project and the actual status. Before optimization, ash circulation is used (called "fine ash circulation" in Figure 1) where fly ash is circulated into the gasifier to minimize bed material consumption and to increase the amount of catalytic substances in the system. Coarse ash circulation was not implemented at the beginning of the project. During the optimization of the ash loops, a gravity separator was implemented in the system to separate bed material particles elutriated with the flue gas path from fly ash ("coarse ash circulation"). The second balance shows the status after the optimization project after the implementation of the coarse ash circulation and after turning off the fine ash circulation.
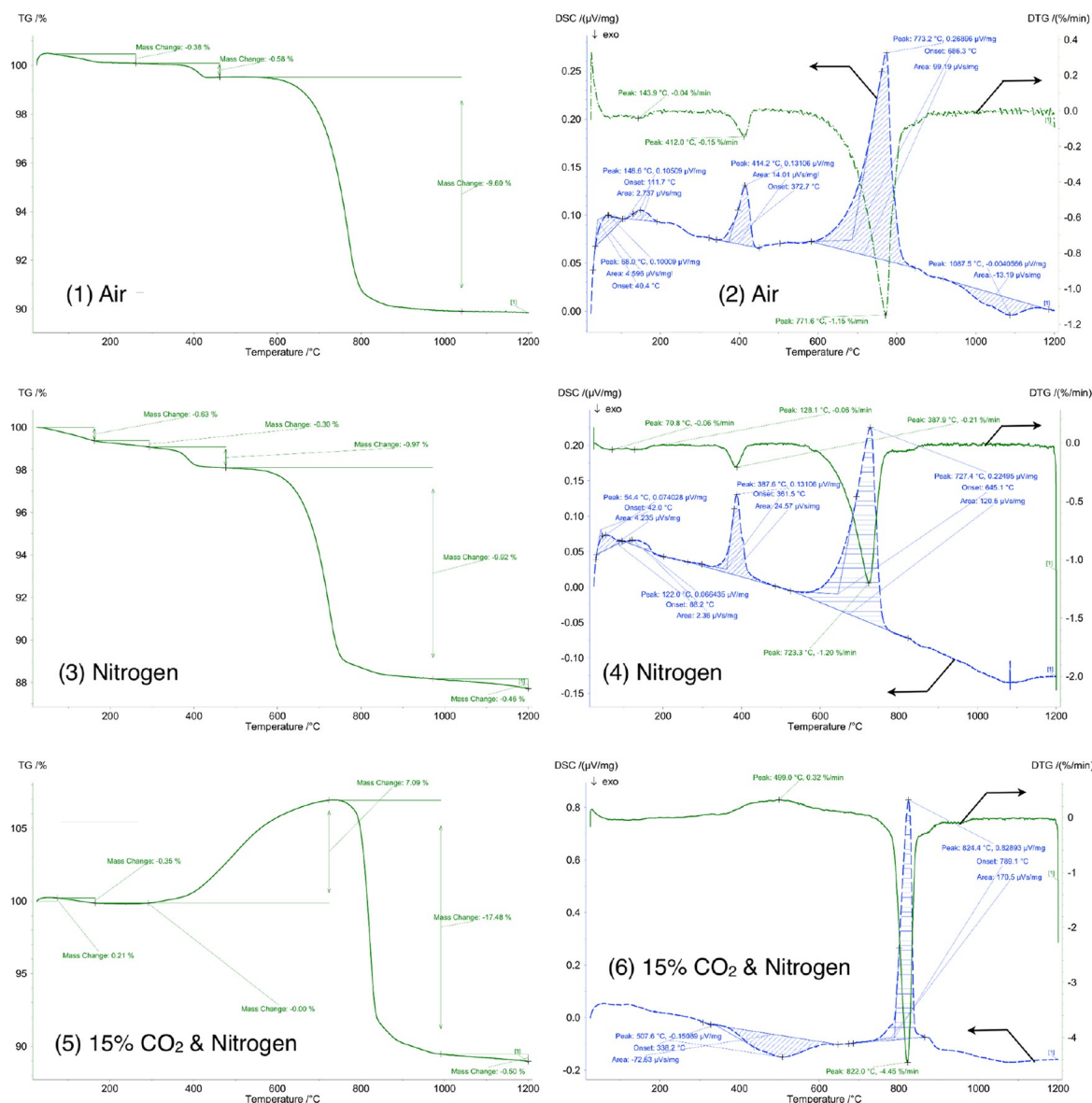
Figure 4. Thermal analysis of fly ash with particle size <200 μm in different atmospheres.

RESULTS

The composition of the biomass ash has a significant influence on fouling, slagging, and bed material agglomeration tendencies in the plant because it is the only source of components with low melting points. The quality of the biomass is constantly determined by the operational personnel in terms of water content but not ash content, bark content, or wood type. Table 7 shows the average biomass ash compositions and their standard deviations from samples taken in the years 2010 and 2011. The main component of the biomass ash is calcium oxide, which represents about half of the weight, followed by silicon oxide and potassium oxide. Magnesium oxide, phosphorus oxide, aluminum oxide, and sodium oxide are detectable in the low percentage range. The composition of the biomass ash is typical for hardwood ash as shown in literature.[32]

Precoat material is used for precoating the product gas filter and is added to the system. The precoat material described in Table 8 shows a typical composition of the natural mineral dolomite, whose main components are calcium and magnesium oxide, with a high ignition loss at 1050 °C, when the carbonates are released. Other elements are available in the low percentage range, such as sodium oxide, silicon oxide, and aluminum oxide.

The elemental composition of the olivine, which is used in the plant as a bed material, shows the main components magnesium oxide, silicon oxide, and iron oxide (Table 9). Other elements are available in low concentrations.
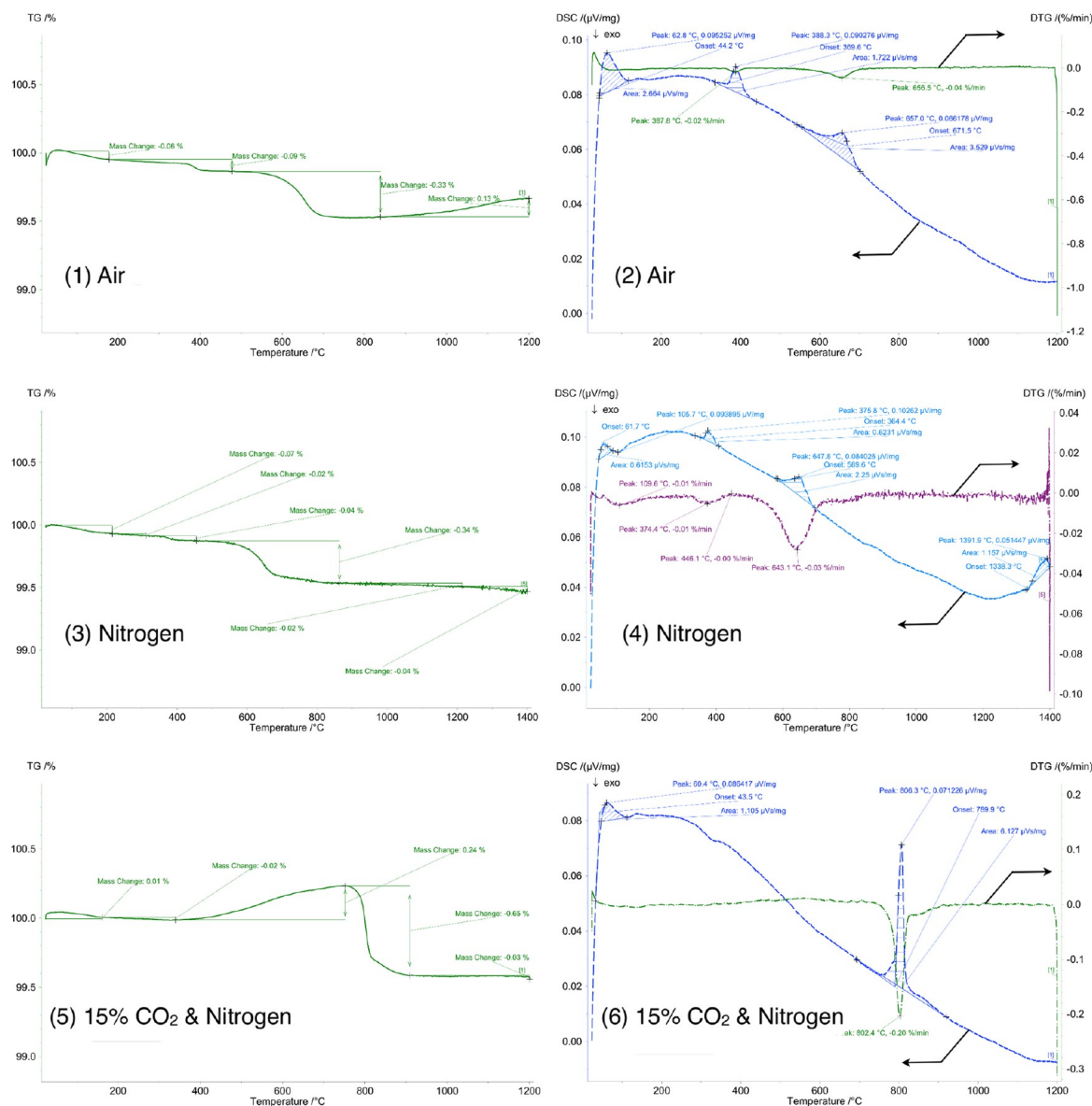
Figure 5. Thermal analysis of fly ash with particle size >200 μm in different atmospheres.

An overview of the composition of the fine ash (particles <200 μm) and coarse ash (particles >200 μm), which leave the process and enter the ash container, is shown in Table 10. Coarse ash consists of the main components of olivine, such as magnesium oxide, silicon oxide, and iron oxide, but also significant contents of calcium oxide (nearly 12 wt %) and potassium oxide (nearly 4 wt %), which originate from biomass ash. This is in agreement with the study presented earlier.[10] Fine ash mainly consists of calcium oxide, silicon oxide, magnesium oxide, and also potassium oxide. A high content of iron oxide is available, and other elements were detected such as sodium oxide, phosphorus oxide, and aluminum oxide. Important for the fouling tendency is the amount of potassium oxide, which is detectable in the fine ash, where it represents

Table 11. Analysis of the fly Char before Optimization of the Ash Loops

		dry base	raw
water content	wt %		0.91
carbon content	wt %	26.14	25.9
hydrogen content	wt %	0.48	0.48
nitrogen content	wt %	0.06	0.06
ash content (db)	wt %	73.32	
upper heating value	kJ/kg	8301	8225
lower heating value	kJ/kg	8196	8097

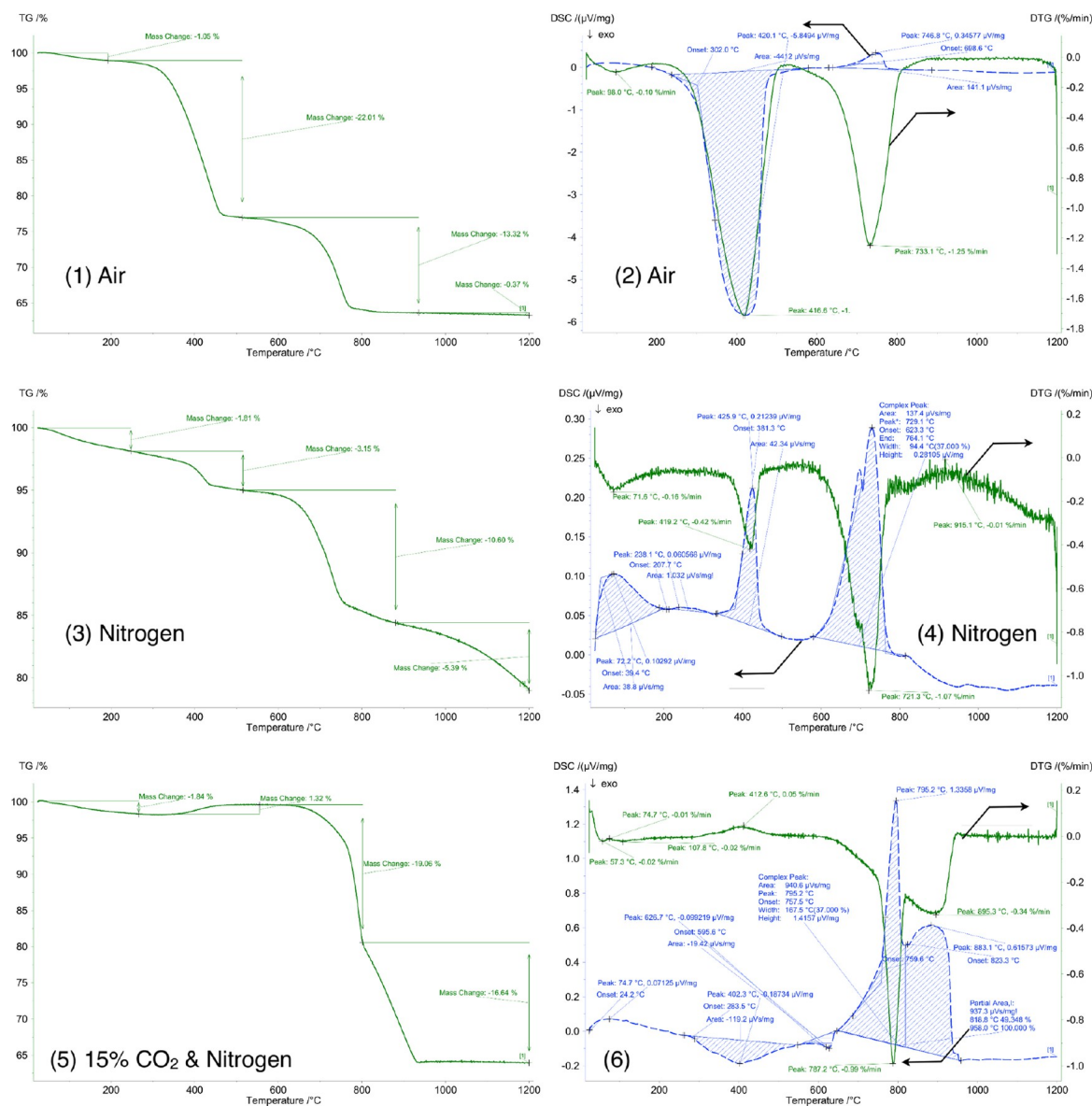around 7 wt %, and in the coarse ash, where it represents only 4 wt %.

Figure 6. Thermal analysis of fly char in different atmospheres.

The thermal behavior of the fine fraction of fly ash in different atmospheres is shown in Figure 4. Two main peaks can be seen up to 1200 °C. At temperatures lower than 100 °C, small changes in weight are detectable. A weight loss with an endothermic signal in the DSC at around 400 °C and a significant endothermic weight loss at temperatures of around 720 to 820 °C are detectable. The results in air and nitrogen are similar; a significant change can be seen in the mixture of nitrogen with 15% CO_2. In a CO_2-rich atmosphere, an endothermic weight loss at 400 °C is not indicated but an increase in weight can be seen at temperatures higher than 400 °C with a strong endothermic peak at 820 °C.

The weight loss at temperatures around 100 °C is considered to be caused by the evaporation of water. An endothermic peak with weight loss at around 400 °C, which is not seen in the CO_2-rich atmosphere, is considered to be due to the calcination of magnesium carbonate. In the CO_2-rich atmosphere this is interfered by the adsorption of CO_2 on calcium oxide, which can be seen from the increase in the weight. Decomposition of calcium hydroxide is not considered at temperatures around 400 °C because it is expected at temperatures around 550 °C. The combustion and decomposition of organic matter (unburned wood) are not considered to happen because a peak can also be seen in the nitrogen atmosphere.

The thermal analysis of the coarse ash fraction of the fly ash shows properties similar to those of the fine ash but less pronounced (Figure 5). In contrast to the fine ash, an increase in weight can be seen at temperatures higher than 900 °C.

The weight loss of the fine ash fraction is around 10% while that of the coarse ash fraction is around 0.5%.

Coarse fly ash is considered to consist mainly of bed material, which is confirmed by the iron content. An increase in weight in the thermal analysis at temperatures higher than 900 °C might be caused by the oxidation of magnetite[33] or by the decomposition of fayalite with the oxidation of iron.

The investigations of the properties of the fly char include a fuel analysis because of the high carbon content of the char. The fuel analysis is shown in Table 11 and reveals that the fly char consists mainly of ash and carbon. The heating value justifies the utilization of the fly char as a fuel in the combustion reactor. The elemental analysis shown in Table 12 reveals the

Table 12. Elemental Analysis of Inorganic Matter of Fly Char[a]

	mean value (wt %)	SD
Na_2O	1.94	1.36
MgO	25.02	2.83
Al_2O_3	2.38	0.63
SiO_2	22.13	2.17
P_2O_5	1.18	0.22
SO_3	0.38	0.26
K_2O	6.09	0.94
CaO	33.11	5.95
Fe_2O_3	5.24	0.19
Cl	0.52	n/a
others	2.0	
loss on ignition 1050 °C, 1 h		36%

[a]Sample date, 2010.

highest concentrations of the substances calcium oxide, magnesium oxide, silicon oxide potassium oxide, and iron oxide.

The thermal analysis of fly char in different gas atmospheres (Figure 6) shows two significant endothermic peaks in air and nitrogen atmosphere at around 417 °C and around 730 °C. A low weight loss can be detected at temperatures up to 100 °C. In a mixture of 15% CO_2 in nitrogen, an exothermic peak can be seen at temperatures around 412 °C and a complex endothermic weight loss can be seen at temperatures between 795 and 880 °C.

The thermal analysis of the fly char showed combustion in air (exothermic peak) at 400 °C. In nitrogen atmosphere an endothermic weight loss can be seen at around 400 °C, which is considered to be due to the decomposition of magnesium carbonate. The low amount of oxygen in the char excludes the pyrolysis of organic matter, which could be also expected at this temperature. The endothermic weight loss at around 730 °C in the air and nitrogen atmosphere is considered to be caused by the decomposition of calcium carbonate and dolomite.[34] This reaction interferes in the CO_2-rich atmosphere with the CO_2-gasification of carbon with the peak at 880 °C.

The nature of fouling at the air preheater varies. The texture of the fouling varies from powder debris to hard and rocky material, which is difficult to remove. Soft and hard layers can be observed within one position but also at different locations. Due to the need for high availability of the plant, the inspection intervals for the heat exchanger are around four weeks and an exact determination of the formation of the fouling is not possible. The results of analyses of two different samples with different textures are shown in Table 13. Fouling that disaggregates easily to a powder has calcium oxide as its main

Table 13. Elemental Analysis of Fouling at the Air Preheater

sample date	Oct. 3, 2010	Sept. 7, 2010
description	hard fouling at air preheater—untreated	fouling at air preheater that disaggregates easily
component	wt %	wt %
Na_2O	1.17	1.22
MgO	25.89	18.37
Al_2O_3	1.28	2.31
SiO_2	16.72	18.91
P_2O_5	1.68	1.92
SO_3	0.18	0.21
K_2O	9.15	3.40
CaO	36.29	47.81
Fe_2O_3	4.81	4.12
Cl	0.18	0.22
others	2.67	1.48
loss on ignition 1050 °C, 1 h	13.94%	3.71%

component, accounting for nearly half of the mass of the sample. Magnesium and silicon oxide are detectable in about the same amount. The hard and rocky fouling shows a higher magnesium oxide concentration and lower calcium oxide and silicon oxide concentrations. Potassium oxide is significantly more highly concentrated in hard fouling, where it represents around 9 wt %, compared to 3.4 wt % in soft fouling.

The thermal analysis of the fouling shown in Figure 7 gave different results compared to coarse ash and fine ash. The TGA shows a constant and significant weight loss of 8 to 10 wt % up to 1200 °C. The weight loss can be seen over the whole temperature range but increases at temperatures higher than 800 °C, and this is independent from the gaseous atmosphere. The DSC signal shows various endothermic peaks. Significant endothermic weight losses can be determined at around 100 °C, at 509 °C in air (526 °C in nitrogen and 532 °C in CO_2– nitrogen respectively), around 755 to 791 °C depending on the atmosphere, 864 to 978 °C, and above 1000 °C.

The first peak of the thermal analysis of the fouling occurs at temperatures around 100 °C, which is considered to be caused by evaporation of water. A significant peak can be observed at 509–530 °C, which is similar to the temperature at which the recrystallization of $K_2O·SiO_2$[35] takes place and the similar temperature at which α-quartz is modified to β-quartz (573 °C).[36]

A peak at 755–791 °C with a high weight loss in air and nitrogen atmosphere and a moderate weight loss in CO_2-rich atmosphere might be caused by the decomposition of dolomite, calcium carbonate, or spurrite.[37−39] In the CO_2-rich atmosphere, this peak can be seen at 791 °C but the peak at 879 °C has a significantly higher weight loss. A high partial pressure of CO_2 can shift the decomposition of carbonates ($CaCO_3$ or spurrite) to higher temperatures. An overlapping of different reactions is suggested, where released CO_2 reacts with another component and is only released at higher temperatures. At temperatures between 864 and 878 °C, a recrystallization of quartz in β-tridymite[40] without weight loss is expected. Arvelakis et al.[38] showed that a mixture of K_2CO_3 and SiO_2 reacts to form potassium silicates at this temperature, leading to a weight loss because of the released carbonates.

In the nitrogen and CO_2-rich atmosphere, significant decomposition and melting can be seen (endothermic DSC signal with a weight loss), which agrees with the findings of Arvelakis et al.[38] that at temperatures higher than 1000 °C excessive decomposition and release in the gas phase of potassium rich compounds (KCl, K_2CO_3, K_2SO_4) as KOH are occurring.
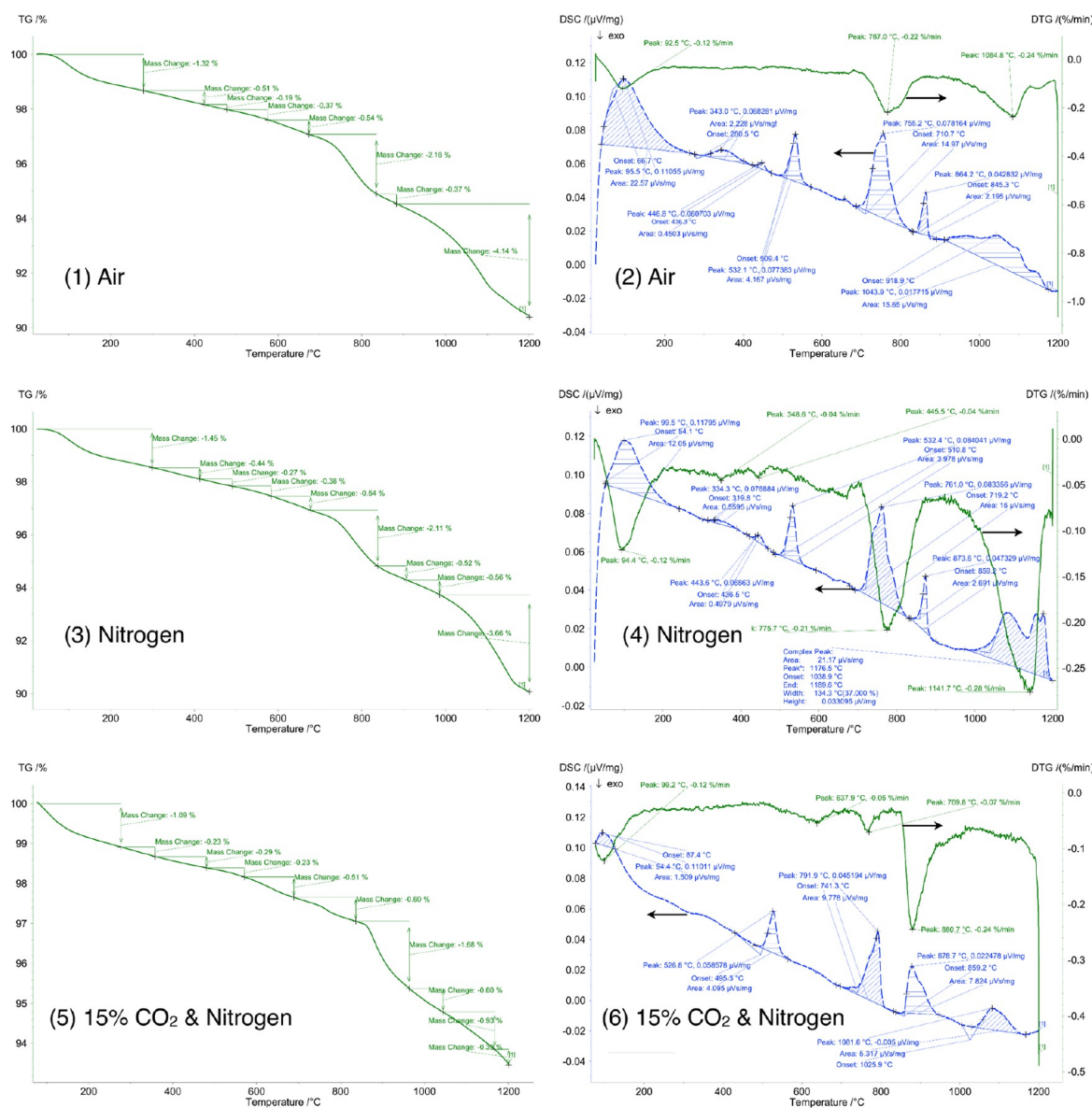
Figure 7. Thermal analyses of fouling at the air preheater in different atmospheres.

The results of the elemental composition of the fouling in the cyclone are shown in Table 14. The elemental analysis confirms the visual impression of the inhomogeneity of the fouling over its thickness. Bed material particles can be visually detected in sample C, which is confirmed by the high iron content of the sample. The amount of potassium in samples A and B, 23.6 and 19.1%, respectively, is significantly higher than is expected from the biomass ash. Calcium oxide content is lower in all samples compared to biomass ash.

Ash Balances. The ash balances were carried out for different operation modes of the ash loops. The status at the beginning of the optimization project is shown in Figure 8. A high amount of ash (coarse and fine) is circulated back into the gasifier before being released into the container to reduce

bed material consumption and to increase the amount of catalytic substances in the system. It can be seen that this circulation of fine ash and coarse ash increases the total amount of ash in the system significantly. Considering that potassium is assumed to be responsible for fouling, the total input and output, respectively, from the system is 2.6 kg/h, while the potassium flow in the fly char is 16.8 kg/h. A significant amount of potassium is transferred from the combustion reactor to the gasification reactor via the siphon.

The status after the optimization of the ash loops is shown in Figure 9. The coarse ash circulation is fed into the combustion reactor while the fine ash circulation is turned off and all fine ash is released into the container. A significant reduction of the fine ash in the system can be seen. The amount of potassium

Table 14. Elemental Composition of the Fouling in the Cyclone (Main Components)

	cyclone sample A total sample (wt %)	cyclone sample B total sample (wt %)	cyclone sample C total sample (wt %)
Na_2O	0.53	0.35	2.88
MgO	11.09	14.82	28.51
Al_2O_3	1.22	2.51	0.89
SiO_2	25.84	29.34	36.84
P_2O_5	0.75	0.96	0.30
SO_3	0.13	0.03	0.06
K_2O	23.63	19.13	9.98
CaO	33.13	27.88	13.07
Fe_2O_3	2.36	3.42	6.03
Cl	0.08	0.06	0.44
others	1.26	1.50	0.99

that is transferred between combustion reactor and gasification reactor is reduced to 1.6 kg/h, which is around half of the amount of potassium that enters the plant with the biomass.

■ DISCUSSION

Discussion of Analyses of Inorganic Matter. The elemental analysis of biomass ash, precoat material (dolomite), and bed material did not reveal unexpected results. Combustion plants using alternative fuels such as straw and energy plants with high concentrations of chlorine, phosphor, and sulfur often show a fouling tendency.[29,41,42] These elements are detectable only in low concentrations in this study and are not considered to be the main reason for fouling in this case.

The reason is considered to be the interactivity between the inorganic flows that enter the plant: biomass ash, precoat material, and bed material. The influence of the interaction with the bed material was discussed and presented in earlier studies.[10−12] The tendency for fouling shows that interaction between biomass ash, abrasion of the bed material, and precoat material is happening. A comparison of the composition of the coarse fraction of the fly ash with used bed material[10] shows that the coarse fraction of the fly ash mainly consists of bed material.

The potassium content, which is considered to be responsible for fouling tendencies, is nearly doubled in the fine fly ash compared to coarse fly ash. The origin of potassium oxide is mainly the biomass ash.

The fuel analysis and elemental analyses of the fly char did not show unexpected results. The elemental composition of the inorganic fraction of fly char is similar to the fine fraction of the fly ash. Mass balances showed that the concentration of potassium in the fly char is higher than would be expected from the biomass ash.

The carbon in the fly char is considered to be bound closely to the ash due to the concentration of the ash component and condensation of gaseous inorganic species while cooling the product gas. According to the mechanism and modification of potassium of van Lith et al.,[25] potassium is available in organic species such as organic acids or bound on phenols.

Considering the elemental composition of the fouling at the air preheater, a high concentration of potassium and also calcium oxide and magnesium oxide can be seen. Fouling after fast fluidized bed combustion is described in the literature with a higher concentration of alkaline and alkaline earth metals compared to the composition of the biomass,[43] which can also be seen in this study. The difference in potassium

content between loose agglomerates of ash and hard fouling at the air preheater is significant. The difference in the morphology of the fouling might be caused by variations of the operation conditions in the plant. High variation of the fuel water content between 20 and 40% causes variations in the operation of the combustion chamber such as temperature, oxygen concentration, and retention time.

The assumption that potassium is responsible for fouling is confirmed by the elemental analyses of the fouling in the cyclone. The surface of the fouling has a potassium concentration of around 24% by weight. Samples from the inside of the fouling and closer to the refractory lining showed lower concentrations of potassium oxide but higher concentrations of silicon oxide and magnesium oxide. The amount of calcium decreases on the inside of the fouling. Operational experience showed that the fouling formed rapidly within three days, which can be seen from the amount of bed material that leaves the cyclone with the flue gas. Operation of the plant is still possible for some weeks after the formation of fouling in the cyclone. The growth of the fouling is expected to be lower during this period, which explains the high potassium content at the surface of the fouling.

Thermal analyses of fly ash (coarse and fine) and fly char were similar except for the high carbon content of fly char, which combusts in an air atmosphere and is gasified in a CO_2-rich atmosphere at temperatures higher than 800 °C. Thermal analyses of fouling showed a high weight loss and a complex behavior. Due to the long retention time at the tube sheet of the heat exchanger, slow reactions are expected, which can cause recrystallization.

The analyses of the inorganic matter are only snapshots of conditions that can occur in the system. The standard deviation of the fuel ash analysis shows high variation in the ash composition of the fuel. This is evident because biomass is bought from various fuel suppliers and the wood yard management is mainly based on the fuel water content. These single analyses are not sufficient to draw conclusions about the behavior of the inorganic matter in the system, and mass balances of inorganic matter need to be considered.

Discussion of Mass Balances of Inorganic Matter. The ash balances showed that the circulation of ash and the setup of the loops can lead to the transportation of ash through the reactors in amounts many times higher than the amount of inorganic matter, which is introduced into the system. This can lead to an accumulation of different substances within the system. Considering the potassium balances, a transfer of potassium from the combustion reactor to the gasification reactor can be detected in all the balances. This transfer leads to potassium concentrations in the fly char that are higher than expected with the mixture of abraded bed material and precoat material. The fly char also consists of unconverted char, which is mainly carbon. According to the findings of Novaković et al.,[26] potassium is released to the gas phase, which is enhanced by the presence of water, calcium oxide, and high temperatures. The release of potassium is also pronounced in gasification atmospheres.[27,28] Based on this knowledge, a close connection between potassium that is released to the gas phase and char can be expected due to the condensation processes of gaseous potassium during cooling of the product gas.

During combustion of fly char in the combustion reactor, the high carbon content of the char (see Table 11) leads to high combustion temperatures, which are responsible for the release of potassium into the gas phase. Scala et al.[44] showed
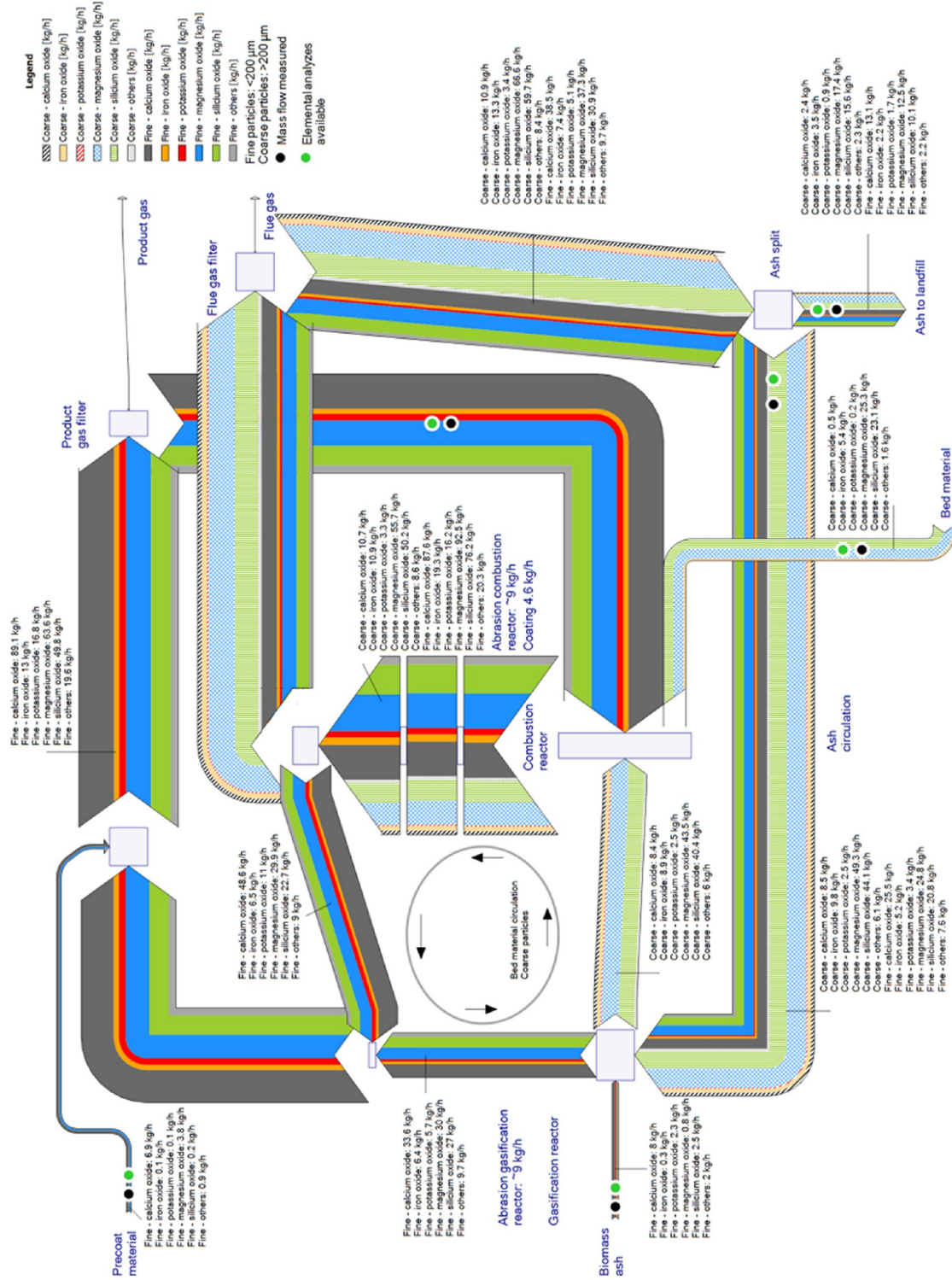
Figure 8. Mass balance of inorganic matter before optimization.
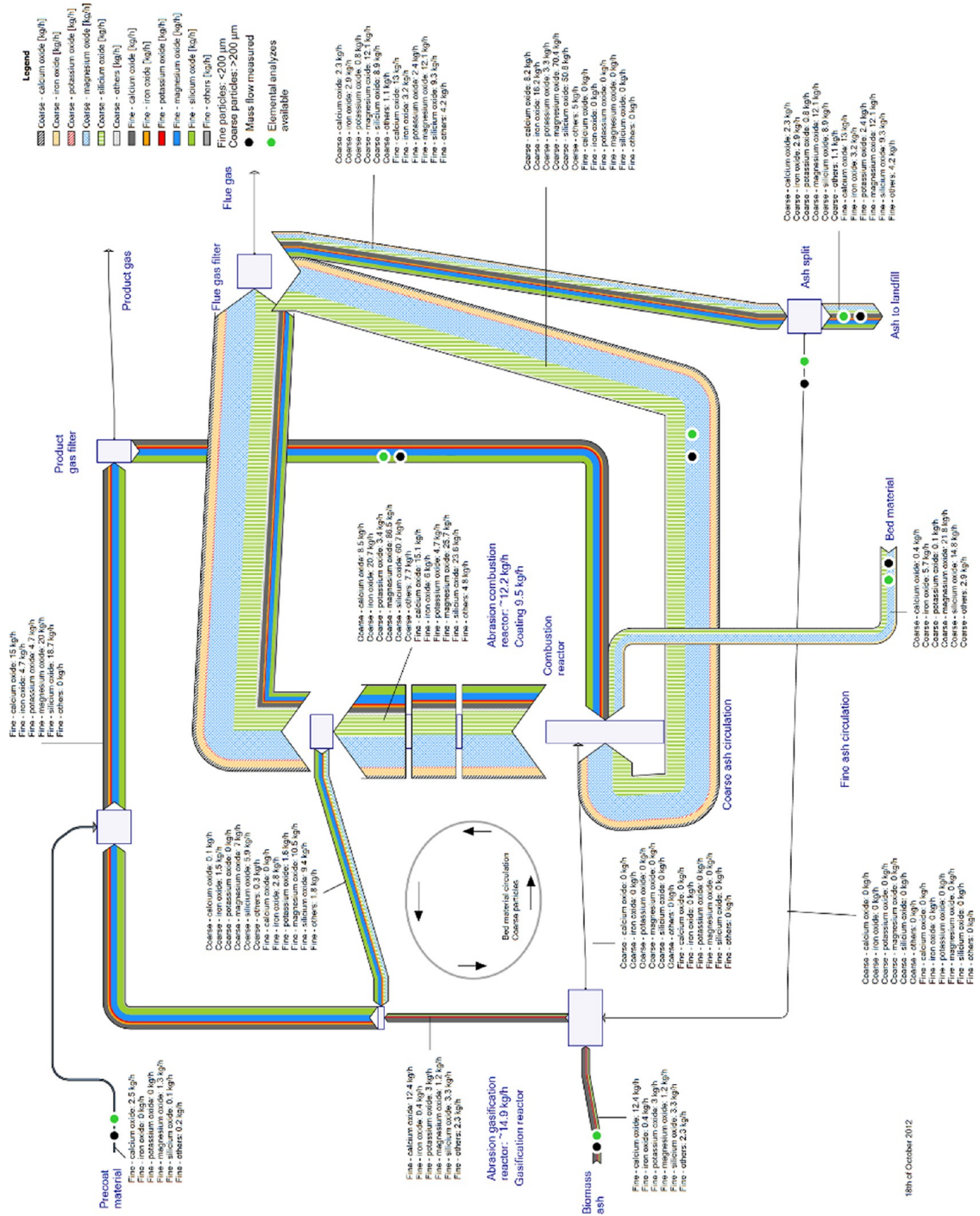
Figure 9. Mass balance of inorganic matter with coarse ash circulation into the combustion reactor and fine ash turned off.

that agglomeration takes place around burning char particles because their temperature is the highest temperature in the fluidized bed.

Low potassium release rates can be achieved by low temperatures, low water content in the combustion reactor, and low calcium content in the system. The temperatures are linked to the demand for a proper gasification temperature and also the bed material circulation rate between the gasification and combustion reactors and the excess air ratio in the combustion reactor. Keeping the excess air ratio in the combustion chamber high will decrease the adiabatic combustion temperature of the burning char particles and reduce the potassium release rate.

The mechanism for the transfer of potassium from the combustion reactor to the gasification reactor is unknown. Different possibilities are suggested: (a) Due to the higher release rate of potassium in the combustion reactor, the potassium concentration in the bed material particles is increased and potassium is released in the gasification reactor. Gaseous potassium is considered to be available in cavities of the bed material.[10] (b) The release rate of potassium is higher in the gasification reactor due to the reducing atmosphere. The fraction of potassium that is bound to the bed material is higher in the combustion reactor compared to the gasification reactor. This can be in the form of potassium carbonate (liquid or solid) in the combustion reactor, which is reduced to potassium hydroxide in the gasification reactor. (c) A higher temperature and the oxidizing conditions in the combustion reactor lead to partly melting silicates that are attached to the bed material and transferred with the bed material into the gasification reactor, where potassium is released to the gas phase.

Sampling of bed material in the combustion chamber and the gasifier is not possible due to high temperatures. The difference in potassium concentration in the bed material between combustion reactor and gasifier can be considered to be below the detection limit of the analysis. Further investigations are required to clarify the mechanism of the overflow of potassium between combustion reactor and gasification reactor.

■ CONCLUSION

The following conclusions can be drawn from the analyses and balances of inorganic matters in the DFB plant presented in this paper:

- Ash loops can lead to significantly higher material streams and to an accumulation of substances with low melting points in the system.
- Potassium, which is considered to be mainly responsible for fouling, slagging, and bed material agglomeration in this case, is transferred from the combustion reactor to the gasification reactor. The mechanism of the transfer is still unknown.
- An accumulation of potassium can be seen in the fly char.
- The concentration of potassium in fine ash is nearly twice that in the coarse ash and bed material.

For the operation of the DFB plants, the following recommendations are given:

- A reduction of potassium in the system can be achieved by consequent and immediate discharge of fine ash. Recirculation of fine ash should be avoided.
- The melting behavior of ashes and the catalytic activity of the bed material are influenced significantly by the inorganic loops. Accurate measurement and control of ash and bed material streams are recommended.

- The high concentration of inorganic matter in the fly char, which is assumed to be closely bound to the char, demands accurate control of the fly char entering the combustion chamber as well as accurate control of the combustion air to avoid temperature variations and to keep the adiabatic combustion temperature of the particles as low as possible.
- A convective path for cooling the flue gas is recommended to cool inorganic matter before it comes into contact with a tube sheet of heat exchangers or tubes. It is also suggested that this may be useful while cooling the product gas.

■ AUTHOR INFORMATION

Corresponding Author
*Phone: + 43 (0) 3322 42606-156. Fax: + 43 (0) 3322 42606-199. E-mail: friedrich.kirnbauer@bioenergy2020.eu.
Notes
The authors declare no competing financial interest.

■ ACKNOWLEDGMENTS

■ REFERENCES

(1) Valmari, T.; Lind, T. M.; Kauppinen, E. I.; Sfiris, G.; Nilsson, K.; Maenhaut, W. *Energy Fuels* **1998**, *13*, 379−389.
(2) Davidsson, K. O.; Amand, L. E.; Steenari, B. M.; Elled, A. L.; Eskilsson, D.; Leckner, B. *Chem. Eng. Sci.* **2008**, *63*, 5314−5329.
(3) E4Tec. *Review of Technologies for Gasification of Biomass and Wastes; NNFCC Publications Final Report*, 9th ed.; NNFCC: York, U.K., 2009; p 130.
(4) Hofbauer, H.; Rauch, R.; Loeffler, G.; Kaiser, S.; Fercher, E.; Tremmel, H. In *Proc. 12th European Conf. Biomass Bioenergy*, Amsterdam, The Netherlands, 2002; p 4.
(5) Kotik, J. *Über den Einsatz von Kraft-Wärme-Kopplungsanlagen auf Basis der Wirbelschicht-Dampfvergasung fester Biomasse am Beispiel des Biomassekraftwerks Oberwart*; Vienna University of Technology: Vienna, Austria, 2010 (in German).
(6) Klotz, T. A regional energy-supply-showcase—The 15 MW fuel-power biomass gasification plant Villach. *International Seminar on Gasification*, Gothenburg, 2010.
(7) SWU Stadtwerke Ulm/Neu-Ulm GmbH. *Strom und Wärme aus der Natur*; http://www.swu.de/fileadmin/Content/PDFs/Energie_Wasser/Web_Flyer_HGASenden_16032012.pdf (accessed March 8, 2013) (in German).
(8) Bolhar-Nordenkampf, M.; Hofbauer, H.; Bosch, K.; Rauch, R.; Aichernig, C. In *Proc. Int. Conf. Biomass Utilisation*, Phuket, Thailand, 2003; Vol. *1*, pp 567−572.
(9) Koppatz, S.; Pfeifer, C.; Rauch, R.; Hofbauer, H.; Marquard-Moellenstedt, T.; Specht, M. *Fuel Process. Technol.* **2009**, *90*, 914−921.
(10) Kirnbauer, F.; Hofbauer, H. *Energy Fuels* **2011**, *25*, 3793−3798.
(11) Kirnbauer, F.; Wilk, V.; Kitzler, H.; Kern, S.; Hofbauer, H. *Fuel* **2012**, *95*, 553−562.
(12) Kirnbauer, F.; Wilk, V.; Hofbauer, H. *Fuel* **2012**, *108*, 534−542.
(13) Hofbauer, H.; Rauch, R.; Bosch, K.; Koch, R.; Aichernig, C. In *Pyrolysis and Gasification of Biomass and Waste*; Bridgwater, A. V., Ed.; CPL Press: Newbury, Berks, U.K., 2003; pp 527−536.
(14) Pronobis, M. *Fuel* **2006**, *85*, 474−480.

(15) Plaza, P.; Griffiths, A. J.; Syred, N.; Rees-Gralton, T. *Energy Fuels* **2012**, *23*, 3437−3445.

(16) Teixeira, P.; Lopes, H.; Gulyurtlu, I.; Lapa, N.; Abelha, P. *Biomass Bioenergy* **2012**, *39*, 192−203.

(17) Valmari, T.; Lind, T. M.; Kauppinen, E. I.; Sfiris, G.; Nilsson, K.; Maenhaut, W. *Energy Fuels* **1998**, *13*, 390−395.

(18) Miles, T. R.; Baxter, L. L.; Bryers, R. W.; Jenkins, B. M.; Oden, L. L. *Biomass Bioenergy* **1996**, *10*, 125−138.

(19) Nielsen, H. P.; Baxter, L. L.; Sclippab, G.; Morey, C.; Frandsen, F. J.; Dam-Johansen, K. *Fuel* **2000**, *79*, 131−139.

(20) Miles, T. R.; Baxter, L.; Bryers, R. W.; Jenkins, B. M.; Oden, L. L. *Alkali Deposits Found in Biomass Power Plants*, NREL/TP-433-8142; NREL: Golden, CO, 1995.

(21) Boström, D.; Br008ström, M.; Skoglund, N.; Boman, C., Backman, R.; Öhman, M.; Grimm, A. *Ash Transformation Chemistry during Energy Conversion of Biomass*; LULEÅ University of Technology: Saariselkä, Lapland, Finland, 2010.

(22) Boström, D.; Skoglund, N.; Grimm, A.; Boman, C.; Öhman, M.; Broström, M.; Backman, R. *Energy Fuels* **2012**, *26*, 85−93.

(23) Kracek, F. C.; Bowen, N. L.; Morey, G. W. *J. Phys. Chem.* **1929**, *33*, 1857−1879.

(24) Scala, F.; Chirone, R. *Biomass Bioenergy* **2008**, *32*, 252−266.

(25) van Lith, S. C.; Jensen, P. A.; Frandsen, F. J.; Glarborg, P. *Energy Fuels* **2008**, *22*, 1598−1609.

(26) Novaković, A.; van Lith, S. C.; Frandsen, F. J.; Jensen, P. A.; Holgerson, L. B. *Energy Fuels* **2009**, *23* (7), 3423−3428.

(27) Sams, D. A.; Talverdian, T.; Shadman, F. *Fuel* **1985**, *64*, 1208−1214.

(28) Dayton, D. C.; French, R. J.; Milne, T. A. *Energy Fuels* **1995**, *9*, 855−865.

(29) Grimm, A.; Öhman, M.; Lindberg, T.; Fredriksson, A.; Boström, D. *Energy Fuels* **2012**, *26*, 4550−4559.

(30) Kirnbauer, F.; Hofbauer, H. *Powder Technol.* **2013**, *245*, 94−104.

(31) Cencic, O.; Rechberger, H. *J. Environ. Eng. Manage.* **2008**, *18*, 3−7.

(32) Vassilev, S. V.; Baxter, D.; Andersen, L. K.; Vassileva, C. G. *Fuel* **2010**, *89*, 913−933.

(33) Fredriksson, H. O. A.; Lancee, R. J.; Thüne, P. C.; Veringa, H. J.; Niemantsverdriet, J. W. H. *Appl. Catal., B* **2012**, 1−23.

(34) L'Vov, B. V. *Thermochim. Acta* **1997**, *303*, 161−170.

(35) Roedder, E. Silicate melt systems. *Phys. Chem. Earth* **1959**, *3*, 224−297.

(36) Bragg, W.; Gibbs, R. E. *Proc. R. Soc. A* **1925**, *109*, 405−427.

(37) Engler, P.; Santana, M. W.; Mittleman, M. L.; Balazs, D. *Thermochim. Acta* **1989**, *140*, 67−76.

(38) Arvelakis, S.; Jensen, P. A.; Dam-Johansen, K. *Energy Fuels* **2004**, *18*, 1066−1076.

(39) Goswami, G.; Padhy, B. P.; Panda, J. D. *J. Therm. Anal. Calorim.* **1989**, *35*, 1129−1136−1136.

(40) Kracek, F. C.; Brown, N. L.; Morey, G. W. *J. Phys. Chem.* **1937**, *41*, 1183−1193.

(41) Zintl, F.; Strömberg, B.; Björkman, E. *Biomass for Energy and Industry: 10th European Conference and Technology Exhibition, Proceedings of the International Conference*, Wuzburg, Germany, June 8−11, 1998; pp 8−11.

(42) De Geyter, S. *The role of sulphur in preventing bed agglomeration during combustion of biomass.* M.S. Thesis. Umeå University, Sweden, 2006

(43) Jenkins, B. M.; Baxter, L. L.; Miles, T. R. *Fuel Process. Technol.* **1998**, *54*, 17−46.

(44) Scala, F.; Chirone, R. *Energy Fuels* **2006**, *20*, 120−132.

Publication VI

F. Kirnbauer, M. Koch, R. Koch, C. Aichernig, H. Hofbauer, The role of inorganic matter in the optimization of a dual fluidized biomass steam gasification plant, Fuel Processing Technology 2013 (submitted).

The role of inorganic matter in the optimization of a dual fluidized biomass steam gasification plant

Friedrich Kirnbauer,* Markus Koch**, Reinhard Koch**, Christian Aichernig[+], Hermann Hofbauer[++]

* Bioenergy 2020+ GmbH, Wiener Straße 49, A-7540 GÜSSING

** Biomasse-Kraftwerk Güssing GmbH, Wiener Straße 49, A-7540 GÜSSING

+ Repotec Umwelttechnik GmbH, Europastraße 1, A-7540 Güssing

++ Vienna University of Technology, Institute of Chemical Engineering, Getreidemarkt 9/166, 1060 Vienna, Austria

Friedrich Kirnbauer, Bioenergy 2020+ GmbH, Wiener Straße 49, A-7540 GÜSSING, Phone: + 43 (0) 3322 42606-156, Fax: + 43 (0) 3322 42606-199, E-mail: friedrich.kirnbauer@bioenergy2020.eu

Abstract

Biomass steam gasification using dual fluidized bed gasifiers is a promising technology to generate electricity and heat from carbon dioxide-neutral sources. The currently difficult market for the utilization of biomass makes optimization necessary, in terms of increasing both plant electrical efficiency and availability. The preconditions for optimization of a dual fluidized bed industrial-scale gasification plant were developed during analyses of inorganic matter at the plant in Güssing/Austria, assisted by investigations and test runs carried out in a pilot-scale plant at the Vienna University of Technology. These findings were applied at the plant in Güssing and are presented in this study. The main optimization steps included a reduction in gasification temperature, a simplification of ash loops, and an upgrade of the gas engine to actual state of the art.

The optimization was evaluated in terms of mass and energy balance, and plant availability. The electrical efficiency of the plant increased from 21 to 23.8%, with a fuel water content around 30%

due to the optimization work. Plant availability was increased from an average of 6600 operating hours per year to 7440 hours in 2012 due to a reduction in fouling tendency.

KEYWORDS: Gasification, biomass, plant optimization, inorganic matter

1 Introduction

Biomass represents a carbon-neutral source for the generation of electricity, heat and liquid biofuels, with a low impact on climate change.

However, those involved in the thermal utilization of biomass in Austria have encountered several problems in recent years, including: (a) a significant increase in fuel prices within the last decade [1]; (b) feed-in tariffs for electricity did not increase in line with fuel prices [2]; (c) the technology for the generation of electricity from biomass faces various problems in general, mainly related to ash behavior [3-5] and the small scale of plants; (d) as well as new technologies associated with operational problems resulting from the plant operators' lack of experience.

A promising technology for the generation of electricity and heat from biomass which was successfully demonstrated in industrial-scale of 8 to 15 MWth is biomass steam gasification in a Dual Fluidized Bed (DFB) reactor. The first industrial-scale plant went into operation in Güssing/Austria in 2002, with the technology's subsequent introduction to the market taking place in recent years with applications in Oberwart/Austria, Villach/Austria and Senden/Germany.

The complex framework surrounding the utilization of biomass in general and biomass steam gasification in particular makes improvement of the technology crucial. The demands facing biomass steam gasification plants for the generation of electricity and heat include reaching an availability of around 8000 h per year, as well as electrical efficiencies higher than 25% for plant sizes of around 10 MW_{th} [6,7]. An optimization scheme aimed at making a significant impact on the commercial success of a plant will likely include the utilization of fuels other than woody biomass in order to reduce fuel costs. Having a competitive advantage over combustion plants will bring product flexibility by producing not only electricity and heat, but also fuels for transportation such as Fischer-Tropsch Diesel, BioSNG (Synthetic natural gas), mixed alcohols and synthetic chemicals, in a process also known as polygeneration [8,9].

This paper documents recent activity undertaken concerning the optimization of a DFB biomass steam gasification plant in Güssing/Austria, aimed at meeting the demands of the market described above. Results obtained from scientific research [10,11], test runs in a 100 kW pilot plant [12,13] and analysis of the industrial-scale plant in Güssing [14] were applied to the operation of the latter, with the aim of increasing its technical and economic efficiency. This includes an increase in the electrical efficiency and availability of the plant.

The optimization program was accomplished via simulation of mass and heat balances in order to evaluate its success.

2 Materials and methods

Most of the studies were carried out at the combined heat and power (CHP) plant in Güssing/Austria. In the following section, the process of the Güssing plant is described and the differences between the demo plant at Güssing and state of the art technology are summarized. An overview of the optimization steps undertaken is given and the method selected for the evaluation of this optimization is described.

2.1 DFB gasification process

The basic principle of biomass steam gasification in a DFB reactor is the separation of endothermic gasification from exothermic combustion; the combustion of a part of the fuel provides the heat required for gasification, which is transferred to the gasification reactor via bed material.

A simplified flow sheet of the plant is shown in Figure 1. Biomass is fed into the gasifier which is operated in bubbling bed mode using steam as a fluidization as well as gasification agent. Bed material also containing char is transferred to the combustion reactor, where the char is combusted in a fast fluidized bed regime. Air is used for fluidization in the combustion reactor. The required heat for gasification is transferred via the bed material that is separated from the flue gas in the cyclone positioned after the combustion reactor, and transported back into the gasifier. The flue gas is further cooled and the fly ash separated in the flue gas filter.

Figure 1: Flow sheet of the gasification plant in Güssing/Austria
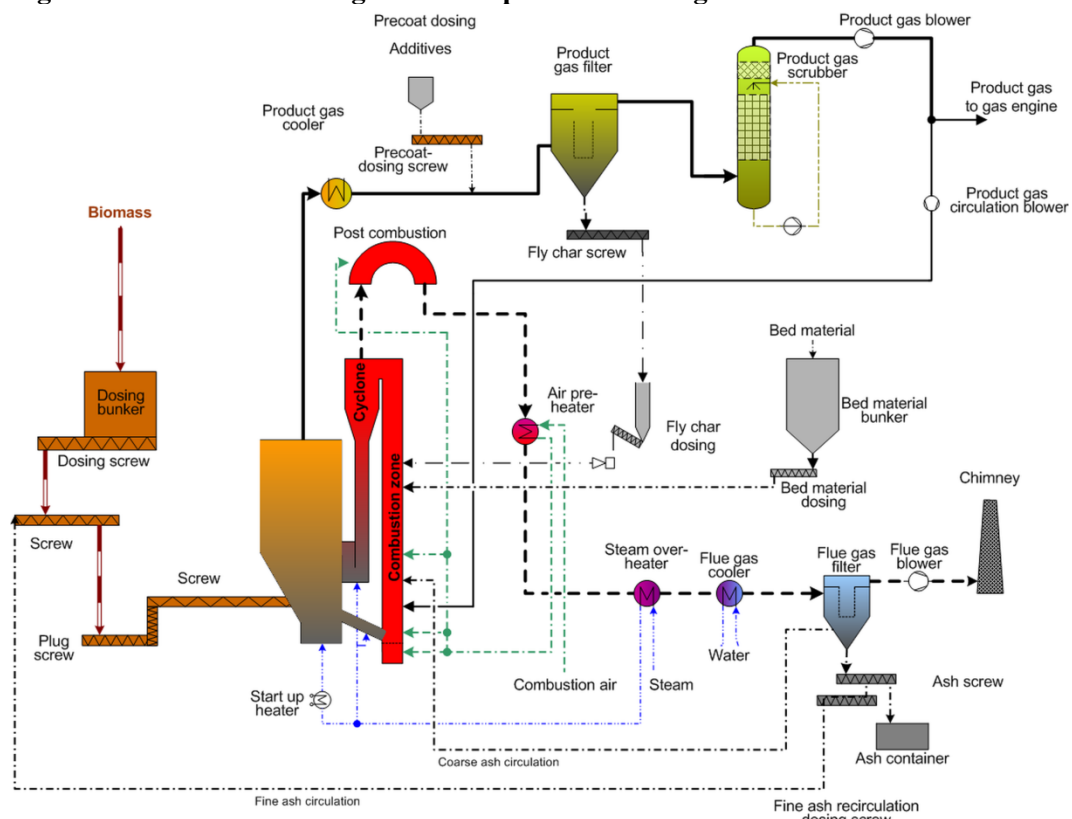
After leaving the gasifier the product gas is cooled and particles separated from the gas stream by the product gas filter. The fly coke from the product gas filter contains inorganic matter such as biomass ash, additives, and products of bed material abrasion, as well as unconverted char and tar. In order to utilize the remaining combustible substances, the fly coke is burnt in the combustion zone. After separation of the particles from the product gas in the product filter, the gas is washed in a rapeseed methyl ester (RME) scrubber to remove water and tars. The cleaned gas is then utilized in a gas engine to produce electricity and heat. A small amount of the product gas is also used to control the temperature of the combustion zone (product gas circulation). The plant is well described elsewhere in the literature [10,12,13,15-18].

Wood chips are used as fuel, with a water content of the fuel delivered varying at between 20 and 45% of fuel weight. Since no biomass dryer is installed at the plant the fuel is used at actual high water content. As the behavior of inorganic matter is investigated in this paper a special focus is given to the origin of these substances. The average composition of the biomass ash is shown in Table 1. Olivine is used as bed material due to its good catalytic properties [19-23]. The composition of a typical olivine sample utilized in the Güssing plant is shown in Table 2.

A dolomite powder is employed for precoating of the product gas filter, with the powder leaving the product gas path with the fly char and introduced into the combustion reactor [14].

Table 1: Average composition of biomass ash (from 3 samples) according to XRF analysis (db, except moisture content) [14]

	Wood chip ash average
	wt.%
Na_2O	2.77
MgO	5.13
Al_2O_3	2.57
SiO_2	15.36
P_2O_5	2.36
SO_3	1.26
K_2O	12.40
CaO	52.47
MnO	1.67
Fe_2O_3	1.73
Cl	0.42
others	1.85
Moisture content	26.25
Ash content	1.42

Table 2: Elemental analysis of unused (fresh) olivine (db) [10]

|	Olivine
	wt.-%
MgO	46.8
SiO_2	39.8
CaO	0.9
Fe_2O_3	10.3
K_2O	0.32
Na_2O	0.43
Al_2O_3	0.40
MnO	0.15
P_2O_5	0.03
Cl	0.10
SO_3	0.06
others	0.71

<u>2.2 The state of the art for DFB biomass steam gasification plants</u>

Due to the demo character of the Güssing plant, the potential for its improvement in terms of design and engineering was determined and applied in later plants.

One of the main differences between the scale of the Güssing prototype plant and those constructed in the following years is the size of the combustion reactor and flue gas pathway. While the Güssing plant was designed for 15% fuel water content, later plants were constructed with higher levels in mind due to the low availability of wood chips and wood residues with water content of around 15% on the Austrian and European markets. However, the plant at Güssing now operates using fuel with significantly higher water content (20-45%). Besides the larger size of the combustion chamber, a low temperature biomass dryer positioned prior to the gasifier in more modern plants can be considered state of the art.

The flue gas path in the Güssing plant includes a post combustion chamber followed by a shell and tube heat exchanger, with the flue gas contained inside the tubes. In contrast, the current state of the art design for flue gas transport involves convection after the post combustion chamber in order to cool the gas to below the melting temperature of all ash components. A comparison of both flue gas pathways is shown in Figure 2.

Figure 2: Comparison of flue gas handling at the Güssing plant (A) and the current state of the art (B)
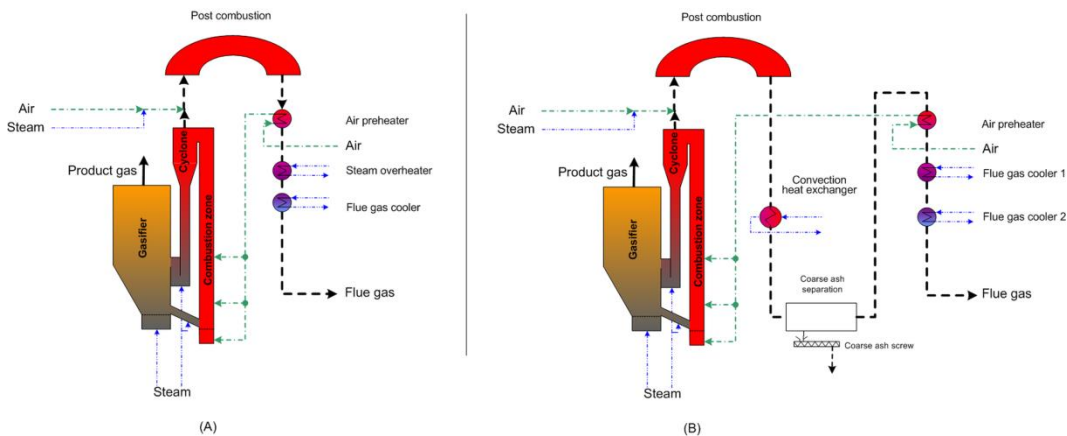

The Güssing plant currently operates at levels unsuited to its size. This results in the fouling and slagging of the combustion chamber, cyclone and at the first heat exchanger (air preheater) [14], issues which are not seen in newer plants such as that e.g. in Oberwart/Austria. Nevertheless, the operating conditions and scale of the Güssing plant, as well as the resulting problems, can be used to form the basis for developing a better understanding of the DFB gasifier in terms of inorganic matter. Indeed, various research activities have recently been carried out in order to understand the behavior of inorganic matter in the system, and to increase the efficiency and operation time of the plant.

Investigation of the employed bed material has revealed that the olivine particles are modified during long-term utilization; interaction with biomass ash leads to the formation of two calcium-rich layers on the surface of the particles (Figure 3). Whereas the inner layer is homogenous and consists mainly of calcium and silicate, the outer layer is similar in composition to the fly ash [10].

Tests carried out in a 100 kW pilot plant at the Vienna University of Technology have revealed that these Ca-rich layers have a significant influence on the catalytic activity of the bed material. Firstly, the water gas shift reaction is enhanced, leading to higher hydrogen and CO_2 yields and lower CO concentrations in the product gas. Secondly, the concentration and amount of tar species in the product gas is reduced significantly. Finally, the decomposition of primary tars is enhanced and the formation of secondary tars reduced [12].

Figure 3: SEM image of used olivine [10]
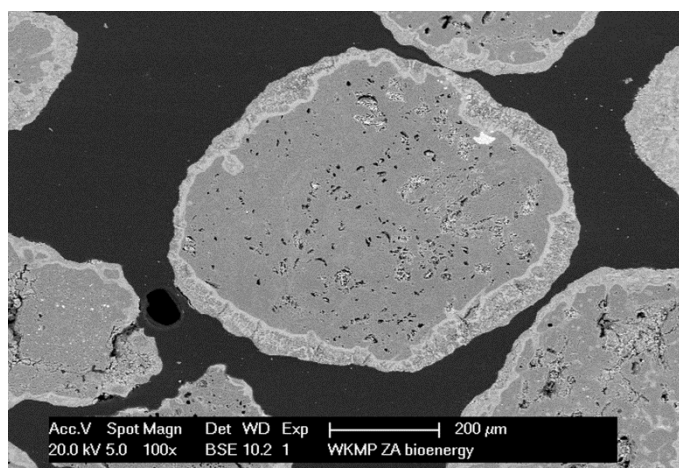
Temperature variation at the 100 kW pilot plant also demonstrated that the gas composition changes when lowering the temperature from 850°C to 750°C, with lower concentrations of hydrogen and carbon monoxide and higher concentrations of carbon dioxide and methane observed. In addition, the volumetric concentration of tars in the product gas increases slightly between 850°C and 800°C, but nearly doubles when decreasing the gasification temperature to 750°C [13].

Pröll et al. [24] used simulations with the software IPSEpro to reveal the potential for increasing plant efficiency by reducing the gasification temperature. An increase in the cold gas efficiency of the plant from 64% to 67% could be achieved by lowering the gasification temperature from 850°C to 800°C, with the electrical efficiency also increasing accordingly.

However, a reduction in the plant's gasification temperature was recently considered to be impossible because of the accompanying increase in product gas tar concentration, which would result in fouling of the product gas filter (mainly with naphthalene). Studies using fresh olivine in a pilot plant confirmed this theory, with tar concentrations increasing to values higher than 5 g/Nm³ when the gasification temperature was lowered to 800°C [25].

Nevertheless, the discovery of layer formation on the bed material particles and its importance of tar reduction as described above have opened the way for further optimization steps to be implemented at the plant.

A reduction in the gasification temperature would likely not only increase the electrical efficiency of the plant, but also decrease both the tendency for fouling in the combustion chamber and flue gas path, and unplanned plant downtime.

2.3 Optimization steps

The investigation of inorganic matter, specifically the nature of its modification and its influence on gasification and plant operation, formed the basis for optimization work at the industrial-scale plant in Güssing.

Previously-acquired data regarding the modification of the bed material [10] and its influence on gasification properties [12,13], as well as the accumulation of low melting species in the system by ash loops [14], resulted in the development of the following optimization steps:

(a) The catalytic activity of bed material increases with retention time in the system [12,13]. A high retention time of the bed material in the system should be aimed.

(b) The source of low melting species such as potassium is fine wood ash [14]. Fine ash should therefore be released from the process immediately and not recycled back into the gasifier.

(c) High concentrations of potassium can be found in the fly char burnt in the combustion chamber [14]. Accurate dosing of fly char is therefore required to ensure perfect combustion conditions in the combustion reactor.

(d) High catalytic activity of the bed material enables temperature reduction in the gasification and combustion reactors [13].

Based on these four steps, the following optimization and modernization procedure was carried out at the Güssing DFB gasification plant during the period from 2009 to 2012:

- Reducing ash loops by turning off the ash circulation and immediately releasing fine ash from the system.
- Focusing on bed material consumption and its retention time in the system via the installation of coarse ash circulation after the cyclone in order to compensate for the latter's malfunction.
- Improving constant fly char dosing into the combustion reactor.
- Focusing on the control of combustion air inside the combustion reactor.
- Reducing the gasification temperature from 850 - 870°C to a target of 830°C.
- Reducing the volume of product gas in the combustion reactor by lowering temperatures inside the combustion reactor, improving bed material circulation, and air staging.
- Increasing the efficiency of the gas engine to state of the art level by the supplier of the engine.

The above optimization procedure was carried out stepwise by the plant operator. After the temperature was reduced inside the gasification reactor, the plant was operated for 12 months at the new set points before the optimization process was evaluated.

2.4 Evaluation of optimization

Evaluation of optimization success was carried out using a variety of different methods. The plants' distributed control system (DCS) logs not only important process data such as temperature, pressure, flows etc., but also the operation time of the gas engine, power load of the generator, and the accumulation of produced electricity. These data were all taken into account in the evaluation of plant availability. The average availability for the years 2005 to 2011 was taken as a reference, although 2008 data were not considered due to a test campaign for an EU research project being carried out which had a negative impact on plant availability. The years between 2002 (plant start-up) and 2004 were also not considered representative because of the likely impact of the start-up phase and the early optimization process required for the new technology.

Biomass water content is measured regularly by plant staff upon delivery. During this process, samples are taken at different locations in the truck (logs and wood chips, partly delivered as logs and partly as wood chips) and the water content determined. The dry substance is then calculated for each truck and the water content allocated. The cumulative distribution was calculated on the basis of variation in dry wood water content. The results presented here include values for the whole of 2009 and 2012. Later modification of water content due to precipitation or evaporation was not considered.

Gas analyses for the 2009 reference point were carried out using a Rosemount NGA 2000 gas analyzer (CH_4, CO, CO_2, H_2 and O_2), with N_2, C_2H_4, C_2H_6 and C_3H_8 measured in a Syntech Spectras GC 955 gas chromatograph.

Gas analyses in 2012 were performed on a Clarus 500 gas chromatograph (GC; Perkin Elmer). This GC was equipped with three different columns - one molecular and two non-polar (Porapak) sieves - connected via two automated valves and a 500 µl injection loop. Helium was used as the carrier gas. Two types of detector were employed: a thermal conductivity detector (TCD) for permanent gases (O_2, N_2, CO, CO_2), and a flame ionization detector (FID) for hydrocarbons up to a carbon number of three. Hydrogen concentrations were calculated as 100 minus the sum of the gas concentrations recorded by the two detectors.

Mass and energy balance calculations were performed for the whole plant in order to evaluate the success of the optimization process in terms of changes in plant efficiency. For this purpose the IPSEpro simulation software program was used, with the model library described by Pröll and Hofbauer [26]. Process values recorded by the plant's DCS were taken as the basis of these calculations, with standard deviations statistically determined and then corrected according to the experience of the operation team. Gas composition was measured via GC and implemented into the model.

A second simulation of plant status in 2012 using again the software IPSEpro was carried out, including the impact of a low temperature biomass tower dryer. Operational values for the dryer were taken from that at the DFB gasification plant in Oberwart [27].

The efficiency of the gasification plant was evaluated in terms of both cold gas efficiency, which represents the relationship between the heating-value-based chemical energy of the product gas and thermal fuel power (Eq (1)), and electrical efficiency (Eq (2)).

$$\eta_{chem} = (m_{PG}*lhv_{PG})/(m_{fuel}*lhv_{fuel}) = P_{chem,PG}/P_{th} \tag{1}$$

$$\eta_{el,brut} = P_{el}/P_{th} \tag{2}$$

Bed material investigations have previously been carried out in earlier work at Güssing [10]; the present study summarizes bed material sample data in relation to the composition of produced gas. Samples were obtained after plant shut down and cooling, with their elemental composition analyzed via X-ray fluorescence (XRF) and calculated as oxides. Samples for XRF were melted in a Merck Spectromelt at 1050°C and dumped on a 400°C stainless steel plate. The analyses were then carried out using a PANalytical Axios Advanced analyzer under vacuum atmosphere with a rhodium anode, an excitation voltage of 50 kV and a tube current of 50 mA. Bed material calcium oxide levels are related to the carbon monoxide content of the product gas, both of which are presented here. Average gas composition during the last hour of plant operation (before shut down and sampling) was determined and taken for reference. Samples were obtained in the period from March 2010 to January 2012, at gasification temperatures of around 850°C to 870°C. Sample carbon monoxide content provides an indication of the enhancement of the water-gas shift reaction [12,28].

3 Results

The operational parameters of the Güssing gasification plant varied considerably in both 2009 and 2012, likely as a result of variation in fuel water content, as shown in Figure 4. Despite this, two points (29th of October 2009 and 15th of October 2012) were chosen which represent an ordinary operation as the basis for simulation with IPSEpro performing mass and energy balances.

Figure 4: Water content of delivered biomass
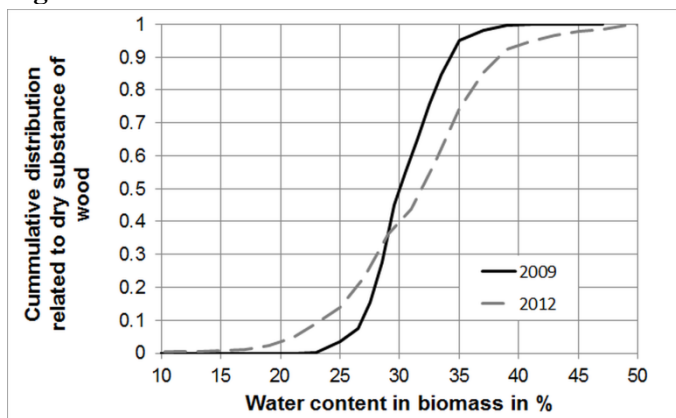
The reference product gas composition values are shown in Table 3. As the Table reveals, whereas hydrogen content decreased between 2009 and 2012, levels of the main components all increased. In contrast, the concentration of higher gaseous hydrocarbons such as ethane, propane and propene fell significantly.

Table 3: Comparison of product gas composition before and after optimization

Species		Status before optimization (2009) [29]	Status after optimization (2012)
		vol-%$_{db}$	*vol-%$_{db}$*
Hydrogen	H_2	39.4	34.4
Carbon monoxide	CO	21.5	24.2
Carbon dioxide	CO_2	23.5	24.9
Methane	CH_4	9	11.2
Ethylene	C_2H_4	2.72	3.5
Nitrogen	N_2	1.3	1.3
Higher gaseous hydrocarbons		2.58	0.2
Oxygen	O_2	n.a.	0.3

Table 4: Performance parameters of the Güssing CHP plant before and after optimization

Origin of values		Initial plant design value	Reference 2009	After optimization 2012	Potential with biomass dryer
		-	Measured and simulated	Measured and simulated	Simulated
Fuel water content	*%*	15	32.2	28.3	36 - dried to 20
Gasification temperature	*°C*		866.2	844.0	844.0
Amount of fuel (ds)	*kg/h*		2070	1790	1660
Fuel power	*kW*	8000	9420	8250	7830
Net power of product gas (LHV)	*kW*	5600	6160	5720	5720
Generator output	*kW*	2000	1980	1960	1960
Heat output	*kW*	4500	4150	4100	3550
Product gas in combustion chamber	*Nm³/h*		316	77	77
Cold gas efficiency	$\eta_{chem,G}$ *[%]*	0.70	65.4	69.4	76.6
Electrical efficiency	$\eta_{el,brut}$ *[%]*	25	21.0	23.8	26.2

The results of the simulation are shown in Table 4. The gasification temperature in the reference year of 2009 was 866°C, a figure which was state of the art at the time. As a result of subsequent temperature reduction in the gasifier, a gasification temperature of 844°C (typical value after reduction) was used in the calculation of plant status after optimization. Electrical efficiency rose from 21% in 2009 to 23.8% after optimization, representing an increase of 13%. These values are confirmed by the amount of wood purchased during the year; with similar generator load, the fuel input decreased accordingly. Cold gas efficiency increased from 65.4% to 69.4%, an improvement of 6%.

The installation of a low temperature biomass dryer would increase plant electrical efficiency to 26.2% and cold gas efficiency to 76.6%. Heat output used in a district heating system would decrease from 4.1 MW to 3.5 MW as a result of drying of the biomass, as this heat would be consumed then for drying purposes.

The optimization measures described above had a significant influence on plant availability, reducing downtime associated with unscheduled shutdowns (Figure 5). The mean availability of the gas engine between 2005 and 2011, excluding the year 2008, was around 6600 h with a maximum of 6950 operating hours per year. Plant optimization could increase this value to 7442 hours.

Figure 5: Comparison of plant availability before and after optimization (yearly average)
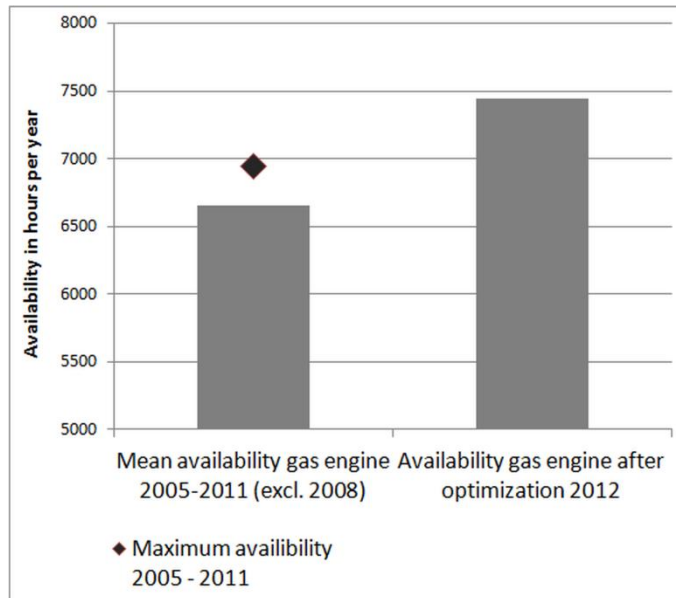
As mentioned earlier the relationship between bed material calcium content and product gas carbon monoxide content is shown in Figure 6 (at 850-870°C gasification temperature). The results of test runs carried out in the 100 kW pilot plant at the Vienna University of Technology are included for comparison and can be taken as a reference for bed material containing no calcium oxide.

Figure 6: Relationship between bed material calcium oxide content and product gas carbon monoxide content (Pilot plant values see [12])
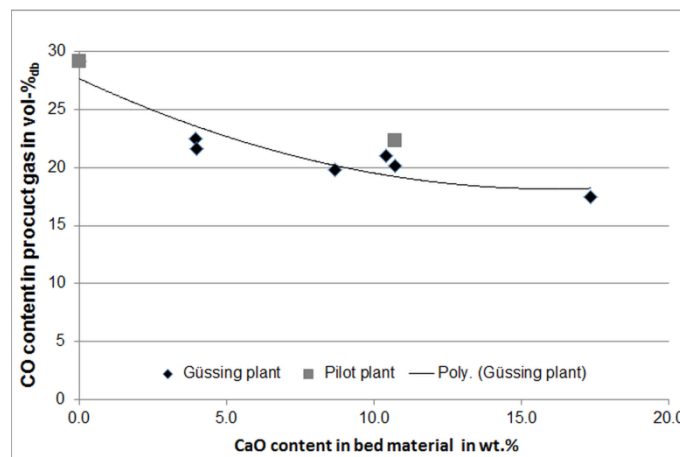
4 Discussion

Fuel water content is an important parameter for gasifier performance. Analysis of fuel water content at the gasification plant in Güssing revealed significant variations between 20 and 40%. Considering the influence of this parameter on both the heating value of the fuel and on the cold gas efficiency of the plant [26], the difference in fuel water content between initial plant design (15%) and that actually used in plant operation (average 30%) would mean the impact is likely significant.

The focus on high bed material retention time and an immediate discharge of fine ash increased plant availability in two ways: i) product gas composition is more stable, leading to less impact on the gas engine, and ii) downtime due to fouling is decreased, as observed in the availability figures for 2012 (Figure 5). Accurate dosing of fly char into the combustion reactor further reduced fouling tendencies in the combustion reactor and flue gas path. Operational experience has shown that variation in fly char dosing and subsequent worsening in combustion can lead to immediate fouling of the two aforementioned areas.

The suggested mechanism of ash transformation in the combustion reactor is shown in Figure 7; the elements indicated in this diagram are not considered to be oxides but rather bound in different minerals. Inorganic matter is introduced into the combustion chamber with char, which is transferred with the bed material from the gasification reactor via the chute, as well as fly char from the product gas filter. Organic matter is burnt in the combustion reactor and inorganic matter released from the particles. These burning particles are the source of heat in fluidized beds and are, therefore, associated with the highest temperatures [30]. Inorganic matter released from the burning material either melts or is released into the gaseous phase or is released as solid particles. The release rate of potassium, which forms compounds with the lowest melting temperatures, is considered crucial for the initiation of fouling and is influenced by temperature, the amount of calcium in the system and water content [31]. Not only is the temperature affected by that of the fluidized bed, but the local temperature of burning particles is also influenced by the excess air ratio and the adiabatic combustion temperature of the particle.

Figure 7: Mechanisms of ash transformation (adapted from Frandsen et al. [5])
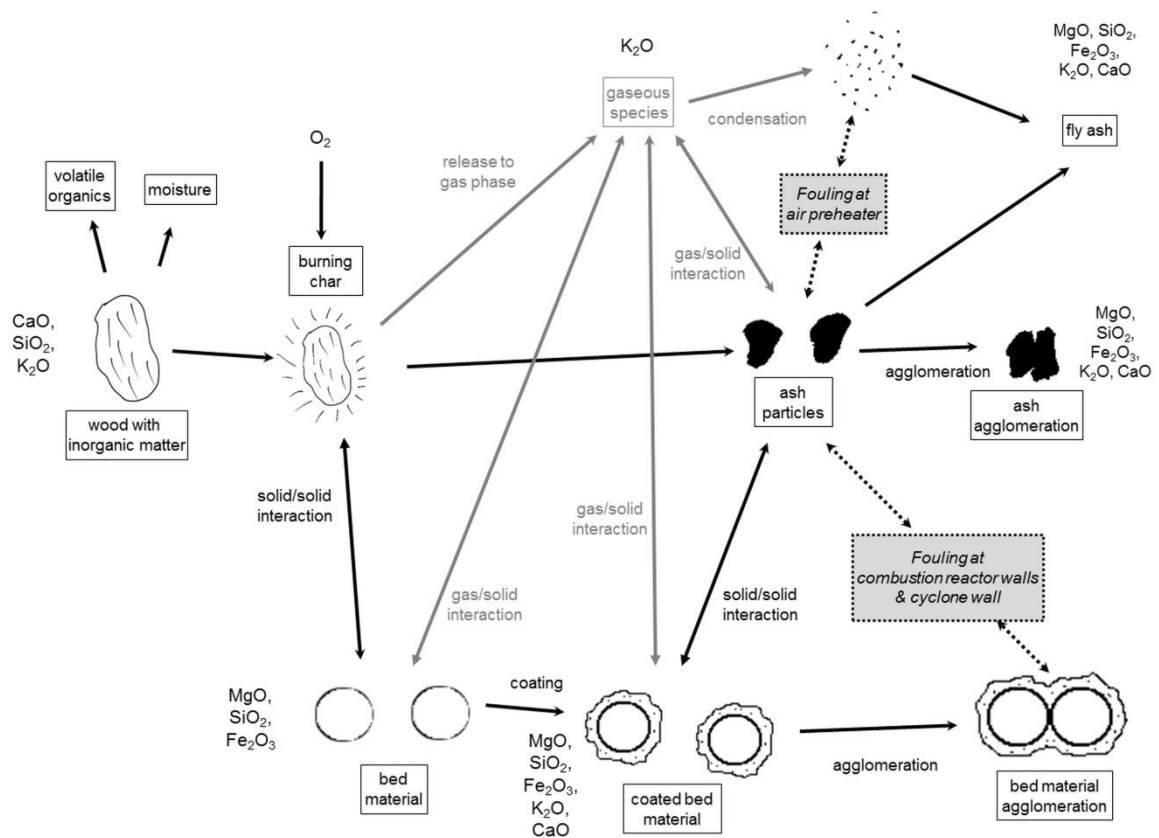
Inorganic matter released into the gaseous phase condenses after cooling in the heat exchangers, which can result in fouling, presumably as a result of a reaction which takes place during condensing and cooling with other inorganic matter in the fly ash solid phase.

Due to the high reactivity of the gaseous species, e.g. potassium, a reaction with solid or melted matter can be expected [32]. Such reactions are considered to increase the risk of fouling in high temperature sections of the combustion reactor and cyclone [14].

Due to the high temperatures which occur locally around burning char particles, the ash components of the fuel which are released can react with the bed material to form the observed layers around the bed material particles [10]. One possible suggestion for the mechanism of layer formation was given in an earlier study [11].

Temperature variation carried out in a 100 kW pilot plant at the Vienna University of Technology has demonstrated that the impact of bed material catalytic activity due to the calcium rich layer on the bed particles on tar concentrations is greater than that of a decrease in gasification temperature to 800°C [13].

A reduction in the target temperature of gasification from 850-870°C to 830-850°C brought no disadvantages in terms of tar-induced plugging of the product gas cooler. Lower gasification temperatures resulted in a decrease in the combustion temperature inside the combustion reactor, with

the same circulation rate of bed material between the combustion and gasification reactors. Demand for product gas recirculation into the combustion reactor for controlling the gasification temperature decreased significantly (see Table 4). Variations in air staging inside the combustion reactor influence both the circulation rate and the amount of char that is transferred from the gasification reactor to the combustion reactor; as a result the demand for the combustion of product gas in the combustion reactor can be further reduced.

Analysis of overall efficiency revealed that besides the two weeks shut-down required for regular plant maintenance, the remaining downtime is largely caused by fouling at the air preheater in the flue gas pathway. Optimization enabled plant downtime due to fouling at the air preheater to be reduced. The installation of a biomass dryer would decrease the load of the combustion reactor because less energy would be required for water evaporation in the gasifier, as well as reducing the risk of air preheater fouling. The installation of a low temperature biomass dryer would, therefore, significantly increase plant efficiency.

5 Conclusions

The analysis of inorganic matter, accompanied by test runs carried out at a 100 kW pilot plant, has provided important information regarding the operation and optimization of the industrial-scale dual fluidized bed gasification plant in Güssing as well as for all other DFB gasification plants in operation.

A focus on control inorganic matter and bed material composition was able to improve plant operation, with reduced fouling tendency observed in terms of inorganic matter.

Gasification temperatures in the DFB biomass gasifier can be reduced to 830°C with no subsequent problems for tar condensation in the product gas path. This procedure can be considered suitable for plants operating using woody biomass.

The flue gas path should be designed so that the gas is cooled via convection to temperatures below the initial melting temperature of potassium silicates (approximately 600 °C). A similar design is recommended for the product gas path when utilization of potassium-rich fuels is planned. Future research should examine the influence of fuels other than woody ash on fouling and bed material layer formation.

Electrical efficiencies of 23% can be obtained when employing fuel with 33% water content. The installation of a biomass dryer would increase efficiency to 26%, while still higher values could be achieved with the implementation of an Organic Rankine Cycle (ORC) to utilize heat at temperatures of around 450°C, as shown in the CHP in Oberwart/Austria [27].

Biomass steam gasification in a DFB reactor represents a competitive alternative for the generation of heat and electricity, with the potential for high availabilities and electrical efficiencies (>30 %) in even small-scale industrial plants.

Further investigation is required regarding the utilization of biomass fuels other than woody biomass. The interaction between fuel ash and olivine bed material has been observed to vary with different fuels [33].

Definitions

Cold gas efficiency	η_{chem}	%
Electrical efficiency	$\eta_{el,brut}$	%
Mass flow of product gas	m_{PG}	$kg*s^{-1}$
Lower heating value of product gas	lhv_{PG}	$J*kg^{-1}$
Mass flow of fuel	m_{fuel}	$kg*s^{-1}$
Lower heating value of fuel	lhv_{fuel}	$J*kg^{-1}$
Net power of product gas (basis lower heating value)	$P_{chem,PG}$	kW
Thermal fuel power (basis lower heating value)	P_{th}	kW
Generator output	P_{el}	kW
Volume percentage, dry basis		$vol\text{-}\%_{db}$

Acknowledgments

References

[1] Alakangas E, Junginger M, van Dam J, Hinge J, Keränen J, Olsson O et al. EUBIONET III—Solutions to biomass trade and market barriers. Renewable and Sustainable Energy Reviews 2012;16:4277–90.

[2] Ökostrombericht 2012. Austria: Energie-Control; 2012.

[3] Valmari T, Lind TM, Kauppinen EI, Sfiris G, Nilsson K, Maenhaut W. Field Study on Ash Behavior during Circulating Fluidized-Bed Combustion of Biomass. 1. Ash Formation. Energy Fuels 1998;13:379–89.

[4] Davidsson KO, Amand LE, Steenari BM, Elled AL, Eskilsson D, Leckner B. Countermeasures against alkali-related problems during combustion of biomass in a circulating fluidized bed boiler. Chemical Engineering Science 2008;63:5314–29.

[5] Frandsen FJ. Ash Research from Palm Coast, Florida to Banff, Canada: Entry of Biomass in Modern Power Boilers. Energy Fuels 2009;23:3347–78.

[6] Evans A, Strezov V, Evans TJ. Sustainability considerations for electricity generation from biomass. Renewable and Sustainable Energy Reviews 2010;14:1419–27.

[7] Nussbaumer T. Combustion and Co-combustion of Biomass: Fundamentals, Technologies, and Primary Measures for Emission Reduction. Energy Fuels 2011;17:1510–21.

[8] Chen Y, Adams TA, Barton PI. Optimal Design and Operation of Static Energy Polygeneration Systems. Ind Eng Chem Res 2012;50:5099–113.

[9] Williams RH, Larson ED, Liu G, Kreutz TG. Fischer–Tropsch fuels from coal and biomass: Strategic advantages of once-through ("polygeneration") configurations. Energy Procedia 2009;1:4379–86.

[10] Kirnbauer F, Hofbauer H. Investigations on Bed Material Changes in a Dual Fluidized Bed Steam Gasification Plant in Güssing, Austria. Energy Fuels 2011;25:3793–8.

[11] Kirnbauer F, Hofbauer H. The Mechanism of Bed material Coating in Dual Fluidized Bed Biomass Steam Gasification Plants and its Impact on Plant Optimization. Powder Technology, 2013 (submitted for publication).

[12] Kirnbauer F, Wilk V, Kitzler H, Kern S, Hofbauer H. The positive effects of bed material coating on tar reduction in a dual fluidized bed gasifier. Fuel 2012;95:553–62.

[13] Kirnbauer F, Wilk V, Hofbauer H. Performance improvement of dual fluidized bed gasifiers by temperature reduction: The behavior of tar species in the product gas. Fuel 2012:1–9.

[14] Kirnbauer F, Koch M, Koch R, Aichernig C, Hofbauer H. The behaviour of inorganic matter in a dual fluidized bed steam gasification plant. Energy Fuels, 2013 (submitted for publication).

[15] Hofbauer H, Rauch R, Loeffler G, Kaiser S, Fercher E, Tremmel H. Six years experience with the FICFB-GASIFICATION process. Amsterdam, The Netherlands; 2002.

[16] Bolhar-Nordenkampf M, Hofbauer H, Bosch K, Rauch R, Aichernig C. Biomass CHP Plant Güssing - Using Gasification for Power Generation. In: K. Kirtikara (Ed.), Self-published, Phuket, Thailand; 2003, p. 567–72.

[17] Koppatz S, Pfeifer C, Rauch R, Hofbauer H, Marquard-Moellenstedt T, Specht M. H2 rich product gas by steam gasification of biomass with in situ CO2 absorption in a dual fluidized bed system of 8 MW fuel input. Fuel Processing Technology 2009;90:914–21.

[18] Hofbauer H, Rauch R, Bosch K, Koch R, Aichernig C. Biomass CHP Plant Güssing - A Success Story. In: Bridgwater AV, editor. Pyrolysis and Gasification of Biomass and Waste, CPL Press; 2003, p. 527–36.

[19] Pfeifer C, Koppatz S, Hofbauer H. Catalysts for dual fluidised bed biomass gasification—an experimental study at the pilot plant scale. Biomass Conv Bioref;2011:1–12.

[20] Devi L, Craje M, Th ne P, Ptasinski KJ, Janssen FJJG. Olivine as tar removal catalyst for biomass gasifiers: Catalyst characterization. Applied Catalysis, a: General 2005;294:68–79.

[21] Devi L, Ptasinski KJ, Janssen FJJG, van Paasen SVB, Bergman PCA, Kiel JHA. Catalytic decomposition of biomass tars: use of dolomite and untreated olivine. Renewable Energy 2005;30:565–87.

[22] Devi L, Ptasinski KJ, Janssen FJJG. Decomposition of Naphthalene as a Biomass Tar over Pretreated Olivine: Effect of Gas Composition, Kinetic Approach, and Reaction Scheme. Ind Eng Chem Res 2005;44:9096–104.

[23]   Devi L, Ptasinski KJ, Janssen FJJG. Pretreated olivine as tar removal catalyst for biomass gasifiers: investigation using naphthalene as model biomass tar. Fuel Processing Technology 2005;86:707–30.

[24]   Pröll T, Rauch R, Aichernig C, Hofbauer H. Fluidized bed steam gasification of solid biomass-Performance characteristics of an 8 MWth combined heat and power plant. International Journal of Chemical Reactor Engineering 2007;5:1–19.

[25]   Hofbauer H, Rauch R. Stoichiometric water consumption of steam gasification by the FICFB-Gasification process. In: Bridgwater AV, editor. Progress in Thermochemical Biomass Conversion, Oxford, UK and Innsbruck, Austria: Blackwell Science Ltd; 2000, p. 199–208.

[26]   Pröll T, Hofbauer H. Development and Application of a Simulation Tool for Biomass Gasification Based Processes. International Journal of Chemical Reactor Engineering 2008;6.

[27]   Kotik J. Über den Einsatz von Kraft-Wärme-Kopplungsanlagen auf Basis der Wirbelschicht-Dampfvergasung fester Biomasse am Beispiel des Biomassekraftwerks Oberwart. PhD Thesis. Vienna University of Technology; 2010 (in German).

[28]   Kern S, Pfeifer C, Hofbauer H. Reactivity tests of the water–gas shift reaction on fresh and used fluidized bed materials from industrial DFB biomass gasifiers. Biomass and Bioenergy VL;2013.

[29]   Aigner I. Co-gasification of coal and wood with steam in a dual fluidized bed gasifier. PhD Thesis. Vienna University of Technology; 2010.

[30]   Scala F, Chirone R. An SEM/EDX study of bed agglomerates formed during fluidized bed combustion of three biomass fuels. Biomass and Bioenergy 2008;32:252–66.

[31]   Novaković A, van Lith SC, et al. Release of Potassium from the Systems K−Ca−Si and K−Ca−P†. Energy Fuels 2012;23.

[32]   Boström D, Skoglund N, Grimm A, Boman C, Öhman M, Broström M, et al. Ash Transformation Chemistry during Combustion of Biomass. Energy Fuels 2012;26:85–93.

[33]   Grimm A, Öhman M, Lindberg T, Fredriksson A, Boström D. Bed Agglomeration Characteristics in Fluidized-Bed Combustion of Biomass Fuels Using Olivine as Bed Material. Energy Fuels 2012;26:4550–9.

Lebenslauf

Dipl.-Ing. Friedrich Kirnbauer

Embelgasse 49/11,
A - 1050 Wien
Mobil: +43 (0)676 974 33 22
E-Mail: f.kirnbauer@me.com

Persönliche Daten:

Geboren am:	04. Oktober 1977 in Wien
Nationalität	Österreich
Familienstand:	Verheiratet

Ausbildungsweg:

5/2009 - heute	Doktoratsstudium der techn. Wissenschaften Verfahrenstechnik
	Technische Universität Wien - Institut für Verfahrenstechnik, Umwelttechnik und Techn. Biowissenschaften/E166
	Dissertation: *„The impact of inorganic matter in the performance of a dual fluidized bed biomass steam gasification plant"* bei Prof. Dr. Hermann Hofbauer
10/1998 - 02/2005	Studium der Verfahrenstechnik an der TU-Wien, Studienzweig: Apparate- und Anlagenbau, Schwerpunkt: Verfahrenstechnik und Energie
	Thema der Diplomarbeit: *"Experimental investigations of different high temperature desufurization sorbents to couple a Solid Oxide Fuel Cell with a biomass gasifier"* bei Prof. Dr. Hermann Hofbauer
	Abschluss: Diplom-Ingenieur (TU)
05/2004 - 10/2004	Versuche zur Diplomarbeit bei SINTEF/NTNU in Trondheim/Norwegen
06/1997	Externistenreifeprüfung über das Oberstufenrealgymnasium mit bildnerischer Erziehung
09/1996 - 06/1997	Maturalehrgang an der Rudolf Steiner - Schule Wien Pötzleinsdorf
1984 – 1996	Rudolf Steiner - Schule Wien Pötzleinsdorf

Publikationen:

F. Kirnbauer, M. Koch, R. Koch, C. Aichernig, H. Hofbauer, *The role of inorganic matter in the optimization of a dual fluidized biomass steam gasification plant*, 2013 (submitted).

F. Kirnbauer, M. Koch, R. Koch, C. Aichernig, H. Hofbauer, *The behaviour of inorganic matter in a dual fluidized bed steam gasification plant*, Energy Fuels **2013**. DOI: 10.1021/ef400598h

F. Kirnbauer, H. Hofbauer, *The Mechanism of Bed Material Coating in Dual Fluidized Bed Biomass Steam Gasification Plants and its Impact on Plant Optimization*, Powder Technology **2013**, 245, 94-104. DOI: 10.1016/j.powtec.2013.04.022.

Kirnbauer, F.; Wilk, V.; Hofbauer, H. *Performance improvement of dual fluidized bed gasifiers by temperature reduction: The behavior of tar species in the product gas*. FUEL **2012**, *108*, 534–542.

Kirnbauer, F.; Wilk, V.; Kitzler, H.; Kern, S.; Hofbauer, H. *The positive effects of bed material coating on tar reduction in a dual fluidized bed gasifier*. FUEL **2011,** 95, 553-562.

Kirnbauer, F.; Hofbauer, H. *Investigations on Bed Material Changes in a Dual Fluidized Bed Steam Gasification Plant in Güssing, Austria*. Energy Fuels **2011**, 25, 3793–3798.

Arbeitserfahrung:

5/2009 - heute	**Bioenergy2020+ GmbH**

Außenstelle Güssing, Wienerstraße 49, A - 7540 Güssing,

www.bioenergy2020.eu

Researcher,

Optimierung eines Biomassekraftwerks nach dem Prinzip der Zweibett-Wirbelschicht-Dampf-Vergasung, Analyse von aschebasierten Vorgängen (Fouling, Slagging, Agglomeration). Optimierung des Wartungs- und Instandhaltungs-managements.

Projektleitung des Umbaus des Rauchgasweges eines Biomassekraftwerks nach dem Prinzip der Zweibett-Wirbelschicht-Dampf-Vergasung

11/2005 - 3/2009	**Andritz AG, Mechanical Pulping Systems**

Eibesbrunnergasse 20, A - 1120 Wien, www.andritz.com

Prozessingenieur, stellvertretender Gruppenleiter Prozessdesign

Faserlinienauslegung, P&ID Fließbilder, Massenbilanzen, Equipment-, Rohrleitungs- und Pumpenauslegung, Prozess- & Betriebsanleitung

Inbetriebnahme und Optimierung von Anlagen vor Ort

Standardisierung im Engineering, Aufbau einer CAE-Datenbank (Comos PT), Training und Koordination des Comos PT Teams

Budget und Personalplanung

Fremdsprachen:

Englisch	Verhandlungssicher
Russisch	Maturaniveau. Ab der 1. Klasse Volksschule
Portugiesisch	Grundkenntnisse.

PC Kenntnisse:

Gute Kenntnisse für MS Windows, MS Office (incl. VBA), MS Visio, MS Project, Comos PT, AutoDesk Inventor, Catia V5, Mac OS-X

Zivildienst:

10/1997 - 09/1998 Johanniter Unfall-Hilfe Bereich Wien als Sanitäter im Krankentransport.

Hobbys:

Sport   Segeln, Mountainbiken, Laufen (Vienna City Marathon 2003), Skitouren

Sonstiges:

Führerschein der Klasse B, Befähigungsausweis zur Führung von Segel- und Motoryachten im Fahrtenbereich 2

Wien, am 26. Juni 2013